FINAL REPORT:
DETECTION, PREDICTION, IMPACT, AND MANAGEMENT OF INVASIVE PLANTS USING GIS

Keith T. Weber, editor
GIS Director
Idaho State University
GIS Training and Research Center
Pocatello, Idaho 83209-8130

FINAL REPORT:
DETECTION, PREDICTION, IMPACT, AND MANAGEMENT OF INVASIVE PLANTS USING GIS

Keith T. Weber, Editor

Contributing Investigators

Keith T. Weber, Principal Investigator (webekeit@isu.edu), Idaho State University, GIS Training and Research Center, Campus Box 8130, Pocatello, ID 83209-8130.

Nancy F. Glenn, Co-Principal Investigator (glennanc@isu.edu), Idaho State University, Department of Geosciences, Campus Box 8072, Pocatello, ID 83209-8072.

Matthew Germino, Co-Principal Investigator (germmatt@isu.edu), Idaho State University, Department of Biological Sciences, Campus Box 8007, Pocatello, ID 83209-8007.

Project web-site: http://giscenter.isu.edu/research/techpg/nasa_weeds/template.htm

ACKNOWLEDGEMENTS
This study was made possible by a grant from the National Aeronautics and Space Administration Goddard Space Flight Center. ISU would also like to acknowledge the Idaho Delegation for their assistance in obtaining this grant.

Recommended citation style:
Streutker, D. R., and N. F. Glenn. 2006. *LiDAR Measurement of Sagebrush Steppe Vegetation Heights*. Pages 33-50 in K. T. Weber (Ed), Final Report: Detection, Prediction, Impact, and Management of Invasive Plants Using GIS. 196 pp.

Table of Contents

DETECTION, PREDICTION, IMPACT, AND MANAGEMENT OF INVASIVE PLANTS USING GIS

Executive Summary

Significant Findings and Achievements

- While high spatial resolution satellite imagery seems to offer numerous advantages to the scientific community to assess and monitor rangeland ecosystems, they are currently of limited application due to cost and, more importantly, unreliable accuracy of patchy targets. This is a function of geo-registration error (RMS~5.0m) that routinely exceeds the absolute spatial resolution of the imagery (2.4m) (chapters 1, 5, and 6).

- High spatial resolution satellite imagery has limited applicability for large study areas because the method in which these data are acquired is not systematic, but rather scheduled. A large study area may be imaged over a period of several weeks. While the imagery can be atmospherically corrected to achieve a seamless and "color-balanced" product, this temporal resolution is not satisfactory for rangeland applications where the phenological state of plants changes fairly rapidly throughout the growing season.

- The accuracy of invasive weed classifications is strongly influenced by co-registration between imagery and field training sites. Since most training sites are acquired using GPS, the accuracy and precision of GPS receivers is extremely important (chapters 5 and 14).

- Reliable classification of rangeland ecosystems is a function of minimum target cover. It appears that targets need to exist at a percent cover of nearly 1/3rd (33%) within each pixel to assure reliable classification results (>70% users accuracy).

- We developed LiDAR statistical tools for detection and characterization of rangeland vegetation (chapter 3). LiDAR routinely underestimated the height of vegetation and it appears that a minimum mass of vegetation (i.e., the interior of the shrub rather than the surface canopy) was required to return the LiDAR signal. This known and consistent underestimation allows LiDAR data to be applied to numerous rangeland ecosystems studies.

- We developed LiDAR/hyperspectral data fusion methods for rangeland vegetation (chapter 2). This methodology increased overall classification accuracy (from 74% to 89%) and provided vegetation structure information previously unavailable with standard image classification techniques.

- We are applying the LiDAR methodologies pioneered by this study to areas with wind erosion/deposition. Two proposals have been submitted to continue this research.

- The effect of livestock grazing on vegetation composition in rangeland ecosystems is dependent upon stocking level and spatial distribution. As a result, we have begun investigating the temporal effect of livestock grazing animals on sagebrush-steppe rangelands.

- Vegetation structure and cover becomes variable in space and time after fire, particularly when sites were grazed extensively before the fire. We predict that where and when vegetation indices are low during the growing season, there must be resources available to exotic plants, making invasions possible (chapters 4 and 9).

- Soil water becomes more available after fire --at depth-- due primarily to the loss of sagebrush (chapter 10).

- Spotted knapweed, which appears representative of Eurasian forbs, has major growth advantages over other plants. The extra advantages arise from its ability to tap into deep soil water that is available when sagebrush or other deep-rooted species are not present (e.g., following fire). This growth advantage is linked to superior photosynthesis and morphological features of knapweed (and probably most exotic forbs of rangelands) conferring greater efficiency in its use of soil resources. Soil resources are a key driver of invasions (chapter 13).

- We addressed how invasive plants persist in the long term and felt it was necessary to first investigate factors affecting reestablishment of the community existing before fire. Herbs come back immediately (chapter 10), but sagebrush is slow to reestablish. We found recovery of mountain sagebrush is negatively affected by neighboring herbs, particularly forbs (chapters 8 and 9). The effect appears linked more to competition over nitrogen (or similar elements) rather than water (WNAN). As rangelands become enriched with forbs as a result of invasive plants like knapweed and other Eurasian forbs, we expect sagebrush recovery after fire to be more sluggish than it currently is.

- One student completed his Graduate Certificate in Geotechnologies (Luke Sander) through this research, while two others completed their Master degree (Ryan Baum and Katie DeCristina). Three students were partially funded by this study which ultimately will result in completion of doctoral degrees (Bhushan Gokhale, Judson Hill, and Erik Jackson) (degrees are expected to be conferred in August 2006).

- Public outreach events associated with this study were very successful. Over 200 people (ranchers, range scientists, range managers, and geospatial scientists) were exposed to our research at the annual Geo-spatial and Range Sciences Conference. Several have become very involved and have used products produced through our research in the ranch/range planning.

Rangeland Health Modeling with Quickbird Imagery

Bhushan Gokhale. Idaho State University, GIS Training and Research Center, Campus Box 8130, Pocatello, Idaho 83209-8130. (**gokhbhus@isu.edu**)

Keith T. Weber. Idaho State University, GIS Training and Research Center, Campus Box 8130, Pocatello, Idaho 83209-8130. (**webekeit@isu.edu**)

ABSTRACT

Rangeland health is very important for ranchers, farmers and land management agencies. It is also important to identify different rangeland health parameters and evaluate their impact on rangeland health. This study obtained various data describing rangeland health conditions in southeastern Idaho and prepared a rangeland health model using Quickbird multispectral satellite imagery. Five elements were chosen to evaluate rangeland health: presence of cheatgrass (*Bromus tectorum*), bare ground exposure, litter, percent shrub cover, and percent grass cover. A field survey collected information (percentage, dimensions etc.) for all the above parameters (n=424). These data was used to create 'training sites', which were then used to "teach the software" what each parameter "looks like" within the satellite imagery. IDRISI, a raster based software application, was used to perform various data analysis operations using individual bands and vegetation indices derived from the Quickbird imagery. Data redundancy was reduced using Principal Component Analysis (PCA). Spectral signature extraction was performed using the training sites and components created during the PCA process. Signatures were purified and then classified using maximum-likelihood. The purification process improved overall image classification accuracy by removing outliers and other non-typical training sites. Accuracy was determined by creating an error matrix and calculating the Kappa statistic for the each classification. All rangeland health parameter models as well as a slope and soil erodibility model were then combined in a multi-criteria evaluation to produce a rangeland health model. The rangeland health model was validated in 2005 and produced overall accuracies of 62-91% when a 15pt and 25pt error margin was applied, respectively.

Keywords: rangeland health, multispectral imagery, Quickbird, Principal Component Analysis (PCA), maximum likelihood

INTRODUCTION

Rangelands occupy approximately 801 million acres in the continental United States. Healthy rangelands are important for wildlife, recreationists, ranchers, farmers, land management agencies, and many rural economies. Typically, definitions of rangeland health consist of several parameters describing evidence of soil erosion (rills, water flow patterns, gullies, and wind-scoured areas), bare ground exposure, litter amount and its movement, plant functional and structural groups, noxious and invasive plants, and soil resistance to erosion etc. (Pellant et. al 2000). Thus, rangeland health assessments are a function of several complex parameters. Indeed, rangeland health has been defined as the degree to which the integrity of the soil, vegetation, water and air as well as the ecological processes of the rangeland ecosystem are balanced and sustained (Pyke D. A. et al., 2002).

Water cycle, energy flow, and nutrient cycles are the three primary components of basic ecological processes. These processes support certain species of plants and animals within a normal range of variation. It is complicated and expensive to directly measure the site integrity and status of ecological processes due to the complexity of the processes and their interrelationships. Therefore biological and physical attributes are many times used as parameters of site integrity and functionality of the ecological processes and eventually, overall rangeland health (Pellant et. al 2000).

Various rangeland health parameters have been used in rangeland monitoring and resource inventories by land management agencies for a long time. These parameters are components of a system which are used to gauge soil or site stability, hydrologic function and the integrity of the biotic community for selected rangeland ecological sites. No single parameter of ecosystem health can address the complexity of ecological processes well. Therefore using a suite of key parameters has been suggested (Pellant et. al 2000).

Some studies have produced a number of parameters for assessing rangeland health. O'Brien (2003) and others studied rangeland health parameters (noxious weeds, ground cover, species composition and shrub cover) for evaluation of rangeland health. They also studied reliability and precision of the parameters (O'Brien et. al 2003).

This study deals with a similar suite of rangeland health parameters. GIS and remote sensing techniques were used to develop the model and perform an accuracy assessment. The result was a rangeland health index model based, initially upon bare ground exposure.

We developed the following working definition of rangeland health for this study: Healthy rangelands exhibit effective water cycles as indicated by minimal bare earth exposure and minimal evidence of soil erosion. In addition, the vegetation present will be a mixture of grasses, forbs, and shrubs that act synergistically to provide quality forage and habitat for wildlife and grazing animals. Litter will be present and biodegrading. Very little if any litter will be decomposing through oxidation.

OBJECTIVES

Several factors can influence rangeland health and may possess a complex connection among them. This study will identify the factors which can serve as rangeland health parameters. The primary objectives of the study are as follows:

- Obtain field data related to various rangeland health parameters for the study area.

- Develop a binary suitability model for each of the parameter using high resolution Quickbird satellite imagery and field data.
- Assess the accuracy of each suitability model.
- Develop a rangeland health model using all suitability models.

THE STUDY AREA:

The study area, known as the Big Desert, lies in southeastern Idaho, approximately 71 km northwest of Pocatello. The center of the study area is roughly located at 113º 4' 18.68" W and 43º 14' 27.88" N (figure 1) (Sander and Weber 2005). This area is managed by the Bureau of Land Management (BLM) and exhibits a large variety of native species as well as invasive species. The area is a sagebrush-steppe semi-desert which is bordered by geologically young lava formations to the south and west. Irrigated agricultural lands border the study area to its north, south and east. The area has a history of livestock grazing and wildfire occurrence (Weber and McMahan 2003).

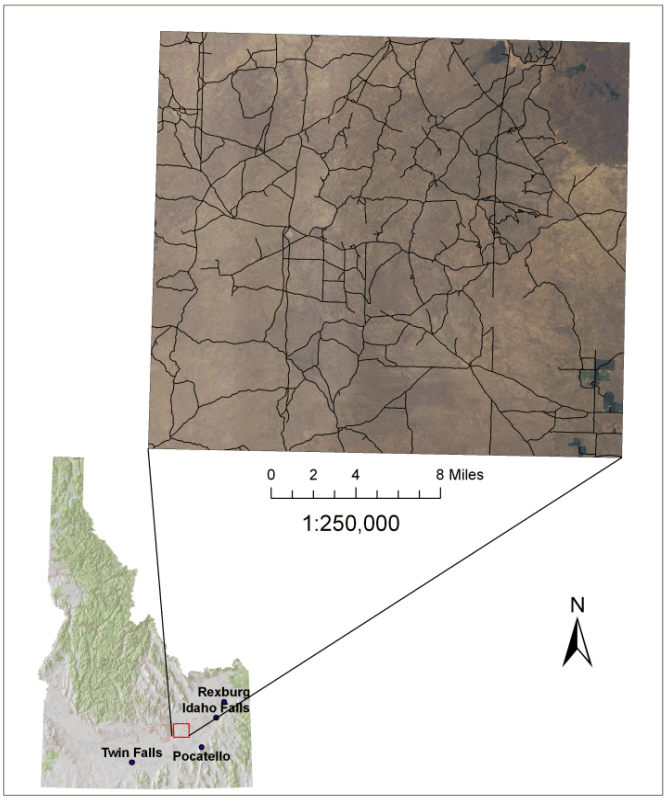

Figure 1. The Big Desert study area in southeastern Idaho.

METHODS

Rangeland health is a function of several different (and complex) factors. Based upon our working definition of rangeland health, seven parameters were selected for the study. They are as follows:

1. Invasive plants (Cheatgrass or *Bromus tectorum*) are plants which are not part of the original local ecological system. These plants tend to grow in greater abundance for the particular rangeland system (Pellant et al 2000). For this study *Bromus tectorum* which is well known as cheatgrass, was identified as the primary invasive species in the study area. This plant is a problematic invasive species for Idaho's rangelands. It can germinate in spring or fall and is known to colonize areas quickly following a fire. During most of its life cycle, cheatgrass provides poor forage for livestock. In addition, it is considered a

fire promoter as its early senescence provides great quantities of fine fuel to carry late summer wildfires (Vavra et al., 1999).

2. Bare ground is defined as exposed mineral or organic soil which is susceptible to raindrop splash erosion. It represents the entire surface that is not covered by vegetation, litter, standing dead vegetation, gravel, rocks and visible biological crust (Pellant et al 2000). Bare ground does not contribute towards healthy rangelands. Therefore, bare ground is considered a key component in our assessment of rangelands health.

3. Grass cover plays a role in energy flow and nutrient cycling. Grasses comprise a group of species with the same root and/or shoot structure, and similar photosynthetic pathways. Thus they can be treated as a single functional or structural group (Pellant et al 2000).

4. Shrub cover, similar to grasses, can also be treated as a functional or structural group. Percent shrub cover was assessed as part of the rangeland health model.

5. Litter cover was defined as any dead plant material which is in contact with the soil surface. Litter supplies essential organic material for onsite nutrient cycling. It dissipates the energy of raindrop splashes as well as overland flows thereby preventing soil erosion. (Pellant et al 2000).

6. Slope is an important factor influencing rangeland health. Higher slopes tend to result in higher runoff potential which can result in more erosion, especially if a steep slope area is coincident with bare ground. A slope of $\geq$10% would possess sufficient potential to damage rangelands especially where bare ground is present as well.

7. Erodibility is a function of bare ground, slope, and soil material. Soil cohesion is essential for healthy rangelands. Clayey soils exhibit less erodibility whereas silty soils tend to be more erodable where slope and bare ground are constant. Knowledge of these two factors was necessary to develop our rangeland health model. Therefore it was decided that both slope and soil erodibility models would be included in the final rangeland health model along with the first five parameter models described above.

It was understood that reliable bare ground detection was absolutely essential for rangeland health modeling and was treated as the main building block of our rangeland health model. The slope model was included in the model only where bare ground was present. Depending upon steepness of the slope (< 10% or $\geq$10%) shrub, grass, and litter were given appropriate weights (figure 2). In this part of the model, the rangeland health index (RH) would range from 0 to 60 (zero indicating very poor rangelands and 60 indicating moderately healthy rangelands). If bare ground was not present (indicating >50% cover by litter or live plants) then factors such as soil erodibility, shrub and grass presence were considered. Soil erodibility was not including in the previous segment as it was determined that soil material type was insignificant under high bare ground exposure. These factors along with shrub, grass, and litter were similarly assigned appropriate weights. In this part of the model the RH index would vary from 30 to 100 (where the value 100 indicates very health rangelands). Figure 2 gives all assigned weights used in this study. This model is driven by the bare ground model. The maximum rangeland health index is 100 and the minimum is 0.

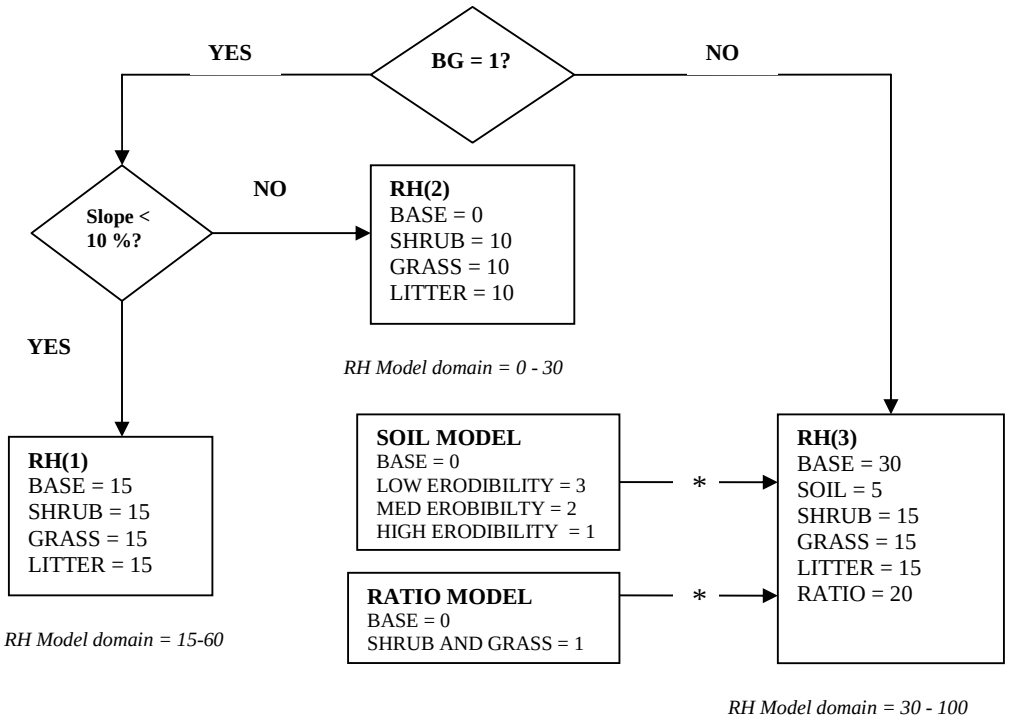

Figure 2. A flowchart illustrating the conceptual approach for the rangeland health model developed in this study.

All rangeland health parameter models except slope and soil erodibility were developed using supervised classification (an image processing technique). The soil erodibility model was readily available from the statewide soil database; STATSGO. The Slope model was developed using a digital elevation model (with 30x30m pixels) of the study area and the 'Surface Analysis' module of IDRISI software.

A total of 253 field samples were collected during 2003 for the first five models' development and 171 samples were collected in 2004 for model validation. All sample points were randomly located across the study area. A Trimble GeoXT GPS receiver (+/-1m with a 95% CI) was used to record the location of each sample point. At each sample points, data describing percent cover of grasses and shrubs, dominant weed (cheatgrass, leafy spurge etc.) and shrub species, fuel load, sagebrush age, GAP vegetation classification, presence of microbial crust, litter type, and available forage was recorded. In addition, four photographs were taken at each point. Visual estimation was used to estimate percent bare ground, litter, shrub, and grass using the following categories: 1. None, 2. 1-5%, 3. 6-15%, 4. 16-25%, 5. 26-35%, 6. 36-50%, 7. 51-75%, 8. 76-95%, and 9. >95% (Sander and Weber 2005).

Quickbird satellite imagery was used for predictive modeling of cheatgrass, bare ground, litter, grass, and shrub presence. The imagery is comprised of four multispectral bands each using 2.4 x 2.4 meter pixels. The wavelengths sensed by each band were as follows:

- *Blue: 450 to 520 nanometers*
- *Green: 520 to 600 nanometers*
- *Red: 630 to 690 nanometers*
- *Near-Infrared: 760 to 900 nanometers*

ArcGIS and IDRISI software were used to 1) convert field samples into training sites (i.e., coded for cheatgrass presence/absence), 2) calculate various vegetation indices (e.g., normalized difference vegetation index), and 3) perform image processing and classification.

The individual rangeland health parameter models based upon satellite imagery were developed using the following sequence of steps.

- Create 'training-sites' using field sample points
- Create Vegetation Indices using processed Quickbird bands
- Principal Components Analysis
- Signature Extraction
- Classification - Maximum Likelihood
- Accuracy Assessment

1. ***Training sites*** – Training sites were used to allow the image processing software to generate spectral signatures for the target of interest (i.e., cheatgrass). Each training site consists of a geographic location and sample attribute (e.g., 1=cheatgrass presence or 2=cheatgrass absence). To be considered a cheatgrass presence training site, the field sample had to contain ≥16% cheatgrass. To be considered a bare ground presence training site, the field sample has to contain ≥50% bare ground. The field sampling points (vector shapefiles) were converted into raster training sites (TIFF format) for use in IDRISI. Those pixels containing a training site were given a value (1 (presence) or 2 (absence)) where all other pixels (unknown) retained a value of zero.

2. ***Vegetation Indices-*** Various vegetation indices were calculated to better capture the vegetation characteristics of the study area and potentially improve our modeling results. These indices are relative measures of actively photosynthesizing vegetation present within each pixel (USWCL 2005). Different vegetation indices can be produced using different combinations/ratios of red and infrared bands and by including additional parameters such as slope and intercept of soil line and soil adjustment factors. Normalized Difference Vegetation Index (NDVI) is perhaps the most common, while the soil adjusted vegetation index (SAVI) also considers the reflectance of bare ground and its behavior in the red and near-infrared bands. Thus SAVI may offer a more accurate characterization of communities where bare ground is frequently encountered.

3. Eight vegetation indices were calculated for this study using the VEGINDEX module of IDRISI program. These indices were then evaluated for their relevance using Principal Components Analysis (PCA).

4. ***Principal Components Analysis (PCA) –*** In remote sensing PCA is used as a data reduction and noise removal technique. PCA produces a new set of images from a set of input images. The images of the new set are called components. The components are uncorrelated with each other and are ordered by the amount of variance described in the original input images (Eastman 2003).

   The first two or three components from a PCA typically describe nearly all the variability contained in the input imagery. Subsequent components introduce

redundancy, outliers, and noise. Therefore these components can be eliminated from further processing without losing any important data.
We performed PCA using the four bands of Quickbird imagery along with eight vegetation indices. The PCA analysis produced a set of component images. Based on these results a subset of images (describing about 97% of total variance) was selected to be used for signature extraction.

5. ***Signature Extraction***- Spectral signature is also known as spectral response pattern and the concept is very similar to the human concept of color. A spectral signature provides a description of the magnitude that light energy is reflected by the target in different regions of the electromagnetic spectrum. Thus it plays a key role in the interpretation of remotely sensed data. Figure 3 shows how light is reflected, absorbed, and transmitted from a particular object. The MAKESIG module of IDRISI was used to develop cheatgrass signatures from PCA component images.

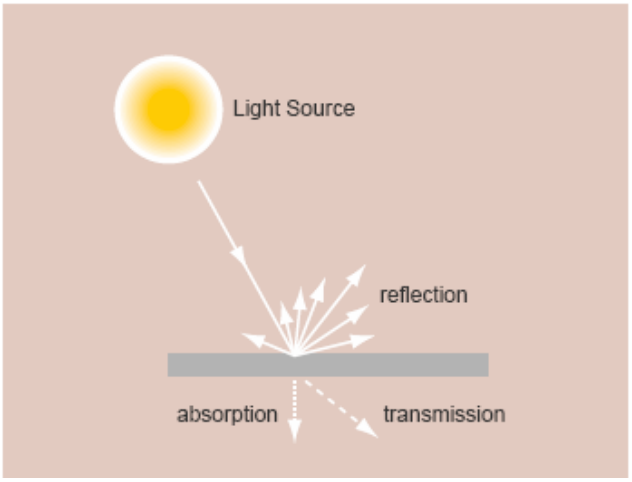

Figure 3. Light behavior of a surface (source: Eastman 2003, IDRISI Kilimanjaro Guide).

6. ***Maximum Likelihood Classification***- Maximum Likelihood Classification was used for image classification. This classification is a type of hard classifier. The hard classifier makes a definitive decision about the land cover class to which each pixel belongs (Eastman 2003).

7. The classification uses information present in the signature file to determine which class each pixel belongs to (i.e., cheatgrass presence or cheatgrass absence). Equal probability was assigned to each of the signature class. Therefore 50 percent probability was assigned to each class.

8. ***Error Assessment***- This step is also known as validation. While there are different ways to judge the accuracy of a model, we chose to use a standard contingency table (or error matrix) and the Kappa statistic. An error matrix measures the agreement between ground truth data with the developed model.

   The ERRMAT module was used for error assessment of the cheatgrass model. We calculated kappa (how much better or worse the classification performed

relative to a chance classification) (Titus et. al. 1984), overall, commission, and omission errors.

9. ***Purification-*** signature purification is sometimes necessary to achieve reliable results. The PURIFY module of IDRISI performs parametric and non-parametric purification. In parametric purification, the training pixel vector is retrieved from the images and the Mahalanobis distance to the mean of the class is calculated. The user is required to specify a typicality threshold which ranges from 0 to 1. A zero typicality threshold indicates that all the pixels will be kept in the data set while value 1 implies that nearly all pixels will be eliminated save for those equal to the mean. Based on the threshold, each pixel's typicality is evaluated (using Mahalanobis distance). A pixel with typicality value less than the threshold is dropped from the new data set (Eastman 2003). Signature purification was performed in the study and a new set of purified signatures was created and used for a second iteration maximum likelihood classification.

The purification-classification process was repeated iteratively to develop the most reliable model or until it was apparent that a reliable model was not possible. A reliable model was one having a user's accuracy of 75% or better.

RESULTS AND DISCUSSION

All models were produced following the methodology described above. Some models were improved through purification while others were not. This appears to be a function of training site variability and how much seperability existed between target and non-target signatures (Richards 1993, Lillesand and Kiefer 2000). Figure 4 show the resulting bare ground model. Figures 5 and 6 show the resulting soil erodibility and slope models, respectively.

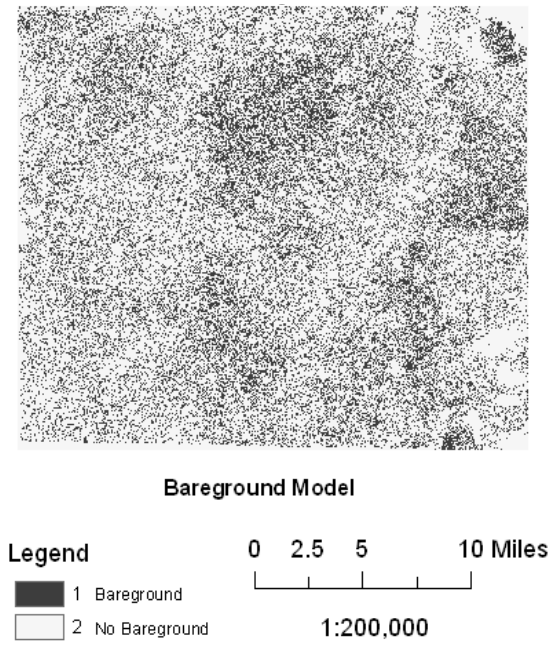

Figure 4. The resulting binary model for bare ground. Dark pixels predict ≥50% bare ground exposure.

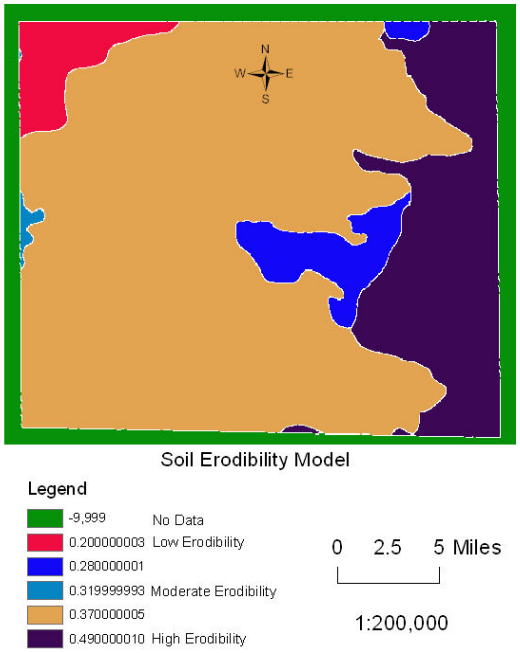

Figure 5. The resulting soil erodibility model for the Big Desert study area. The model was developed following RUSLE using STATSGO soils data.

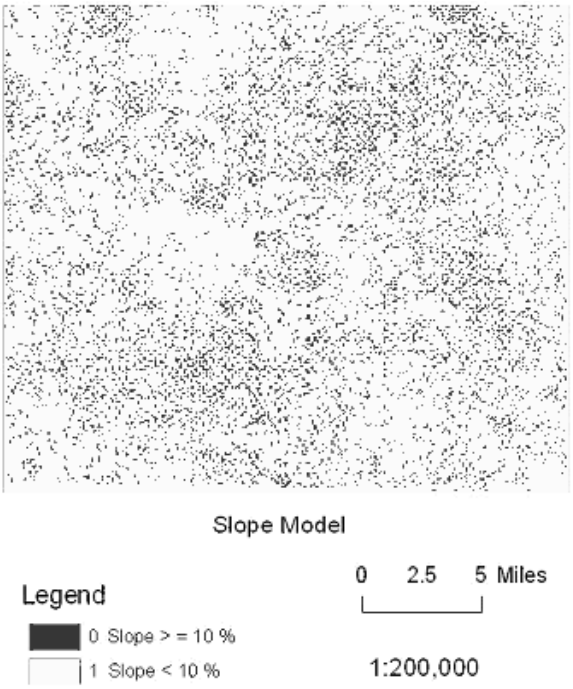

Figure 6. The resulting binary slope model generated using SRTM DEM data. Dark pixels indicate steeper slopes whereas light pixels indicate gentle slopes.

The results of model validation for bare ground, shrub, grass, litter and cheatgrass component models are given in tables 1-5.

Table 1 – Error Matrix for the bare ground model developed using purified signature

		Ground truth			
		Presence	Absence	Total	Commission
Model	Presence	28	4	32	0.12
	Absence	6	36	42	0.14
	Total	34	40	74	
	Omission	0.18	0.10		0.13

Bare ground - Overall Kappa = 0.7267

Table 2 – Error Matrix for the shrub model developed using purified signature

		Ground truth			
		Presence	Absence	Total	Commission
Model	Presence	10	3	13	0.23
	Absence	0	25	25	0.00
	Total	10	28	38	
	Omission	0.00	0.11		0.08

Shrub - Overall Kappa = 0.8143

Table 3 – Error Matrix for the grass model developed using un-purified signature

		Ground truth			
		Presence	Absence	Total	Commission
Model	Presence	18	54	72	0.75
	Absence	11	150	161	0.07
	Total	29	204	233	
	Omission	0.38	0.26		0.28

Grass - Overall Kappa = 0.2176

Table 4 – Error Matrix for the litter model developed using un-purified signature

		Ground truth			
		Presence	Absence	Total	Commission
Model	Presence	12	43	55	0.78
	Absence	2	176	178	0.01
	Total	14	219	233	
	Omission	0.14	0.20		0.19

Litter - Overall Kappa = 0.2787

Table 5 – Error Matrix for the cheatgrass model developed using un-purified signature

		Ground truth			
		Presence	Absence	Total	Commission
Model	Presence	18	55	73	0.75
	Absence	8	152	160	0.05
	Total	26	207	233	
	Omission	0.31	0.26		0.27

Cheatgrass - Overall Kappa = 0.2383

It is evident from tables 1 and 2 that the purification process worked well to improve the bare ground and shrub models. Although more than 60% of the training sites were lost during the signature purification process, the resulting models show higher overall accuracy and Kappa index (i.e. overall accuracy of 87% for the bare ground model and 92% for the shrub model with a Kappa index of agreement (KIA) of 0.7267 for the bare ground model and 0.8143 for the shrub model.

The purification process did not consistently improve either overall accuracy or Kappa indices for all models. Although purification did improve the overall accuracy of the grass, litter, and cheatgrass models (i.e. 72 %, 81% and 73 % respectively), the Kappa index for these models (KIA = 0.2176, 0.2787 and 0.2383 respectively) were very low indicating the classification was little better than a lucky random classification. Due to the patchy nature of grass, litter, and cheatgrass within the study area, purification was not advantageous. While very common, percent cheatgrass/grass cover ranged only up to 36% (with no training sites exceeded 36% cover). This means that even for cheatgrass/grass presence training sites, roughly two-thirds of each pixel was covered by non-target objects. We anticipated that by using imagery with high spatial resolution (i.e., Quickbird with 2.4x2.4m pixels) that the mixed-pixel affect would be minimized and allow for more reliable classification. Indeed, this is not the case. Further, using high-spatial resolution imagery introduced another difficulty in our processing; co-registration between imagery and training sites (Weber 2006).

Studying the cheatgrass and grass models and associated error matrices (tables 3 and 5) we see similarity in the results (i.e. overall accuracy of 72 % for grass and 73 % for cheatgrass and KIA = 0.2176 for grass and 0.2383 for cheatgrass). The obvious explanation is that cheatgrass and other grasses yield similar spectral signatures. This is an important observation, because it illustrates that even with relatively high radiometric resolution of Quickbird imagery (11bit), cheatgrass cannot be differentiated reliably from other grasses within the study area.

A primary source of error in all the models is poor co-registration (RMS = 5.20 m) between training sites locations and Quickbird imagery regardless of our attempts to eliminate this error using a ground control shapefile collected in the field. Still, the best RMS achieved was 5.20 m. When one considers the size of each pixel (2.40m) this implies a positional error of approximately two pixels. In other words, our cheatgrass training sites were likely shifted up to 2 pixels away from the actual pixel containing the target. This error propagated through the model and likely contributed to the very low accuracies in all models describing targets.

The seven individual parameter models provided the basic elements to produce a final rangeland health model. The parameter models were processed through the "Image Calculator" module of IDRISI software to produce a rangeland health model (Figure 7).

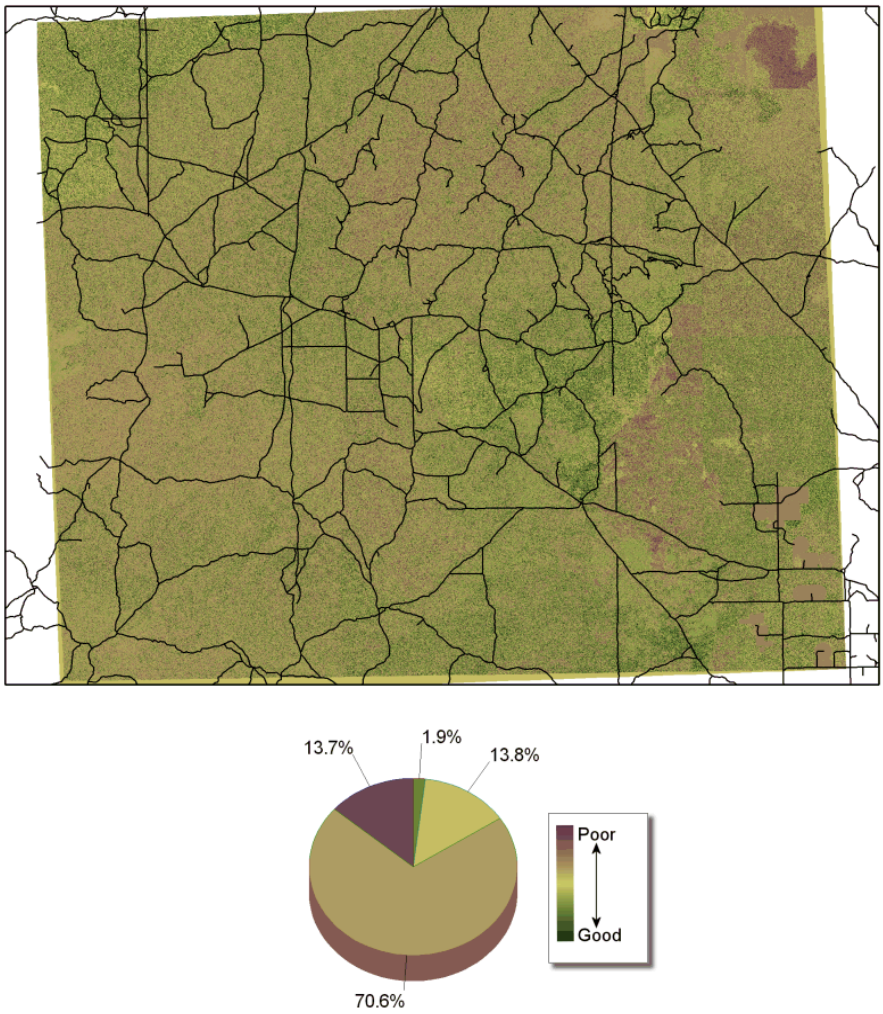

Figure 7. The rangeland health model for the Big Desert study area.

Similar to the individual parameter models, the rangeland health model was validated using rangeland health parameter values calculated from 189 field observations made during the summer of 2005. Note: for slope and soil erodibility parameters the modeled values were used since they could not be easily calculated in the field). Not surprisingly, no field observation values were exactly the same as modeled values. However, when reasonable confidence intervals were applied the rangeland health model showed much better corroboration with field observations (table 6).

Table 6. Validation of rangeland health model with 15 and 25pt error margins applied.

	Accuracy (+/- 15pts)	Accuracy (+/- 25pts)	n
RH1	75%	97%	68
RH3	55%	88%	121
Total	62%	91%	189

CONCLUSIONS

Grass, cheatgrass, and litter cannot be modeled reliably (>75% overall accuracy) using Quickbird multispectral imagery. The overall accuracy of the grass and cheatgrass models never exceeded 73%. Purification did not improve accuracy for grass, litter, and cheatgrass models. We speculate that training sites dominated (>50%) by grass/cheatgrass/litter are required to achieve reliable results. This is probably true of all target/species differentiations except in those cases where the target has a distinctive spectral signature or texture. In addition, it appears that grass and cheatgrass produced nearly identical spectral signatures which resulted in similar overall accuracy and KIA.

The bare ground and shrub models produced very high overall accuracy (approximately 87% and 92% respectively). A distinct spectral signature may be the reason for such good classification results. The purification process was used and resulted in improved overall accuracy and KIA for these models. To further improve these models will require the use of imagery that is better co-registered with field data. This can only be accomplished using numerous ground-based control points which are visible within the imagery to eliminate co-registration error and the resulting loss of accuracy propagated by this error.

While not ideal for rangeland ecosystems, the RUSLE model was used in this study to estimate soil erodibility levels. Future versions of this model will attempt to make use of soil erodibility models designed for rangelands such as the rangeland hydrology and erosion model (Moffet et al 2006).

The rangeland health index model produced fairly reliable results. To accomplish this we did not attempt to differentiate annual invasive grasses from other types of grasses and thereby improved the model through generalization. Further research is required to fully examine the potential of high-spatial resolution imagery for rangeland management and the ability of remotely sensed imagery to reliably model rangeland health along with the parameters selected in this study.

MANAGEMENT IMPLICATIONS

This model can be applied fairly easily to rangelands throughout the intermountain west. It should be understood however, that not all areas may have the potential to achieve a rangeland health index of 100. For this reason, the model and its results require careful interpretation by experienced range scientists who are familiar with the site being analyzed.

ACKNOWLEDGEMENTS

This study was made possible by a grant from the National Aeronautics and Space Administration Goddard Space Flight Center. ISU would also like to acknowledge the Idaho Delegation for their assistance in obtaining this grant.

LITERATURE CITED

Eastman, R. J., 2003. IDRISI Kilimanjaro Guide to GIS and Image Processing. Clark University Laboratory.

Lillesand T. M. and R. W. Kiefer. 2000. Remote Sensing and Image Interpretation. 4th Ed. John Wiley and Sons, New York, NY. 724pp.

Moffet, C., S. Van Vactor, and F. Pierson. 2006. Rangeland Hydrology and Erosion Model. URL = http://rhem.nwrc.ars.usda.gov/index.php visited 1-March-2006.

O'Brien R.A., Johnson C.M., Wilson A. M. and Elsbernd V. C., Indicators of Rangeland Health in the Intermountain West, June 2003.

Pellant M., Pyke D.A., Shaver P. and Herrick J. E., Interpreting Indicators of Rangeland Health – Version 3, Technical reference 1734-6, 2000

Richards, J.A., 1993. Remote Sensing Digital Image Analysis, Springer-Verlag, New York, NY. 363 pp.

Sander L. and K. T. Weber. 2005. Range Vegetation Assessment in the Big Desert, Upper Snake River Plain, Idaho, GIS Training and Research Center. URL = http://giscenter.isu.edu. Visited 1-March-2006.

Titus, K., J. A. Mosher, and B. K. Williams. 1984. Chance-corrected classification for use in discriminant analysis: ecological applications. Am. Midl. Nat. 111:1-7.

USWCL 2005. How a vegetation index works. URL=http://www.uswcl.ars.ag.gov/epd/remsen/Vi/VIworks.htm, visited 19-July-2005.

Vavra M., W. A. Laycock, and R. D. Pieper. 1999. Ecological Implications of Livestock Herbivory in the West, Society of Range Management.

Weber, K. T. 2006. Challenges of Integrating Geospatial Technologies into Rangeland Research and Management. REM 59(1):38-43.

Weber K. T. and B. J. McMahan. 2003. Field Collection of Fuel Load and Vegetation Characteristics Wildfire Risk Assessment Modeling: 2002 Field Sampling Report. URL = http://giscenter.isu.edu/Research/techpg/nasa_wildfire/Final_Report/Documents/Chapter2.pdf

Mapping Sagebrush Distribution Using Fusion of Hyperspectral and LiDAR Classifications

Jacob T. Mundt, Department of Geosciences, Boise Center Aerospace Laboratory, Idaho State University, 322 E. Front Street, Suite 240, Boise, ID 83702 (mundjaco@isu.edu)

David R. Streutker, Department of Geosciences, Boise Center Aerospace Laboratory, Idaho State University, 322 E. Front Street, Suite 240, Boise, ID 83702 (stredavi@isu.edu)

Nancy F. Glenn, Department of Geosciences, Boise Center Aerospace Laboratory, Idaho State University, 322 E. Front Street, Suite 240, Boise, ID 83702 (glennanc@isu.edu)

ABSTRACT
The applicability of high spatial resolution hyperspectral data and small-footprint Light Detection and Ranging (lidar) data to map and describe sagebrush in a semi-arid shrub steppe rangeland is demonstrated. Hyperspectral processing utilized a spectral subset (605 nm to 984 nm) of the reflectance data to classify sagebrush presence to an overall accuracy of 74 percent. With the inclusion of co-registered lidar data, this accuracy increased to 89 percent. Furthermore, lidar data were utilized to generate stand specific descriptive information in areas of sagebrush presence and sagebrush absence. The methods and results of this study lay the framework for utilizing co-registered hyperspectral and lidar data to describe semi-arid shrubs in greater detail than would be feasible using either dataset independently or by most ground based surveys.

Keywords: remote sensing, shrubs, rangelands

INTRODUCTION

Wyoming big sagebrush *(Artemisia tridentata Spp. wyomingensis)* is an important rangeland shrub associated with the Intermountain West shrub steppe environment. Many vertebrate species utilize habitats within sagebrush to maintain viable populations (e.g., pygmy rabbit *(Brachylagus idahoensis)*, sage grouse *(Centrocercus urophasianus)*, and sharp-tailed grouse *(Tympanuchus phasianellus)*). As sagebrush communities in the Intermountain West become increasingly fragmented due to agricultural and urban growth, range fires, and invasive weeds, critical habitats and historic grazing/browsing regimes become threatened (NPCC, 2004). Thus, land managers and conservation agencies need accurate tools to inventory and assess these semiarid shrubs. This study combines the strengths of passive, high spatial resolution, hyperspectral reflectance imagery and active, small-footprint Light Detection and Ranging (lidar) pulse data to assess sagebrush distribution and stand structure information, exceeding the mapping ability of either dataset alone.

The study area for this project covers nine square kilometers within the Idaho National Engineering and Environmental Laboratory (INEEL) in southeastern Idaho (Figure 1). The vegetative composition of the sagebrush ecosystem in the study area commonly includes Wyoming big sagebrush, green rabbitbrush *(Chrysothamnus viscidiflorus)*, Russian thistle *(Salsola kali)*, and winterfat *(Ceratoides lanata)*. Associated native grasses include thick-spiked wheatgrass *(Elymus lanceolatus)*, bottlebrush squirreltail *(Elymus elymoides)*, Indian ricegrass *(Oryzopsis hymenoides)*, needle-and-thread grass *(Stipa comata)*, and Nevada bluegrass *(Poa secunda)* (ESER, 2004).

Two large fires burned across separate regions of the study area, the first in 1974 and the second in 2000. Wildfires are naturally occurring disturbances in semi-arid rangelands, and it may take decades for sagebrush to re-establish a viable population following a disturbance (Colket, 2003). Thus, in the burned areas, sagebrush is dominantly absent, having been replaced by increased populations of green rabbitbrush, cheatgrass *(Bromus tectorum)*, native grasses, and Russian thistle. Additionally, land managers have seeded some burned areas with crested wheatgrass *(Agropyron desertorum)* in an attempt to increase botanical diversity.

PREVIOUS WORK

Remote sensing techniques have the unique ability to capture a spatial and temporal snapshot of an ecosystem that can feasibly be used to establish geographic context and perform spatial interrogation of ecological health and inventory (Patil and Myerst, 1999). Remotely sensed data also have the potential to provide large-scale information on vegetation in semi-arid and arid rangelands (Tueller, 1987). Multispectral sensors have been used for more than 30 years to characterize vegetation across the globe, while hyperspectral instruments came into widespread use in the 1990s. Warren and Hutchison (1984) document the utility of remote sensing for holistic change detection in shrub/grass rangeland. Other studies have demonstrated success at mapping ecological resources in semiarid systems using high spectral resolution data (e.g., Elmore *et al*., 2000; Lewis *et al*., 2000; Okin *et al*., 1999), and the use of multiple or fractional end-members has been shown to increase classification confidence in semi-arid environments (e.g., Roberts *et al*., 1998). Okin *et al*. (2001), however, encountered complications in discrimination of spectrally indeterminate arid shrubs using high spectral resolution field data. Significant soil exposure and an increased level of non-linear spectral mixing in semi-arid environments likely influenced these complications (Huete and Jackson, 1988; Huete *et al*., 1985; Musick, 1984; Ray and Murray, 1998).

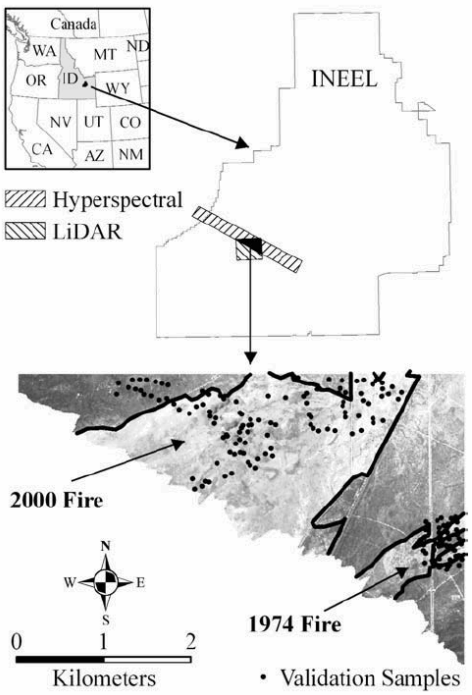

Figure 1. Location of the study area within the Idaho National Engineering and Environmental Laboratory (INEEL). In the hyperspectral image of the study area, dark lines bound the burned areas and points represent field validation sites.

While lidar is newer technology than passive reflectance remote sensing, recent studies have demonstrated the applicability of small (1 m or less) and large (10 m to 25 m) footprint lidar data to precisely characterize forest canopies. Waveform returns from large-footprint lidar sensors such as the Scanning Lidar Imager of Canopies by Echo Recovery (SLICER) and Laser Vegetation Imaging Sensor (LVIS) have successfully been used to measure variables such as tree height, canopy structure, leaf area index (LAI), and biomass (e.g., Drake *et al*., 2002; Harding *et al*., 2001; Hofton *et al*., 2002). Similarly, small-footprint lidar has been used to determine tree height and LAI in various forest types (e.g., Drake *et al*., 2002; Popescu *et al*., 2002; Riaño *et al*., 2004).

Relative to the number of forestry studies, little work has addressed lidar applications in rangeland ecosystems. Height profiles created by non-scanning lidar sensors have been used to measure plant height and canopy cover in a rangeland environment (Weltz *et al*., 1994) and to model rangeland surface roughness (Ritchie *et al*., 1995). Other studies have demonstrated the applicability of scanning lidar combined with multispectral video imagery to map shrub coppice dunes in desert grasslands (Rango *et al*., 2000).

Hyperspectral and lidar data have fundamentally different characteristics. Lidar data are irregularly spaced monochromatic near-infrared laser pulses (postings) emitted by and reflected back to the sensor. The postings are distributed in a pseudorandom fashion and are thus assumed to statistically represent the terrain characteristics. Conversely, hyperspectral data are intensity values of radiation reflected from a contiguously recorded surface across a broad range of narrow electromagnetic bandwidths. Though these differences imply complications for data fusion, some recent work has quantitatively related lidar and reflectance datasets. Popescu and Wynne (2004) used multispectral imagery to distinguish between deciduous and pine trees, thereby enhancing lidar-dependent tree height models. Additionally, Hudak *et al*. (2002) successfully fused Landsat

ETM imagery with lidar to improve tree height calculation. Lee and Shan (2003) combined lidar with multispectral Ikonos imagery to improve upon supervised classification accuracies in a coastal environment, and Blackburn (2002) used lidar to mask tree gaps while using hyperspectral Compact Airborne Spectrographic Imager (CASI) data to estimate photosynthetic pigments in forest plantations.

METHODS

DATA COLLECTION

This study fuses hyperspectral data collected in July 2002 with lidar data collected approximately two months later. The hyperspectral data were acquired by the HyVista Corporation of North Ryde, New South Wales, Australia. The dataset has a spatial resolution of 4.6 m 4.6 m and contains 126 spectral bands between 450 *n*m and 2,500 *n*m, with spectral bandwidths of approximately 10 *n*m in the visible and near-infrared and 20 *n*m in the short-wave infrared. The lidar data were collected by the Airborne 1 Corporation of El Segundo, California using a 25 KHz scanning pulsed laser at a wavelength of 1,067 *n*m. The dataset contains 13.3 million postings within the study area (approximately 1.2 postings per square meter) where each lidar posting has a diameter of approximately 25 cm. Two returns (first and last) were recorded for each posting, and each return included a time stamp, the *X*, *Y*, and *Z* coordinates, and an intensity value.

A field survey in the summer of 2004 collected 157 differentially corrected Global Positioning System (GPS) validation samples within the study area (Figure 1). Each validation sample was acquired as a point location, attributed by fractional coverage of sagebrush, grass, rabbitbrush, and bare ground (oblique field estimates) to a search radius of approximately 15 m. In addition to the point data samples, GPS polygon samples and line features were also collected around geographically distinctive features in the study area (e.g., rock outcrops, sand dunes, and roads) to assist in the assessment of image registration errors.

Although there was a two-year period between image acquisition and field data collection, we assume negligible changes in the sagebrush ecosystem. Independent test plot measurements of mature sagebrush canopy indicate a variation in cover between 5 percent and 10 percent over two-year intervals (Inouye, personal communication, 2004). Additionally, the study area is neither heavily grazed nor public land, and no major range fires or other disturbances occurred in the area between the time of data collection and the time the validation was performed.

HYPERSPECTRAL PROCESSING

The hyperspectral data were atmospherically corrected by the vendor using the MODTRAN4 radiative transfer code (Berk *et al*., 1999). Exploratory data evaluation identified an inconsistency in cross-track illumination, which was rectified using a multiplicative correction algorithm built into the Environment for Visualizing Images (ENVI) software (RSI, 2004). Further evaluation revealed generally higher reflectance in the visible wavelengths within the fire scars as compared to areas of mature sagebrush. We hypothesized that these differences were the result of variation in vegetative composition and increased soil exposure. Preliminary unsupervised classifications, performed to explore the spectral variability within the data, determined that areas of sagebrush on the west side of the study area were spectrally distinct from areas of sagebrush on the east side. This artifact was correlated to a change in soil composition, with the east portion of the study area typified by thick floodplain sediments and the west portion by aeolian sands overlying basalt.

Hyperspectral data were classified utilizing the Mixture Tuned Matched Filtering (MTMF) algorithm. MTMF is a partial unmixing algorithm that combines the strengths of linear spectral

unmixing and statistical matched filtering to produce a Matched Filter (MF) score (estimate of target abundance) and a measure of infeasibility (Boardman, 1998).

MTMF classifications utilizing the full spectral range of the hyperspectral dataset overestimated sagebrush presence within the burn scars. Comparison of spectral profiles derived from areas of both sagebrush presence and sagebrush absence illustrated strong similarities across the spectral range of the dataset (Figure 2). In the visible and near-infrared, however, the profiles deviate slightly. Accordingly, the data were reprocessed using only the spectral range from 605 *n*m to 984 *n*m (27 spectral bands), and the resulting classification generated a qualitatively improved representation of sagebrush distribution.

MTMF classification requires the input of spectral training endmembers. While the objective of this study is to map the distribution of sagebrush, it is notable that there is a certain amount of heterogeneity within a sagebrush stand (e.g., dead brush, rabbitbrush, grasses, and soil exposure may vary locally) (Huete and Jackson, 1988). In this study, areas referred to as *sagebrush* are realistically only partially *Artemisia tridentata*, and it is assumed that no sagebrush stand will be an *Artemisia tridentata* monoculture. Thus, from an ecological perspective, it is important to consider any vegetative compositional variance within the sagebrush ecosystem when mapping. To model this variance, training areas were input in block (polygon) form (Chen and Stow, 2002). Iterative data classification demonstrated that a single sagebrush endmember (derived from an area of sand overlying basalt soils) effectively mapped sagebrush locally, but was not effective across the entire study area. We hypothesized that this anomaly was dominantly due to variability in underlying soil texture and composition. The addition of a second block endmember derived from an area of sagebrush underlain by floodplain sediments also performed well locally, and visually complemented the first endmember classification.

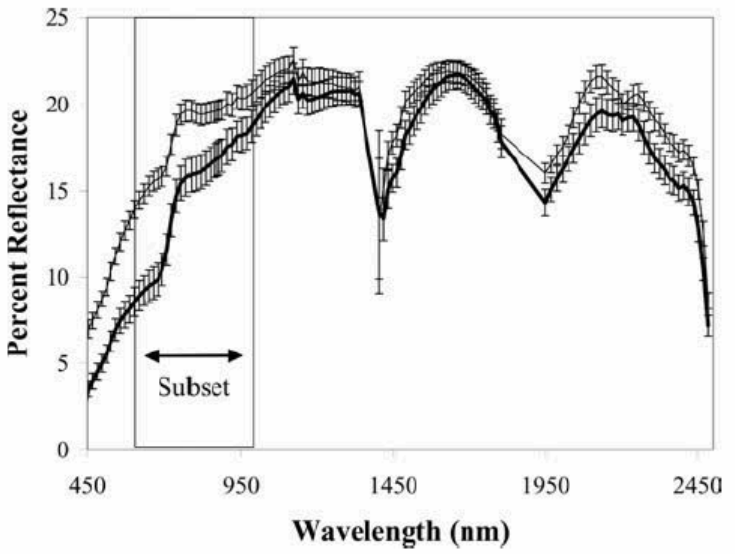

Figure 2. Spectral profiles derived from burned (upper spectra, 22 sample mean) and unburned (lower spectra, 18 sample mean) areas. Typical burned areas lack any sagebrush, while the unburned areas had relatively high percent sagebrush cover. The spectral range used for the final hyperspectral analysis is noted.

As MTMF is a linear operator with MF scores representing sub-pixel target abundance, the two endmember classifications, in the form of MF values, were arithmetically summed to derive a composite sub-pixel abundance of the target. An arithmetic average of the two bands of infeasibility was calculated and combined with the summed MF scores, generating a composite

MTMF classification. This composite classification represented both sagebrush endmembers, and more appropriately estimated sagebrush abundance across the entire study area.

LIDAR PROCESSING

The lidar data over the study area were collected in 22 separate flight lines, each approximately 300 m wide. The vendor performed a GPS validation survey to constrain the absolute accuracy of the lidar coordinates to approximately 1 m in the horizontal direction and 25 cm in the vertical direction (two-sigma; Flood, 2004). A similar accuracy was determined in the study area using assessment methods modeled after Latypov (2002) which calculated the error between individual flight lines in areas of overlap.

Relative error within individual flight lines was considerably lower, approximately 10 cm in the horizontal direction and 5 cm in the vertical direction. Relative errors of this size can be expected when using a properly calibrated lidar sensor under normal operating conditions (Airborne 1, 2001). After using the time stamp of each posting to separate the data into individual flight lines, the relative vertical error within each flight line was estimated by calculating the standard deviation of the heights of points collected over a flat surface. The roofs of three structures and the surfaces of two cooling ponds, each spanning at least 75 m^2 and assumed to be topographically invariant, were used in this analysis. The horizontal accuracy of the lidar points was determined using a similar methodology applied to five different vertical walls of multi-story buildings, each of which is at least 5 m wide. Coordinates of lidar posts reflected from the walls were extracted and fit to a flat vertical plane, and the relative horizontal accuracy was estimated as the standard deviation of the points about this plane. In order to preserve the highest possible relative accuracy, subsequent processing considered all flight lines individually.

As the study area is relatively devoid of major topographic features and semi-arid rangeland canopies are fairly open, the first return lidar data were used to characterize both the terrain and the vegetative canopy. Using a single lidar dataset instead of attempting to merge the first and last pulse datasets (each of which contain over ten million points within the study area) kept the overall processing requirements to a minimum and avoided the introduction of problems associated with detecting multiple returns at a similar height (Hodgson *et al*., 2003).

Individual lidar postings were grouped into 5 m 5 m cells, where the lowest point in each cell was assumed to represent the ground surface. Using these ground points, an initial ground surface was interpolated across the study area using a thin plate spline (Meinguet, 1979). Heights above this surface were calculated for the remaining data points, and resulting values of zero or less were reclassified as ground points. The ground surface was re-interpolated iteratively until all lidar points were classified as either ground or non-ground (99 percent of the points converged after two iterations). Of all lidar points, 21 percent were classified as ground, and the remaining 79 percent were classified as non-ground. All resulting ground points were used to interpolate a final ground surface, and above-ground height values were calculated for all remaining (non-ground) points. The final height points were combined from all individual flight lines into a single dataset, and were subsequently grouped into 4.6 m cells (the same spatial resolution as the hyperspectral data). Surface roughness values were derived for each cell by computing the standard deviation of all height values, which generated a surface roughness raster matching the spatial resolution of the hyperspectral data (Figure 3).

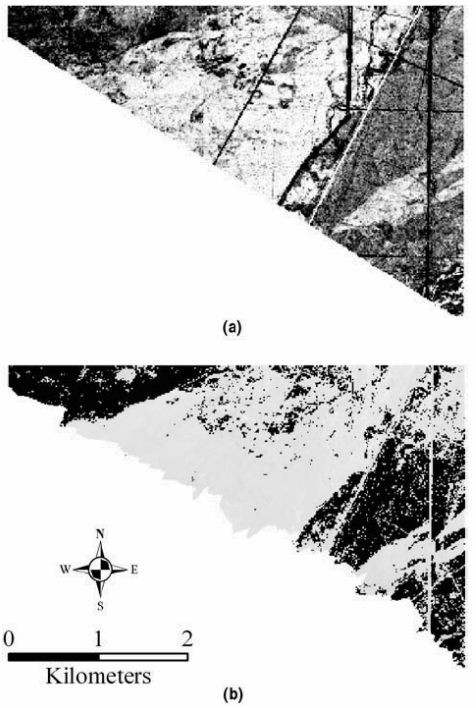

Figure 3. Map of surface roughness within the study area (a), and a final MTMF sagebrush presence distribution map (b). Surface roughness ranges from 0 cm (white regions) to over 300 cm (dark regions).

In addition to surface roughness, lidar data were used to calculate several variables describing the physical properties of all vegetation in the study area. The mean height of each pixel was calculated as the average of all heights within the pixel, including the ground postings, while the mean vegetation height was calculated as the average height of only the non-ground postings. The highest single posting in each pixel was recorded (tallest vegetation) as was the fraction of lidar postings within each pixel that were classified as bare ground.

CO-REGISTRATION

Co-registration is the process of assigning exactly the same spatial context to two raster geographic datasets such that when overlain, pixels correspond to exactly the same geographic location. Previous work demonstrated that small differences in co-registration can lead to large errors, and that for quantitative analysis in semi-arid environments, co-registration must be accurate to between 0.5 and 1 pixel (Townshend, 1992).

Lidar intensity data were interpolated into a raster with the same spatial resolution as the hyperspectral reflectance data (4.6 m). The hyperspectral band 43 (1,062 *n*m) corresponded most closely with the wavelength of the lidar laser (1,067 *n*m). This band was overlaid with both the interpolated lidar intensity data and five differentially corrected GPS ground control points. The lidar data were internally consistent and representative of GPS features (e.g., roads discernable in the image were straight and correctly positioned as compared to the GPS centerlines), and demonstrated less than one pixel error with respect to the GPS ground control points. The hyperspectral data expressed an image shift from the lidar dataset that averaged approximately 20 m between GPS ground control points and image projected locations. A first-order polynomial transform was applied to the hyperspectral dataset using sixteen image-derived ground control points discernable in both datasets (lidar intensity data used as the base image). Following the

transform, agreement between the lidar and hyperspectral images was within one pixel at the GPS ground control points.

Away from the GPS ground control points, the hyper-spectral image displayed geometric anomalies with a local shift between one and three pixels (compared to the lidar image). The lower geometric accuracy of the hyperspectral data is likely due to turbulent atmospheric conditions during data collection. Further, lidar geocorrection routines utilize differentially corrected GPS transects and real-time communication with mobile base stations for enhanced accuracy. Nine image control points were used to calculate a mean residual geometric error of 11.5 m (standard deviation of 3 m) between lidar and hyperspectral equivalent locations. Because these anomalies were small scale and randomly distributed across the study area, both datasets were re-sampled to three hyperspectral pixels (13.8 m). The hyperspectral data were re-sampled using a pixel aggregate function, while lidar point height data were interpolated to an equivalent raster resolution. The resulting datasets did not have quantifiable geometric errors with respect to each other or to any of the GPS ground control data.

Due to the possibility of uncertainties being generated and propagated by repeatedly projecting and re-sampling data as necessary for co-registration, both the hyperspectral and lidar data were processed in raw (reflectance and point, respectively) format. The analysis products were then geometrically transformed with the intent of preserving the integrity of the raw data while minimizing processing requirements.

CLASSIFICATION AND FUSION

Hyperspectral MTMF classification products were evaluated using scatterplots of MF versus infeasibility values. Pixels with MF values greater than zero and infeasibility values less than seven were considered to contain sagebrush. Classification accuracies for sagebrush presence and absence were calculated using error matrices and methods according to Congalton and Green (1999). Because field validation surveys (15 m diameter plots) were collected at approximately the same spatial scale as the resolution of the re-sampled and co-registered imagery (13.8 m pixels), validation plots were buffered by 0.5 pixels (6.9 m) to ensure that representative accuracies were determined. MF scores were extracted for the true positive field validation plots (field observed sagebrush coinciding with image classified sagebrush) as estimates of sub-pixel sagebrush components. Where multiple image pixels occurred within a single plot, the average value of all corresponding MF scores was used. The extracted MF values were correlated to field estimated sagebrush cover for each validation plot to evaluate the ability of MTMF to predict sub-pixel abundances of sagebrush. Positive MF values were rescaled to range between zero and one (representing 0 to 100 percent cover).

Lidar roughness values were extracted for all field validation plots and were considered on a pixel-by-pixel basis. Separate distributions were drawn for sagebrush presence and sagebrush absence validation plots, and were compared using significance testing. The distribution of roughness values for sagebrush presence and absence plots overlap, yet are found to be statistically distinguishable according to an F-test for sample variances (Table 1).

Table 1. The statistical properties of the lidar-derived surface roughness values corresponding to the sagebrush present and sagebrush absent field validation sites

Lidar Roughness	Sagebrush Absent	Sagebrush Present
Mean (cm)	7.0	9.1
Median (cm)	5.8	8.1
Integer Mode (cm)	5	8
Standard Deviation (cm)	4.5	3.6
Number of Samples	88	64

F Statistic 1.57.
F_{Crit} (α = 95%) 1.48.

Roughness values representing sagebrush were determined iteratively. The lowest roughness values were associated with smooth surfaces (e.g., paved roads or short grass), while the highest roughness values represented tall anthropogenic features (e.g., power poles). An upper roughness threshold of 75 cm (approximately 18 standard deviations above the mean: Table 1) was determined appropriate for removing most tall anthropogenic features. When plotted against MF values, roughness values generate two distinct groupings, one with slightly lower mean and lower MF values (correlated to sagebrush absence) and the other with a slightly higher mean and higher MF values (correlated to sagebrush presence: Figure 4). The lower roughness threshold was incrementally adjusted and accuracies calculated at each increment, and an optimal lower roughness value of 6.5 cm was determined.

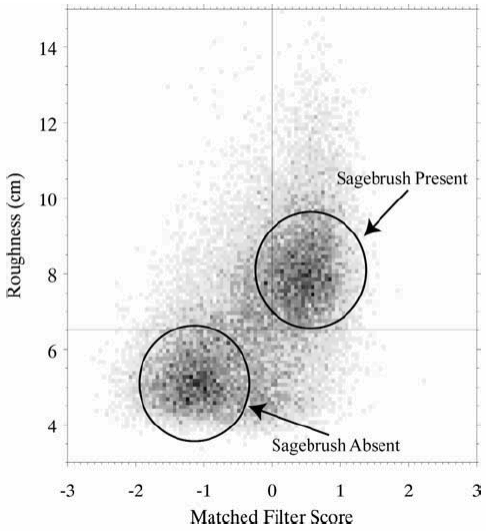

Figure 4. Scatterplot of Matched Filter (MF) score versus surface roughness for the entire study area, illustrating the relationship between areas of sagebrush presence (higher MF and higher roughness) and sagebrush absence (lower MF and lower roughness). Lines represent the roughness threshold of 6.5 cm and the MF threshold of zero that were used to generate sagebrush classifications.

Because both MF scores and lidar roughness were correlated to sagebrush presence (Table 1; Figure 4), sagebrush was re-classified using a minimum MF value of zero, a maximum infeasibility value of seven, and roughness values between 6.5 cm and 75 cm. Image re-classification using fused hyperspectral and lidar variables resulted in a more accurate and detailed sagebrush distribution map for the study area. The sagebrush classification was then augmented by the vegetative structure information derived using the lidar data. Population statistics for each of the previously derived lidar variables (roughness, mean height, mean

vegetation height, tallest vegetation, and percent bare ground) were tabulated for all pixels classified as either sagebrush present or sagebrush absent (Table 2; Figure 5). As in image classification, areas with very high surface roughness (greater than 75 cm) were eliminated from this analysis.

Table 2. The mean, median, variance, and f-value (95% confidence level) of lidar height products for sagebrush present and sagebrush absent image classified areas of the entire study area. These values were calculated using 15,273 pixels from areas classified as sagebrush present and 28,601 pixels from areas classified as sagebrush absent. Values are presented as sagebrush "not present/present"

Lidar Variable	Mean	Median	Standard Deviation	F-Statistic (F_{crit} = 1.02)
Mean Pixel Height (cm)	7.8/9.6	7.1/9.2	3.5/2.8	1.52
Mean Vegetation Height (cm)	10.0/11.9	9.0/11.3	4.2/3.2	1.72
Percent Bare Soil	7.0/19.4	6.0/18.2	4.5/4.3	2.50
Roughness (cm)	6.8/9.2	5.9/8.5	3.8/3.5	1.17
Tallest Vegetation (cm)	34.1/53.2	30.0/51.0	15.2/16.4	1.17

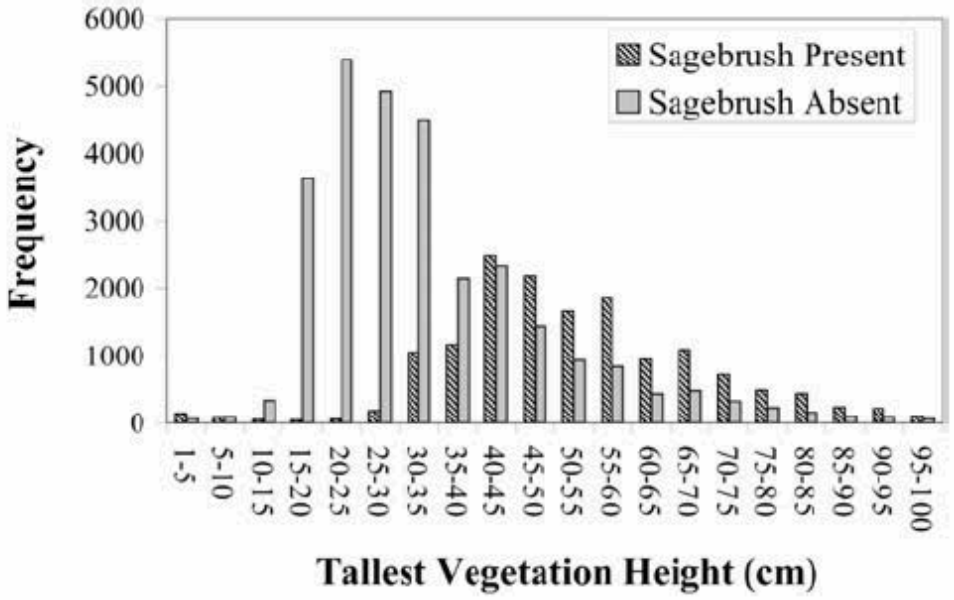

Figure 5. Histograms of lidar-derived tallest vegetation heights for both the sagebrush present (higher mean) and sagebrush absent (lower mean) classified areas.

RESULTS

All classification accuracies are summarized in Table 3. Sagebrush was successfully mapped from hyperspectral imagery using MTMF, resulting in producer's, user's, and overall accuracies of 91 percent, 64 percent, and 75 percent, respectively, with no infeasibility constraint. The inclusion of a maximum infeasibility threshold of seven resulted in producer's, user's, and overall accuracies of 72 percent, 75 percent, and 74 percent, respectively. Subsequent attempts at lowering the infeasibility threshold generated unacceptable producer's accuracies. Fusion of lidar roughness values as a third variable in sagebrush classification increased producer's, user's, and

overall accuracies to 84 percent (12 percent increase), 92 percent (17 percent increase), and 89 percent (15 percent increase), respectively. However, no significant correlation (R^2 0.02) was found between field estimates of sagebrush canopy cover and MF scores.

Table 3. Accuracy assessment results for multiple sagebrush classification strategies are investigated. Accuracies were calculated using 88 validation polygons with sagebrush presence and 152 polygons with sagebrush absence.

Classification Strategy	Producer's Accuracy	User's Accuracy	Overall Accuracy
MF greater than 0	91%	64%	75%
MF greater than 0 AND Infeasibility less than 7	72%	75%	74%
MF greater than 0 AND Roughness between 6.5 and 75 cm	88%	86%	87%
MF greater than 0 AND Infeasibility less than 7 AND Roughness between 6.5 and 75 cm	84%	92%	89%

With relatively good constraint on sagebrush distribution, vegetative structure information derived from lidar data was cross-tabulated against the final classification of sagebrush presence and absence. All tested populations were found to be significantly distinguishable according to an F-test for sample variances (95 percent confidence: Table 2). Overall, pixels with sagebrush present had significantly greater mean heights, mean vegetation heights, roughness, and percent bare ground than did pixels with no sagebrush present. The maximum vegetation height for areas of sagebrush presence was also significantly greater in general than in areas of sagebrush absence. Further, histograms of tallest vegetation height clearly indicate that areas with sagebrush have higher population means and medians than do areas with no sagebrush (Figure 5).

DISCUSSION

Hyperspectral classification utilizing the full electromagnetic range of the data resulted in highly confused classifications of the distribution of sagebrush in a semi-arid rangeland. This corresponds with results published by Okin *et al*. (2001) in that semi-arid partial-cover canopies with bright soil backgrounds are difficult to discriminate. The separation of sagebrush from background vegetation was optimized based on empirical evaluations of the spectral relationships shown in Figure 2, which substantially increased the quality of the sagebrush classification. We hypothesize that spectrally subsetting the data removed a significant portion of soil-dominated reflectance ranges confusing the classifications. Further, the use of multiple target endmembers increased classification accuracy in this study. It is notable that in large areas where holistic variability becomes difficult to model, the inclusion of all necessary endmembers may be difficult. These results indicate that future studies in areas of low variability or highly constrained parameters can produce useful results (e.g., indicator plots or key ecologic zones), though this methodology would be difficult over large and diverse areas.

MTMF classification did not discern representative sub-pixel abundances of sagebrush. While it is likely that some degree of error in sagebrush percent cover estimation confused the relationship between the MF score and the actual sub-pixel component, we infer that there are additional complications. For example, MTMF calculates the image mean as spectral background, which is expected to be distinct from the target (Mundt *et al*., in review). In this study, the target is a large

component of the dataset, and it is possible that some of the target spectral properties were interpreted as background, confusing the classification. This limitation is demonstrated in Figure 4, where the cluster of sagebrush present pixels crosses into negative MF space. While MTMF may not be the best approach to sub-pixel component estimation in this scenario, it still visually outperformed Linear Spectral Unmixing and Spectral Angle Mapping in iterative sagebrush presence and absence classifications.

This study used a simple sum of individual classification MF values to represent the composite sagebrush abundance (MF) distribution. Combination of linear unmixing endmembers in this context is not well documented, and we hypothesize that alternative approaches may also be effective (e.g., non-linear or weighted combinations). The summation of MF variables in this study is justified as we were able to generate a distribution map in which we have high confidence (Figure 3). Further, other empirical combinations of MF and infeasibility classifications (e.g., using geometric instead of arithmetic means) did not produce significantly different products.

While no correlation was found between MF scores and field estimates of sagebrush canopy cover, pixels with sagebrush presence generally had higher MF scores than pixels with sagebrush absence (Figure 4). Further, in most areas of sagebrush presence, field validation estimated 30 percent cover, which is near the mean (as well as the median and mode) of the rescaled MF distribution (Table 2). In light of this, we hypothesize that the MF scores may potentially be useful, though they are likely confused by high degrees of mixing in an indeterminate spectral endmember (Okin *et al*., 2001).

Lidar data significantly improved hyperspectral classifications and added useful stand structure information in a semi-arid rangeland. Though typical rangeland vegetation heights are of the same order as the absolute vertical accuracy of small-footprint lidar scanners (Table 2), it is possible to measure such heights if attention is paid to preserving the high relative accuracy throughout the processing. In this study, high vertical accuracy was maintained by processing the lidar data in individual flight lines and as raw, irregularly spaced posting data. This allowed for the measurement of heights as small as 5 cm and for the production of height and roughness maps which effectively describe a large number of geographic features in addition to sagebrush presence, including roads, railroads, power lines, drainage canals, and fences. It is further notable that most sagebrush in the study area was significantly taller than the vertical precision of the lidar data (Figure 5).

Co-registration of high spatial resolution data is processing and time intensive, yet provides a significantly more useful product than either of the parent models for discrimination and description of sagebrush. Fusion of classification products increased overall accuracies by 14 percent over standard hyperspectral processing. We assert that the fundamental differences between the two sensors adds significantly to the potential discrimination of semi-arid shrubs as long as the vegetative ecosystems are relatively static or the datasets are acquired in rapid succession. The increase in accuracy resulting from data fusion may justify the added processing time and cost in areas where precision monitoring is necessary or key environmental indicators are present.

One of the major limitations of the co-registration process is the requirement to re-sample both datasets to a lower spatial resolution to accommodate geometric error. Although the hyperspectral imagery in this study was re-sampled to one-third of its acquired spatial resolution, it still maintained higher spatial resolution than high altitude Airborne Visible Infrared Spectrometer (AVIRIS) instrument, which has had documented success in the context of

vegetation discrimination (Merenyi *et al*., 2000). The lidar data were spatially re-sampled to a small fraction of their original resolution, yet were significantly useful in this study. Furthermore, because lidar data are geometrically precise, invaluable ecological descriptions for high-resolu-tion inventory and monitoring can be derived from the lidar data at a finer spatial scale than classifications from hyper-spectral data.

General field observations of sagebrush in the study area found a mean height of approximately 50 cm and a maximum height of approximately 1 m, while vegetation in areas of sagebrush absence was most commonly shorter than 50 cm (with rabbitbrush often reaching heights of approximately 30 cm). These field relationships are supported by the derived lidar products (Figure 5). Analyses using lidar-derived variables such as this have implications for high-resolution habitat monitoring, biomass/fuel load calculations, and numerous other objectives that may not be efficiently interpreted by field survey crews.

CONCLUSIONS

This study introduces the utility of hyperspectral data for mapping sagebrush communities, demonstrates the applicability of lidar data to describe semi-arid shrubs, and successfully fuses the two datasets to generate improved classification accuracies and stand structure descriptions. These products are desirable in the context of long term monitoring, and may potentially be useful in habitat analysis or biomass calculations. Figure 4 clearly indicates the correlation between surface roughness and sagebrush presence; and fires scars (including sagebrush islands) are plainly visible in the final sagebrush distribution map (Figure 3). Spectral subsetting and multiple spectral endmember classification helped to minimize the spectral confusion introduced by partial cover canopies and soil variability. Sub-pixel components could not be accurately modeled in this study, likely due to complex mixing in semi-arid partial canopies. While accuracies from MTMF classification of sagebrush distribution were intermediate (75 percent overall accuracy), the inclusion of lidar-derived roughness notably increased the ability to map the distribution of sagebrush (89 percent overall accuracy). Following the generation of accurate and co-registered maps of sagebrush distribution and vegetative structure, quantitative statistics were derived that described sagebrush stands in terms of vegetation heights and percent bare ground. The methods and results of this study lay the framework for utilizing co-registered hyperspectral and lidar data to describe semi-arid shrubs in greater detail than would be feasible for most ground based surveys. Although it is currently not reasonable to use these methods to inventory or monitor large scale vegetative ecosystems (e.g., semi-arid shrubs in the Southwest U.S.), we assert that these methods are useful where small-scale precision has implications for large-scale inventory or land management objectives.

ACKNOWLEDGMENTS

This work was supported by the Idaho National Environmental and Engineering Laboratory (INEEL) through the Idaho State University – INEEL Partnership for Integrated Environmental Analysis Education Outreach Program. Additional support was provided by a grant from the National Aeronautics and Space Administration (NASA) Goddard Space Flight Center and the NOAA Environmental Technology Laboratory (ETL). We thank Ron Rope, Shane Cherry, and Tanya Johnson for field and office assistance. Finally, we thank our two anonymous reviewers for their helpful comments.

This study was made possible by a grant from the National Aeronautics and Space Administration Goddard Space Flight Center. ISU would also like to acknowledge the Idaho Delegation for their assistance in obtaining this grant.

LITERATURE CITED

Airborne 1, 2001. Briefing Note BN#01; LiDAR Accuracy, Airborne 1 Corporation, El Segundo, California, 24 p.

Berk, A., G.P. Anderson, L.S. Bernstein, P.K. Acharya, H. Dothe, M.W. Matthew, S.M. Adler-Golden, J.H. Chetwynd, S.C. Richtsmeier, B. Pukall, C.L. Allred, L.S. Jeong, and M.L. Hoke, 1999. MODTRAN4 radiative transfer modeling for atmospheric correction, Proceedings of the AVIRIS Airborne Geosciences Workshop, Pasadena, California (JPL, Publication 99–17, Pasadena, California).

Blackburn, G.A., 2002. Remote sensing of forest pigments using airborne imaging spectrometer and LIDAR imagery, Remote Sensing of Environment, 82:311–321.

Boardman, J.W., 1998. Leveraging the high dimensionality of AVIRIS data for improved sub-pixel target unmixing and rejection of false positives: Mixture Tuned Matched Filtering, Proceedings of the 7th Annual JPL Airborne Geoscience Workshop (JPL, Publication 97–1, Pasadena, California), p. 55.

Chen, D., and D. Stow, 2002. The effect of training strategies on supervised classification at different spatial resolutions, Photogrammetric Engineering & Remote Sensing, 68(11):1155–1161.

Colket, E.C., 2003. Long-Term Vegetation Dynamics and Post-Fire Establishment Patterns of Sagebrush Steppe, M.S. thesis, University of Idaho, Moscow, Idaho, 144 p.

Congalton, R.G., and K. Green, 1999. Assessing the Accuracy of Remotely Sensed Data: Principles and Practices, Lewis Publishers, Boca Raton, Florida, 137 p.

Drake, J.B., R.O. Dubayah, D.B. Clark, R.G. Knox, J.B. Blair, M.A. Hofton, R.L. Chazdon, J.F. Weishampel, and S.D. Prince, 2002. Estimation of tropical forest structural characteristics using large-footprint LiDAR, Remote Sensing of Environment, 79:305–319.

Elmore, A.J., J.F. Mustard, S.J. Manning, and D.B. Lobell, 2000. Quantifying vegetation change in semi-arid environments: Precision and accuracy of spectral mixture analysis and the Normalized Difference Vegetation Index, Remote Sensing of Environment, 73:87–102.

ESER, 2004. INEEL Environmental Surveillance, Education and Research program; INEEL vegetation, an overview, URL: http://www.stoller-eser.com/Flora/vegetation.htm, S.M. Stoller Corporation, Idaho Falls, Idaho (last date accessed: 12 October 2005).

Flood, M. (editor), 2004. American Society for Photogrammetry and Remote Sensing Guidelines – Vertical Accuracy Reporting for Lidar Data, ASPRS, Bethesda, Maryland, 15 p.

Harding, D.J., M.A. Lefsky, G.G. Parker, and J.B. Blair, 2001. Laser altimeter canopy height profiles: Methods and validation for closed-canopy, broadleaf forests, Remote Sensing of Environment, 76:283–297.

Hodgson, M.E., J.R. Jensen, L. Schmidt, S. Schill, and B. Davis, 2003. An evaluation of LIDAR- and IFSAR-derived digital elevation models in leaf-on conditions with USGS Level 1 and Level 2 DEMs, Remote Sensing of Environment, 84:295–308.

Hofton, M.A., L.E. Rocchio, J.B. Blair, and R. Dubayah, 2002. Validation of vegetation canopy LiDAR sub-canopy topography measurements for a dense tropical forest, Journal of Geodynamics, 34:491–502.

Hudak, A.T., M.A. Lefsky, W.B. Cohen, and M. Berterretche, 2002. Integration of LiDAR and Landsat ETM data for estimating and mapping forest canopy height, Remote Sensing of Environment, 82:397–416.

Huete, A.R., and R.D. Jackson, 1988. Soil and atmosphere influences on the spectra of partial canopies, Remote Sensing of Environment, 29:89–105.

Huete, A.R., R.D. Jackson, and D.F. Post, 1985. Spectral response of a plant canopy with different soil backgrounds, Remote Sensing of Environment, 17:37–53.

Latypov, D., 2002. Estimating relative LiDAR accuracy information from overlapping flight lines, ISPRS Journal of Photogrammetry and Remote Sensing, 56:236–245.

Lee, D.S., and J. Shan, 2003. Combining LiDAR elevation data and IKONOS multispectral imagery for coastal classification mapping, Marine Geodesy, 26:117–127.

Lewis, M., V. Jooste, and A. DeGasparis, 2000. Hyperspectral discrimination of arid vegetation, Proceedings of the 28th International Symposium on Remote Sensing of Environment, 27–31 March, Cape Town, South Africa, pp. 148–151.

Meinguet, J., 1979. Multivariate interpolation at arbitrary points made simple, Journal of Applied Mathematics and Physics, 30:292–304.

Merenyi, E., W.H. Farrand, L.E. Stevens, T.S. Melis, and K. Chhibber, 2000. Mapping Colorado River ecosystem resources in Glen Canyon: Analysis of hyperspectral low-altitude AVIRIS imagery, ERIM Proceedings of the 14th International Conference on Applied Geologic Remote Sensing, 06–08 November, Las Vegas, Nevada, pp. 44–51.

Mundt, J.T., D.R. Streutker, and N.F. Glenn, In Review. Partial unmixing of hyperspectral imagery: Theory and methods, Remote Sensing of Environment.

Musick, H.B., 1984. Assessment of Landsat multispectral scanner spectral indexes for monitoring arid rangeland, IEEE Transactions on Geoscience and Remote Sensing, GE-22(6):512–519.

NPCC, 2004. Upper Snake Subbasin Assessment, Northwest Power and Conservation Council, Portland, Oregon, 75 p.

Okin, G.S., D.A. Roberts, B. Murray, and W.J. Okin, 2001. Practical limits on hyperspectral vegetation discrimination in arid and semiarid environments, Remote Sensing of Environment, 77:212–225.

Okin, W.J., G.S. Okin, D.A. Roberts, and B. Murray, 1999. Multiple endmember spectral mixture analysis: Endmember choice in an arid shrubland, Proceedings of the 8th Annual AVIRIS Airborne Geoscience Workshop (JPL, Publication 99–17), Pasadena, California, pp. 323–332.

Patil, G.P., and W.L. Myerst, 1999. Environmental and ecological health assessment of landscapes and watersheds with remote sensing data, Environmental Health, 5(4):221–224.

Popescu, S.C., and R.H. Wynne, 2004. Seeing the trees in the forest: Using LiDAR and multispectral data fusion with local filtering and variable window size for estimating tree height, Photogrammetric Engineering & Remote Sensing, 70(5):589–604.

Popescu, S.C., R.H. Wynne, and R.F. Nelson, 2002. Estimating plot-level tree heights with LiDAR: Local filtering with a canopy-height based variable window size, Computers and Electronics in Agriculture, 37:71–95.

Rango, A., M.J. Chopping, J.C. Ritchie, K. Havstad, W. Kustas, and T. Schmugge, 2000. Morphological characteristics of shrub coppice dunes in desert grasslands of southern New Mexico derived from scanning LiDAR, Remote Sensing of Environment, 76:26–44.

Ray, T.W., and B.C. Murray, 1998. Nonlinear spectral mixing in desert vegetation, Remote Sensing of Environment, 55:59–64.

Riaño, D., F. Valladares, S. Condés, and E. Chuvieco, 2004. Estimation of Leaf Area Index and covered ground from airborne laser scanner (LiDAR) in two contrasting forests, Agricultural and Forest Meteorology, 124:269–275.

Ritchie, J.C., K.S. Humes, and M.A. Weltz, 1995. Laser altimeter measurements at Walnut Gulch watershed, Arizona, Journal of Soil and Water Conservation, 50(5):440–442.

Roberts, D.A., M. Gardner, R. Church, S.L. Ustin, G.J. Scheer, and R.O. Green, 1998. Mapping chaparral in the Santa Monicamountains using multiple endmember spectral mixture models, Remote Sensing of Environment, 65:267–279.

RSI, 2004. ENVI User's Guide (Version 4.1), Research Systems Incorporated, Boulder, Colorado, 1,084 p.

Townshend, J.R.G., 1992. The impact of misregistration on change detection, IEEE Transactions on Geoscience and Remote Sensing, 30(5):1054–1060.

Tueller, P.T., 1987. Remote sensing science applications in arid environments, Remote Sensing of Environment, 23:143–154.

Warren, P.L., and C.F. Hutchison, 1984. Indicators of rangeland change and their potential for remote sensing, Journal of Arid Environments, 7:107–126.

Weltz, M.A., J.C. Ritchie, and H.D. Fox, 1994. Comparison of laser and field measurements of vegetation height and canopy cover, Water Resources Research, 30(5):1311–1319.

LiDAR Measurement of Sagebrush Steppe Vegetation Heights

David R. Streutker, Department of Geosciences, Idaho State University, Boise, ID. (stredavi@isu.edu)

Nancy F. Glenn, Department of Geosciences, Idaho State University, Boise, ID. (glennanc@isu.edu)

ABSTRACT
Small footprint LiDAR data were used to detect and characterize vegetation in a semi-arid sagebrush steppe environment in southeastern Idaho. Processing the raw data in individual flightlines maintained the high relative accuracy of the dataset and allowed for the detection of sub-meter vegetation. First return LiDAR pulse data were used to both determine the ground surface as well as calculate vegetation heights. Surface roughness maps based on vegetation heights were found to best capture the variability of the canopy and accurately distinguish burned and unburned areas. Field validation of a sagebrush presence and absence classification based on a single roughness threshold value indicate an overall accuracy of 86%. The LiDAR-determined vegetation heights are moderately well correlated to those measured in the field, though the LiDAR heights uniformly underestimate the field heights. This underestimation is believed to be due to signal threshold limits within the LiDAR sensor, producing heights corresponding to the interior of the shrub canopy rather than the top.

Keywords: remote sensing, vegetation, rangelands

INTRODUCTION

Though a relatively young remote sensing technology, LiDAR (light detection and ranging, also referred to as laser altimetry or airborne laser swath mapping) has quickly demonstrated great potential to precisely characterize vegetative systems. Within forest canopies, both small (1 m or less) and large (10-25 m) diameter footprint LiDAR systems have found widespread success in the measurement of various ecological parameters. Waveform returns from large footprint LiDAR sensors such as the Scanning LiDAR Imager of Canopies by Echo Recovery (SLICER) and Laser Vegetation Imaging Sensor (LVIS) have successfully been used to measure variables such as tree height, canopy structure, leaf area index (LAI) and biomass (Drake et al., 2002; Harding et al., 2001; Hofton et al., 2002). Similarly, small footprint LiDAR data have been used to determine tree height and LAI in various forest types (Popescu et al., 2002; Riaño et al., 2004). Beneath the canopy, Seielstad and Queen (2003) have also used small footprint LiDAR data to measure fuel loads of coarse woody debris on the forest floor.

Despite the fact that rangelands make up an estimated 70% of the planet's land area (West, 1999), little work has addressed LiDAR applications in rangeland ecosystems relative to the large number of forestry studies. Height profiles created by profiling LiDAR sensors have been used to measure plant height and canopy cover in a rangeland environment (Weltz et al., 1994) as well as to model rangeland surface roughness (Ritchie et al., 1995). Other studies have demonstrated the applicability of scanning LiDAR combined with multispectral video imagery to map shrub coppice dunes in desert grasslands (Rango et al., 2000).

The purpose of this study is to investigate the utility of small footprint LiDAR for detecting and characterizing vegetation in a semi-arid sagebrush steppe. Sub-meter accuracies are currently achievable with LiDAR technology, allowing for the discrimination of short vegetation types. This study seeks primarily to determine the capability of LiDAR to detect the presence of sagebrush and other types of low shrub. Upon positive detection, the ability to quantify various ecological variables such as shrub height and ground cover is explored. The methods described here are similar to those used in Glenn et al. (2006) and Mundt et al. (2006), but are presented in more detail and with attention to validation, both qualitative and quantitative.

Sagebrush (*Artemisia tridentata*) is one of the most dominant species of vegetation in the intermountain West, with sagebrush communities present in all 11 western states (Bunting et al., 1987). Many vertebrate species utilize habitats within sagebrush steppe ecosystems to maintain viable populations, such as pygmy rabbit *(Brachylagus idahoensis)*, sage grouse *(Centrocercus urophasianus)*, and sharptailed grouse *(Tympanuchus phasianellus)*. However, due to pressures from invasive species, grazing practices, agriculture, and altered fire regimes, sagebrush populations have been in decline throughout the last century. An estimated 3 million acres of public lands in the intermountain West have become dominated by invasive grasses such as cheatgrass (*Bromus tectorum*) or medusahead (*Taeniatherum caput-medusae*) (West, 1999), while big sagebrush in the Upper Snake subbasin alone has decreased an estimated 42% from historic levels (NPCC, 2004). In many areas, there has been a complete loss of the sagebrush ecosystem (Knick, 1999).

As sagebrush communities in the intermountain West become increasingly fragmented or disturbed due to agricultural and urban growth, range fires, and invasive weeds, critical habitats and historic grazing/browsing regimes become threatened (NPCC, 2004). For instance, sagebrush communities can require 15 years or more to return to preburn conditions following a fire (Bunting et al., 1987; Humphrey, 1984). Many sagebrush communities have a long history of disturbance (Knick and Rotenberry, 1997) and require active restoration techniques (Hemstrom et

al., 2002; McIver and Starr, 2001). As a result, land managers and conservation agencies are in need of accurate tools to inventory and assess sagebrush ecosystems.

As in the case of forest canopies, LiDAR has the capability to provide information about rangeland vegetation structure such as heights, densities, and biomass, properties which may not readily be determined through the use of passive remote sensing. A study by Mundt et al. (2006) has shown that LiDAR can be used successfully to improve upon a hyperspectral classification of sagebrush presence/absence in southern Idaho. This study aims to demonstrate the potential of LiDAR to be a powerful and complementary tool in monitoring rangelands, both in pristine condition or after a disturbance.

STUDY AREA

The study area for this investigation is located within the United States Sheep Experiment Station (USSES), a facility of the United States Department of Agriculture (USDA) Agricultural Research Service (ARS). This facility is located near Dubois, Idaho, in the northeastern Snake River Plain. The study area itself is located in the northeast corner of the USSES and is approximately 5 km long and 1 km wide, with a total area of 6.9 km2 (Figure 1). The terrain of the study area is gently rolling rangeland, with elevations between 1777 and 1866 m.

The dominant vegetation within the study area is mountain sagebrush (*Artemisia tridentata ssp. vaseyana*), while secondary shrub types include green rabbitbrush (*Chrysothamnus viscidiflorus*) and horsebrush (*Tetradymia canescens*). The average height of these shrubs within the study area is generally no more than one meter. Grasses and forbs include thickspike wheatgrass (*Elymus lanceolatus spp. lanceolatus*), Plains reedgrass (*Calamagrostis montanensis*), Idaho fescue (*Festuca idahoensis*), and bushy bird's beak (*Cordylanthus ramosus*). Two controlled fires have occurred within the study area in recent years, both of which are indicated in Figure 1. The latter was in the northern part of the study area and took place in the fall of 2002, just prior to the acquisition of the LiDAR data. The earlier burn occurred in the eastern part of the study area in 1995. In areas where the fires were more intense, the sagebrush stems were burned completely to the ground, while in less intensely burned areas remnants of shrub stems and branches remain. The ecosystem within the 1995 burn is still recovering, albeit quite slowly. Seven years later, at the time of the data collection, the area was yet dominated by bare ground and grasses, with some sparse low brush.

This study area was selected for two principal reasons. The first is that the terrain has mild topography, making it amenable to vegetation discrimination without the complexities of rugged terrain. The second reason is that the burned areas provide a bare, non-vegetated state with which to compare and contrast the results from the vegetated areas.

METHODS

DATA CHARACTERISTICS AND ACCURACY

The LiDAR data were acquired in the fall of 2002 by the Airborne 1 Corporation of El Segundo, California, using an Optech ALTM 2025 LiDAR System. The sensor, which acquires data at a rate of 25 kHz, was mounted on a fixed wing aircraft flying with a minimum airspeed of approximately 100 kt. Both first and last pulse datasets were acquired, each consisting of over eight million individual postings having an average separation of 0.9 m (producing a post density of 1.2 m-2). The data were collected in nine separate flightlines, each approximately 300 m wide, resulting in flightline overlap of roughly 50%. All flightlines were then combined to form the final datasets. Each data point includes a Global Positioning System (GPS) time stamp and intensity value, as well as the spatial coordinates in three dimensions. The data were collected

from an altitude of approximately 750 m, resulting in a footprint diameter of roughly 20 cm for each laser pulse.

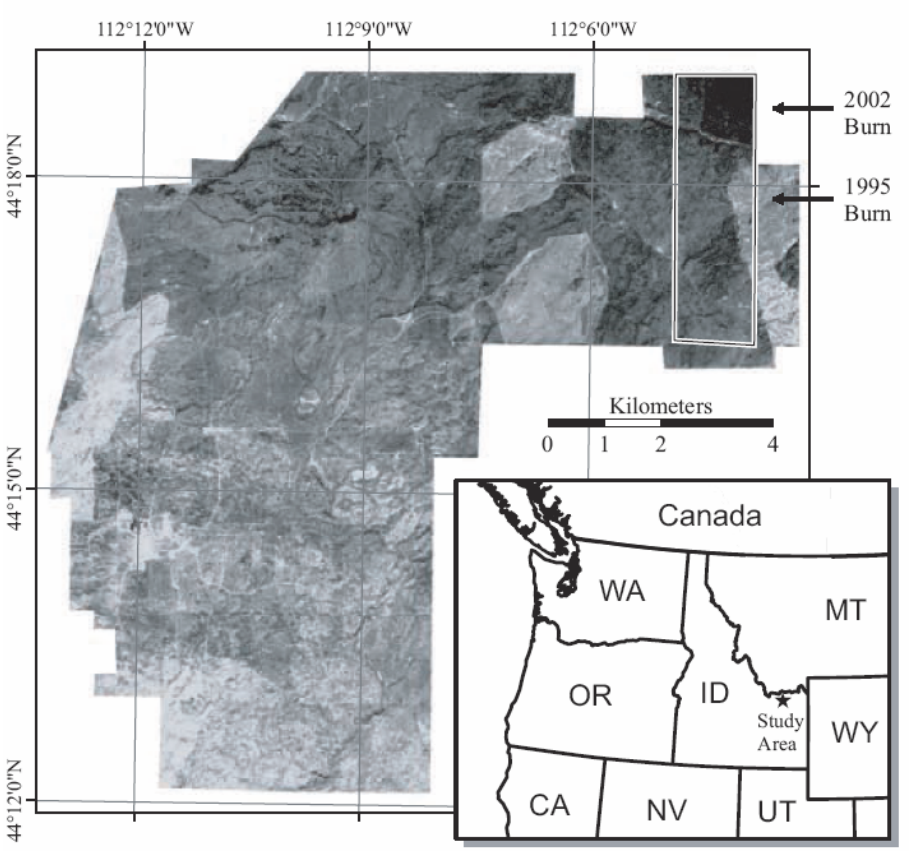

Figure 1. A figure of the study area, outlined within the United States Sheep Experiment Station. The base map is a QuickBird image, acquired in October of 2002. The two burns within the study area are identified. The inset shows the location of the study area (as a star) within the state of Idaho.

Once the LiDAR data were collected, both the absolute and relative accuracies of the dataset were determined. The absolute accuracy of LiDAR data determines how accurate the individual coordinates of each point are with respect to an absolute coordinate system or datum. Relative accuracy, on the other hand, determines how accurately individual points are located with respect to each other and provides a measure of the internal consistency within the dataset.

The vendor performed a GPS validation survey concurrent to the LiDAR acquisition and was able to constrain the absolute accuracy of the LiDAR coordinates to 22 cm in the vertical direction and 1 m in the horizontal direction (two-sigma; ASPRS, 2004). A comparable vertical accuracy was also determined using assessment methods modeled after Latypov (2002), which calculate the error between individual flightlines in areas of overlap.

One of the simplest ways to measure relative error is by performing a statistical analysis of a collection of points returned from a flat surface. Such surfaces may include a standing body of water, a flat and nonvegetated area of ground (e.g. a dry lakebed or parking lot), or the wall or roof of a building. LiDAR points that are returned from these surfaces are expected to lie on a flat plane, and thus any deviation away from a flat plane provides a measure of the relative accuracy (vertical accuracy in the case of bodies of water and rooftops, horizontal accuracy in the case of building walls).

Analyses in previous studies using LiDAR data collected on the same campaign as this study, though in different areas of southern Idaho, determined vertical and horizontal relative accuracies of 5 cm and 10 cm, respectively (Glenn et al., 2006; Mundt et al., 2006). As this study area contains no buildings or standing bodies of water, the vertical relative accuracy was estimated using flat areas of bare ground. Even if these bare areas contain minor topographic variability, they can still serve to determine an upper bound of the relative accuracy. Within the study area, numerous separate bare ground locations were distributed among multiple flightlines, each of which contained at least 50 LiDAR points with standard deviation of 5 cm or less. Relative accuracies of this magnitude can be expected when using a properly calibrated LiDAR sensor under normal operating conditions (Airborne 1, 2001). Figure 2 shows a histogram of the standard deviation of elevation over the entire study area, based on 25 m2 parcels. As can be seen from the shaded portion of the figure, several thousand such locations exist with standard deviation of 5 cm or less, indicating that the vertical accuracy of the sensor is within this limit.

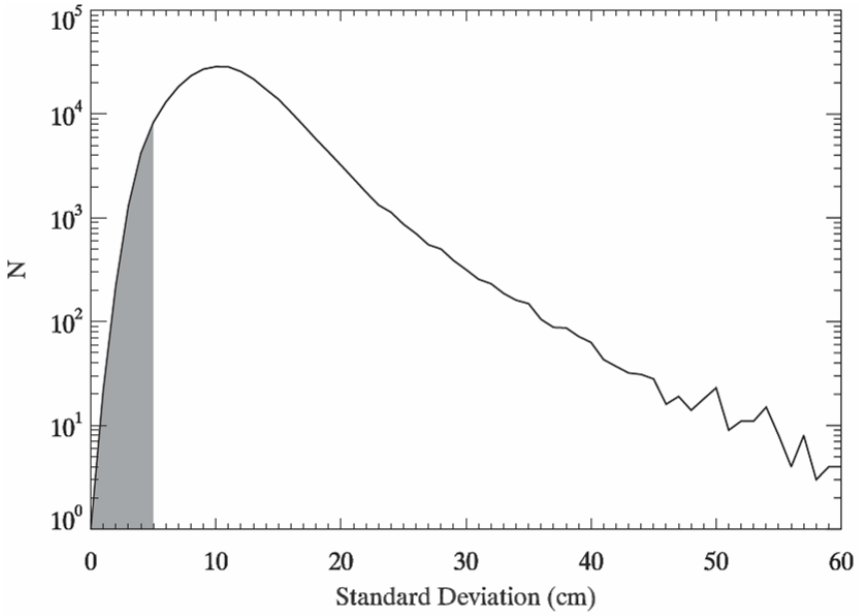

Figure 2. A histogram of standard deviations of elevation over 25 m2 parcels for the entire study area. The shaded portion represents those areas with a standard deviation of 5 cm or less.

Fifty-two ground control points (GCPs) were collected throughout the study area, primarily at road intersections and other easily identifiable features, with the use of a differentially-correctable Trimble GeoXT GPS unit. Due to the high vertical accuracy of the data, in combination with the available intensity data, many of these features were identifiable within the LiDAR dataset. Thus the GCPs were used to geometrically register the LiDAR dataset (which involved a datum conversion) and resulted in an RMS error of 0.75 m. The dataset was registered as a whole, without separating the individual flightlines. The calculated registration error is in general agreement with the absolute horizontal accuracy quoted by the vendor.

Initial field investigation of the study area found that the canopy cover was generally low throughout the site, exposing a large amount of bare ground. Because of this, in addition to the fact that the study area is relatively devoid of major topographic features, the first return LiDAR data were used to characterize both the terrain and the vegetative canopy. Using a single-return LiDAR dataset instead of attempting to merge the first and last return data kept the overall

processing requirements to a minimum and, more importantly, avoided the introduction of problems associated with detecting multiple pulse returns at a similar height (Hodgson et al., 2003).

As stated earlier, the study area was chosen for this investigation in part because of its gentle topography, which would in turn aid in the extraction of vegetation heights from the LiDAR data. Figure 3 shows a semivariogram of the elevation data at lag distances up to 500 m. One can see from the figure that the semivariogram is parabolic near the origin, indicative of a Gaussian model of semivariance and characteristic of extremely continuous terrain (Isaaks and Srivastava, 1989). This result supported the premise that the ground could be modeled as a smooth and continuous surface.

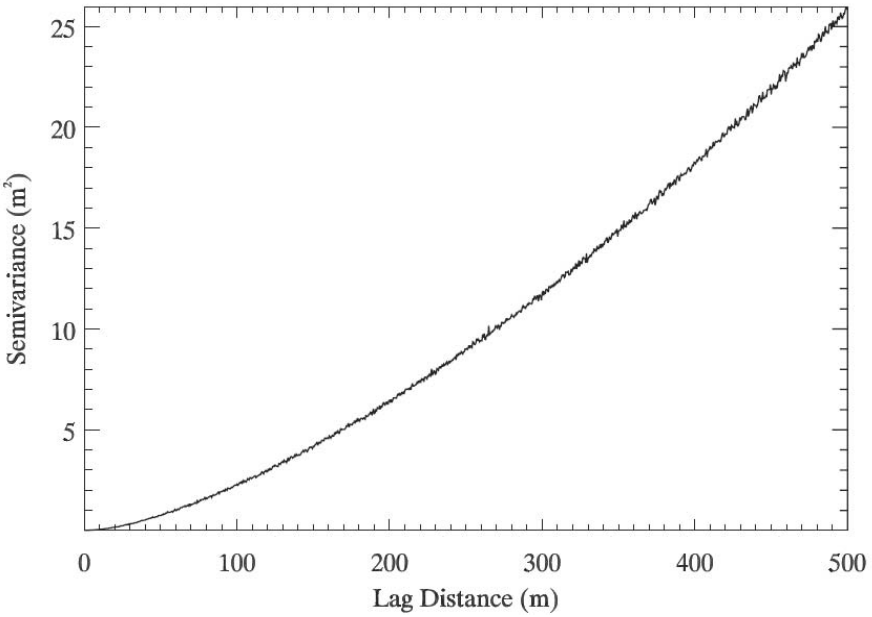

Figure 3. A semivariogram of elevation heights for the study area.

HEIGHT CALCULATION

The LiDAR data were divided into 5 m × 5 m grid cells, each of which contained between 5 and 50 individual LiDAR points, depending on the local point density. Even though only the first return data were used in this study, it was assumed that, due to the open canopy, some fraction of the returned pulses were reflected entirely from the ground, without encountering any canopy cover. As such, the lowest point within each cell was assumed to have fully penetrated the canopy and been returned from the ground surface. With the use of these initial ground points, spaced an average of 5 m apart, a preliminary ground surface was interpolated across the entire study area using a thin plate spline (Meinguet, 1979). Due to local terrain irregularities, some low points, though not the absolute lowest in each cell, were as a result located below the initially interpolated ground surface. Points that lay on or below the ground surface were therefore reclassified as additional ground points. A new ground surface was then re-interpolated using the increased collection of ground points. This process was iterated until all LiDAR points were classified as either ground or non-ground. Ninety-eight percent of the points converged after two iterations of this procedure. All resulting ground points were used to interpolate a final ground surface, and heights above this surface were calculated for all remaining non-ground points.

Initial investigations determined that regions of poor relative vertical accuracy (25 cm or more) existed in many areas due to the overlap of multiple flightlines. Because this inaccuracy was greater than the majority of vegetation heights, the vegetation component was obscured and computed vegetation heights were inaccurate. However, when the methodology described above was applied to each of the flightlines individually instead of to the dataset as a whole, the relative accuracy increased considerably across all flightlines to the 5 cm level that was desired. In order to preserve the highest possible accuracy, the processing of vegetation heights was performed by considering all flightlines individually. Upon calculation of heights within each flightline, all flightlines were recombined into a single dataset.

As noted previously, the LiDAR dataset has a point density of 1.2 m-2 and a footprint diameter of approximately 20 cm. This results in the sampling of less than 10% of the actual surface throughout the entire region. In this way LiDAR can only be considered as a sampling method, providing a statistical measure of the surface topography. In terms of vegetation, only a small fraction of all plants are therefore sampled. This led to the consideration of statistical products to quantify the topography and any derived properties, such as vegetation heights or ground cover.

RASTERIZATION

The point data were used to produce maps of various ecological properties, primarily mean height and surface roughness. This was done by dividing all of the point data into 5 m grid cells and statistically analyzing the data within each cell. The mean height was computed as the mean of all individual height values within the cell, while the surface roughness value was determined by calculating the standard deviation of the heights. Both products included the zero-height ground points so as to be characteristic of the data in entirety. Several other products were similarly calculated, such as the mean vegetation height (which excluded ground points) and tallest height within each cell. The percentage of vegetative cover was also calculated as the ratio of the number of non-ground points to the total number of points within each cell.

VALIDATION

A validation campaign was carried out in the fall of 2004. One hundred and sixty-eight validation points were collected throughout the study area with a GPS unit. Each validation point consisted of the type of ground cover at that location (sagebrush, grass, burned remnants and litter, or bare ground) and the height of the vegetation, measured to the nearest 5 cm. When individual shrubs were measured, the maximum height of the shrub was recorded and the GPS point was centered on it. The field validation points also included an ocular estimate of the overall ground cover within a radius of 50 cm. These points were collected in three transects throughout the study area, one through an unburned area, one through the 1995 burn, and one through the 2002 burn. The number of validation points collected in each transect was roughly equal.

In order to investigate the relationship between the field and LiDAR measurements, the heights were compared using a spatial buffer. Due to the difficulty of precisely locating individual LiDAR points in the field, the field points were buffered horizontally when compared to the LiDAR point data. (A spatial buffer allows the absolute location of a point to vary within a specified radius.) The height of each sagebrush field point was compared to the highest individual LiDAR point within the buffered area, as the highest LiDAR point would most likely represent the shrub corresponding to the field measurement. Initially, the buffer size was varied in order to determine the optimal buffer radius. Based on 104 sagebrush points, it was found that the highest correlation between the field-measured heights and the LiDAR-calculated heights occurred at a buffer radius of approximately 1.5 m. (The analysis was restricted to sagebrush field points only, as bare ground field points would be unlikely to show significant spatial dependence.) Figure 4 shows the correlation coefficient (r) versus buffer size up to a buffer radius of 3.5 m. The

correlation weakens for both larger and smaller radii, indicating that this buffer size was optimal for capturing isolated shrubs. The resulting buffer is large enough to accommodate horizontal inaccuracies and yet small enough to prevent confusion between multiple shrubs. Thus a buffer of 1.5 m was used throughout the remainder of the validation. It is interesting to note that the optimal buffer size is roughly equal to the sum of the horizontal LiDAR accuracy (calculated above) and the general accuracy of the GPS unit (<1 m).

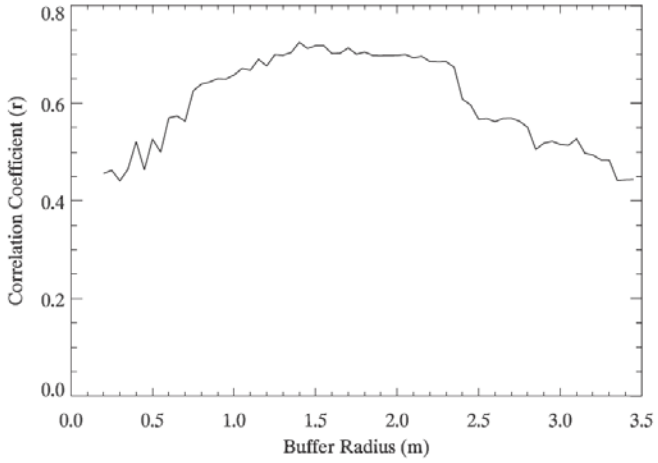

Figure 4. A plot of correlation coefficient versus buffer size for all sagebrush field points.

RESULTS

An example cross-section of the resulting height data is shown in Figure 5. In the upper figure, the black line shows the first pulse LiDAR data and represents the top of the rangeland canopy. The grey line below it is the ground surface, calculated via the method explained above. In the lower figure, the ground elevations have been subtracted from the LiDAR data, resulting in the vegetation heights alone which are shown with the grey line. The black line represents the surface roughness, calculated as the standard deviation of the heights over 5 m intervals. As identified in the diagram, the cross-section intersects a boundary between burned and unburned areas. The burned side has correspondingly lower vegetation heights and surface roughness than the unburned side.

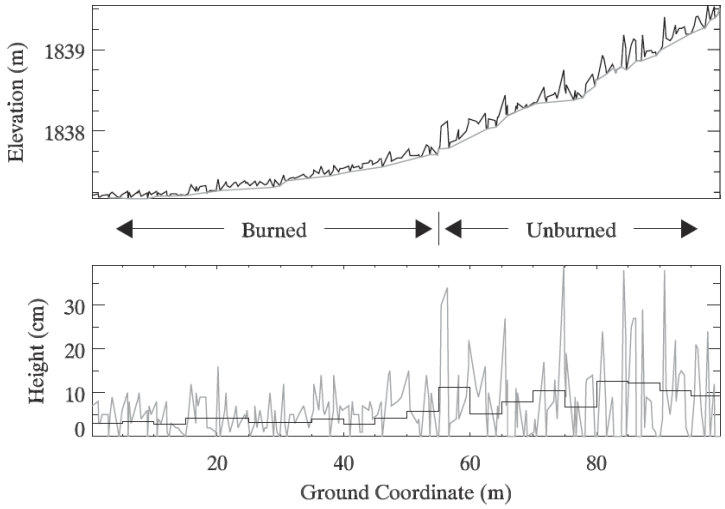

Figure 5. A cross-section of the elevation data showing the individual vegetation heights above the ground surface. The upper figure shows the raw LiDAR points (black) above the interpolated ground surface (grey). The lower figure shows the corresponding individual vegetation heights (grey) and the surface roughness, calculated over 5 m intervals (black).

VEGETATION HEIGHTS

Of the first pulse LiDAR points, 21% were classified as ground and the remainder as non-ground. Figure 6 shows images of the mean vegetation heights across the northern half of the study area, rasterized to 5 m pixels. Figure 6a shows the heights calculated from the entire dataset as a whole, while Figure 6b shows the heights calculated from the dataset after separating the flightlines. As shown in Figure 6a, the overlapping flightlines caused a north-south striped pattern of anomalous heights due to the degraded accuracy. These stripes disappear in Figure 6b, allowing the burned and unburned areas to be much more distinguishable and even revealing unimproved roads throughout the site. The height values calculated from the separated flightlines and represented in Figure 6b are used for the remainder of the analysis.

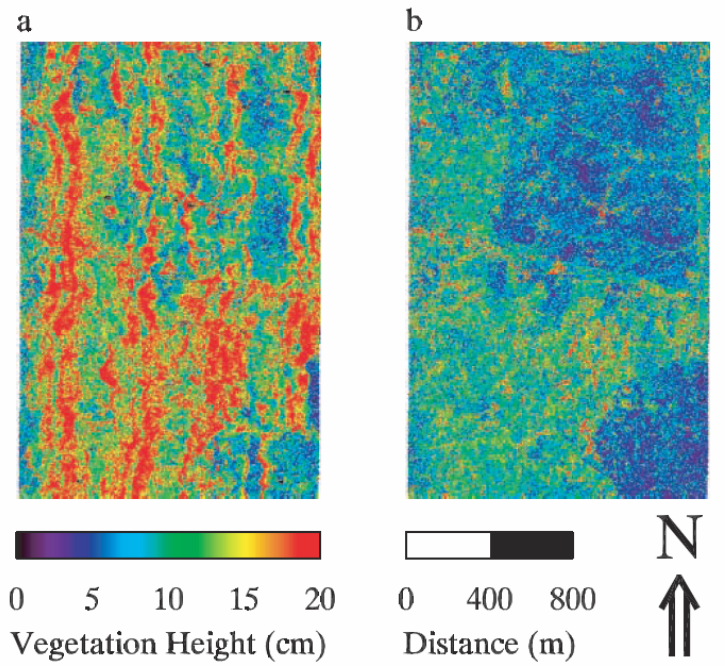

Figure 6. Maps showing mean vegetation height rasters over a subset of the study area. a) The vegetation heights calculated from the combined dataset. b) The vegetation heights calculated from individual flightlines.

Figure 7 is a histogram showing all individually calculated height values throughout the study area. The calculated non-ground heights range from 1 cm to 343 cm (likely a tree) and have a mean of 12 cm, a median of 9 cm, and a mode of 5 cm. Ten percent of the height measurements are equal to or greater than 25 cm, while the tallest 1% are equal to or greater than 45 cm. Within the sage dominated areas, the mean vegetation height is 13 cm. The mean heights in the 1995 and 2002 burns are 8 cm and 9 cm, respectively.

The histograms in Figure 8 compare the vegetation heights from the burned and unburned areas. In the figure, the solid line represents the unburned area, while the dotted line represents the 1995 burn and the dashed line represents the 2002 burn. As expected, the vegetation heights are greater in the unburned area than in the burned areas. Table 1 shows the statistical properties of the heights within each subset. (The vegetative fraction listed in the table is calculated as the ratio of non-ground points to the total number of points throughout the entire subset.)

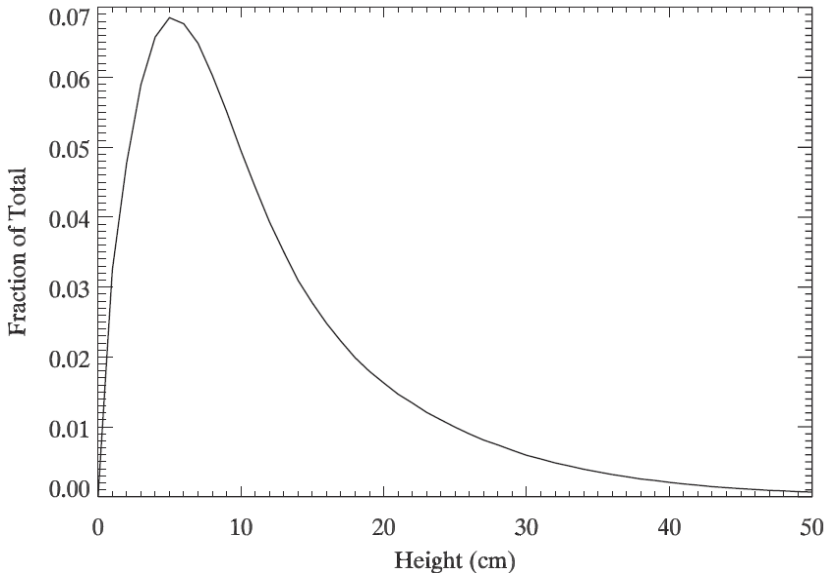

Figure 7. A histogram of individual vegetation heights for the entire study area.

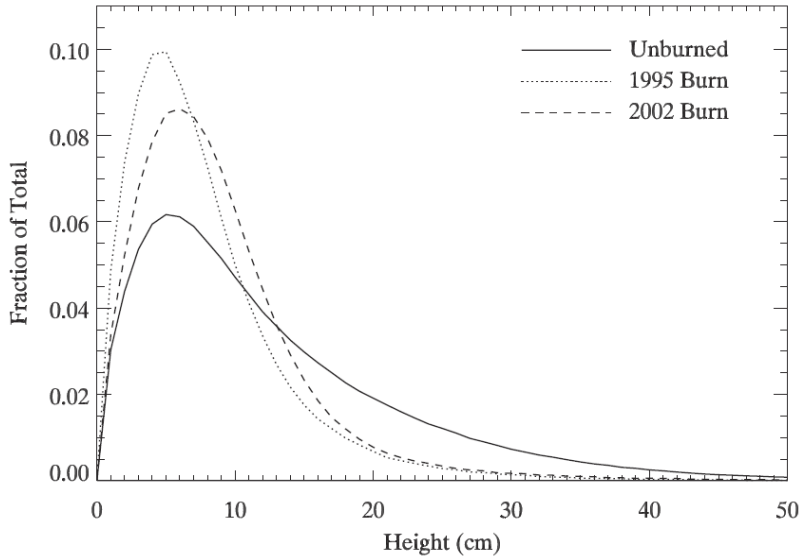

Figure 8. A histogram comparing the vegetation heights of burned and unburned areas.

Table 1. Vegetation height statistics for the burned and unburned areas.

Area	Mean Height (cm)	Median Height (cm)	Standard Deviation (cm)	Height of 95th Percentile (cm)	Vegetation Fraction
Unburned	13	10	10	33	0.801
1995 Burn	8	6	6	19	0.766
2002 Burn	9	8	7	20	0.765

SURFACE ROUGHNESS

Due to the irregular and open nature of the sagebrush canopy, surface roughness, calculated as the standard deviation of the vegetation heights, was found to better capture the variability of the canopy than other statistical measures, such as mean height or skewness. The calculated surface

roughness values ranged from near zero to 2.5 m. Unburned, sage dominated areas have a mean surface roughness value of 10 cm, while both of the burned areas have a lower surface roughness mean of 5 cm. Figure 9 shows a histogram of surface roughness for both burns as well as an unburned region. Unlike the vegetation heights, the histograms of surface roughness demonstrate high separability of the burned areas from the unburned area, as evidenced by the two distinct peaks. From the figure, we see that the burned and unburned areas may be separable using a threshold value near 6 cm, where the burned and unburned histograms intersect. Table 2 shows the statistical properties of each subset calculated from the rasterized maps.

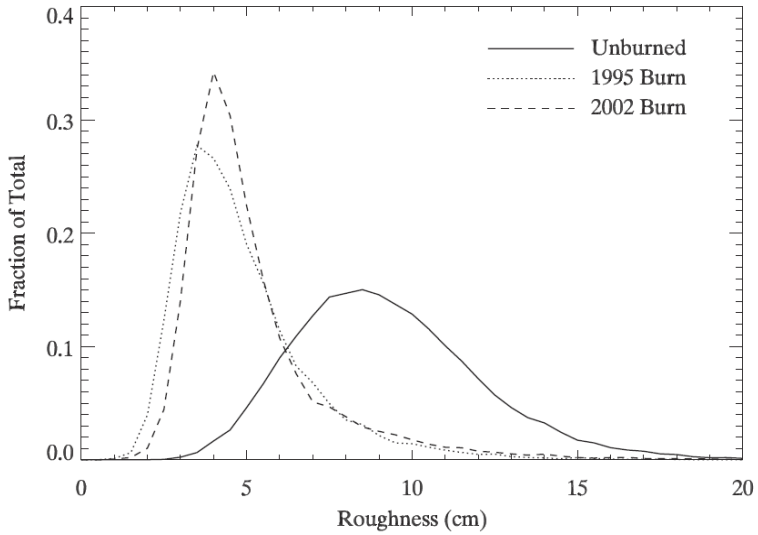

Figure 9. A histogram comparing the surface roughness of burned and unburned areas.

Table 2. Vegetation statistics after rasterization for the burned and unburned areas.

Area	Mean Height (cm)	Mean Roughness (cm)	Tallest Height (cm)	Average Terrain Slope (%)	Vegetation Fraction
Unburned	10.5	9.5	36.6	3	0.81
1995 Burn	6.0	5.1	19.1	3	0.76
2002 Burn	6.8	5.4	19.6	5	0.76

Figure 10 compares the map of surface roughness to a multispectral image (pan-sharpened QuickBird, acquired within weeks of the LiDAR data) of the northern half of the study area. The contrast of the burned to unburned areas is quite visible in the surface roughness map, with clear boundaries between the two regions. Nearly all of the burned areas from both the 1995 and 2002 fires are clearly visible in the map of surface roughness. In comparison to the map of mean height in Figure 6b, the map of surface roughness appears to better demonstrate changes in overall landcover.

VALIDATION

Of the 168 validation points collected in the field, 104 were classified as sage, 5 as grass, 4 as rock, 13 as bare ground, and 42 as burned remnants. The first validation test was simply a presence/absence accuracy assessment for sagebrush, following the method of Congalton and Green (1999). The classification is based on the surface roughness calculation, using a simple threshold value for presence and absence. (Roughness values greater than the threshold indicate sagebrush presence, while values less than the threshold indicate absence.) Sagebrush presence was based on direct field observation, while points categorized as bare ground, rock, or grass in the field were classified as sagebrush absence. (Burned remnants were excluded from the analysis

as no distinction was made in the field between remnants that remained standing and remnants that had burned almost entirely to the ground.) The error matrix in Table 3 shows the bivariate frequency distribution for sagebrush presence and absence using a threshold value of 5 cm, which produced the highest accuracies. As can be seen from the table, the 5 cm threshold classifies the sagebrush presence quite well, to Producer's and User accuracies of 88% and 94%, respectively. While the Producer's accuracy of sagebrush absence is also reasonably high at 74%, the User accuracy of sagebrush absence is a relatively poor 57%. This indicates confusion between sagebrush present in the field and points classified as absent in the LiDAR classification. The overall accuracy of the classification is 86%.

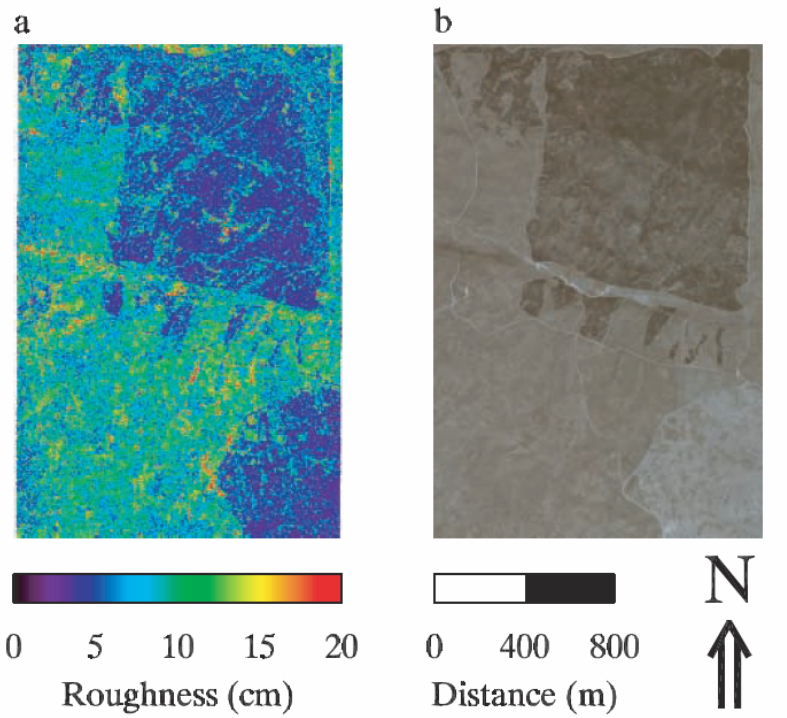

Figure 10. A comparison of a) a map of the calculated surface roughness to b) a true-color QuickBird scene for the northern half of the study area.

Table 3. Error matrix for the field validation of sagebrush presence and absence.

	Field Present	Field Absent	Total	User Accuracy
LiDAR Present	92	6	98	94%
LiDAR Absent	12	16	28	57%
Total	104	22	126	
Producer's Accuracy	88%	72%		86% (Overall)

The field-measured heights were then compared directly to the individual LiDAR-calculated heights, as well as to the local surface roughness. The comparison of field-measured and LiDAR-calculated heights resulted in a correlation coefficient of r = 0.64. When the comparison is restricted to field measurements of sagebrush only, the correlation increases to 0.72. Figure 11 shows a scatterplot of the LiDAR-derived heights versus field heights for all of the field measurements. Though the correlation is weak, a test of correlation shows it to be significant at 99% confidence (Davis, 1986). The correlation between field height and LiDAR roughness values was similar, at 0.70. A linear regression analysis determines that Hfield = 1.5 × HLiDAR + 25 cm best describes the data. The dashed line in Figure 11 represents this regression, while the dotted line signifies an ideal 1:1 association.

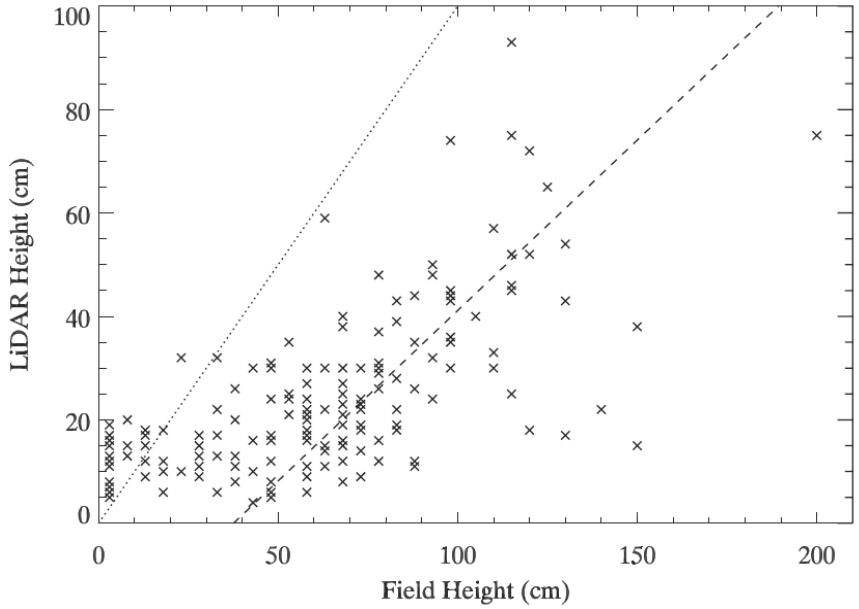

Figure 11. A comparison of individual field-measured height values versus LiDAR-determined height values. The dashed line is a best-fit linear regression to the data, while the dotted line represents a 1:1 correspondence.

DISCUSSION

Regardless of the methods used to generate or compare them, the LiDAR heights are consistently lower than the field measurements. Most sources of error, such as in field survey methods or due to sensor inaccuracies, are stochastic and would not contribute to an overall reduction in the LiDAR heights. The LiDAR heights, on the other hand, appear to be systematically lower than the field measurements in almost all areas. When a linear regression is performed on the LiDAR and field heights, the LiDAR heights are found to be approximately half as high as the field heights, as shown in Figure 11. This could be due to the inherent properties of the LiDAR scanner or the method by which the heights are determined from the LiDAR data. Also apparent in the figure is the lack of correlation between LiDAR and field heights below approximately 20 cm. It may be that this represents an operational lower limit for height determination.

Due to the two-year interval between acquisition of the LiDAR data and the collection of field points, some growth may have occurred affecting the accuracy of the validation. These effects could vary depending on which regions of the study area are in question: the 2002 burn, the 1995 burn, or the unburned area. Within the 2002 burn, all recent vegetation (generally consisting of grasses) was ignored and only burned remnants were measured. These remnants are assumed to be unchanged over the two year interval, and thus should not be a source of error. It was also assumed, based in part on field observation, that only minor canopy changes occurred within the 1995 burn or unburned areas. Independent test plot measurements indicate that sagebrush canopy varies by roughly 10% over a two-year interval (Inouye, private communication), equivalent to approximately 10 cm in the context of this study. While this may contribute to the overall underestimation of heights by LiDAR, it would represent only a minor component of the discrepancy.

Overall, the sagebrush presence/absence classification based on surface roughness performed well. However, the User accuracy of sagebrush absence was a rather poor 57%, indicating that a significant amount of sagebrush was not detected by the LiDAR analysis. In fact, the average

field-measured height of the sagebrush at these locations was 54 cm, implying that the LiDAR data simply missed these shrubs. This is not altogether surprising, considering that the width of the shrubs themselves is on the order of 1 m, roughly the same as the absolute horizontal accuracy of the LiDAR data.

This reflects the most difficult step in this study, which was trying to compare LiDAR data points, having a footprint diameter of approximately 20 cm, with ground truth data that has been co-registered to 0.75 m, an inaccuracy several times the width of the footprint. As a result, it was not possible within the scope of the study to determine the exact location of each LiDAR footprint on the ground, but only to within one meter or so. It was therefore necessary to buffer the data, introducing a significant uncertainty. One consequence of this is the likelihood that a large number of the LiDAR pulses were reflected not from the top of the canopy, but instead from the shoulders of the individual shrubs. This is most certainly the case in some portion of the measurements, and would indeed serve to decrease many of the calculated heights. However, it must then also be concluded that some fraction of the pulses were reflected from the top of the crowns and, barring other sources of error, should produce accurate heights. Yet, as shown in Figure 11, this appears not to be the case. In fact, if the shorter, uncorrelated points are excluded, the vast majority of the remaining points lie well below the 1:1 line.

This in turn leads to the question of whether or not the LiDAR pulse penetrates some distance into the canopy before it is reflected. Unfortunately, the current literature does not discuss the minimum detection threshold for common LiDAR sensors. The low LiDAR heights calculated in this study seem to indicate the possibility that the pulse does not reflect sufficiently from the absolute top of the vegetation, but does in fact penetrate into the canopy to some extent before a detectable reflection occurs. Therefore the LiDAR calculated heights would be systematically lower than the field measured heights, necessitating an approximation such as incorporating a scale factor and/or a correction constant into the height derivation. Such a correction would likely be vegetation specific, depending on the overall density of the target. In the case of sagebrush, this scale factor appears to be between 1.5 and 2.0. A scale factor may also accommodate other types of inaccuracies, such as that due to reflections from shrub shoulders discussed above.

The local canopy coverage does seem to play a role in how well the LiDAR measures the vegetation structure. As stated previously, the correlation between field measured height and LiDAR measured height is 0.64, while the correlation between field measured height and LiDAR measured roughness is 0.70. However, when restricted to validation points where the canopy coverage is 50% or more (49 points, as determined by field observations), these correlations increase to 0.78 and 0.79, respectively.

Although the accuracies of the classification increase with canopy cover, too dense of a canopy would likely lower the accuracies. As stated earlier, the last pulse data were not used in this study for the principle reason that current LiDAR systems do not seem to be able to discriminate multiple returns from similar heights, due to signal detection threshold and timing limits within the LiDAR sensor, the vertical width of the individual laser pulses, and inaccuracies in co-registering multiple returns both vertically and horizontally. As such, it was necessary to use the first pulse data to characterize both the rangeland canopy and the ground surface. One of the limitations of this methodology is that it is appropriate only for an open canopy. If the canopy is too dense, to the point of preventing a sufficient number of ground returns with which to generate an accurate ground surface, then this methodology would be unlikely to produce accurate results. There would also be a balance between maximum canopy cover and terrain variability. The terrain of this study area in this investigation is relatively gentle, and therefore requires fewer

ground points for an accurate interpolation. A more rugged and variable terrain would require more ground points and therefore a more open canopy.

Although the vegetation heights within the two burned areas are quite similar, the heights within the more recent 2002 burn are, paradoxically, slightly higher than within the older 1995 burn. The difference is so small as to be below the accuracy of the study, though the heights within the 1995 burn would be expected to be higher. It is not known why this difference exists, though possible explanations include the poor recovery of the ecosystem within the 1995 burn, differences in burn severity between the two burns, the seeming inability of the LiDAR algorithms to detect very low height brush and grass, or some combination of these factors. As noted in Table 2, the area of the 2002 burn has a slightly higher average slope than that of the 1995 burn, which also may have influenced the LiDAR height determination.

It is probable that the methods used to estimate vegetation fraction (the results of which are shown in Tables 1 and 2) overestimated the overall vegetation cover. This is not unexpected, however, in that it was calculated as simply a ratio of vegetation returns to the total number of returns. The ground returns, by definition, are assumed to contain no vegetation within their footprint. The non-ground returns, on the other hand, need only contain a minimal amount of vegetation to provide detection. This produces a bias toward non-ground points, effectively oversampling the vegetation cover.

It is also uncertain as to whether or not this methodology can detect or characterize rangeland grasses. The study area was relatively lacking in grassy areas, with only five validation points classified as such in the field. Due to the problem detecting low sagebrush and the uncertainty regarding pulse return threshold limits discussed above, it is questionable whether the current methodology would be able to distinguish grass from bare ground.

CONCLUSIONS

This study showed that LiDAR data can be successfully used to detect and characterize vegetation in a rangeland environment. However, relative vertical accuracies on the order of 5 cm are required to resolve low vegetation heights and care was needed in order to preserve this accuracy throughout the study. As such, all data were processed and heights calculated in raw point format, without rasterization. This also required the processing of all data in individual flightlines, and recombining into a single dataset only at the time of analysis.

In a sagebrush dominated area, the mean LiDAR-derived vegetation height was found to be 12 cm, while the individual vegetation heights ranged as high as 343 cm. Surface roughness calculations were found to be a useful measure of surface variability within this ecosystem and better distinguished ecological regimes than other types of statistical measure. Burned and unburned areas were found to be easily identifiable using LiDAR-determined height measurements and statistical analysis. A roughness value of 5 cm was found to classify sagebrush presence and absence to an overall accuracy of 86%.

While LiDAR data have been used a great deal in the study of forest ecosystems, this study shows that they can also be of significant use in rangelands or other low-canopy regions. Possible uses include biomass and fuel load estimation, determining burn severity and rates of recovery following disturbance, and habitat characterization, such as the identification of sage grouse leks (large areas of bare ground used for display and courting). The success shown in classifying sagebrush presence and absence indicates that this methodology may be of use in determining burn boundaries, even if a significant amount of time passes between the burn and the data acquisition. There is also the potential for possible inclusion into ongoing ecological studies at the

station, such as evaluating the impact of various sheep grazing practices on sagebrush health (Bork et al., 1998; Seefeldt and McCoy, 2003). However, further investigations are necessary to better estimate actual sagebrush heights and densities from LiDAR measurements. The applicability of these methods in more rugged terrain or denser canopy must also be addressed, as well as the possibility of including data containing multiple returns.

ACKNOWLEDGEMENTS
This study was made possible by a grant from the National Aeronautics and Space Administration Goddard Space Flight Center. ISU would also like to acknowledge the Idaho Delegation for their assistance in obtaining this grant.

The authors would like to acknowledge Steve Seefeldt and the United States Sheep Experiment Station for their assistance in this study. We also wish to thank Jacob Mundt and Matt Germino of Idaho State University for their insightful suggestions during the preparation of this manuscript. Finally, we appreciate the helpful comments of our three anonymous reviewers.

LITERATURE CITED
Airborne 1 (2001). LiDAR accuracy. *Briefing Note BN#01*, Airborne 1 Corporation, El Segundo, California, 24 pp.

ASPRS (2004). Guidelines - vertical accuracy reporting for lidar data. *1.0*, American Society for Photogrammetry and Remote Sensing, Bethesda, Maryland, 15 pp.

Bork, E. W., West, N. E., & Walker, J. W. (1998). Cover components on long-term seasonal sheep grazing treatments in three-tip sagebrush steppe. *Journal of Range Management, 51*, 293-300.

Bunting, S. C., Kilgore, B. M., & Bushey, C. L. (1987). Guidelines for prescribed burning sagebrush-grass rangelands in the northern Great Basin. *General Technical Report INT-231*, Intermountain Research Station, United States Department of Agriculture Forest Service

Congalton, R. G., & Green, K. (1999). *Assessing the Accuracy of Remotely Sensed Data: Principles and Practices*. Boca Raton, Florida: CRC Press 137 pp.

Davis, J. C. (1986). *Statistics and Data Analysis in Geology*. New York: John Wiley & Sons 646 pp.

Drake, J. B., Dubayah, R. O., Clark, D. B., Knox, R. G., Blair, J. B., Hofton, M. A., Chazdon, R. L., Weishampel, J. F., & Prince, S. D. (2002). Estimation of tropical forest structural characteristics using large-footprint lidar. *Remote Sensing of Environment, 79*, 305-319.

Glenn, N. F., Streutker, D. R., Chadwick, J., Thackray, G. D., & Dorsch, S. (2006). Analysis of LiDAR-derived topographic information for characterizing and differentiating landslide morphology and activity. *Geomorphology, 73*, 131-148.

Harding, D. J., Lefsky, M. A., Parker, G. G., & Blair, J. B. (2001). Laser altimeter canopy height profiles: Methods and validation for closed-canopy, broadleaf forests. *Remote Sensing of Environment, 76*, 283-297.

Hemstrom, M. A., Wisdom, M. J., Hann, W. J., Rowland, M. M., Wales, B. C., & Gravenmier, R. A. (2002). Sagebrush-steppe vegetation dynamics and restoration potential in the interior Columbia Basin, U.S.A. *Conservation Biology, 16,* 1243-1255.

Hodgson, M. E., Jensen, J. R., Schmidt, L., Schill, S., & Davis, B. (2003). An evaluation of LIDAR- and IFSAR-derived digital elevation models in leaf-on conditions with USGS Level 1 and Level 2 DEMs. *Remote Sensing of Environment, 84,* 295-308.

Hofton, M. A., Rocchio, L. E., Blair, J. B., & Dubayah, R. (2002). Validation of Vegetation Canopy Lidar sub-canopy topography measurements for a dense tropical forest. *Journal of Geodynamics, 34,* 491-502.

Humphrey, L. D. (1984). Patterns and mechanisms of plant succession after fire on *Artemisia*-grass sites in southeastern Idaho. *Vegetatio, 57,* 91-101.

Isaaks, E. H., & Srivastava, R. M. (1989). *Applied Geostatistics*. New York: Oxford University Press 561 pp.

Knick, S. T. (1999). Requiem for a sagebrush ecosystem? *Northwest Science, 73,* 53-57.

Knick, S. T. and Rotenberry, J. T. (1997). Landscape characteristics of disturbed shrubsteppe habitats in southwestern Idaho (U.S.A.). *Landscape Ecology, 12,* 287-297.

Latypov, D. (2002). Estimating relative LiDAR accuracy information from overlapping flight lines. *ISPRS Journal of Photogrammetry & Remote Sensing, 56,* 236-245.

McIver, J. and Starr, L. (2001). Restoration of degraded lands in the interior Columbia River Basin: Passive vs. Active approaches. *Forest Ecology and Management, 153,* 15-28.

Meinguet, J. (1979). Multivariate interpolation at arbitrary points made simple. *Journal of Applied Mathematics and Physics, 30,* 292-304.

Mundt, J. T., Streutker, D. R., & Glenn, N. F. (2006). Mapping sagebrush distribution using fusion of hyperspectral and lidar classifications. *Photogrammetric Engineering & Remote Sensing, 72,* 47-54.

NPCC (2004). Upper Snake subbasin assessment. Northwest Power and Conservation Council, Portland, Oregon, 75 pp.

Popescu, S. C., Wynne, R. H., and Nelson, R. F. (2002). Estimating plot-level tree heights with lidar: Local filtering with a canopy-height based variable window size. *Computers and Electronics in Agriculture, 37,* 71-95.

Rango, A., Chopping, M. J., Ritchie, J. C., Havstad, K., Kustas, W., & Schmugge, T. (2000). Morphological characteristics of shrub coppice dunes in desert grasslands of southern New Mexico derived from scanning LIDAR. *Remote Sensing of Environment, 76,* 26-44.

Riaño, D., Valladares, F., Condés, S., & Chuvieco, E. (2004). Estimation of leaf area index and covered ground from airborne laser scanner (lidar) in two contrasting forests. *Agricultural and Forest Meteorology, 124,* 269-275.

Ritchie, J. C., Humes, K. S., & Weltz, M. A. (1995). Laser altimeter measurements at Walnut Gulch watershed, Arizona. *Journal of Soil and Water Conservation, 50*, 440-442.

Seefeldt, S. S. and McCoy, S. D. (2003). Measuring plant diversity in the tall threetip sagebrush steppe: Influence of previous grazing management practices. *Environmental Management, 32*, 234-245.

Seielstad, C. A. and Queen, L. P. (2003). Using airborne laser altimetry to determine fuel models for estimating fire behavior. *Journal of Forestry*, *101*, 10-15.

Weltz, M. A., Ritchie, J. C., & Fox, H. D. (1994). Comparison of laser and field measurements of vegetation height and canopy cover. *Water Resources Research*, *30*, 1311-1319.

West, N. E. (1999). Managing for biodiversity of rangelands. In W. W. Collins, & C. O. Qualset (Eds.), *Biodiversity in Agroecosystems* (pp. 101-126). Boca Raton, Florida: CRC Press

Interactive Effects of Fire, Grazing, and Precipitation on Long-Term Variability in Remotely Sensed Indices of Vegetation

Ryan E. Baum, Department of Biological Sciences, Idaho State University, Pocatello ID 83209-8007.

Matthew J. Germino, Department of Biological Sciences, Idaho State University, Pocatello ID 83209-8007. (**germmatt@isu.edu**)

ABSTRACT
We evaluated the interactive effects of fire and grazing disturbances on satellite-derived measures of vegetation, particularly as they vary in space and time with yearly precipitation (PPT), over 20 years and nearly 300 km^2 of semiarid sagebrush-steppe. Some grazing systems may promote shrub cover and fire temporarily excludes dominant sagebrush species, so we also compared spatio-temporal patterns of disturbed areas with undisturbed areas with and without sagebrush within sagebrush-steppe ecosystems at the Idaho National Lab, in cold desert of the Great Basin, USA.

Remote sensing was used to calculate a soil-adjusted vegetation index ($MSAVI_2$) from Landsat satellite data, for the period of peak biomass in each year from 1984-2004. Differences in the mean or coefficient of variation (CV) of $MSAVI_2$ were determined for sites that (1) were either unburned in the previous 70 years, or burned in 1994, 1995, or 1996, and (2) either had livestock grazing excluded since 1950, or have been regularly grazed over the past century. Correlations of mean and CV of $MSAVI_2$ and 3 year sliding averages of PPT were determined for each disturbance type, for the 8-10 years following each fire. Livestock grazing did not affect mean $MSAVI_2$, and fire led to increases in mean $MSAVI_2$ in the second year after burning only. In contrast, the CV of $MSAVI_2$ among pixels within one image (i.e. spatial variation; $CV_{spatial}$) was lower in grazed compared to ungrazed areas, and increased for 1-3 years following fire. Short-term effects of fire on CV of $MSAVI_2$ were more persistent on grazed lands, and occurred irrespective of significant climate variability among burn years. Yearly $CV_{spatial}$ of $MSAVI_2$, but not mean $MSAVI_2$, was correlated with PPT ($r^2 = 0.47 – 0.70$). The slope of the relationship between $CV_{spatial}$ of $MSAVI_2$ and PPT was least positive in grazed areas, but 78% steeper (and steepest of all disturbance regimes) in grazed areas that had also burned. In undisturbed areas, mean $MSAVI_2$ and the slope of yearly $CV_{spatial}$ of $MSAVI_2$ and PPT were about 40% greater in grasslands than in areas dominated by sagebrush.

Longer-term disturbance effects are more apparent in the spatio-temporal variability of greenness as measured by $MSAVI_2$, rather than in mean responses of $MSAVI_2$. Variability in $MSAVI_2$ had complex responses to interactions of disturbances, as indicated by negative responses to grazing, positive responses to fire, but even more positive responses to the combination of grazing and fire. Conversion of vegetation type, as well as modification of responses to yearly changes in PPT, are likely ways that fire and grazing alter spatio-temporal variability of $MSAVI_2$.

Keywords: Disturbance, fire, geographic information systems, grazing, MSAVI, precipitation, remote sensing, sagebrush-steppe, spectral vegetation indices.

INTRODUCTION

Like most ecosystems, sagebrush (*Artemisia*) steppe in western North America experiences combinations of natural and anthropogenic disturbances. Sagebrush steppe is affected by annual variations in precipitation, abrupt disturbances such as fire, and disturbances such as livestock grazing that occur persistently over longer periods (Anderson and Inouye, 2001). Disturbances cause changes in communities and ecosystems (Pickett and White, 1985) that could modify climate-productivity relationships over the vast areas of sagebrush steppe in which they occur. Many studies investigated separate effects of fire or grazing on semiarid rangeland function (Anderson and Holte, 1981; Anderson and Inouye, 2001; Wambolt et al., 2001; Diaz-Delgado et al., 2002; Washington-Allen et al., 2004), but less is known about interactive effects of disturbances (Valone, 2003; Geiger and McPherson, 2005). Additionally, ecosystem responses to disturbance have mostly been studied at the small-scale, plot level (e.g., Anderson and Holte, 1981; Anderson and Inouye, 2001; West and Yorks, 2002), therefore, little quantitative information exists over large spatial and temporal scales (e.g., Washington-Allen et al., 2004) to help address the potentially complex effects of multiple disturbances on ecosystem structure and function. Large scale assessments of effects of weather variation, fire, and livestock grazing disturbances are needed to better match the scale at which rangeland management occurs as well as for global assessment of vegetation-climate relationships. Evaluations at larger scales are also important because ecological relationships can be scale dependent (e.g., Stohlgren et al., 1999; Small and McCarthy, 2003).

Remote sensing can provide periodic measures of vegetation over large areas that exceed measurement capabilities of traditional, ground-based assessments (Washington-Allen et al., 2004). Previous studies derived spectral vegetation indices (SVI's) from remotely sensed ratios of red and near-infrared reflectance to examine greenness of vegetation in rangeland ecosystems (e.g., Graetz and Gentle, 1982; Pickup and Foran, 1987; Graetz et al., 1988; Smith et al., 1990; Pickup et al., 1993; Elmore et al., 2000; Ramsey et al., 2004; Wallace et al., 2004). Greenness of earth surfaces, as measured by SVIs, is affected by chlorophyll concentrations and leaf abundance in the vertical plane (ie. leaf area index, "LAI", # leaf layers/unit ground area). SVIs are a valuable tool for large-scale assessment of ecosystem responses to precipitation and land-use (Paruelo and Lauenroth, 1998; Paruelo et al., 2001; Washington-Allen et al., 2004).

This study utilized a 20-year archive of Landsat data to determine the interactive effects of fire, livestock grazing, and precipitation change on the spatial and temporal variability of SVI's in sagebrush-steppe, relative to background variability in undisturbed areas. Water availability in these semi-arid rangelands is limited and highly variable in time (Anderson and Inouye, 2001), and primary production in semiarid lands can be tightly linked to variation in rainfall (LeHouerou et al., 1987). Long-term grazing tends to promote shrub cover (Laycock, 1967; Anderson and Holte, 1981; Brotherson and Brotherson, 1981; Anderson and Inouye, 2001) and fire temporarily promotes grass cover (Humphrey, 1984; Wambolt et al., 2001; West and Yorks, 2002). We hypothesized that lands with histories of grazing, fire, or no disturbance would not differ much in mean responses, but that histories of fire and grazing would lead to greater variability in SVIs in years following disturbance, due to changes in the sensitivity of SVIs to annual precipitation and conversions of community type. Thus, in addition to calculating mean SVIs, we assessed how disturbances and precipitation affected the stability of SVIs in space and time, measured as coefficient of variation of SVIs.

METHODS

Areas dominated by Wyoming Big Sagebrush (*Artemisia tridentata* Nutt ssp. *wyomingensis* Beetle and Young) with different fire and grazing histories since 1939 were identified from Bureau of Land Management (BLM) Geographic Information Systems (GIS) data within the Idaho National Laboratory (INL; Fig. 1; version 9, ArcGIS, ESRI, Redlands CA, USA). The INL is located on the Eastern Snake River Plain (Idaho), and was ideal for this study because of its relatively flat topography and large homogenous management units (livestock grazing allotments) where wildfires have occurred frequently

over the last two decades. Areas within 1 km buffers of wildfire perimeters were categorized as follows: 1) *Rest*, undisturbed areas where no fires have occurred since at least 1939, and livestock grazing has been excluded since 1950; 2) *Grazed*, areas within BLM grazing allotments that have been actively grazed since 1950; 3) *Burned*, non-grazed areas that have burned once from mid-late summer in 1994 – 1996 and not any other time since 1939; and 4) *Grazed/burned*, areas within BLM grazing allotments that have been actively grazed since 1950 and burned once from 1994 – 1996. No pixels within 90 m of boundaries of burn or grazed areas were included. We focused our study on areas that burned in 1994, 1995, or 1996 because they encompassed years of significant variation in precipitation, and provided 8 – 10 years of recovery after fire. Fires occurred elsewhere on the INL during our study period, but they were too recent to allow for adequate assessment of temporal variation in SVI's following fire. BLM summer stocking rates of domestic livestock (cattle and sheep) varied little over the last 20 years and ranged from 12.4 to 33.5 acres/active animal unit month (AUM). Grazing was excluded from burned areas for two years following fire.

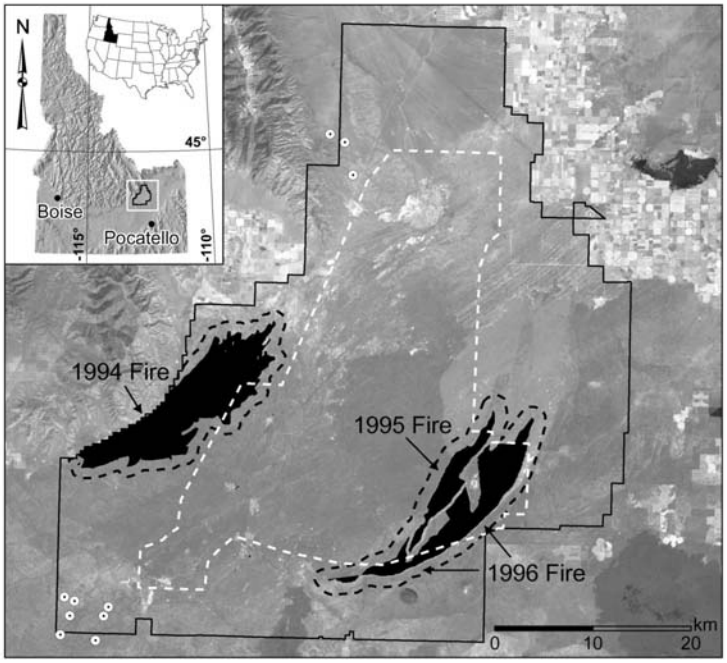

Figure 1. Map of the Idaho National Laboratory (INL, bound by solid black line) located on the Upper Snake River Plain (inset map; coordinates for Idaho) and the arrangement of four disturbance types in three replicate blocks around the 1994, 1995, and 1996 fires. Burn areas are shown in black, and livestock grazing has been excluded from area inside white dashes since 1950. Sampling areas within 1-km of burns are bound by black dashes. White circles indicate livestock watering sites for two grazing allotments on the INL. Image is derived from Landsat data.

We examined spatial and temporal variability in SVIs among lands with different histories of disturbance, in one cloud-free Landsat 5 Thematic Mapper (TM) or 7 Enhanced Thematic Mapper (ETM+) image per year. Image sampling dates were selected for 19 of the years from 1984 – 2004, in a 37-day window centered on 27-June. Fires in occurred from mid July through August, weeks after the Landsat sampling dates of the same years, and 11 to nearly 12 months prior to the next image acquisition. We were unable to use more sampling dates per year, due to cloud cover or data gaps. Landsat sampling dates corresponded to the peak summer growing season for sagebrush-steppe, as estimated by Paruelo and Lauenroth (1995 and 1998) for the INL using the maximum normalized difference vegetation index (NDVI) derived from Advanced Very High Resolution Radiometer (AVHRR) data. Pixels (30 m

resolution) were converted to at-satellite reflectance, coregistered, and radiometrically normalized with relative corrections for atmospheric attenuation using the empirical, multiple-date, regression method (Jensen, 1996).

The "second modified soil-adjusted vegetation index" ($MSAVI_2$, Qi et al. 1994) was calculated to quantify the greenness of sagebrush-steppe vegetation (version 4.1, ENVI, Research Systems Inc, Boulder CO, USA). $MSAVI_2$ minimizes soil background influences on vegetation signals by enhancing the red (band 3, 630-690 nm) and near-infrared (band 4, 750-900 nm) reflectance ratios (Qi et al., 1994). It was calculated as:

$$MSAVI_2 = \frac{2*(\text{band 4}) + 1 - \sqrt{(2*(\text{band 4}) + 1)^2 - 8*(\text{band 4} - \text{band 3})}}{2}$$

Total vegetation cover is commonly less than 50% or even 25% of ground area in sagebrush-steppe at the INL (Anderson and Inouye 2001; R. Blew, unpublished data). MSAVI has been used to quantify sparse vegetation cover in arid and semi-arid rangelands, and significantly correlates to field measures of canopy and areal ground cover (Senseman and Bagley, 1996; Purevdorj et al., 1998; McGwire et al., 2000). In arid environments with less than 25% vegetation cover, MSAVI had a higher and more constant sensitivity over the full range of plant cover compared to other soil-adjusted SVI's (Rondeaux et al.; 1996). Other soil-adjusted SVI's require constant, empirically defined, soil adjustment factors to minimize soil influences on canopy spectra (e.g., SAVI, soil-adjusted vegetation index), and are therefore difficult to apply in assessing impacts of disturbances that alter soil exposure (Rondeaux et al.; 1996). Defining an appropriate soil adjustment factor for pixels across an entire image, where the quantity and type of vegetation and soil is not constant, is likely to cause non-systematic errors in estimates of variation in SVI's among pixels that differ in soil exposure due to disturbance regime or variation in precipitation. $MSAVI_2$ is a variant of MSAVI that does not rely on pre-determined soil correction factors, because soil is adjusted for inductively by a term that varies inversely with the amount of vegetation present in each pixel (Qi et al., 1994). $MSAVI_2$'s increased sensitivity to vegetation is important for assessing the year-to-year variability of disturbed sagebrush-steppe rangelands where the total cover of vegetation is relatively low and soil exposure varies considerably with disturbance and precipitation.

Our analyses focused on calculations of mean $MSAVI_2$, the coefficient of variation (CV) of $MSAVI_2$ among years ("$CV_{temporal}$ of $MSAVI_2$"; CV = SD / mean * 100), and CV of $MSAVI_2$ among pixels with a year (i.e. within one image, "$CV_{spatial}$ of $MSAVI_2$"). Fire effects on $MSAVI_2$ were determined by comparing post-fire mean and CV of $MSAVI_2$ in both burned and non-burned (i.e. rest) lands the first and subsequent growing seasons after fire. Distances to livestock watering troughs had no effects on $MSAVI_2$, as assessed by examining variation in $MSAVI_2$ among areas that were either within 30 m, or were 30 m to 100 m, 100 m to 500 m, or 500 m to 1000 m from watering troughs (data not shown; troughs locations in Fig. 1). Thus, we examined all pixels within grazing allotments for assessments of grazing impacts.

To estimate the potential for interconversions of community type between shrub and grassland to explain disturbance effects on $MSAVI_2$, we compared mean and CV of $MSAVI_2$ between areas that were grazed, burned, or grazed/burned, to those areas that were undisturbed and either contained sagebrush or had no sagebrush and were dominated by grass. Vegetation communities were identified from previous field surveys and vegetation classifications of the INL (Kramber et al., 1992, and subsequent monitoring by R. Blew for US Department of Energy).

Statistical Analyses

Areas containing each of the four disturbance regime types (undisturbed rest, grazed, burned, and grazed/burned) around each of the 1994, 1995, or 1996 burns were our unit of replication, resulting in n=3 complete blocks of disturbance types (Fig. 1). One-way ANOVA was used to detect differences in

mean or CV of $MSAVI_2$ among the four disturbance types within individual years (i.e., within one image). Repeated-measures MANOVA was used to detect differences among disturbance or community types (sagebrush or grass in undisturbed areas) when comparisons included sampling over multiple years. The significance of differences in the relationship between precipitation (PPT) and mean or CV of $MSAVI_2$ among the disturbance and community types were investigated using linear, least-squares regression. Relationships between PPT and $MSAVI_2$ over years were examined using sliding averages of PPT each the image year (cumulative from January to image date; 'yearly PPT') and total cumulative PPT in each of the two previous years. Cumulative yearly PPT had greater correlations with $MSAVI_2$ (higher r^2 values) than did water-year PPT (cumulative from October to image date) or growing-season PPT (cumulative from April to image date). Anderson and Inouye (2001) also found that ground-based measures of cover at INL were best correlated with 3-year sliding averages of yearly PPT, compared to other statistical representations of PPT. Precipitation data were from the INL Central Facilities Area station (Western Regional Climate Center, Desert Research Institute, Reno NV). Over the study period, three-year averages of yearly PPT ranged from 246.7 mm to 77.34 mm, with the highest PPT occurring in 1985 and 1995, and the lowest PPT occurring in 1990 and 2001-2004 (Fig. 2). One-way ANOVA and Kruskal-Wallis tests were used to detect differences in the slope of the relationships between PPT and mean or CV of $MSAVI_2$ among the disturbance types, with three replicates of each disturbance type, as described above.

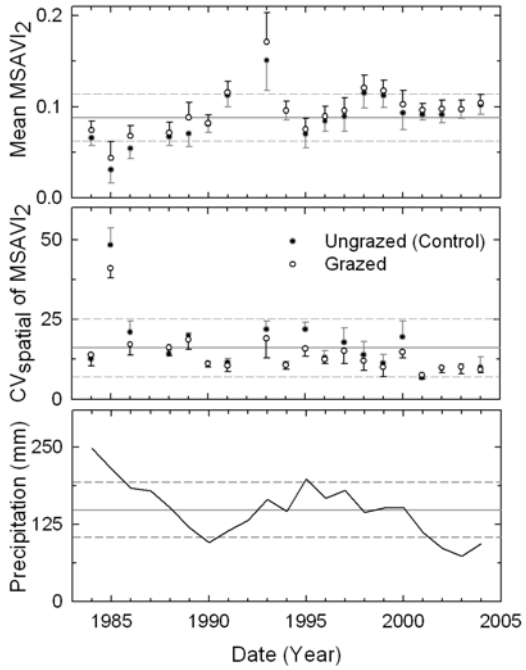

Figure 2. Mean and $CV_{spatial}$ (%) of $MSAVI_2$ for unburned pixels of ungrazed (rest, solid symbols) and grazed areas (open) on the INL from 11 June to 17 July in 1984 – 2004; and sliding, 3-yr averages of yearly precipitation during the study period. Errors for individual data points are shown as + or – 1 SD, and are not shown in ± for clarity. Solid and dashed horizontal lines show mean ± 1 SD values for rest areas over all 20 years.

RESULTS

Mean $MSAVI_2$ of undisturbed lands fluctuated significantly over the 20-year period, ranging from 0.03 in 1985 to 0.l5 in 1993 (Fig. 2; $F_{18,56} = 12.60$, $P < 0.0001$). Mean $MSAVI_2$ among the 20 years ranged from 0.03 to 0.15 in sagebrush and 0.06 to 0.22 in grasslands (data not shown; $F_{1,37} = 2.94$, $P = 0.10$ for mean differences). Mean $MSAVI_2$ over the whole study period was not different between undisturbed-rest and

grazed areas (Fig. 2). Variation in $MSAVI_2$ among years ($CV_{temporal}$ of $MSAVI_2$) was similar among undisturbed sagebrush (29.6%) and grasslands (31.6%); and ungrazed (29.6%) and grazed (27.8%) areas (Fig. 2, top panel). $CV_{spatial}$ of $MSAVI_2$ (variation in $MSAVI_2$ among pixels within each image) varied significantly among years in undisturbed areas (6–48%, $F_{18,56} = 32.96$, $P < 0.0001$), but varied only marginally among years in grazed areas (8–41%, $F_{18,72} = 1.82$, $P = 0.11$; Fig. 2).

History of disturbance and time since fire had a significant, interactive effect on mean $MSAVI_2$ in the second growing season after fire, only (Fig. 3; $F_{6,16} = 3.51$, $P < 0.05$). Specifically, mean $MSAVI_2$ in grazed and ungrazed areas alike increased 40% in the second growing season following fire ($F_{1,18} = 28.31$, $P < 0.0001$), compared to average background increases of 14% in pixels of unburned areas surrounding each burn (Fig. 3; $F_{1,18} = 12.96$, $P < 0.001$). There were otherwise no differences in mean $MSAVI_2$ among disturbance types over all 8-10 growing seasons after fire, with mean values ± 1 SD ranging from only 0.10 ± 0.01 in undisturbed rest areas to 0.11 ± 0.02 in grazed/burned areas. Inter-annual variability ($CV_{temporal}$) of $MSAVI_2$ following all fires combined was up to 2-fold greater in pixels in burned (15.9%) and grazed/burned areas (16.2%) compared to rest (6.6%) and grazed-only areas (7.3%; calculations for Fig. 3; $F_{3,12} = 7.63$, $P < 0.05$).

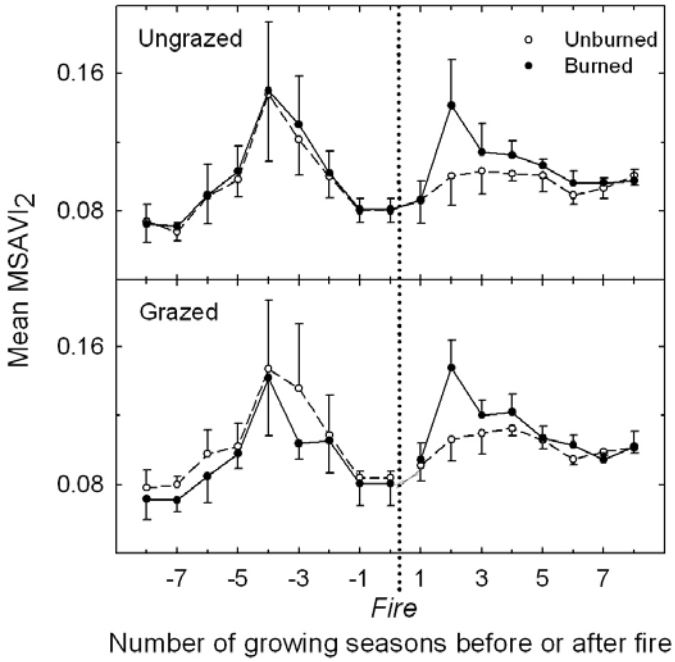

Figure 3. Mean $MSAVI_2$ (+ or – 1 SE) from 11 June to 17 July among ungrazed (top panel) and grazed lands (bottom panel) before or after fire. Solid vertical line shows time of fire in late summer of either 1994, 1995, or 1996; and scale on x-axis is year relative to year of fire. N = 3 burn-year blocks.

$CV_{spatial}$ of $MSAVI_2$ was 37% greater in burned and grazed/burned areas compared to rest and grazed-only areas in the first post-fire year (Fig. 4; $F_{3,11} = 3.12$, $P = 0.09$). Post-fire recovery (decreases) of $CV_{spatial}$ of $MSAVI_2$ to levels observed in unburned areas appeared to occur more quickly in ungrazed compared to grazed areas ($F_{3,8} = 3.10$, $P = 0.09$), and by the fourth year after fire, no significant differences in $CV_{spatial}$ of $MSAVI_2$ were detectable among disturbance types. $CV_{spatial}$ of $MSAVI_2$ of undisturbed rest areas decreased progressively following burning of neighboring areas, after 1994-1996 (Fig. 4; $F_{2,16} = 6.16$, $P = 0.01$), corresponding to a trend of decreasing yearly PPT.

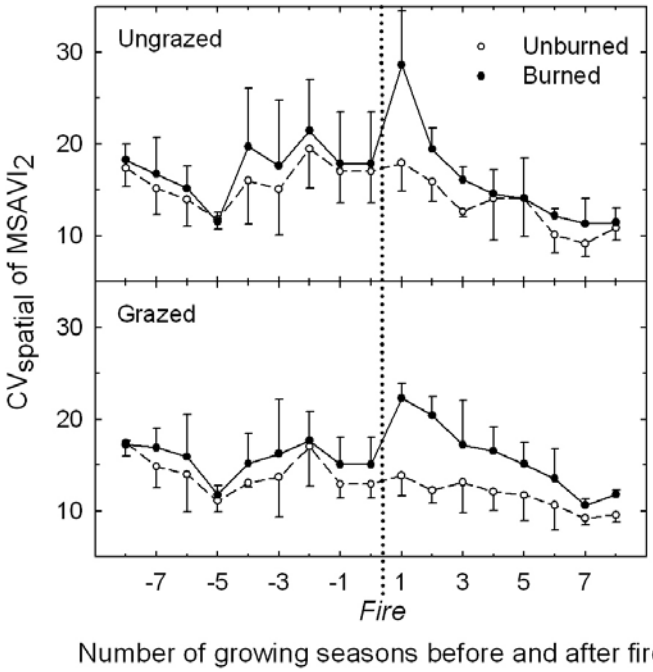

Figure 4. Mean CV of $MSAVI_2$ (+ or – 1 SE) among pixels ($CV_{spatial}$) for ungrazed (top) and grazed lands (bottom) before or after fire (N = 3 burn-year blocks). See Fig. 3 for plotting details.

Mean $MSAVI_2$ was weakly or uncorrelated with sliding, three-year averages of cumulative yearly PPT for lands in all disturbance types alike (Table 1), in contrast to greater correlations of $CV_{spatial}$ of $MSAVI_2$ and yearly PPT (Table 2). Moreover, greater correlations of $CV_{spatial}$ of $MSAVI_2$ and PPT were detected in burned areas than in undisturbed rest areas and grazed plots. Specifically, mean r^2/P values for the regressions in all burn-year blocks were 0.57/0.03 and 0.59/0.06 in grazed/burned and burned areas, compared to 0.43/0.06 in undisturbed rest areas and an insignificant 0.26/0.35 in grazed areas that did not burn (calculated from Table 2). The slope of the relationship between $CV_{spatial}$ and PPT in burned areas was 51% steeper than in rest areas, and 78% steeper than in grazed areas ($F_{3, 11} = 10.80$, $P = 0.03$, Fig. 5, Table 2). Mean ± SE slopes of the relationship between $CV_{spatial}$ and PPT in over the three undisturbed areas around each burn were 41% steeper in grasslands (0.15± 0.01) than in sagebrush (0.11± 0.01; $F_{1, 5} = 10.80$, $P = 0.03$).

DISCUSSION

Previous, ground-based studies measured mean changes in plant cover of sagebrush-steppe in response to wildfire or grazing disturbances (e.g., Laycock, 1967; Brotherson and Brotherson, 1981; Humphrey, 1984; Wambolt, 2001; West and Yorks, 2002). However, we found that variability of $MSAVI_2$ was more sensitive to disturbance than mean $MSAVI_2$ for 8 – 10 years following fire. Spatio-temporal variability in greenness among 30 x 30 m units of ground area and years emerged as more responsive than average greenness over km^2 and decades. Mean $MSAVI_2$ among burned lands increased only in the second growing season following fire compared to unburned lands (Fig. 3), but mean $CV_{spatial}$ of $MSAVI_2$ was greater in fire-disturbed lands for up to three growing seasons after fire (Fig. 4). These immediate responses to fire (within 3 years) were consistently observed despite climate variations among the burn years (Figs. 2-4). In addition to these shorter-term responses, longer-term variability following fire appeared to result from increased coupling of $CV_{spatial}$ of (but not mean) $MSAVI_2$ to inter-annual changes in precipitation (Fig. 5). Thus, fire and grazing influenced the stability (or, spatio-temporal constancy) of $MSAVI_2$ measures in sagebrush-steppe in ways that were more persistent and different from effects that might result from their direct, immediate impacts of vegetation removal.

Table 1. Correlations of yearly mean $MSAVI_2$ and sliding three-year averages of cumulative yearly precipitation, in each disturbance type and burn-year block (burns in 1994, 1995, or 1996), as well as portions of undisturbed rest areas dominated by sagebrush or grassland. N indicates the number of years following each fire up to 2004 included in regression analyses.

	Burn year	**r^2**	***P***	**Slope**	**N**
Sagebrush, in rest	1994	0.186	0.214	0.000	10
	1995	0.017	0.741	0.000	9
	1996	0.002	0.903	0.000	8
Grassland, in rest	1994	0.006	0.834	0.000	10
	1995	0.073	0.483	0.000	9
	1996	0.177	0.300	0.000	8
Rest	1994	0.376	0.060	0.000	10
	1995	0.036	0.624	0.000	9
	1996	0.253	0.204	0.000	8
Grazed	1994	0.071	0.458	0.000	10
	1995	0.035	0.629	0.000	9
	1996	0.147	0.349	0.000	8
Burned	1994	0.223	0.169	0.000	10
	1995	0.343	0.097	0.000	9
	1996	0.171	0.309	0.000	8
Grazed/Burned	1994	0.025	0.662	0.000	10
	1995	0.416	0.061	0.000	9
	1996	0.281	0.177	0.000	8

Although mean $MSAVI_2$ significantly increased among burned areas in the second growing season following fire, it appeared to recover to levels similar to nearby unburned lands by the third growing season after fire. These results contrast previous findings of post-fire vegetation recovery in Mediterranean oak-pine ecosystems, where NDVI (normalized difference vegetation index) derived from Landsat decreased substantially following fire, but recovered to pre-fire levels after about a decade (Diaz-Delgado et al., 2002). Post-fire increases in SVI's in sagebrush-steppe may be attributable to lower standing biomass and corresponding leaf area before fire in shrubland compared to forests, which allows for relatively quicker regeneration of leaf area to equal or greater levels than pre-fire conditions in shrub steppe. Resprouting annual and perennial grasses and forbs tend to increase in abundance in response to fire in sagebrush steppe (Humphrey, 1984; West and Yorks, 2002), probably in compensation to overall reductions of dominant sagebrush, a non-resprouting species that recovers slowly after fire (>decades). Plants that initially colonize burns also can be enriched in the soil nutrients that temporarily become more available after fire, and correspondingly can have greater LAI or concentrations of chlorophyll (DeBano et al. 1998), and thereby could express more greenness to satellite sensors. Our observations of greater mean $MSAVI_2$ in burned compared to unburned pixels corresponds with greater $MSAVI_2$ and SVI values in grassland compared to sagebrush communities measured here and by others (Kremer and Running,

1993; Paruelo and Lauenroth, 1995; Weiss et al., 2004; Bradley and Mustard, 2005). Although sagebrush has greater biomass per unit ground area than grasses, much of the biomass is non-photosynthetic. Thus, short-term increases in $MSAVI_2$ after fire may result in part from conversion to grasses and intrinsically greater greenness of grasslands, though the duration and magnitude of changes of fire-induced changes in $MSAVI_2$ were less than expected if changes were entirely attributable to conversion to grassland. Progressive reductions in $MSAVI_2$ towards rest levels following the 2nd post-fire year could reflect establishment of new plants on otherwise unvegetated soil, and dilution of growth resources, leaf area, and chlorophyll from a few colonizing plants to greater horizontal plant cover.

Table 2. Correlations of yearly $CV_{spatial}$ of $MSAVI_2$ and sliding three-year averages of cumulative yearly precipitation, in each disturbance type and burn-year block (1994, 1995, or 1996), as well as portions of undisturbed rest areas dominated by sagebrush or grassland. N indicates the number of years following each fire up to 2004 included in regression analyses.

	Burn year	**r^2**	***P***	**Slope**	**N**
Sagebrush, in rest	1994	0.545	0.015	0.104	10
	1995	0.440	0.051	0.098	9
	1996	0.633	0.018	0.124	8
Grassland, in rest	1994	0.505	0.021	0.149	10
	1995	0.392	0.071	0.137	9
	1996	0.576	0.029	0.175	8
Rest	1994	0.466	0.030	0.057	10
	1995	0.355	0.091	0.075	9
	1996	0.456	0.066	0.064	8
Grazed	1994	0.647	0.005	0.058	10
	1995	0.080	0.460	0.015	9
	1996	0.064	0.545	0.014	8
Burned	1994	0.631	0.006	0.080	10
	1995	0.568	0.019	0.105	9
	1996	0.556	0.034	0.186	8
Grazed/Burned	1994	0.701	0.003	0.124	10
	1995	0.465	0.043	0.086	9
	1996	0.556	0.034	0.186	8

Our measurements of less spatio-temporal variability of $MSAVI_2$ in grazed lands compares with similar findings from ground-based studies (Adler and Lauenroth, 2000; Adler et al., 2001), but contrasts greater variability detected in $MSAVI_2$ following fire (Figs. 4-5). Less spatio-temporal variability in grazed lands might reflect removal of patches of greater herbaceous growth in wet years or patches by livestock (as suggested by Anderson and Inouye, 2001). Grazing and fire effects on spatio-temporal variability could also result partly from interconversion of community types, as discussed for mean responses of $MSAVI_2$. Specifically, relative decreases or increases in variability of $MSAVI_2$ following grazing or fire,

respectively, correspond with promotion of shrubs by grazing and exclusion of shrubs by fire. Spatial variability in $MSAVI_2$ was less in undisturbed sagebrush compared to grass-dominated communities, especially in relation to annual changes in precipitation (Table 2). Similarly, NDVI variability in time was greater in areas dominated by annual grass compared to shrubs, in other regions of the Great Basin (Bradley and Mustard, 2005). Plots with higher shrub densities tended to exhibit less variability in cover from year-to-year than plots with low shrub densities, over 45 years of ground-based monitoring at INL (Anderson and Inouye, 2001). Similarly, ground measures of cover varied less for Wyoming big sagebrush than herbaceous and annual species, in response to drought (West and Yorks, 2002; also estimated from ground data in Passey et al., 1982). Less spatio-temporal variability of $MSAVI_2$ in sagebrush compared to herb-dominated communities, especially in response to variable PPT, could result from the evergreen habit of sagebrush, which enables retention of leaf area produced in favorable conditions through less favorable periods. As noted for mean responses of $MSAVI_2$, the magnitude and duration of fire-induced changes in variability in $MSAVI_2$ were not fully matched by changes that would be expected from conversion to grassland alone. Thus, other factors that we cannot identify likely contributed to changes in variability in greenness among 30 x 30 m ground areas following fire.

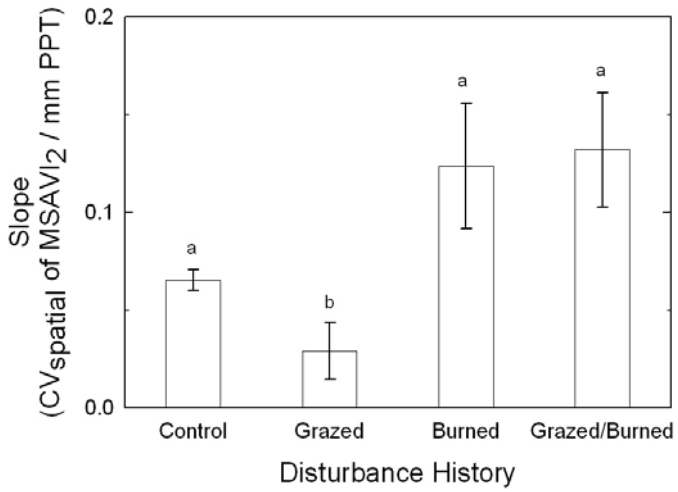

Figure 5. Mean slopes (± SE) of relationships between sliding 3-yr averages of cumulative yearly precipitation (PPT, from April 1 to image date) and post-fire $CV_{spatial}$ of $MSAVI_2$ among pixels, for lands with different histories of disturbance. Values are means for replicate areas matched to the 1994, 1995, or 1996 burns (n=3). See Table 2 for regression statistics.

More persistent increases in $CV_{spatial}$ of $MSAVI_2$ following fire on grazed compared to ungrazed lands may be attributable to more than conversion of shrubs to grasses (Fig. 4). Greater fuel loads result from promotion of shrub over grass cover by livestock grazing, leading hotter fires (DeBano et al., 1998). Increased fire severity may lead to greater site alterations (e.g. changes in soil physical properties) than just exclusion of shrubs, leading to greater spatial and temporal variability in $MSAVI_2$ following fire. Also, fewer herbs prior to burning should lead to fewer resprouting herbs in the first year after fire on grazed lands, and post-fire heterogeneity in establishment of new herbs could contribute to greater spatio-temporal variability in $MSAVI_2$.

SUMMARY

Semiarid shrub-grasslands cover a large portion of the global land area, and are regularly affected by fire, grazing, and variability in precipitation (Frank and Inouye 1994). Grazing and fire effects were less evident in average greenness over kilometers^2 and decades than in spatial variability of greenness at the scale of 30 x 30 m areas and yearly timesteps. Interactive effects of grazing and fire may be complex, as indicated by decreased spatio-temporal variability of greenness in response to grazing, but increases in

response to fire, and especially grazing followed by fire. Patches of landscapes appear to vary in their sensitivity to fire, and the combination of fire, grazing, and precipitation. Longer-term effects of fire and grazing appear to result from modification of the linkage between spatio-temporal variability of greenness and variability in PPT. Changes in spatio-temporal variability are an important issue for efforts to utilize multispectral satellite imagery, such as Landsat, to map community types or assess responses of ecosystem productivity to climate variability. Legacies of disturbances affect the certainty of multi-spectral signatures related to vegetation, particularly as they relate to climate variability over large scales.

ACKNOWLEDGEMENTS
This study was made possible by a grant from the National Aeronautics and Space Administration Goddard Space Flight Center. ISU would also like to acknowledge the Idaho Delegation for their assistance in obtaining this grant. Ronald C. Rope (INL), Glenn Guenther and Brett Herres (US Department of Interior, Bureau of Land Management) provided site information and access, and Richard Inouye, Teri Peterson, and Nancy Glenn provided helpful comments.

LITERATURE CITED

Adler, P.B. and Lauenroth, W.K. (2000) Livestock exclusion increases the spatial heterogeneity of vegetation in Colorado shortgrass steppe, *Applied Vegetation Science* 3, 213-222.

Adler, P.B., Raff, D.A. and Lauenroth, W.K. (2001) The effect of grazing on the spatial heterogeneity of vegetation. *Oecologia*, 128, 465-479.

Anderson, J.E. and Holte, K.E. (1981) Vegetation development over 25 years without grazing on sagebrush-dominated rangeland in southeastern Idaho. *Journal of Rangeland Management*, 34, 25-29.

Anderson, J.E. and Inouye, R.S. (2001) Landscape-scale changes in plant species abundance and biodiversity of a sagebrush steppe over 45 years. *Ecological Monographs*, 71, 531-556.

Bradley, A.B. and Mustard, J.F. (2005) Identifying land cover variability distinct from land cover change: Cheatgrass in the Great Basin. *Remote Sensing of Environment* 94, 204-213.

Brotherson, J.D. and Brotherson, W.T. (1981) Grazing impacts on the sagebrush communities of central Utah. *Great Basin Naturalist*, 41, 335-340.

Daddy, F., Trlica, M.J. and Bonham, C.D. (1988) Vegetation and soil water differences among big sagebrush communities with different grazing histories. *Southwestern Naturalist*, 33, 413-424.

DeBano, L.F., Neary, D.G. and Ffolliott, P.F. (1998) Fire's effects on ecosystems. John Wiley and Sons, Inc., New York, NY. 333 pp.
Diaz-Delgado, R., Francisco, L., Pons, X., and Terradas, J. (2002) Satellite evidence of decreasing resilience in Mediterranean plant communities after recurrent wildfires, *Ecology*, 83, 2293-2303.

Foran, B.D. and Pickup, G. (1987) The use of spectral and spatial variability to monitor cover change on inert landscapes. *Remote Sensing of Environment*, 23, 351-363.

Geiger, E.L. and McPherson, G.R. (2005) Response of semi-desert grasslands invaded by non-native grasses to altered disturbance regimes. *Journal of Biogeography*, 32, 895-902.

Graetz, R.D., and Gentle, M.R (1982) The relationships between reflectance in the Landsat wavebands and the composition of an Australian semi-arid shrub rangeland. *Photogrammetric Engineering and Remote Sensing*, 48, 1721-1730.

Humphrey, L.D. (1984) Patterns and mechanisms of plant succession after fire on Artemisia-grass sites in southeastern Idaho. *Vegetatio*, 57, 91-101.

Jensen, J.R. (1996) Introductory digital image processing. Prentice-Hall, Inc., Upper Saddle River, NJ. 318 pp.

Kramber, W.J., R.C. Rope, J.E. Anderson, J. Glennon, and A. Morse. 1992. Producing a vegetation map of the Idaho National Engineering Lab using Landsat thematic mapper data. American Society for Photogrammetry and Remote Sensing/American Congress on Surveying and Mapping Annual Meeting Technical Papers Vol. 1:217-226.

Kremer, R.G., and Running, S.W. (1993) Community type differentiation using NOAA/AVHRR data within a sagebrush-steppe ecosystem. *Remote Sensing of Environment*, 46, 311-318.

Lauenroth, W.K., and Sala, O.E. (1992) Long-term forage production of North American shortgrass steppe. *Ecological Applications*, 2, 397-403.

Laycock, W.A. (1991) Stable states and thresholds of range condition on North American rangelands: A viewpoint. *Journal of Range Management*, 44, 427-433.

Laycock, W.A. (1967) How heavy grazing and protection affect sagebrush-grass ranges. *Journal of Range Management*, 20, 206-213.

Le Houerou, H.N., Bingham, R.L. and Skerbek, W. (1988) Relationship between the variability of primary production and the variability of annual precipitation in world arid lands. *Journal of Arid Environments*, 15, 1-18.

McGwire, K., Minor, T. and Fenstermaker L. (2000) Hyperspectral mixture modeling for quantifying sparse vegetation cover in arid environments. *Remote Sensing of Environment*, 72: 360-374.

Milchunas, D.G. and Lauenroth, W.K. (1993) Quantitative effects of grazing on vegetation and soils over a global range of environments. *Ecological Monographs*, 63, 327-366.

Passey, H.B., Hugie, V.K., Williams, E.W. and Ball, D.E. (1982) Relationships between soil, plant community, and climate on rangelands of the Intermountain West. Technical Bulletin Number 1669. USDA Soil Conservation Service, Washington, D.C., USA.

Paruelo, J.M., Burke, I.C. and Lauenroth, W.K. (2001) Land-use impact on ecosystem functioning in eastern Colorado, USA. *Global Change Biology*, 7, 631-639.

Paruelo, J.M. and Lauenroth, W.K. (1998) Interannual variability of NDVI and its relationship to climate for North American shrublands and grasslands. *Journal of Biogeography*, 25, 721-733.

Paruelo, J.M. and Lauenroth, W.K. (1995) Regional patterns of normalized difference vegetation index in North American shrublands and grasslands. *Ecology*, 76, 1888-1898.

Pickett, S.T.A. and White P.S.E. (1985) The ecology of natural disturbance and patch dynamics. Academic Press, Orlando, FL.

Pickup, G., Chewings, V.H. and Nelson D.J. (1993) Estimating changes in vegetation cover over time in arid rangelands using Landsat MSS data. *Remote Sensing of Environment*, 43, 243-263.

Pickup, G. and Foran, B.D. (1987) The use of spectral and spatial variability to monitor cover changes on inert landscapes. *Remote Sensing of Environment*, 23, 351-363.

Purevdorj, T., Tateishi, R., Ishiyama, T. and Honda Y. (1998) Relationship between percent vegetation cover and vegetation indices. *International Journal of Remote Sensing*, 19, 3519-3535.

Qi, J., Chehbouni, A., Huete, A.R., Kerr, H. and Sorooshian, S. (1994) A modified soil adjusted vegetation index. *Remote Sensing of Environment*, 48, 119-126.

Ramsey, R.D., Wright, Jr. D.L., and McGinty. C. (2004) Evaluating the use of Landsat 30m Enhanced Thematic Mapper to monitory vegetation cover in shrub-steppe environments. *Geocarto International*, 19, 39-47.

Reed, B.C., Brown, J.F., VanderZee, D., Loveland, T.R., Merchant, J.W. and Ohlen, D.O. (1994) Measuring phenological variability from satellite imagery. *Journal of Vegetation Science*, 5, 703-714.

Rondeaux, G., Steven, M. and Baret, F. (1996) Optimization of soil-adjusted vegetation indices. *Remote Sensing of Environment*, 55, 95-107.

Senseman, G.M. and Bagley, C.F. (1996) Correlation of rangeland cover measures to satellite-imagery-derived vegetation indices. *Geocarto International*, 11, 29-38.

Small, C.J. and McCarthy B.C. (2003) Spatial and temporal variability of herbaceous vegetation in an eastern deciduous forest, *Plant Ecology*, 164, 37-48.

Stohlgren, T.J., Binkley, D., Chong, G.W., Kalkhan, M.A., Schell, L.D., Bull, K.A., Otsuki, Y. Newman, G., Bashkin, M. and Son, Y. (1999) Exotic plant species invade hot spots of native plant diversity, *Ecological Monographs,* 69, 25-46.

Valone, T.J. (2003) Examination of interaction effects of multiple disturbances on an arid plant community, *Southwestern Naturalist*, 48, 481-490.

Wallace, J.F., Caccetta, P.A. and Kiiveri. H.T. (2004) Recent developments in analysis of spatial and temporal data for landscape qualities and monitoring, *Austral Ecology*, 29, 100-107.

Wambolt, C.L., Walhof, K.S. and Frisina, M.R. (2001) Recovery of big sagebrush communities after burning in south-western Montana, *Journal of Environmental Management*, 61, 243-252.

Washington-Allen, R.A., Ramsey, R.D. and West, N.E. (2004) Spatiotemporal mapping of the dry season vegetation response of sagebrush steppe, *Community Ecology*, 5, 69-79.

Weiss, J.L., Gutzler, D.S., Coonrod, J.E. and Dahm, C.N. (2004) Long-term vegetation monitoring with NDVI in a diverse semi-arid setting, central New Mexico, USA. *Journal of Arid Environments*, 58, 248-271.

West, N.E. and Yorks, T.P. (2002) Vegetation responses following wildfire on grazed and ungrazed sagebrush semi-desert. *Journal of Range Management*, 55, 171-181.

West, N.E. and Young, J.A. (2000) Intermountain valleys and lower mountain slopes. In: M.G. Barbour and W.D. Billings (eds), *North American Terrestrial Vegetation*. 2nd ed. Cambridge Univ. Press, New York, NY. pp. 255-284.

West, N.E., Rea, K.H. and Harniss, R.O. (1979) Plant demographic studies in sagebrush-grass communities of southeastern Idaho. *Ecology,* 60, 376-388.

Whitford, W.G. (2002) Ecology of Desert Systems. Academic Press, London. 343 pp.

Challenges of Integrating Geospatial Technologies into Rangeland Research and Management

Keith T. Weber, GIS Director, Idaho State University, GIS Training and Research Center, Campus box 8130, Pocatello, ID 83209-8130. (webekeit@isu.edu)

ABSTRACT
With the development and commercial availability of sub-meter spatial-resolution satellite imagery, geospatial tools can accommodate the needs of range professionals better than ever before. However, with these new tools comes a new set of challenges. Range managers and range scientists must now: 1) better understand and take advantage of the geotechnical tools at their disposal, 2) collect field observations/measurements in ways that act synergistically with these tools, and 3) utilize high-accuracy global positioning system receivers. To produce reliable rangeland models it is important to collect field data which corresponds with what the satellite "sees". Further, it is frequently necessary to use high-resolution imagery which subsequently necessitates the use of high-accuracy global positioning system receivers to ensure field data is recorded in the correct pixel and properly co-registered. This paper describes the results of research and experimentation that have lead to the development of techniques to improve geo-spatial rangeland applications. For optimal classification accuracy, field data collected for use in remote sensing applications should estimate/measure ground cover using general vegetation community types and must never exceed 100%. Further, the field sample sites used for classification must be located using a global positioning system receiver with accuracy ≤50% of the size of satellite imagery pixels (e.g., if Landsat imagery is used –with 28.5m pixels—the GPS receiver must be able to achieve ±14m accuracy with 95% confidence). Finally, a series of best practices are suggested to help range managers and range scientists better understand and implement geo-spatial technologies.

Keywords: GIS, Remote Sensing, Global Positioning System, range science.

INTRODUCTION

Sampling vegetation in the field that results in an accurate description of rangelands is an age-old problem (Pechanec and Pickford 1937; Daubenmire 1958) and collecting field or ground-truth data is critical to the success of any remote sensing or GIS project. However, applying traditional ecological vegetation sampling techniques directly to geotechnical studies frequently fails to yield highly accurate and reliable classifications (Witt and Weber 2001).

In July 1972, Landsat Multi-Spectral Scanner was launched into orbit (USGS 2003). This remote sensing satellite offered natural resource scientists the first significant platform on which to analyze the earth's surface for landscape-level vegetation characteristics. Whereas this satellite represented an enormous advance in geotechnical capabilities, it fell far short of the needs and demands of the range community, due to the sensor's spatial resolution (pixel size of 80 meters) and the small number of spectral bands (4) , detailed (and reliable) models of shrub cover or bare earth exposure was not possible. In addition, the heterogeneity and complexity of rangeland plant communities and the fact that individual plant cover and leaf area index are low compared with forested ecosystems resulted in relatively low classification accuracies, <75% overall accuracy (McMahan et al. 2000, Johnson et al. 2001). Today, high-spatial resolution multispectral satellite imagery (pixel size of <5 meters) are commercially available, so are sophisticated hyperspectral remote sensing platforms that record over 100 spectral bands of data across the electromagnetic spectrum. Coupled with thousands of global positioning system (GPS) base stations and state-of-the-art GPS receivers, the range community has the ability to analyze the earth's surface with unprecedented resolution and reliability.

While these readily available technologies have the potential to accurately and reliably monitor rangelands, they also bring with them a new set of challenges. To obtain successful analyses and classifications ($\geq$ 75% overall accuracy; Goodchild et al. 1994, Pettingill, J. pers. comm.2002), high-spatial resolution remote sensing imagery (pixel size < 2.5 meters) must be geo-registered very well (root mean square error (RMS) $\leq$ 1m) and field observation points must be accurately located ($\pm$ 1m). Generally, any single point can be geolocated only to within $\pm$ 0.5 pixel for raster and grid data. When using Landsat TM imagery, this means the horizontal positional accuracy of field locations could not exceed $\pm$ 14 m Such generous error margins are easily satisfied today with even fairly simple GPS receivers (Serr et al. 2005). However, when using high-spatial resolution imagery, acceptable horizontal positional accuracy is concomitantly reduced. For example, the horizontal positional accuracy required of data used with Digital Globe's Quickbird imagery (pixel size of 2.4 m) is $\pm$ 1.2 m. To satisfy the latter accuracy requirement involves the use of more sophisticated GPS receivers and more stringent data collection protocols. Classification accuracy is substantially decreased with poor geolocation accuracy (Peleg and Anderson 2002).

In addition to these considerations and challenges, to extract reliable information from hyperspectral remote sensing data requires the application of advanced classification tools such as fuzzy classification (McMahan et al. 2003), spectral angle mapper (Kruse et al. 1993), or mixture-tuned match filtering (Boardman 1998, Parker-Williams and Hunt 2002, 2004; Mundt 2003).

This paper will present three challenges confronting range managers and range scientists using the geotechnologies in their decision-making process. These challenges are: 1) to better understand and take advantage of geotechnical tools, 2) to collect field observations/measurements in ways that act synergistically with these tools, and 3) to utilize high-accuracy global positioning system receivers for image rectification and co-registration with

field observation sites. These challenges and potential solutions will be described. Following this, a series of best practices will be suggested.

METHODS

To determine optimal field sampling design for sagebrush-steppe rangeland remote sensing studies in southeastern Idaho, we compared two vegetation sampling techniques. The first followed more traditional vegetation sampling techniques and consisted of a 20 m base line directly north of each randomly located sample point. At 10 m increments (0, 10, and 20 m) along the base line, three 25 m transects were read east of the base line. Ground cover was recorded along each transect at 1 cm resolution using a steel tape measure and meter-stick placed perpendicular to the ground surface. All cover intersecting the meter-stick was classified as bare soil, rock, litter, herbaceous, graminoid, or woody plants. Percent cover for each class of vegetation was then calculated. While an accurate record of the vegetation found at each site was collected, total ground cover frequently exceeded 100%, making application of these data very difficult for remote sensing classification unless they were generalized. The second vegetation sampling technique consisted of simple ocular estimates of ground cover (using the same cover type categories listed above) found within the area occupied by one pixel which was presumed to be centered over each randomly located sample point. This method was designed to estimate the percent cover "seen" by a satellite. Percent cover was estimated using categorical breaks of 0%, 1-5%, 6-15%, 16-25%, 26-35%, 36-50%, 51-75%, 76-95%, and 96-100% (Weber and McMahan 2003).

We experimented with numerous classifications using both types of field data and report here the result of two of those classifications. The first attempts a very detailed classification using seventeen cover classes (Table 1). The second uses simplified cover category data generalized into seven classes (Table 2). In both cases Landsat 5 thematic mapper data was used, which has a spatial resolution of 28.5 x 28.5 meter pixels. Following this, validation of each model was performed using traditional boot-strap estimation techniques (Efron 1979, McMahan and Weber 2003) and Kappa statistic (Titus et al. 1984; Congalton and Green 1999). Boot-strap estimation is a technique whereby a sub-set of hypothetical samples is drawn from an original larger sample set. These sub-sets are then iteratively analyzed and accuracy determined using the inverse or unused sub-set. To readily compare both types of field data for this paper, separability was calculated using the Transformed Divergence Index (Richards 1993, Lillesand and Kiefer 2000). Separability statistics calculate the statistical “distance” between classification categories. The separability value of the spectral signatures derived for each class of training site provides a measure of classification accuracy. In essence, this statistic determines how discrete each category or class of data is, based on the spectral signatures extracted from available imagery. While no minimum number of sites per class was imposed to calculate separability, only those classes containing at least 30 training sites were evaluated in this part of the study. The significant separability threshold was set at 1500 in accordance with values suggested by other authors (Richards 1993).

To explore the potential advantage of using high-spatial resolution imagery, we compared classifications of leafy spurge infestations in southeastern Idaho using Landsat (pixel size of 28.5 m), SPOT 5 (pixel size of 10 m), and Quickbird (pixel size of 2.4 m) satellite imagery. Classifications were made using 253 stratified- random field observation points collected during the summer of 2002. Validation was then performed using standard boot-strap techniques and calculated as an error matrix with Kappa statistic. The criteria used for evaluation were 1) cost-effectiveness and 2) classification accuracy, where an accurate and reliable classification is defined as having $\geq$ 75% accuracy with minimal omission error.

Table 1. Cover classes used for detailed classification of sagebrush-steppe rangelands (total cover could not exceed 100%).

Class	Shrub cover	Grass cover	Rocks/ bare soil/ lichen crust
1- rocks/ bare soil/ lichen crust	1-5%	1-5%	≥36%
2- low grass	1-5%	6-15%	≥36%
3- medium grass	1-5%	16-25%	≥36%
4- high grass	1-5%	26-35%	≥36%
5- low grass/shrub mix	6-15%	6-15%	≥36%
6- medium grass- low shrub mix	6-15%	16-25%	≥36%
7- high grass- low shrub mix	6-15%	≥36%	<36%
8- medium shrub- low grass mix	16-25%	6-15%	≥36%
9- medium grass/shrub mix	16-25%	16-25%	<36%
10- medium grass/shrub with rocks/bare soil/ lichen crust	16-25%	16-25%	≥36%
11- high shrub	26-35%	1-5%	≥36%
12- high shrub- low grass mix	26-35%	6-15%	<36%
13- high shrub – low grass mix with rocks/bare soil/ lichen crust	26-35%	6-15%	≥36%
14- high shrub- medium grass mix	26-35%	16-25%	≥36%
15- very high shrub	≥36%	1-5%	≥36%
16- very high shrub- low grass mix	≥36%	6-15%	<36%
17- very high shrub- low grass mix with rocks/ bare soil/ lichen crust	≥36%	6-15%	≥36%

Table 2. Cover classes used for general sagebrush-steppe rangeland classification (total cover could not exceed 100%).

Class	Shrub cover	Grass cover	Rocks/ bare soil/ lichen crust
1- grass with rocks/ bare soil/ lichen crust	<16%	≥16%	≥26%
2- grass	<16%	≥16%	<26%
3- shrubs with rocks/ bare soil/ lichen crust	≥16%	<16%	≥26%
4- shrubs	≥16%	<16%	<26%
5- grass and shrub mix with rocks/ bare soil/ lichen crust	≥16%	≥16%	≥26%
6- grass and shrub mix	≥16%	≥16%	<26%
7- rocks/ bare soil/ lichen crust	<16%	<16%	≥26%

To consistently satisfy geo-registration and co-registration requirements and effectively use available high-spatial resolution imagery requires the use of sophisticated GPS receivers and the implementation of more stringent data collection protocols. To establish these protocols we experimented with three types of GPS receivers (Trimble ProXR, Trimble GeoXT, and Trimble GeoExplorer II). A primary differences between these receivers is that the ProXR and GeoXT are 12-channel receivers (i.e., 12 satellites can be connected simultaneously allowing the receiver to select the optimal geometric configuration) whereas the GeoExplorer II is a 6-channel receiver. In addition, the GeoXT can utilize Wide-Area Augmentation System (WAAS) for real-time differential correction. In all experiments, estimations were acquired only when a minimum of 4 concurrent GPS signals were processed, 120 positions were averaged per point with a 95%

confidence interval (CI) to indicate location error, and the mask for Position Dilution of Precision (PDOP) was set at 5.0. Because GPS estimates location based on triangulation, PDOP masks are used to ensure optimal satellite geometry (i.e., the satellites used are not clustered close to one another). All locations were evaluated in raw format as well as post-processed differentially corrected format and evaluated for horizontal positional accuracy relative to the location of the City of Pocatello's ground control points established using traditional survey methods and survey-grade GPS with real-time differential correction from a US Geodetic CORS station (Table 3).

Table 3. Accuracy and precision of global positioning system (GPS) receivers. Values are expressed in meters at the 95% confidence interval using a 120 position average per point (n = 70 points).

GPS Receiver	Accuracy	Precision	Applicable image resolution	Effective map scale
Trimble ProXR	±0.78	±0.46	>1.6m	1:925
Trimble GeoXT[1]	±0.96	±0.66	>2.0m	1:1,100
Trimble Geoexplorer II	±3.25	±2.90	>6.5m	1:3,800

1. Using WAAS real-time differential correction along with post-processing.
Note: All results reported using post-process differential correction.

RESULTS AND DISCUSSION

FIELD SAMPLING FOR RANGELAND REMOTE SENSING

Table 4 describes the separability of 253 training sites into 17 cover categories. Only four categories contained a sufficient number of training sites (>30) to develop reliable spectral signatures. Of these, 3 of the classification categories were found to be statistically separable with Transformed Divergence Index scores exceeding 1500 (Richards 1993, Lillesand and Kiefer 2000) (Table 4). Class 8 is separable from class 13 based upon an increase in shrub cover from 16-25% to 26-35%. Class 8 is also separable from class 15 based upon an increase in shrub cover from 16-25% to ≥36% and a loss of grass cover from 6-15% to 1-5%. Lastly, class 13 is separable from class 15 based upon an increase in shrub cover from 26-35% to >36% and a loss of grass cover from 6-15% to 1-5%. The data were then combined into seven general cover categories (Table 2) and re-evaluated for separability. Seventy-one percent (15 of 21) of these categories were statistically separable with Transformed Divergence Index scores > 1500 (Table 5).

These analyses show that even with high spatial resolution data, there is a limit to the amount of usable information obtained by remote sensing. Even with a sufficient number of training sites, many of the classes in Table 1 would still not be separable because the signatures also depend also on the soil background reflectance (Asner 2004). Reliable sub-species differentiation of plants has not been demonstrated nor has reliable differentiation of similar grasses and shrubs (e.g., differentiating crested wheatgrass from bluebunch wheatgrass) with multispectral imagery. Field observation sites must be collected appropriately for image processing regardless of the desired mapping or modeling result. In other words, field personnel must collect measurements and observations that will correspond with what the satellite "sees" (i.e. collecting data describing functional group and vegetation structure is typically more useful than species level differentiations with multispectral imagery unless the target species has a very distinctive spectral signature (e.g., blooming leafy spurge) present when the imagery was acquired, and at high enough abundance within the imagery to allow for easy detection).

Table 4. Separability of training sites using 17 detailed cover categories calculated using the transformed divergence index.

	C1	C2	C3	C4	C5	C6	C7	C8	C9	C10	C11	C12	C13	C14	C15	C16	C17
C1	0																
C2	0	0															
C3	1999	0	0														
C4	2000	0	1999	0													
C5	1999	0	835	0	0												
C6	1999	0	1995	1829	1999	0											
C7	1761	0	1999	2000	1999	1999	0										
C8	1999	0	5.72	0	61	1999	1999	0									
C9	1999	0	1999	1999	1999	1623	1999	1999	0								
C10	1999	0	1170	0	968	1999	1999	1137	2000	0							
C11	1999	0	608	0	114	1998	1999	107	1999	995	0						
C12	2000	0	1999	0	1999	2000	2000	1999	2000	2000	1999	0					
C13	2000	0	1999	0	199	2000	2000	1999	2000	2000	1999	0	0				
C14	2000	0	2000	2000	1999	1999	1999	121	2000	2000	2000	2000	2000	0			
C15	2000	0	871	0	272	1999	1999	1999	2000	1442	308	1995	2000	2000	0		
C16	1999	0	2000	2000	1999	1999	1999	1999	1999	2000	1999	2000	2000	2000	2000	0	
C17	1426	0	1999	1999	1998	1999	1606	2000	1999	1999	1999	2000	2000	2000	1999	2000	0

Note: Categories with a sufficient number of training sites ($n \geq 30$) are shaded (C5, C8, C13, and C15). Of these, three were statistically separable based on a transformed divergence index ≥ 1500. The separable cover classes are those where shrub cover exceeds 16%, bare ground exceeds 36% and minimal grass cover is present.

Table 5. Separability of training sites using 7 cover categories calculated using the transformed divergence index.

	C1	C2	C3	C4	C5	C6	C7
C1	0						
C2	1973	0					
C3	1999	569	0				
C4	1090	1999	1999	0			
C5	1801	1733	1710	1732	0		
C6	1293	914	7.92	1608	518	0	
C7	2000	2000	2000	2000	2000	2000	0

Note: All categories had a sufficient number of training sites (n>30); pairwise comparisons that are significant different are shaded. The cover class descriptions are give in Table 2.

Achieving accurate and reliable classification (≥ 75% overall accuracy) of rangelands with models built from multispectral satellite imagery requires the use of categorical training site data. Applying training data that is more detailed (i.e., cover data collected at species levels) frequently results in unacceptably poor accuracy.

SELECTION OF APPROPRIATE SPATIAL RESOLUTION

Using imagery with better spatial resolution has allowed researchers to improve classification accuracy relative to platforms such as Landsat TM. Figure 1 illustrates mean classification accuracies using Landsat, SPOT5, and Quickbird for leafy spurge infestation detection in southeastern Idaho. An inverse relationship exists between spatial resolution and overall classification accuracy for leafy spurge detection.

Training sites must be accurately located relative to the imagery. In other words, the field training site must be placed inside the correct pixel. The first step towards that end is to acquire terrain corrected imagery from the vendor whenever possible (it is noted that this is typically the

most expensive package from vendors). Doing this does not preclude the need to collect good control points and further rectify the imagery. Rather it makes the geo-rectification process easier since the imagery is "closer" to its correct location than if it were not terrain corrected.

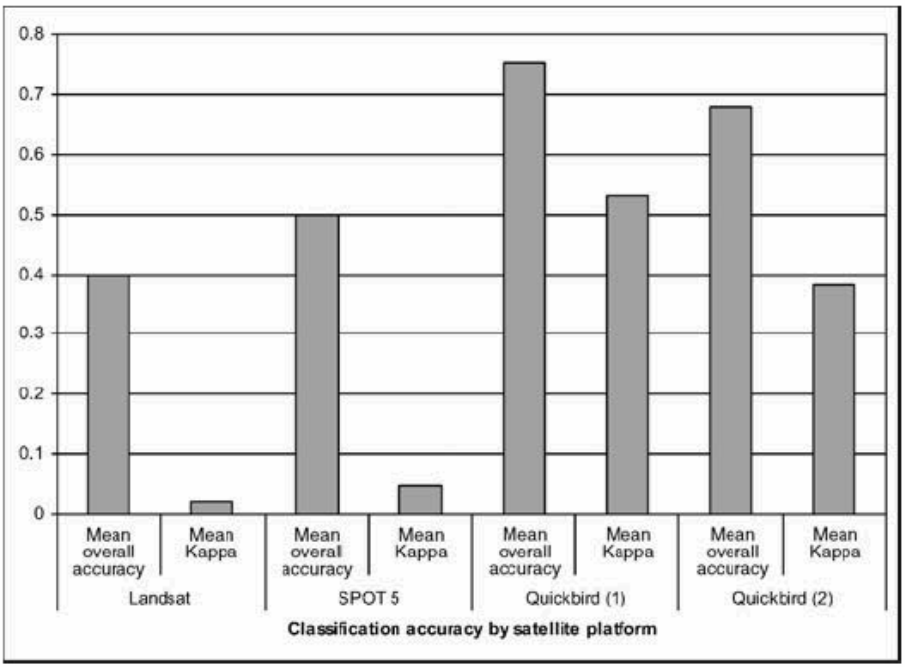

Figure 1. Mean overall accuracy and kappa analysis results for classification of leafy spurge derived from various satellite platforms. Kappa ≥0.35 is significant (maximum likelihood, minimum distance to means, and spectral angle mapper classification techniques were used). Quickbird (1), satellite imagery acquired in early summer. Quickbird (2), satellite imagery acquired in late summer.

An interrelated consideration is the spatial resolution required to address specific problems. In the case study presented above, detection of patchy invasive plant infestations required the use of high-spatial resolution imagery (pixel size of <5 m) to achieve 75% overall classification accuracy. In this case, we observed an inverse relationship between accuracy and spatial resolution. Other rangeland applications may not follow this trend. In fact, there are many applications where Landsat or MODIS imagery is perfectly well suited (Reeves et al. 2001).

SPOT 5 satellite imagery was able to achieve reasonable accuracy (Fig. 1) at a much reduced cost (Table 6). For this reason, SPOT imagery is very attractive and it may be the most cost-effective imagery for the detection of leafy spurge. The cost per km^2 is higher than that of Landsat but substantially lower than that of Quickbird. The overall accuracy (51%) of SPOT imagery for detection of leafy spurge was below the given accuracy requirements; but the 75% overall accuracy requirement was arbitrary. It is important to note however, that because of a fairly low mean kappa value, additional research will be required before a firm conclusion can be made regarding applicability of SPOT imagery for rangeland classification.

In addition to these considerations, the user should also consider temporal aspects of image acquisition, specifically as it relates to the phenology of targeted plant species (Everitt et al. 1995). Figure 1 illustrates the variation in overall accuracy when using imagery acquired in early summer (78%) versus late summer (67%). The phenology of leafy spurge has bright conspicuous flowers in the early summer, which increases its separability from non-target features and helps explain improved detection accuracy during this time period.

Table 6. Comparison of spatial resolution and cost of various satellite platforms.

	Spatial Resolution (meters per pixel)	Minimum Scene size (km^2)	Cost per scene	Cost per km^2	Cost for 32,400km^2
Landsat TM	30	32,400	$650	$0.02	$650
SPOT 5	10	3,600	$3,259[1]	$1.10	$35,640
Quickbird	2.4	64	$1,920	$30.00	$972,000

RECTIFICATION AND REGISTRATION

The Trimble ProXR GPS receiver consistently (95% CI) achieved sub-meter horizontal positional accuracy (± 0.78 m) when a clear view of the sky was available (Bays 2003) and differential correction was used. Likewise, the Trimble GeoXT also achieved sub-meter horizontal positional accuracy (95% CI = ± 0.96 m). In contrast, the Trimble GeoExplorer II GPS receiver achieved horizontal positional accuracy of only 95% CI = ± 3.25 m, which failed to consistently achieve the required accuracy for the Quickbird imagery (±1.2m) even when differentially corrected.

GPS is quickly becoming the most needed yet most misused technology available. This is perhaps because many users are already familiar with recreational-grade GPS receivers. The result is that these users approach GPS research applications with basic familiarity but without a full appreciation of the differences in receiver specific accuracy and error propagation. When using high-spatial resolution imagery, the use of resource-grade GPS receivers is necessary to satisfy horizontal positional accuracy requirements (95% CI = ±1.2m).

At the core of this problem is the fact that users are not simply trying to navigate to a point in the field but rather, are trying to match observations from two independent systems (i.e., imagery and field). To succeed, both systems must use the same datum and projection. The native coordinate system for the GPS is latitude-longitude with WGS84 used as its horizontal datum. Any datum transformations and/or projections (i.e., converting geographic to UTM) can be handled with receiver specific software. Ordering imagery in a specific coordinate system is usually acceptable.

MANAGEMENT IMPLICATIONS

As a result of experiences in the field, a set of best practices has been assembled to guide rangeland scientists in their efforts to integrate geospatial technologies into their profession.

1) Design and collect field observations which match "what the satellite sees".
2) Develop a problem statement that clearly defines the questions you want the geotechnologies to address. As part of this statement, decide upon an acceptable level of error.
3) Understand that cost-effectiveness means the least expensive sensor that satisfies the accuracy requirements. Choosing a sensor that is the least expensive can result in 100% waste of financial resources.
4) Invest in high quality GPS receivers particularly when using high spatial resolution imagery.
5) If real-time differential correction (producing acceptable horizontal positional accuracy (e.g., ±1.2 m) is not available, use post-process differential correction for all GPS acquisitions from nearby base stations.
6) Collect all GPS points using native latitude-longitude and the WGS84 datum. Conversion can be made at a later time using receiver specific software.
7) Establish as accurate a location as possible while in the field. To do this:
    a. Collect a sufficient number of positions per point to account for instantaneous environmental errors (typically 120 positions per point) and ephemeris errors

arising from differences between the anticipated location of a satellite and its true location .

b. Use signals from 4 or more GPS satellites available to the receiver (3D mode). A twelve-channel receiver will provide higher location precision than a six-channel receiver.
c. Establish and follow PDOP and elevation mask protocols.

8) Collect ground control points in the field using clearly identifiable points on the imagery and/or map. For applications using high-spatial resolution imagery, reflective tarps will need to be staked in the field prior to image acquisition so rectification and co-registration is as accurate as possible.
9) Invest in geotechnical training and/or geotechnically trained personnel.

ACKNOWLEDGEMENTS
This study was made possible by a grant from the National Aeronautics and Space Administration Goddard Space Flight Center. ISU would also like to acknowledge the Idaho Delegation for their assistance in obtaining this grant.

LITERATURE CITED

Asner, G. P. 2004. Biophysical remote sensing signatures of arid and semiarid ecosystems. In S. L. Ustin (Ed.) Remote Sensing for Natural Resource Management and Environmental Montoring. Manual of Remote Sensing, Third Edition, Volume 4. Hoboken, NJ: John Wiley & Sons. p. 53-109.

Bays, K. 2003. Draft GPS Data Accuracy Standard. USDI BLM. Available at: http://giscenter.isu.edu/gps_cbs/cached_blmstd_04_22_03.pdf. Accessed 1-August-2005.

Boardman, J. W. 1998. Leveraging the high dimensionality of AVIRIS data for improved subpixel target unmixing and rejection of false positives: Mixture Tuned Matched Filtering. In Summaries of the Seventh Annual JPL Airborne Geoscience Workshop, October 1998, Pasadena CA 581-583.

Congalton, R. G. and K. Green. 1999. Assessing the Accuracy of Remotely Sensed Data: Principles and Practices. Boca Raton, Florida: Lewis Publishers. 160 pp.

Daubenmire, R. F. 1958. A canopy-coverage method for vegetation analysis. Northwest Science 53:43-64.

Efron, B. 1979. Bootstrap methods: another look at the jackknife. Annals of Statistics (7) 1-26.

Everitt, J. H., G. L. Anderson, D. E. Escobar, M. R. Davis, N. R. Spencer, and R. J. Andrascik. 1995. Use of remote sensing for detecting and mapping leafy spurge (Euphorbia esula). Weed Technology, 9:599-609.

Goodchild, M. F., G. S. Biging, R. G. Congalton, P. G. Langley, N. R. Chrisman,, and F. W. Davis. 1994. Final Report of the Accuracy Assessment Task Force. California Assembly Bill AB1580, Santa Barbara: University of California, National Center for Geographic Information and Analysis (NCGIA).

Johnson, T., G. Russel, and K. T. Weber. 2001. GAP Analysis Agreements of Rangeland Vegetative Communities of Southeast Idaho. Available at: http://giscenter.isu.edu/research/techpg/nasa_wildfire/abstracts/GAP_2002_abstract.pdf Accessed 20 January 2004.

Kruse, F.A., A. B. Lefkoff, J. W. Boardman, K. B. Heidebrecht, A. T. Shapiro, A.T., P. J. Barloon, and A. F. H. Goetz. 1993. The Spectral Image Processing System (SIPS) -- Interactive Visualization and Analysis of Imaging Spectrometer Data. Remote Sensing of the Environment. 44:145-163.

Lillesand T. M. and R. W. Kiefer. 2000. Remote Sensing and Image Interpretation. 4th Ed. John Wiley and Sons, New York, NY. 724pp.

McMahan, J. B., K. T. Weber, and J. Sauder. 2003. Fuzzy Classification of Heterogeneous Vegetation in a Complex Arid Ecosystem. In K. T. Weber (Ed), Final Report: Wildfire Effects on Rangeland Ecosystems and Livestock Grazing in Idaho. 209pp. Available at: http://giscenter.isu.edu/research/techpg/nasa_wildfire/Final_Report/Documents/Chapter7.pdf.

McMahan, J. B., K. T. Weber. 2003. Validation Alternatives for Classified Imagery. In K. T. Weber (Ed), Final Report: Wildfire Effects on Rangeland Ecosystems and Livestock Grazing in Idaho. 209pp. Available at: http://giscenter.isu.edu/research/techpg/nasa_wildfire/Final_Report/Documents/Chapter10.pdf.

McMahan, J. B., W. C. Witt, and K. T. Weber. 2000. GAP Analysis Ground-Truthing in Southeastern Idaho. Available at: http://giscenter.isu.edu/research/techpg/lcc/documents/GAP_ABfinal.pdf Accessed 20 January 2004.

Mundt, J. T. 2003. Detection Of Leafy Spurge (Euphorbia esula) In Swan Valley, Idaho, Using Hyperspectral Remote Sensing With Limited Training Data. Master's Thesis, Idaho State University, Department of Geosciences. 107pp.

Parker-Williams, A., and E. R. Hunt, Jr. 2002. Estimation of leafy spurge cover from hyperspectral imagery using mixture tuned matched filtering: Remote Sensing of Environment. 82:446-456.

Parker-Williams, A., and E. R. Hunt, Jr. 2004. Accuracy assessment for detection of leafy spurge with hyperspectral imagery. Journal of Range Management. 57:106-112.

Pechanec, J. F. and G. D. Pickford. 1937. A weight estimate method for determination of range or pasture production. Journal of the American Society of Agronomy. 29:894-904.

Peleg, K. and G. L. Anderson. 2002. FFT regression and cross-noise reduction for comparing images in remote sensing. International Journal of Remote Sensing. 23:2097-2124.

Reeves, M. C., J. C. Winslow, and S. W. Running. 2001. Mapping Weekly Rangeland Vegetation Productivity Using MODIS Algorithms. Journal of Range Management. 54: A90-A105.

Richards, J.A., 1993. Remote Sensing Digital Image Analysis, Springer-Verlag, New York, NY. 363 pp.

Titus, K., J. A. Mosher, and B. K. Williams. 1984. Chance-corrected Classification for use in discriminant analysis: ecological applications. American Midland Naturalist, 111: 1-7.

Serr, K., T. K. Windholz, and K. T. Weber. 2005. Comparing GPS Receivers: A field study. Available at: http://giscenter.isu.edu/research/techpg/nasa_weeds/to_pdf/gps_accuracy_precision.pdf. Accessed 11 May 2005.

USGS. 2003. USGS Landsat Project. Available at: http://landsat.usgs.gov/history.html Accessed 21 October 2003.

Weber, K. T. and J. B. McMahan. 2003. Field Collection of Fuel Load and Vegetation Characteristics for Wildfire Risk Assessment Modeling: 2002 Field Sampling Report. In K. T. Weber (Ed), Final Report: Wildfire Effects on Rangeland Ecosystems and Livestock Grazing in Idaho. 209pp. http://giscenter.isu.edu/research/techpg/nasa_wildfire/Final_Report/Documents/Chapter2.pdf.

Witt, W. C. and K. T. Weber. 2001. Project Report: Land Cover Change Detection Error Assessment. Available at: http://giscenter.isu.edu/research/techpg/lcc/documents/2000_report.pdf Accessed 14-January-2004.

Modeling Cheatgrass using Quickbird Imagery

Bhushan Gokhale, GIS Training and Research Center, Idaho Sate University, Pocatello ID 83209-8130. (gokhbhus@isu.edu)

Keith T. Weber, GIS Director, GIS Training and Research Center, Idaho Sate University, Pocatello ID 83209-8130 (webekeit@isu.edu)

ABSTRACT

Cheatgrass (*Bromus tectorum*) is of growing concern among farmers, ranchers, and researchers in the intermountain west due to its ability to alter rangeland vegetation communities and their associated fire regimes. Quickbird multi-spectral imagery (spatial resolution 2.4 mpp) was used to detect and model cheatgrass presence in southeastern Idaho. Training sites were created using 2003 field data. The four bands of Quickbird imagery were processed using IDRISI software and various vegetation indices were created using the red and near-infrared bands of the Quickbird imagery. Principal Components Analysis (PCA) was performed using eight vegetation indices and the four original bands of data. Redundant data was minimized using results from PCA. Maximum likelihood classification was then used to classify the imagery to model the presence of cheatgrass. The accuracy of the resulting model was assessed using an error matrix and Kappa statistic. An overall accuracy of 73% was achieved through this process.

Keywords: weeds, vegetation indices, signature extraction, maximum likelihood

INTRODUCTION

Cheatgrass (*Bromus tectorum*) is considered a problematic invasive plant in Idaho's rangelands. This annual plant can germinate in spring or fall and is known to colonize areas quickly following a fire. During most of its life cycle, cheatgrass provides poor forage for livestock. In addition, it is considered a fire promoter as its early senescence provides great quantities of fine fuel to carry late summer wildfires (Vavra M. et al., 1999). Understanding the distribution and density of cheatgrass is essential to management. Due to its widespread, yet patchy distribution (cheatgrass is rarely found in excess of 30% cover within our study area) we chose to use Quickbird multispectral imagery to detect and predict the location of cheatgrass.

The main objectives of this study were as follows-

1. Identify areas with current cheatgrass infestation.
2. Develop spectral signatures for cheatgrass extracted from satellite imagery at those locations of known cheatgrass infestation.
3. Develop a cheatgrass prediction model using maximum likelihood classification.
4. Assess the accuracy of the cheatgrass model.
5. Purify the training sites and repeat classification-assessment.

THE STUDY AREA

The study area, known as the Big Desert, lies in southeastern Idaho, approximately 71 km northwest of Pocatello. The center of the study area is roughly located at 113º 4' 18.68" W and 43º 14' 27.88" N (Figure 1) (Sander and Weber 2005). This area is managed by the Bureau of Land Management (BLM) and exhibits a large variety of native species as well as invasive species. The area is a sagebrush-steppe semi-desert which is bordered by geologically young lava formations to the south and west. Irrigated agricultural lands border the study area to its north, south and east. The area has a history of livestock grazing and wildfire occurrence (Weber and McMahan 2003).

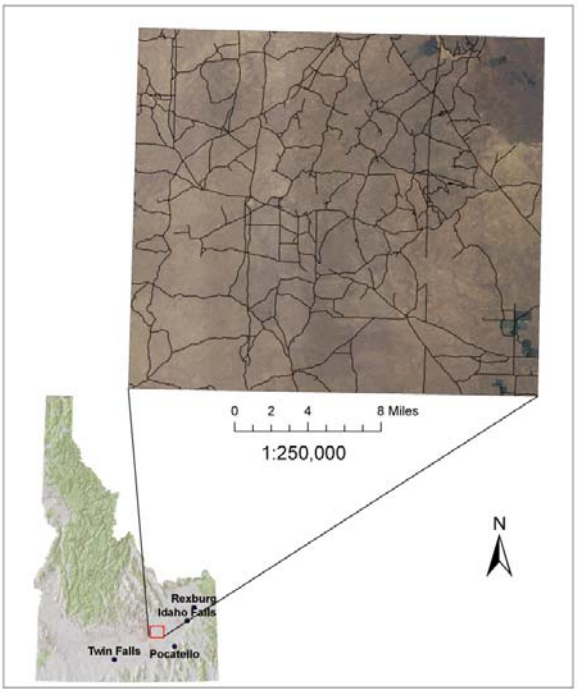

Figure 1. The Big Desert study area in southeastern Idaho.

METHODS

A total of 253 field samples were collected during 2003 for model development and 171 samples were collected in 2004 for model validation. All sample points were randomly located across the study area. A Trimble GeoXT GPS receiver (+/-1m with a 95% CI) was used to record the location of each point. At each of the sample points data describing percent cover of grasses and shrubs, dominant weed (cheatgrass, leafy spurge etc.) and shrub species, fuel load, sagebrush age, GAP vegetation classification, presence of microbial crust, litter type, and forage availability were recorded. In addition, four photographs were taken at each point. Visual estimation was used to describe percent bareground, litter, shrub and grass into one of nine classes (1. None, 2. 1-5%, 3. 6-15%, 4. 16-25%, 5. 26-35%, 6. 36-50%, 7. 51-75%, 8. 76-95%, and 9. >95% (Sander and Weber 2005)).

Quickbird satellite imagery was used for predictive modeling of cheatgrass. The imagery is comprised of four multispectral bands each with 2.4 x 2.4 meter pixels. The wavelengths sensored by each band were as follows:

- *Blue: 450 to 520 nanometers*
- *Green: 520 to 600 nanometers*
- *Red: 630 to 690 nanometers*
- *Near-Infrared: 760 to 900 nanometers*

ArcGIS and IDRISI software were used to 1) convert field samples into training sites (coded for cheatgrass presence/absence), 2) calculate various vegetation indices, and 3) perform image processing and classification.

Paste in these same things from the RH paper…

1. ***Training sites*** – Training sites were used to allow the image processing software to generate spectral signatures for the target of interest (i.e., cheatgrass). Each training site consists of a geographic location and sample attribute (e.g., 1=cheatgrass presence or 2=cheatgrass absence). To be considered a cheatgrass presence training site, the field sample had to contain $\geq$16% cheatgrass. To be considered a bare ground presence training site, the field sample has to contain $\geq$50% bare ground. The field sampling points (vector shapefiles) were converted into raster training sites (TIFF format) for use in IDRISI. Those pixels containing a training site were given a value (1 (presence) or 2 (absence)) where all other pixels (unknown) retained a value of zero.

2. ***Vegetation Indices-*** Various vegetation indices were calculated to better capture the vegetation characteristics of the study area and potentially improve our modeling results. These indices are relative measures of actively photosynthesizing vegetation present within each pixel (USWCL 2005). Different vegetation indices can be produced using different combinations/ratios of red and infrared bands and by including additional parameters such as slope and intercept of soil line and soil adjustment factors. Normalized Difference Vegetation Index (NDVI) is perhaps the most common, while the soil adjusted vegetation index (SAVI) also considers the reflectance of bare ground and its behavior in the red and near-infrared bands. Thus SAVI may offer a more accurate characterization of communities where bare ground is frequently encountered.

3. Eight vegetation indices were calculated for this study using the VEGINDEX module of IDRISI program. These indices were then evaluated for their relevance using Principal Components Analysis (PCA).

4. ***Principal Components Analysis (PCA) –*** In remote sensing PCA is used as a data reduction and noise removal technique. PCA produces a new set of images from a set of input images. The images of the new set are called components. The components are uncorrelated with each other and are ordered by the amount of variance described in the original input images (Eastman 2003).

   The first two or three components from a PCA typically describe nearly all the variability contained in the input imagery. Subsequent components introduce redundancy, outliers, and noise. Therefore these components can be eliminated from further processing without losing any important data.
   We performed PCA using the four bands of Quickbird imagery along with eight vegetation indices. The PCA analysis produced a set of component images. Based on these results a subset of images (describing about 97% of total variance) was selected to be used for signature extraction.

5. ***Signature Extraction***- Spectral signature is also known as spectral response pattern and the concept is very similar to the human concept of color. A spectral signature provides a description of the magnitude that light energy is reflected by the target in different regions of the electromagnetic spectrum. Thus it plays a key role in the interpretation of remotely sensed data. Figure 3 shows how light is reflected, absorbed, and transmitted from a particular object. The MAKESIG module of IDRISI was used to develop cheatgrass signatures from PCA component images.

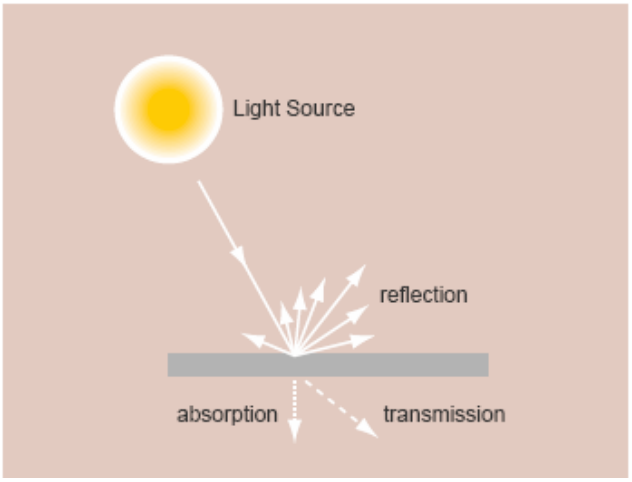

Figure 2. Light behavior of a surface (source: Eastman 2003, IDRISI Kilimanjaro Guide)

6. ***Maximum Likelihood Classification***- Maximum Likelihood Classification was used for image classification. This classification is a type of hard classifier. The hard classifier makes a definitive decision about the land cover class to which each pixel belongs (Eastman 2003).

7. The classification uses information present in the signature file to determine which class each pixel belongs to (i.e., cheatgrass presence or cheatgrass absence). Equal probability was assigned to each of the signature class. Therefore 50 percent probability was assigned to each class.

8. ***Error Assessment-*** This step is also known as validation. While there are different ways to judge the accuracy of a model, we chose to use a standard contingency table (or error matrix) and the Kappa statistic. An error matrix measures the agreement between ground truth data with the developed model.

   The ERRMAT module was used for error assessment of the cheatgrass model. We calculated kappa (how much better or worse the classification performed relative to a chance classification) (Titus et. al. 1984), overall, commission, and omission errors.

9. ***Purification-*** signature purification is sometimes necessary to achieve reliable results. The PURIFY module of IDRISI performs parametric and non-parametric purification. In parametric purification, the training pixel vector is retrieved from the images and the Mahalanobis distance to the mean of the class is calculated. The user is required to specify a typicality threshold which ranges from 0 to 1. A zero typicality threshold indicates that all the pixels will be kept in the data set while value 1 implies that nearly all pixels will be eliminated save for those equal to the mean. Based on the threshold, each pixel's typicality is evaluated (using Mahalanobis distance). A pixel with typicality value less than the threshold is dropped from the new data set (Eastman 2003). Signature purification was performed in the study and a new set of purified signatures was created and used for a second iteration maximum likelihood classification.

RESULTS AND DISCUSSION

Figure 3 shows the cheatgrass model produced using maximum likelihood classification from un-purified training sites. The corresponding error matrix generated using the ERRMAT module of IDRISI is given in table 1.

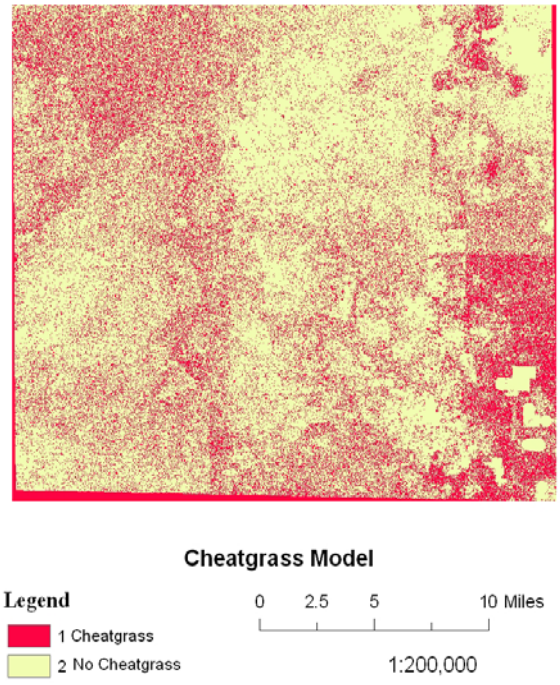

Figure 3. The binary cheatgrass model produced for the Big Desert Study area. Red (dark) pixels represent predicted cheatgrass presense at /or above 16% cover (cover class no. 4).

Table 1 – Error Matrix for a Cheatgrass model developed using un-purified signature files.

		Field Observations			
Model Predictions		Presence	Absence	Total	Commission Error
	Presence	18	55	73	0.75
	Absence	8	152	160	0.05
	Total	26	207	233	
	Omission Error	0.31	0.26		0.27

The model predicted only 18 sites correctly as cheatgrass (Table 1). This resulted in a large error of commission of about 75%. Further examination of the model indicates that eight known cheatgrass training sites were classified as non-cheatgrass sites. This resulted in an error of omission of approximately 30%. The model did well identifying what is not cheatgrass. Considering these results, the overall error of the model was about 27% (making it 73% accurate). The kappa index was 0.2383, indicating little improvement over a simple random classification. Further, such a low Kappa value indicates little reliability in the model. Table 2 shows the error matrix for a second cheatgrass model developed using purified signature files.

Table 2 – Error Matrix for a Cheatgrass model developed using purified signature files.

		Field Observations			
Model Predictions		Presence	Absence	Total	Commission Error
	Presence	20	69	89	0.77
	Absence	5	114	119	0.04
	Total	25	183	208	
	Omission Error	0.20	0.38		0.36

As a result of purification 25 training sites were removed. The overall error of the model was about 36% (or about 64% accurate). The error of omission and commission were very similar to those reported using non-purified signature files (Table 1) and Kappa was 0.2009 indicating the purification process was not beneficial in this case.

A primary source of error in both models is likely poor co-registration between training sites and the Quickbird imagery regardless of our attempts to eliminate the error. While the Quickbird imagery was geo-registered with a ground control shapefile the best RMS achieved was 5.20 m. When considering the pixel size was 2.40 m, this implies a positional error of more than twice the pixel size. In other words, our cheatgrass training sites may have been shifted up to 2 pixels away from the actual pixel containing the target. This error propagated through the model and likely explains the unacceptably low accuracy.

The patchy nature of cheatgrass in the study area is not advantageous to reliable processing. While very common, cheatgrass cover for our training sites ranged between 16 and 36% (no training sites exceeded 36% cover). This means that even for cheatgrass presence training sites, roughly two-thirds of the pixel was covered by non-target objects. It was expected that by using imagery with high spatial resolution (i.e., Quickbird) that the mixed-pixel affect could be minimized and allow for a reliable classification. Indeed, this is not the case. Further, using high-spatial resolution imagery introduced another difficulty; co-registration between imagery and training sites which was discussed earlier.

CONCLUSIONS

While further study is required, cheatgrass currently cannot be modeled reliably (where users' accuracy exceeds 70%) using Quickbird multispectral imagery. The overall accuracy of the

model was 73%; however user's accuracy never exceeded 25%. Purification did not improve accuracy. We speculate that training sites dominated (>50%) by cheatgrass are required to achieve reliable results. This is probably true of all target/species differentiations except in those cases where the target has a distinctive spectral signature or texture. In addition, numerous ground-based control points which are visible within the imagery are required to eliminate co-registration errors and the resulting loss of accuracy propagated by this error.

ACKNOWLEDGEMENTS
This study was made possible by a grant from the National Aeronautics and Space Administration Goddard Space Flight Center. ISU would also like to acknowledge the Idaho Delegation for their assistance in obtaining this grant.

LITERATURE CITED
Eastman, R. J., 2003. IDRISI Kilimanjaro Guide to GIS and Image Processing. Clark University Laboratory.

USWCL 2005. How a vegetation index works. URL=http://www.uswcl.ars.ag.gov/epd/remsen/Vi/VIworks.htm, visited 19-July-2005.

Vavra M., W. A. Laycock, and R. D. Pieper. 1999. Ecological Implications of Livestock Herbivory in the West, Society of Range Management.

Sander L. and K. T. Weber. 2005. Range Vegetation Assessment in the Big Desert, Upper Snake River Plain, Idaho, GIS Training and Research Center. URL = http://giscenter.isu.edu/Research/techpg/nasa_weeds/to_pdf/fieldreport_2003-2004.pdf

Weber K. T. and B. J. McMahan. 2003. Field Collection of Fuel Load and Vegetation Characteristics Wildfire Risk Assessment Modeling: 2002 Field Sampling Report. URL = http://giscenter.isu.edu/Research/techpg/nasa_wildfire/Final_Report/Documents/Chapter2.pdf

Range Vegetation Assessment in the Big Desert, Upper Snake River Plain, Idaho

Luke Sander, Idaho State University GIS Training and Research Center. Campus Box 8130, Pocatello, Idaho 83209-8130

Keith T. Weber, GIS Director, Idaho State University GIS Training and Research Center. Campus Box 8130, Pocatello, Idaho 83209-8130 (webekeit@isu.edu)

ABSTRACT
Vegetation data was collected at 575 randomly located sample points during the summers of 2003 and 2004 (424 in the USDI BLM Big Desert Region (253 in 2003 and 171 in 2004) and 151 in the USDA-ARS Sheep Experiment Station in 2004). We collected data describing percent cover of grasses and shrubs, dominant weed and shrub species, fuel load, sagebrush age, GAP vegetation classification, presence of microbial crust, litter type, forage availability, and photo points. Sample points were stratified by fire, grazing, and rest treatments. A high amount of cheatgrass was found throughout both years as well as a high amount of bare ground. However, in 2004 forage availability increased from 2003 probably due to increased rainfall.

Keywords: vegetation, sampling, GIS, remote sensing, GPS.

INTRODUCTION

Many factors influence landscape changes. Wildfire has been, and will always be, a primary source of broad scale landscape change. After a wildfire occurs a change in both plant community composition and plant structure results. In a completely unaltered system, there are plants and shrubs that establish themselves very quickly. In some systems, native plants are in competition with non-native vegetation that is more aggressive. The increase of non-native vegetation can directly result in the reduction of livestock and wildlife carrying capacities. Fire frequency may also increase. An example of non-native vegetation that out competes native vegetation and increases fire frequency is cheatgrass (*Bromus tectorum*). The Big Desert study area is approximately 71 km northwest of Pocatello and the center of the study area is approximately 113º 4' 18.68" W and 43º 14' 27.88" N. (Figure 1)

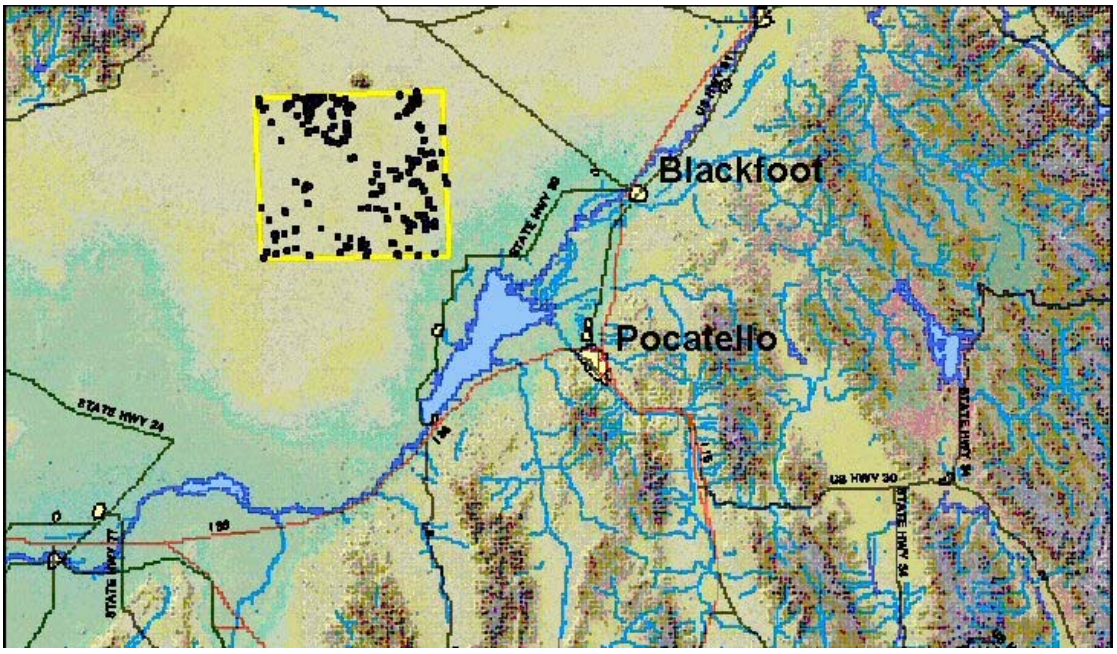

Figure 1. Southeastern Idaho and this study's Area of Concern (bounded in yellow rectangle) .

We assessed research in all possible areas; fire, no fire, grazing and no grazing. After comparing various traits in each of these areas we can create generalizations and these generalizations can then shed light on relationships between these variables and may aid range managers in making decisions about prescribed fire and grazing management.

METHODS

Five hundred and seventy five sample points were randomly generated across the study area. Each point met the following criteria;
1) >70 meters from an edge (road, trail, or fence line)
2) <750 meters from a road.

The sample points were stratified by treatment: 1) fire (within the past 10 years) 2) grazing and 3) rest. In 2004 50 points were created in each of these strata, and 70 in each in 2003. The location of each point was recorded using a Trimble GeoXT GPS receiver (+/-1m with a 95% CI) using native latitude-longitude (WGS 84). Points were occupied until a minimum of 120 positions were acquired and WAAS was used whenever available. All points were post-process differentially corrected using Idaho State

University's GPS community base station. The sample points were then projected into Idaho Transverse Mercator NAD 83 using Trimble's Pathfinder office for datum transformation and ESRI's ArcGIS for projection.

Ground Cover Estimation
Visual estimates were made of percent cover for the following; bare ground, litter and duff, grass, shrub, and dominant weed. Cover was classified into one of 9 classes (1. None, 2. 1-5%, 3. 6-15%, 4. 16-25%, 5. 26-35%, 6. 36-50%, 7. 51-75%, 8. 76-95%, and 9. >95%).

Observations were assessed by viewing the vegetation while looking straight down as we walked the sample site. This was done to emulate what a "satellite sees". In other words we were viewing the vegetation from nadir (90 degree angle).

Fuel Load Estimation
Based upon field vegetation training techniques provided by the BLM office in Shoshone Idaho, we estimated fuel load at each sample point. Visual observations of an area equivalent to a Quickbird pixel, (2.4mpp or approximately 5.76 m^2), centered over the sample point were used to estimate fuel load (table 1).

Table 1. Fuel Load Classes (Tons/Acre)

1.	0.74
2.	1
3.	2
4.	4
5.	>6

These categories were derived from Anderson (1982).

Forage Measurement
Available forage was measured using a plastic coated cable hoop 93 inches in circumference, or 0.44 m^2. The hoop was randomly tossed into each of four quadrants (NW, NE, SE, and SW) centered over the sample point. All vegetation within the hoop that was considered adequate forage for cattle, sheep, and wild ungulates was clipped and weighed (+/-1g) using a Pesola scale tared to the weight of an ordinary paper bag. All grass species (except cheatgrass (*Bromus tectorum*)) were considered forage. The measurements were then used to estimate forage amount in AUM's, pounds per acre, and kilograms per hectare (Sheley, Saunders, Henry 1995)

Microbiotic Crust Presence
Microbiotic crusts (Johnston 1997) are formed by living organisms and their by-products, creating a surface crust of soil particles bound together by organic materials. The presence of microbiotic crust was evaluated at each sample point and recorded as either present or absent. Any trace of a microbiotic crust was defined as "presence".

GAP Analysis
Vegetation cover was described using a list of vegetation cover types from the GAP project (Jennings 1997). The GAP vegetation description that most closely described the sample point was selected and recorded.

Litter Type
Litter was defined as any biotic material that is no longer living. Litter decomposes and creates nutrients for new growth. For the litter to decompose it needs to be in contact with the soil in order for the microbes in the soil to break down the dead substance. If the litter is suspended in the air it turns a gray color and takes an immense amount of time to decompose through chemical oxidation. If it is on

the ground it is a brownish color and decomposes biologically at a much faster rate. The type of litter present was recorded by color: either gray (oxidizing) or brown litter (decaying).

Big Sagebrush (Artemisia tridentata spp.) Age Estimation
Maximum stem diameter of Big sagebrush plants was measured using calipers (+/-1cm) to approximate the age of each plant (Perryman, Olson 2000) A maximum of four samples were taken at each sample point, one within each quadrant (NW, NE, SE, and SW). The sagebrush plant nearest the plot center within each quadrant was measured using calipers (+/-1cm) and converted to millimeters. The age of each big sagebrush plant was then estimated using the following equation (AGE = 6.1003 + 0.5769 [diameter in mm]).

Photo Points
Digital photos were taken in each of 4 cardinal directions (N, E, S, and W) from the sample point.

RESULTS
Percent Cover Bare Ground, Grass, and Microbiotic Crust
2003
Sixty-five percent of all 2003 field samples (*n* = 254) had >50% exposed bare ground. Eighty percent of the samples had <15% grass cover. Microbial crust presence was not recorded for this year. Seventy-two percent of the samples had >5% Cheatgrass.
2004
The dominant weed was nearly always cheatgrass (*n* = 195). Forty-five percent of the sample points had <5% cheatgrass cover. Ninety-three percent of all sample points had grass that covered <15% of the ground. Ninety-six of the sample points had >50% exposed bare ground. Only 4 of the 322 sample points had microbiotic crust present.

Big Sagebrush Age Estimation
2003
The mean age of sagebrush plants was 22.8 yrs (*n* = 514). The minimum age was 8 yrs and the maximum age was 106 yrs (Figure 2).

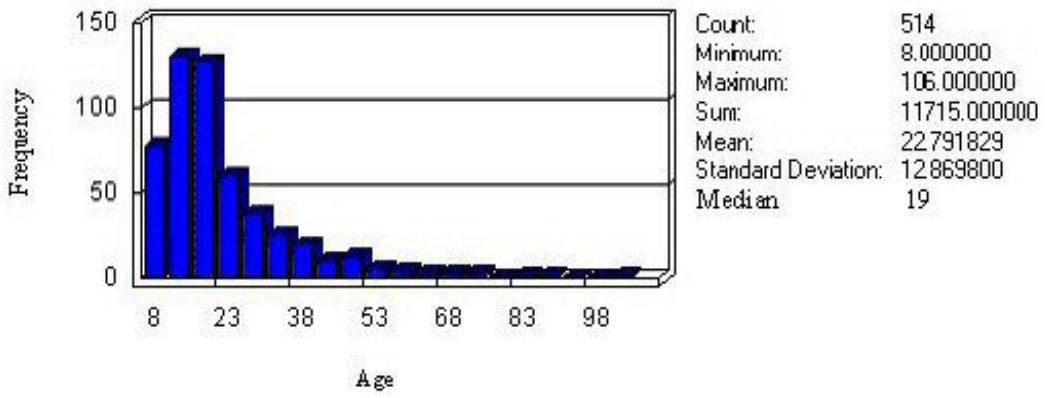

Figure 2. Age distribution of sampled Big Sagebrush plants in the study area (2003).

2004
The mean age of the sagebrush plants was 26.24 yrs (*n* = 227). The minimum age was 6 yrs and maximum age was 111 yrs. (Figure 3).

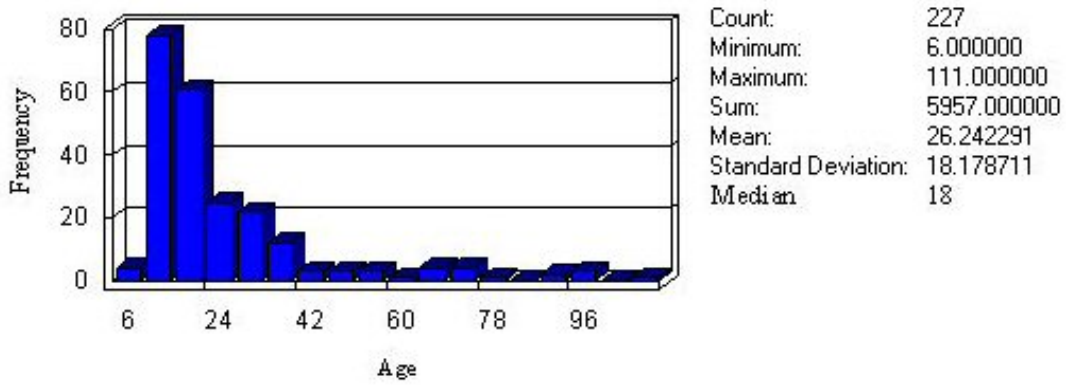

Figure 3. Age distribution of sampled Big Sagebrush plants in the study area (2004).

Forage Measurements

2003

Using AUM Analyzer software (Sheley, Saunders, Henry 1995), forage amount and available Animal Units were calculated for all sample points. Mean forage available was 191.3 kg/ha. The minimum forage available was 11 kg/ha and the maximum forage available was 1724 kg/ha.

2004

Using AUM Analyzer software, forage amount and available Animal Units were calculated for all sample points. Mean forage available was 289.7 kg/ha. The minimum forage available was 6 kg/ha and the maximum forage available was 3961 kg/ha.

CONCLUSIONS

The available forage present on the range in 2004 is higher than what was found in 2003. This is primarily due to greater amount in 2004 (table 2). This also serves to illustrate the potential of Idaho's rangelands.

Table 2. Recent annual precipitation (inches)

Month	2003	2004
May	0.53	1.91
June	0.14	0.56
July	0.00	1.09

The range appeared healthier and greener in 2004 for a longer period of time compared to 2003. There were multiple rainy days during the desert field season in 2004 while there was not one day of rain during the 2003 field season. The increased rainfall did not necessarily increase the amount of vegetation; it merely sustained the greenness of the vegetation for a longer period of time. Bare ground measurements were higher in 2004 than they were in 2003, yet AUM measurements were higher in 2004 than in 2003. These could be factors of the different areas sampled, but with such a difference in bare ground values over the 2 years I think that the vegetation that was already established used the moisture to sustain greenness for a longer period of time.

In 2004 there was a small decrease in cheatgrass from 2003. It was only a 10% difference which is not significant. Sampling in 2005 will be interesting to see the difference a high precipitation year makes in cheatgrass measurements.

In 2004 there was a higher occurrence of Green Rabbitbrush (*Chrysothamnus viscidiflorus*) than was seen in 2003. This occurred primarily in fire disturbed areas. Green Rabbitbrush is typically the first shrub to populate an area after a fire.

Big Sagebrush (*Artemisia tridentata* spp.) age was approximately the same between 2003 and 2004, although this year (2004) there was more points that had no sagebrush. This was most likely simply a function of the random points generated.

Only 4 of 322 sample points had a microbial crust present. "Microbial crust is formed by living organisms and their by-products, creating a surface crust of soil particles bound together by organic materials" (Johnston 1997). These are common in very poor rangelands and they are sometimes one of the last things left alive. They can retain water very well even against an osmotic pull. After seeing only 4 out of 322 sampled points with a positive presence during a high moisture year, continuing to record its presence would be beneficial to see how this crust changes from year to year.

ACKNOWLEDGEMENTS
This study was made possible by a grant from the National Aeronautics and Space Administration Goddard Space Flight Center. ISU would also like to acknowledge the Idaho Delegation for their assistance in obtaining this grant.

LITERATURE CITED
Anderson, Hal E. 1982. Aids to Determining Fuel Models For Estimating Fire Behavior. USDA For. Serv. Gen. Tech. Rep. INT-122. Ogden, Utah

Jennings, Michael. 1997. "Gap Analysis Program". USGS < http://www.gap.uidaho.edu>

Johnston, Roxanna. 1997. Introduction to Microbiotic Crusts. USDA NRCS Gen. Tech. Rep.

Montana State University. "AUM Analyzer" Sheley, Roger. Saunders Steve. Henry, Charles. Reprinted May 2003 < http://www.montana.edu/wwwpb/pubs/mteb133.pdf >

Perryman, B. L., and R. A. Olson, 2000. Age-stem diameter relationships of big sagebrush and their management implications. J Range Management. 53: 342-346.

Ecological Syndromes of Invasion in Semiarid Rangelands and their Implications for Land Management and Restoration

Matthew Germino, Department of Biological Sciences, Idaho State University, Pocatello, ID 83209-8007. (germmatt@isu.edu)

Steven Seefeldt, Rangeland Scientist, USDA, ARS, U.S. Sheep Experiment Station, Dubois, ID 83423.

Judson Hill, Department of Biological Sciences, Idaho State University, Pocatello, ID 83209-8007.

Keith Weber, GIS Director, GIS Training and Research Center, Idaho State University, Pocatello, ID 83209-8130. (webekeit@isu.edu)

ABSTRACT

An understanding of why infestations occur helps land managers target causes and not just symptoms of invasions. Syndromes, which are recurring sets of symptoms that are characteristic of a particular disorder or disease, help link basic and generalizable science with the specific treatment needs of individuals in clinical practice, or sites in land management. We hypothesized that management-related disturbances increase site resources in ways that selectively favor ecophysiological traits of invasive compared to established flora. In rangelands of Montana and Idaho, we measured 1) the effects of prescribed fire and shrub removal on plant community composition and soil water availability, and 2) differences in photosynthesis and water relations in *Centaurea maculosa* (spotted knapweed; CEMA) and established flora (mainly grasses). Soil water increased substantially below about 0.4 m depth in disturbed compared to control plots. Carbon uptake was about 50% greater in CEMA than the grasses, due apparently to greater water uptake from deep soils and correspondingly greater water status in CEMA. These results point to a possible ecological syndrome that may be applicable in some form to vast areas of sagebrush-steppe that 1) are disturbed in ways that 2) cause unusually low abundances of native, deep-rooted perennials, and 3) as a consequence, have unusually abundant deep soil water, and 4) are therefore more easily invaded by CEMA and similar exotic perennial forbs. If correct, this syndrome suggests that managing semiarid communities for complete utilization of soil water may be an important way that rangeland managers can avoid infestations by exotic perennial forbs.

Keywords: invasive plants, fire, semiarid rangelands, sagebrush steppe, ecophysiology, soil water

INTRODUCTION

Exotic plant invasion is probably the greatest ecological problem in the management of semiarid rangelands of the American Intermountain west. Exotic plant infestations in semiarid rangelands have generally been persistent and difficult or impossible to eradicate, and have led to considerable ecological and economic damage. Much research has focused on eradication of invasive plants, while basic factors underlying the invasiveness of certain plants or the susceptibility of sites to invasion have received less attention. A better understanding of why invasions occur should lead to more effective, pro-active management and restoration strategies that prevent invasions from occurring.

Unfortunately, basic research is difficult to conduct on the short-time scales that are most relevant to land management decisions, and also tends to be too expensive to limit in scope to specific sites that concern land managers. Invasive plant management may benefit from adopting means by which clinical practice is linked with basic research in medical disciplines. Clinicians use sets of symptoms to identify disorders in their subjects, then prescribe remedial actions that are based in some way on basic, scientific knowledge of how the disorder functions. This system links the efforts of scientists who seek to provide basic information that can be broadly applied, and clinicians who are concerned with specific subjects.

In contrast to medical systems, restoration of infested rangelands and other habitats has typically focused entirely and usually unsuccessfully on application of unnatural chemicals or biological agents to reduce the abundance of invasive plants. Exotic plant infestations of rangelands may be symptoms of other, currently unknown 'disorders' in ecosystem structure and function that are likely to arise from natural and anthropogenic disturbance. If so, failed efforts to restore infested lands may be due to an emphasis on treating symptoms and not identifying and treating causes of infestations. Prescriptions of fire for agricultural or ecological restoration purposes, grazing, mechanical removal of shrubs, and other management practices are examples of practices which have been associated with invasions and perhaps are causative agents of infestations (e.g., Fig. 1).

Figure 1. A 2004 photo of a near monocultural infestation of leafy spurge (*Euphorbia esula*) in a 1999 prescribed burn at the USSES, with unburned and uninfested sagebrush steppe in the background. Only 0.5 of >200 ha were infested in this area of the otherwise pristine USSES, and it is a small example of much larger problems in nearby rangelands.

Infestations result from dispersal of exotic seed into a site, followed by successful emergence, establishment, persistence, and proliferation of exotic plants within the site. Control of dispersal is a known and practiced aspect of exotic plant management, but infestations still occur and persist in semiarid lands of Idaho and Montana. The objective of our ongoing research is to determine factors

that contribute to the persistence of non-indigenous, invasive, perennial forbs of semiarid rangelands. Previous research (eg. Mack 1985) demonstrated the widespread syndrome of infestations of semiarid lands by annual 'cheatgrass' (*Bromus* sp.) and fire-related mechanisms that contribute to its persistence. However, many exotic, invasive plants in semiarid rangelands of western North America are perennial forbs that can have deep taproots.

This paper describes preliminary findings from our research on basic mechanisms contributing to the success of spotted knapweed (*Centaurea maculosa*) and other, exotic perennial forbs (eg. leafy spurge, *Euphorbia esula*) in sagebrush steppe rangelands. Disturbance is a frequently cited cause of infestations, but few studies provide a comprehensive understanding of how site conditions change in ways that selectively favor invasive compared to native or established plants. Fire and eradication of sagebrush are two common disturbances that are associated with infestation by exotic perennial forbs in the sagebrush steppe. We hypothesized that fire or removal of shrubs cause increases in site resources that selectively favor the maintenance of populations of *Centaurea* compared to native or established plants. Water availability is the most limiting soil resource of semiarid lands, and was therefore our focus. We measured how fire and removal of shrubs affect patterns of soil water availability, and how the productivity and water relations of invasive and native plants respond to changes in availability of soil water.

METHODS

Data presented here synthesize in abbreviated form the major findings from several other papers that are either in review or in preparation for submission elsewhere. Photosynthesis and water relations were measured for *Centaurea maculosa* L. near Bozeman and Helena, Montana and the US Sheep Experimental Station (USSES) near Dubois, Idaho. Native or established vegetation at the Montana sites consisted of sagebrush (*Artemesia tridentata* ssp*. wyomingensi*s), brome grass (*Bromus inermis*), and wheatgrasses (*Psuedoregneria spicata, Agropyron smitthi*), and the USSES site consisted of *Artemesia tridentata* ssp. *vaseyana*, grasses such as *Psuedoregneria spicata, Fescue idahoensis*, and *Poa sp.*,., and forbs such as *Crepis, Erigeron, Balsamorhiza, and Lupinus* sp.. Elevation and mean annual precipitation for each site was 1650 m and 297 mm/yr for the USSES, 1500 m and 440 mm/yr for the Bozeman site, and 1200 m and 295 mm/yr for the Helena Site, respectively (Western Regional Climate Center, Desert Research Institute, Reno, NV).

FIRE AND SHRUB REMOVAL EFFECTS

In September of 2002, 12 replicate areas of the USSES ranging from 0.1 to >100 ha were burned (Fig. 2). In the same month, all sagebrush were mechanically removed using chainsaws in three, 25 x 25 m areas. Subsequently, soil water contents were measured using a neutron probe (CPN, Martinez, CA). Corresponding changes in vegetative cover were determined on the ground using visual estimates of cover in 100 1-m^2 frames that were deployed in a grid-like, stratified sampling scheme (see 'multiplots' in Fig. 2). We calculated the normalized difference vegetation index, which correlates with the vertical abundance or leaf-area index of vegetation, for areas around each soil water sampling location, using Quickbird satellite imagery. The Quickbird imagery had 3 x 3 m pixels, with reflectance measured in four visible wavebands.

INTERSPECIFIC DIFFERENCES IN USE OF SOIL WATER

In 2002 and 2003, we measured photosynthesis and water relations of *Centaurea maculosa* and co-occurring grasses in a greenhouse study and at the Bozeman and Helena sites. Photosynthesis was measured in situ using a portable photosynthesis instrument (model 6400, LiCOR Inc, Lincoln, NE) and plant water potential was measured using a pressure chamber (PMS, Corvallis, OR)

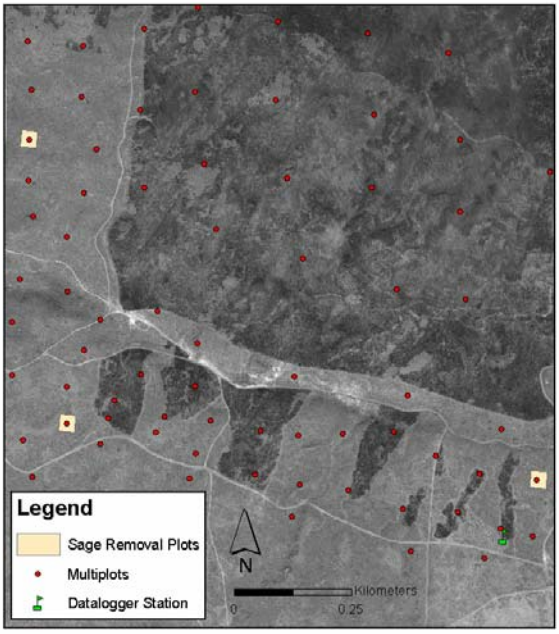

Figure 2. Quickbird image of study site at the USSES.

RESULTS

FIRE AND SHRUB REMOVAL EFFECTS

Over the whole summer of 2003, sites burned in 2002 had 20% greater soil water content than sites that had sagebrush removed or were undisturbed (Fig. 3). In midsummer, burned plots had about 40% less herbaceous cover and 10% lower NDVI than control plots. 'Cut' plots where sagebrush was removed had similar herbaceous cover and 10% lower NDVI than control plots (not shown). In shallow soils (< 30 cm) at early season, water contents became more than 50% greater in burned compared to control plots (Fig. 3). By mid summer, soil water contents had become 15-40% greater in burned compared to control sites, at all soil depths (Fig. 3). Subsequently, evaporative losses from shallow soils diminished any treatment differences except in soils deeper than about 40 cm. By July and especially September, water contents of deeper soils were about 50% greater in burned and shrub removal plots compared to control plots where sagebrush were apparently taking up deep soil water. From July to the end of the growth season, the only soil water contents that appeared to correspond to levels within nominal ranges for plant uptake were in soils deeper than about 50 cm in undisturbed or sagebrush-removed plots.

INTERSPECIFIC DIFFERENCES IN USE OF SOIL WATER

No differences in photosynthesis or photosynthetic water use efficiency (mol CO_2/H_2O) were detected between *C. maculosa* or rangeland grasses in a greenhouse study following growth for 2 months at three water potentials. However, photosynthesis was several fold greater in *Centaurea maculosa* compared to co-occurring rangeland grasses over all sites and sampling dates in the field, and also was more persistent during the driest periods of summer, when other plants senesced (Fig. 4). Photosynthesis was measured in *C. maculosa* when water contents of shallow soils were below nominal values for the permanent wilting point, in August of 2002 (Swan & Wraith, unpublished). When water contents of deep soils became less than levels corresponding to the permanent wilting point during unusually dry conditions of 2003, photosynthesis was no longer detectable in *C. maculosa* (Fig. 4). Photosynthetic water use efficiency appeared similar between *C. maculosa* and established flora under all conditions except the driest of sampling conditions in 2003, when water use efficiency became greater in *C. maculosa* (not shown).

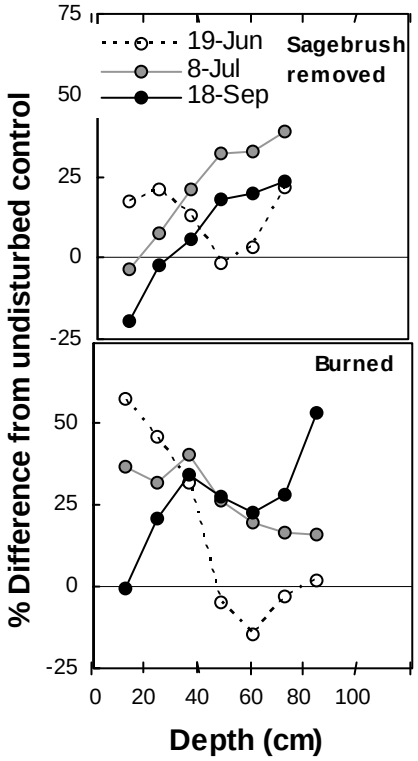

Figure 3. Mean percent difference in soil water content at different depths in sites that were burned or had sagebrush mechanically removed, compared to unburned controls. Data were collected in 2003 and treatments were applied in 2002. N = 3.

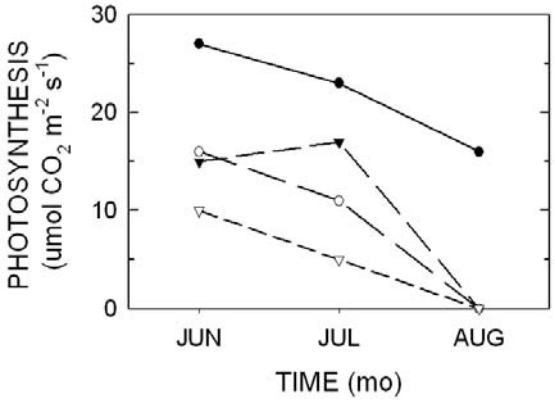

Figure 4. Mean photosynthesis of *C. maculosa* (round symbols), and grasses (triangular, *Bromus inermis Pseudoregneria spicata*) in 2002 (solid) and 2003 (open). N = 2 means, one from each site, and each consisting of 15 replicates.

Plant water potentials decreased 30% less from predawn to midday in *C. maculosa* compared to co-occurring rangeland species, even though *C. maculosa* had much greater evapotranspiration (not shown). Plant water potential in *C. maculosa* decreased only 34 ± 9% from predawn to midday compared with 51 ± 1% and 78 ± 4% decreases in *P. spicata* and *B. inermis*. Accordingly, *C. maculosa*

had midday water potentials that were 183% and 110% greater than *P. spicata* and *B. inermis*, respectively

DISCUSSION

Fire and removal of shrubs, two widespread disturbances of sagebrush steppe rangelands, led to considerable increases in water contents of deep compared to shallow soils and for a substantial period of the growth season (Fig. 3). Photosynthetic carbon uptake appeared much greater in *C. maculosa* compared to other rangeland species, due apparently to greater maintenance of water status during solar periods. Greater maintenance of high water potentials during solar periods with high evapotranspiration in *C. maculosa* compared to grasses could only result from greater uptake of water in CEMA. Measurements of photosynthesis in *C. maculosa* when water contents of shallow but not deep soils were below levels that are within the range of availability to plants, combined with cessation of photosynthesis when deep soil water became depleted below plant-available levels indicates that the extra water taken up by *C. maculosa* compared to grasses is probably from deep soils. These ecophysiological data are evidence that the persistence of *C. maculosa* following initial invasion is enhanced by the availability of deep soil water.

Soil water contents were previously reported to be lower underneath stands of *C. maculosa* as well as *C. solstitialis* compared to similar sites that did not have these species (Sperber 2001, Gerlach 2003). Our findings indicate that differences in how invasive and established plants use soil water can contribute to invasions of semiarid rangelands, in addition to differences in nutrient use and potential allelopathic interactions (e.g., Blicker et al. 2002, 2003; Rideneour and Calloway 2001). Increases in soil water that result from fire and shrub removal are likely to selectively favor *C. maculosa*, and probably similar tap-rooted invasive forbs of rangelands.

Our findings agree with those of Anderson et al. (1987) who demonstrated that intact sagebrush steppe communities nearly completely utilize all available soil water. The manner in which fire or shrub removal affected soil water contents appeared consistent with how these disturbances modified vegetation (Fig. 3). Both disturbances eliminated shrubs, which are the primary native users of deep soil water in these communities, and increases in deep soil water were the most consistent changes observed following these disturbances. Increased water content of shallow soils in early summer following fire likely results from reductions in herbaceous cover.

Our results indicate a potential syndrome of invasion in semiarid rangelands, whereby persistent infestations by herbaceous perennial forbs occur on sites that are disturbed in ways that select against native, deep rooted species and have elevated water contents in deep soils. Two factors indicate the potential generality of this syndrome to those sagebrush-steppe rangelands of western North America that receive most precipitation during winter and therefore have significant deep soil water: 1) the majority of invasive exotic species in these habitats (Pyke 1999) are forbs that are tap rooted like *C. maculosa*, and 2) much sagebrush steppe is disturbed by fire, shrub removal, and other disturbances that happen to select against deep rooted species. A significant portion of sagebrush steppe in slightly drier areas than our study sites is currently dominated by cheatgrass, a shallow-rooted, spring annual, and local land managers and scientist have recognized the susceptibility of these lands to so- called ‘secondary invaders’, which consist primarily of invasive exotic forbs, such as those describe here.

Recurrent, expensive, and potentially hazardous efforts to eradicate *C. maculosa* and similar exotic forbs like leafy spurge (*Euphorbia*), skeletonweed (*Chondrilla*), thistles, and other *Centaurea* species may be treating the symptom instead of causes of their persistence. More effective restoration of infested rangelands might involve identifying and maintaining or increasing the abundance of those species which can best compete for soil water and resources that exotic species need to thrive.

ACKNOWLEDGEMENTS
This study was made possible by a grant from the National Aeronautics and Space Administration Goddard Space Flight Center. ISU would also like to acknowledge the Idaho Delegation for their assistance in obtaining this grant.

Funding for this research was also provided by the United States Department of Agriculture NRI program, and NASA. Thanks also to M. Pokorny and J. Jacobs for inviting this paper for the symposium entitled "Restoration of invasive plants infestations: On the edge between science and management". The use of trade, firm, or corporation names in this publication is for the information and convenience of the reader. Such use does not constitute an official endorsement or approval by the United States Department of Agriculture or the Agricultural Research Service of any product of service to the exclusion of others that may be suitable.

LITERATURE CITED

Anderson, J.E., Shumar, M.L., Toft, N.L. & Nowak, R.S. (1987) Control of the soil water balance by sagebrush and three perennial grasses in a cold-desert environment. *Arid Soil Research and Rehabilitation* 1, 229-244.

Blicker, P.S., Olson, B.E. & Engel, R. (2002) Traits of the invasive *Centaurea maculosa* and two native grasses: Effect of N supply. *Plant and Soil* 247, 261-269.

Blicker, P.S., Olson, B.E. & Wraith, J.M. (2003) Water use and water-use efficiency of the invasive *Centaurea maculosa* and three native grasses. *Plant and Soil* 254, 371-381.

Gerlach, J. D. (2004) The impacts of serial land-use changes and biological invasions on soil water resources in California, USA. *Journal of Arid Environments* 57, 365-379.

Mack RN (1985) Temperate grasslands vulnerable to plant invasions: characteristics and consequences. Biological Invasions: a Global Perspective (eds.) JA Drake, HA Mooney, E diCastri, RH Groves, FJ Kruger, M Rejmanek, M Williamson. John Wiley, Chichester, pp155-173

Pyke, D.A. (1999) Invasive exotic plants in sagebrush ecosystems of the intermountain west. In: *Proceedings: Sagebrush Steppe Ecosystems Symposium*. Bureau of Land Management Publication No. BLM/ID/PT-001001+1150, Boise ID USA

Ridenour, W.M. & Callaway, R.M. (2001) The relative importance of allelopathy in interference: the effects of an invasive weed on a native bunchgrass. *Oecologia* 126, 444-450

Sperber, T.D. (2001) *Soil physical properties and soil water dynamics under spotted knapweed and native grasses*. M.S. Thesis, Montana State University, Bozeman.

Spatial and Temporal Patterns of Sagebrush (*Artemisia tridentata ssp. vaseyana*) Establishment Following Fire

Katherine DiCristina. Idaho State University, Department of Biological Sciences. Pocatello, Idaho 83209-8007.

Matthew Germino. Idaho State University, Department of Biological Sciences. Pocatello, Idaho 83209-8007. (germmatt@isu.edu)

Steven Seefeldt . US Sheep Experiment Station, US Department of Agriculture, Dubois, Idaho 83423

ABSTRACT

Long-term recovery of sagebrush populations following natural and prescribed fires has been inconsistent among sites in the Great Basin. Explanations for this variability are precluded in part by an incomplete understanding of factors affecting sagebrush establishment. Our objective was to determine how establishment of *Artemisia tridentata* ssp. *vaseyana* (mountain big sagebrush) varies in time and space, relative to climate fluctuations and neighboring plant species. We measured year of *A. t. vaseyana* establishment, distances of *A. t. vaseyana* seedlings to surrounding vegetation and community cover in four sites that were burned at different times, 1-8 years prior to sampling. Age distributions in each burn site indicated that seedling establishment occurred only in the first 1-3 years following each fire, irrespective of variations in climate that occurred among burn years. Distances of *A. t. vaseyana* seedlings to herbs became progressively smaller and moreover similar to distances of random locations to herbs, in sites having greater times since burning and correspondingly more herb cover. No spatial relationships were detected between *A. t. vaseyana* seedlings and older shrubs. Temporal patterns of *A. t. vaseyana* establishment reported here differ from relatively gradual and weather-dependent establishment patterns reported for other subspecies of big sagebrush, at lower elevations. Post-fire establishment of *A. t. vaseyana* appeared to be driven by more than episodes of optimal weather, and may be affected by changes in herb cover and seed availability that result from fire.

Keywords: rangeland, fire, sagebrush.

INTRODUCTION

Fire is an important component of disturbance-succession regimes in sagebrush steppe that is managed through suppression and prescribed application. Fire is applied in sagebrush steppe to promote forage production, reduce fuel loads, or restore disturbance for wildlife habitat. Whether, and to what extent application of fire achieves these ecological goals is currently debated, as indicated by much lower levels and higher variability of big sagebrush cover (*Artemisia tridentata*) up to 30 years following fire (Wambolt *et al.*, 2001) compared to studies conducted in earlier decades (Harniss and Murrary**,** 1973). Lack of *A. tridentata* recovery following fire is a major concern for sustaining sage grouse (*Centrocercus urophasianus*) and other wildlife (Leonard *et al*., 2000). Altered rates of *A. tridentata* reestablishment correspond in many cases with invasions by exotic herbs, which sagebrush steppe appears unusually vulnerable to (Brooks and Pyke, 2001). A better understanding of how native herb communities affect reestablishment patterns of key shrub species (e.g., Eliason and Allen, 1997) is needed to assess potential impacts of exotic herbs on ecological processes, such as disturbance-succession cycles.

Resprouting and rapidly colonizing herbs, as well as a few shrubs, tend to dominate burned sagebrush steppe in the decade or so following fire, while the slower-growing *A. tridentata* reestablishes (Harniss and Murray, 1973). Direct observations of interactions between sagebrush seedlings and other species are rare in the literature (e.g. Daubenmire, 1975; Owens and Norton, 1989; Berlow *et al*., 2002), especially for postfire conditions. Seed dispersal and germination have been studied for *A. tridentata* and other aridland shrubs in undisturbed and post-fire situations (e.g. Hassan and West, 1986; Young *et al.*, 1990; Tyler, 1996; Chambers, 2000), but less is known about factors affecting seedling success. High mortality rates during initial seedling establishment indicate the importance of this life history stage for dynamics of *A. tridentata* populations (Daubenmire, 1975; Owens and Norton, 1989).

The objective of this study was to determine spatial and temporal patterns of *A. t. vaseyana* establishment following fire, relative to climate variations and changes in abundance of other native plant species. Temporal patterns of establishment were estimated by determining seedling ages in sites burned 1-8 years prior to sampling. Spatial patterns of establishment relative to neighboring plants were determined by measuring the percent cover, identity and proximity of surrounding vegetation to *A. t. vaseyana* seedlings. We also examined interactions of azimuth orientations and distance of *A. t. vaseyana* seedlings to neighboring vegetation to determine if establishment near or away from neighboring plants might be affected by aboveground interactions, such as shading. Spatiotemporal patterns and correlates of *A. tridentata* establishment could yield important insight on disturbance-succession cycles in semiarid shrublands.

MATERIALS AND METHODS

Site and species.—Research was conducted in sagebrush steppe at the US Sheep Experimental Station (USSES) near Dubois, Idaho (44°14’44” N Latitude, 112°12’47” W. Longitude; 1650 m a.s.l.) where fire and grazing records were available since about 1935. Vegetation in the particular region of the USSES that we examined (<50 km^2) is a diverse sagebrush and perennial herb community that is rare in having almost no invasive or exotic plants. The absence of exotic plants provided an opportunity to examine responses of sagebrush to its native community. The dominant shrub in this community, mountain big sagebrush, *Artemisia tridentata* ssp. *vaseyana* Nutt, shares the drought-deciduous foliage and dimorphic root traits of other subspecies of big sagebrush that occur in warmer and drier sites (*A. t. wyomingensis* and *A. t. tridentata*). Other, less abundant shrubs are *Chrysothamnus viscidiflorus* Nutt., *Tetradymia canescens* DC. and *Purshia tridentata* (Pursh) DC. Perennial bunchgrasses such as *Agropyron dastychium* (Hook.) Scribn., *Festuca idahoensis* Elmer and *Poa sandbergii* Vasey, and short-lived perennials such as

Achillea millefolium L., *Antennaria rosea* Rydb. Gaertn., *Erigeron corymbosus* L., *Phlox longifolia* L. and *Crepis* sp., are common herbs. Soils are fine, loamy, mixed, frigid Calcic Argixerolls derived from wind blown loess or residuum (Natural Resources Conservation Service). Total annual precipitation averaged 297 mm over the last 78 years, with most precipitation occurring as spring snow and early summer rain (Western Regional Climate Center, 'WWRC', Desert Research Institute, Reno NV).

All data were collected from June to July 2003, when herb abundances were at seasonal maxima. Seedlings of *A. t. vaseyana* were individuals less than 30 cm in height above ground and lacking reproductive structures. Adult *A. t. vaseyana* are frequently 1 to 1.5 m in height or taller.

Prescribed burns.—Burns were located within a few km of each other, and areal extents of each burn were 280 ha for the 1995 burn, 207 ha for the 1998 burn, 221 ha for the 1999 burn and 105 ha for the 2002 burn. The four burns were all prescribed, and occurred in fall of their respective years, prior to seed production by the sagebrush community. Grazing has occurred on all sites. Mean animal unit months (aum) from 1968-2003 for the 1995, 1998, 1999 and 2002 burns were 21.3, 8.9, 13.0 and 21.3, respectively. Grazing did not occur in the year prior to or during application of prescribed burns in 1995 and 1999. Short-term and low-intensity grazing (few animals) did occur following the 1998 and 2002 burns.

No seeding of any species occurred during or prior to the study and all sagebrush seedlings emerged from seed that dispersed and germinated naturally. Seed production in *Artemisia tridentata ssp. vaseyana* appears to be fairly consistent from year to year (Young *et al.*, 1989; Harniss and McDonough, 1976). Big sagebrush seedling densities near $2/m^2$ or frequently more were detected following fires on or near the USSES, even several km from unburned plants in large burn areas (Mueggler, 1956). Seeds of *A. t. vaseyana* can remain viable for at least several years in soil, and seedlings in Mueggler's study (1956) apparently germinated primarily from residual seed that endured fire (see also Hassan & West 1996), though seed transported by wind from unburned plants also appeared significant in some cases. Other studies reported narrow dispersal ranges for other species of sagebrush or subspecies of big sagebrush, with seeds most commonly dispersing and germinating within about 1 m from reproductive plants (e.g. Young et al. 1989; Berlow et al. 2002).

Seedling age distributions.—We used a stratified-random method to collect 10 seedlings from each of the 1995, 1998 and 1999 burns, and 30 emergent seedlings from the 2002 burn, for determination of establishment dates of *A. t. vaseyana* seedlings. Seedlings were collected from a 1-m wide, 20-40 m long belt transect in each burn. Only one seedling was collected from clusters of seedlings (eg, several seedlings within a few cm), when clusters were encountered, to ensure spatial dispersion of samples. Establishment dates and ages of seedlings were determined from thin cross sections of the stem, taken within a mm of the stem-root interface, that were stained with 1% basic fuchsin and 0.1% toluene blue. We captured images of each section with a microscope under 40-100x magnification (Remote Capture 2.2, Canon USA) and counted annual growth rings. Interannual (ie. false) or complete absence of rings is supposedly rare in big sagebrush (Maier *et al.*, 2001; Ferguson, 1964). Patterns of establishment among years were compared to precipitation and temperature records for the USSES, obtained from the WWRC. Cumulative precipitation from January to September was determined by summing total precipitation for each month. Average monthly maximum and mean temperatures from May to September were determined by averaging the maximum or mean values reported for each month, respectively.

Neighborhood relationships of seedlings and community cover.—A second stratified-random sampling regime was used to locate *A. t. vaseyana* seedlings for assessment of seedling heights, distances to neighboring plants, and community cover. These locations occurred at random distances of 1 to 100 m from the perimeter towards the center of each burn area. Distances originated at 200 m intervals along the perimeter of burns. Measurements for both actual seedlings and random points were necessary to characterize both the realized and available space for seedlings, respectively. Therefore, we measured distances from random points to neighboring plants, using the same protocol used for assessing neighboring plants for *A. t. vaseyana* seedlings. In all cases, random points did not have sagebrush seedlings, by chance.

Using differentially-corrected global positioning system points of all sampling locations, geographic information systems, and digital elevation models (GeoExplorer, Trimble Inc, CA; ArcGIS version 8, ESRI Inc, Redlands CA; 10 m pixel elevation data from United States Geological Survey), we determined that about 40% of 192 sample points (N = 46-51) that were recorded for all years combined were on flat ground with 0° slopes. The maximum slope was 9.26°, and 95% of sample points that were not on level ground were on <6°slopes.

Distances from the base of each *A. t. vaseyana* seedling, or random point, to the base of the nearest herb (forb or grass) and nearest shrub in each of four cardinal directions (NW, NE, SE, SW) were measured, for a total of eight distances per seedling or random point. The four measured distances were added together and considered the 'sum distance' of each *A. t. vaseyana* seedling or reference point to the surrounding vegetation. This sampling approach allowed us to generate more replicates than possible with techniques similar to Theissen polygons (e.g. Owens and Norton, 1989), but was more robust than simply measuring distance to only the nearest neighboring plant. Heights of all *A. t. vaseyana* seedlings above soil were measured. Ground cover was assessed in 0.5 m^2 plots at the random points using the point intercept method (Floyd and Anderson, 1987), to assess overall differences in the identity and abundance of vegetation in each burn site. Cover classes included shrub, herb, forb, litter, rock and bare soil. The number of seedlings and random points sampled, respectively, were 56 and 16 in the 1995 burn, 75 and 23 in the 1998 burn, 52 and 10 in the 1999 burn, and 89 and 32 in the 2002 burn. We initially did not make measurements of distances and abundances of neighboring plants for random points, leading to less sampling than for seedlings.

Vegetative and other ground cover were also measured in 87, 0.56-m^2 plots at midsummer before and the year after applying the 2002 fire (39 of the 87 plots burned), to further assess how herb cover changes as a result of fire. In each 0.56-m^2 plot, the amount of shrub, grass, forb, bare soil, litter, and rock cover was estimated without the use of point frames to the nearest 5%, except for 1% resolution for classes covering less than 5% of plots.

Statistical analysis.—Our analysis focused on determining whether heights or ages of seedlings, and distances of seedlings or random points to neighbors, varied among sites burned in different years. The 1995, 1998 and 1999 fires occurred as one large patch, and there was no basis for identifying spatial replicates of burns or separate seedling populations within each burn. We therefore caution that although we examined a substantial number of seedlings, our experimental design replicated seedlings but not sites within each burn year. The statistics reported herein are therefore a better measure of the population or community in each burn site, rather than how year of burn affects sagebrush populations.

The significance of mean differences in heights or ages of seedlings in sites with different times since burning was determined using one-way analysis of variance (ANOVA; $\alpha < 0.05$). Three-

way ANOVA was used to determine the significance of mean differences in sum distances to neighboring vegetation among sampling type (seedlings or reference points), type of neighbor (grass, forb and shrub), and burn site (1995, 1998, 1999 and 2002 burn). We tested for differences in each cover class (shrub, grass, forb, bare soil, litter and rock) among each burn site (1995-2002 burn sites) using two-way ANOVA. The significance of changes in each cover class (shrub, grass, forb, bare soil, litter, rock) from before to after the 2002 fire (measurements in 2002 and 2003) was determined for burned and unburned plots using three-way ANOVA, with (1) cover class, (2) burn year, and (3) treatment (burned or unburned) as factors. Two-way ANOVA was also used to determine if distances of *A. t. vaseyana* seedlings to surrounding vegetation were affected by the cardinal orientation of seedling and neighboring plant (NE, SE, NW and SW), and whether distances in each cardinal orientation were similar among each burn site (1995-2002). Distances to neighboring vegetation and cover data were ln or arcsine transformed to satisfy ANOVA requirements for normal distribution. Analyses were conducted using SAS version 8 and JMP version 3.2.2 (SAS Institute, Cary NC).

RESULTS

Frequency distributions of seedling height and age.—Heights of seedlings in sites burned in 1995, 1998 or 1999 were similar, and collectively greater than seedling heights in the 2002 burn ($F_{3,59} = 233.37$, $P < 0.0001$, Fig. 1), where 90% of seedlings were under 5 cm in height. Only one seedling in the 1995 burn, and two seedlings in the 1998 burn were under 5 cm. Correspondingly, seedlings aged in 2004 were considerably younger in sites burned more recently (Fig. 2). All seedlings in the site burned in 2002 established in 2003. In the sites burned in 1999 and 1998, 70% and 50% of seedlings established in the year following fire, respectively, and no establishments were detected after the 3rd year following fire. Similarly, no establishments were detected after the 3rd post-fire year in the site burned in 1995, but seedling establishments were more evenly distributed over the three years following the 1995 fire than observed in the 1999 and 1998 burns (Fig. 2). Mean ± SE ages of seedlings in 2004 were (in years) 1.0 ± 0.0 in the 2002 burn, 3.5 ± 0.3 in the 1999 burn, 4.3 ± 0.3 in the 1998 burn and 7.0 ± 0.3 in the 1995 burn ($F_{3,59} = 1137.05$, $P < 0.0001$). The range of seedlings ages (max. – min. age) within each burn was only 2 years.

No consistent relationships emerged between temperature or precipitation of years that came before, during, or after each fire, and age or height distributions of *A. t. vaseyana* in each burn site (Fig. 3 compared to Fig. 2). The 1995 burn occurred in a relatively wet and cool year and was followed by average conditions, and the 1998 and 1999 burns occurred during relatively wet years and were followed by relatively wet or average conditions. In contrast, weather before, during, and after the 2002 burn was among the warmest and driest in the past century (Fig. 3). Despite these climate variations among burn years, there was a consistent tendency for establishment within the first 3 years following each fire.

Relationships to surrounding vegetation.—Cover of *A. t. vaseyana* and other shrub species (*Chrysothamnus, Tetradymia*) was as much as 10% of ground area in sites burned from 1995-1999 (Fig. 4). Grass cover was about twofold greater in sites burned from 1995-1999 compared to in the 2002 burn ($F_{1,1265} = 5.4$, $P = 0.02$), and there was marginal statistical support for about 50% less soil exposure in sites burned in 1995-1999 compared to in 2002 ($F_{1,1265} = 1.9$, $P = 0.16$, Fig. 4). In the 2002 burn site, herbaceous cover was at least 50% lower and soil exposure threefold greater than before fire in 2002, when grass cover was 30.4 ± 2.1%, forb cover was 24.5 ± 1.8%, and bare soil was 13.4 ± 1.5% ($F_{1,1089} > 10.0$ and $P < 0.002$ for changes in each cover type from 2002-2003; data not shown). No changes in soil exposure were detected in

neighboring, unburned plots from 2002 to 2003, however, forb cover decreased 22% ($F_{1,1089}$ = 4.6, P = 0.03) whereas there was marginal statistical support for a 16% increase in grass cover from 2002-2003 in these control plots ($F_{1,1089}$ = 2.03, P = 0.14).

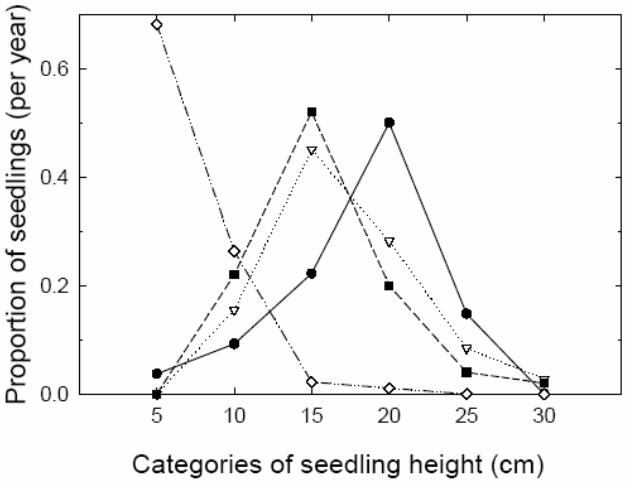

Figure 1. Frequency distribution of heights of A. t. vaseyana seedlings found on sites with different time since fire. The upper value of each 5-cm height category is shown on the x-axis. Seedlings are represented by round symbols in the 1995 burn; triangles in the 1998 burn; squares in the 1999 burn, and diamonds in the 2002 burn. N=52-89 seedlings per burn year.

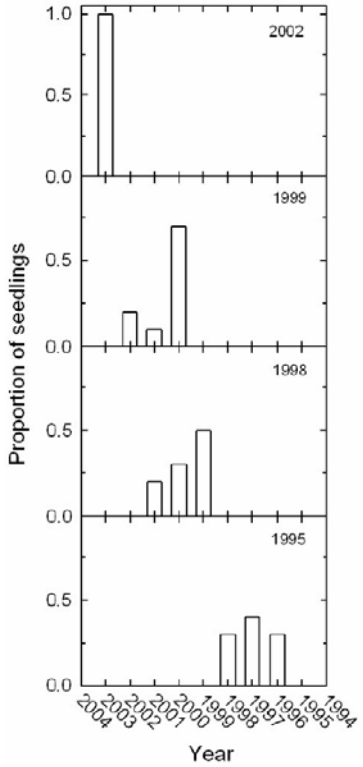

Figure 2. Frequency distribution of year of establishment for seedlings of *A. t. vaseyana* in each burn. N = 10 except in the 2002 burn, where N = 30.

Sum distances of *A. t. vaseyana* seedlings to shrubs did not vary appreciably among the sites burned from 1995-1999 (Fig. 5). Also, distances were similar from of *A. t. vaseyana* seedlings and random points to shrubs, in sites burned from 1995-1999 (Fig. 5). *Artemisia* seedlings in the 2002 burn had almost 3-fold greater sum distances to forbs than in sites burned before 2002 ($F_{1,483} = 83.5$, $P < 0.0001$), and compared to random points in the 2002 burn ($F_{1,483} = 8.4$, $P < 0.01$, Fig. 5). Distances of *Artemisia* seedlings to grasses were 1.4 to 2.5 times greater in the site burned in 2002 compared to sites burned prior to 2002 ($F_{1,483} = 62.2$, $P < 0.0001$), and compared to random points in the 2002 burn ($F_{1,483} = 12.9$, $P < 0.001$). Mean distances of *A. t. vaseyana* seedlings to shrubs and herbs were similar in all cardinal directions, for all burn years (not shown).

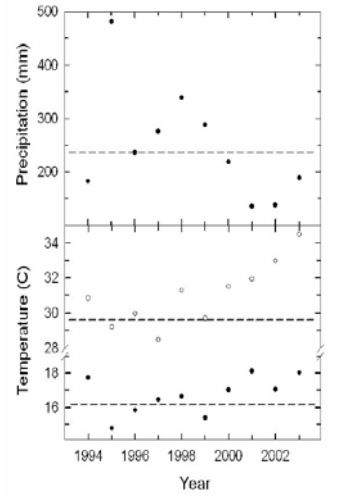

Figure 3. Cumulative precipitation from January-September (top panel) and average monthly maximum and mean temperatures from May-September (open and solid symbols, respectively, in lower panel). Dashed lines show mean values for the past 80 years.

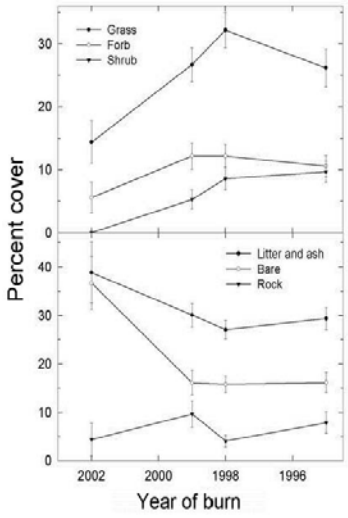

Figure 4. Mean (± 1 SE) percent cover of grass, forbs, shrubs (top panel) and litter, bare soil, and rock (bottom panel) in each burn year. N = 52-89.

DISCUSSION

New establishment of *A. t. vaseyana* in the initial 1-3 years after each fire, followed by no new establishments in the next 4-8 years (Figs. 1, 2), differ considerably from the general perception that sagebrush establishment occurs progressively over decades following fire (Harniss and Murray, 1973; Meyer, 1994). Mueggler (1956) reported substantial seedling establishment (frequently >2 seedlings per m^2) in the first growth season following 4 of 5 burns years at the USSES. Mueggler (1956) also speculated that most seedlings established in the initial postfire year, on a site burned 4 years prior to his sampling. Similarly, in another study at the USSES, juveniles (<15 cm) were about 10 times as abundant as 'seedlings' (presumably new emergents, with low densities near 0.03 individuals/m^2) in a site burned 11 years prior to sampling, reflecting a previous pulse of establishment (Harniss and Murray, 1973).

New establishments of *A. t. vaseyana* as well as *A. t. tridentata* can apparently occur in later stages of succession, decades following fire (Harniss and Murray, 1973; Daubenmire 1975; Young and Evans, 1978, 1989; Wambolt *et al*., 2001). For example, individuals of *A. t. vaseyana* in the youngest seedling size classes were 10-fold more abundant (0.3-0.5 seedlings/ m^2) on unburned sites than on sites burned about 10 years prior to sampling (Harniss and Murray, 1973). Thus, our study combines with Mueggler (1956) and Harniss and Murray (1973) to indicate that new establishment of *A. t. vaseyana* may be most common in sites burned in the previous three years, least evident in sites at intermediate stages of succession, but apparent again in sites having some mature *A. t. vaseyana* after decades of recovery since burning.

Temporal patterns of sagebrush establishment described above are nearly opposite of typical changes in herbaceous cover during disturbance-succession cycles in sagebrush steppe. Herb cover is usually least abundant immediately following and in the first growth seasons after fire, but most abundant thereafter for about a decade, in a variety of *A. t. vaseyana* and other *A. tridentata* communities (Fig. 4; Young and Evans, 1978; West and Hassan, 1985; Akinsoji, 1988; Cook *et al*., 1994, Ratzlaff and Anderson, 1995; Perryman *et al*., 2002, West and Yorks, 2002). Decreases in herb cover in later stages of succession correspond to progressive recovery of mature shrub canopies (Sneva, 1972). Based on these relationships, we propose two possible explanations for the cessation of new establishments of *A. t. vaseyana* in sites burned four or more years before our sampling: 1) negative effects of recolonizing herbs on *A. t. vaseyana* seedlings and 2) depletion of residual seed banks.

Big sagebrush seeds are apparently relatively short-lived in storage and could be similarly so in the field (reviewed in Meyer, 1994). Depletion of big sagebrush seed banks reportedly occurred several years following fires, as a possible result of germination (Young and Evans, 1989). Depletion of seed banks is unlikely to occur near burn edges that are within the dispersal range of unburned shrubs. We found no new establishments after the third post-fire year in the few sampling locations that happened to be near unburned shrubs, similar to in sampling areas that were distant from shrubs (for data in Fig. 2).

Previous reports of neighborhood relationships, seeding trials, and root-exclusion experiments indicated that seedlings of the other species of big sagebrush are negatively affected by neighboring herbs (e.g. Blaisdell 1949, Richenberger and Pyke, 1990; Schuman *et al.*, 1998; Owens and Norton, 1989; Williams *et al.*, 2002). Greater distances of *A. t. vaseyana* seedlings than random points to neighboring herbs, and greater distances of both seedlings and random points to neighboring herbs (Figs. 2, 5) could reflect negative effects of herbs on *A. t. vaseyana* seedlings. Moreover, growth and carbon assimilation were significantly lower in *A. t. vaseyana* seedlings that had smaller distances to neighboring herbs, compared to seedlings located further

from herbs following fire (DiCristina and Germino, in review). Decreased spacing between *A. t. vaseyana* and neighboring herbs in less recently burned areas may have been made possible by deeper rooting in older seedlings compared to shallower root systems that were likely in younger seedlings of more recent burns. Shallower roots of younger *A. t. vaseyana* would be more likely to match shallower rooting patterns typical of herbs.

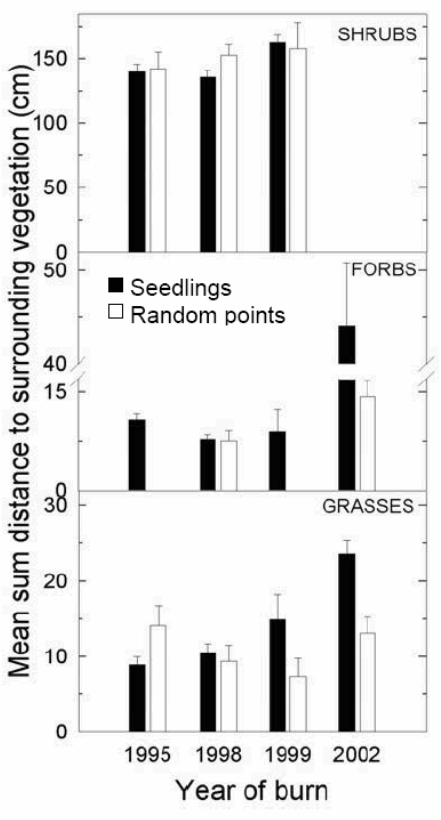

Figure 5. Mean sum distances (+ 1 SE) of Artemisia t. vaseyana seedlings (solid bars) or random points (open bars) to shrubs, forbs, or grasses, in each burn year. N=10-89.

Initially, we anticipated detecting positive or facilitative associations of *A. t. vaseyana* seedlings and adult shrubs, based on speculations by Daubenmire (1975) and findings of Owens and Norton (1989) for other subspecies of *A. tridentata*. Mature shrubs can favorably alter soils, soil water, sunlight and evaporative demand for seedlings in semiarid lands, and thereby could potentially ameliorate the drought conditions which we previously found to limit *A. t. vaseyana* seedling growth (DiCristina and Germino, in review). However, we detected no evidence for direct positive associations of *A. t. vaseyana* seedlings and neighboring plants, and moreover observed no evidence of preferential establishment of *A. t. vaseyana* on north or south aspects of neighboring plants to indicate potential shading effects. Although there was no evidence for direct facilitation, mature shrubs could indirectly facilitate *A. t. vaseyana* establishment by having negative effects on abundances of herbs (Anderson and Inouye, 2001).

Establishment of sagebrush is commonly thought to occur mainly in response to favorable climate conditions that occur sporadically across decades (Daubenmire, 1975; Maier *et al.*, 2001), but the patterns of establishment reported here are closely linked to the fire-induced changes in herb cover (Figs. 1-5). Consistent establishment in years 1-3 following each fire, irrespective of

climate variations (Figs. 2, 3), is some indication that precipitation is commonly abundant enough for *A. t. vaseyana* to germinate and establish in most years. However, survival of newly germinated seedlings may be less likely during intermediate stages of succession (Fig. 2) when herbs are most abundant (Figs. 4) or when emergence could become limited by seed availability. Shrub establishment in communities that have relatively greater plant cover than sites dominated by *A. t. vaseyana* appeared reliant on disturbances that reduce vegetative cover; such as small mammal disturbances that allow *A. rothrocki* to invade montane meadows (Berlow *et al*., 2002) or pulses of shrub establishment following fire in chapparal (Tyler, 1996).

Summary and implications.—Recovery of *Artemisia tridentata* canopies to prefire levels may require decades (Harniss and Murray, 1973; Wambolt *et al.*, 2001), however, initial establishment of *A. t. vaseyana* in the first growth seasons following fire may be more important than previously assumed. Temporal patterns of *A. t. vaseyana* establishment may be attributable to negative relationships of seedlings with neighboring herbs or depletion of seed banks, though further experimental verification of these effects are needed. Competitive displacement of seedlings of other *Artemisia* shrub species by an exotic grass appears contributes to site conversion to grassland (eg. Eliason and Allen 1997), and long-term displacement of *A. t. tridentata* or *wyomingensis* through accelerated of fire frequency by *Bromus tectorum* are well known (reviewed in Brooks and Pyke 2001). Dense and persistant invasions of new exotic forbs (eg. *Centaurea* sp. and thistles) into *A. t. vaseyana* communities are becoming increasingly common, particularly following fires. *Artemisia t. vaseyana* seedlings appeared to require greater distances from forbs than grasses during initial postfire establishment (Fig. 3), indicating that *A. t. vaseyana* may interact differently with herb communities as they become enriched in exotic forbs.

ACKNOWLEDGEMENTS

This study was made possible by a grant from the National Aeronautics and Space Administration Goddard Space Flight Center. ISU would also like to acknowledge the Idaho Delegation for their assistance in obtaining this grant. Richard Inouye provided helpful comments.

LITERATURE CITED

Anderson, J. E. AND R. S. Inouye. 2001. Long term vegetation dynamics in sagebrush steppe at the Idaho National Engineering and Environmental Laboratory. *Ecol. Monogr.*, 71:531-556.

Berlow E. L., C. M. D'antonio And S. A. Reynolds. 2002. Shrub expansion in montane meadows: the interaction of local-scale disturbance and site aridity. *Ecol. Appl*., 12:1103-1118.

Blaisdell, J. P. 1949. Competition between sagebrush seedlings and reseeded grasses. *Ecology*, 30:512-519.

Brooks, M. L. And D. A. Pyke. 2001. Invasive plants and fire in the deserts of North America, p. 1-14. *In*: K.E.M Galley and T.P. Wilson (eds.), Proceedings of the Invasive Species Workshop: the Role of Fire in the Control and Spread of Invasive Species. Fire Conference 2000: the First National Congress on Fire Ecology, Prevention, and Management. Tall Timbers Research Station, Tallahassee, FL.

Chambers, J. 2000. Seed movements and seedling fates in disturbed sagebrush steppe ecosystems: implications for restoration. *Ecol. Appl*., 10:1400-1413.

Daubenmire, R. F. 1975. Ecology of *Artemisia tridentata* subsp. *tridentata* in the state of Washington. *Northwest Sci*., 49:24-35.

Dicristina, K. And M. J. Germino. In review. Correlation of neighborhood relationships, carbon assimilation, and water status of sagebrush seedlings establishing after fire. *West. N. Am. Naturalist*.

Eliason, S. A. And E. B. Allen. 1997. Competition as a mechanism for exotic grass persistence following conversion from native shrubland. *Restor. Ecol*., 5:245-255.

Ferguson, C. W. 1964 Annual rings in big sagebrush. Papers of the Laboratory of Tree-Ring Research No. 1. University of Arizona Press, Tucson, AZ.

Floyd, D. A. and J. E. Anderson. 1987. A comparison of three methods for estimating plant cover. *J. Ecol*., 75:221-228.
Harniss, R. O. And R. B. Murray. 1973. 30 years of vegetal change following burning of sagebrush-grass range. *J. Range Manage*., 26:322-325.

Harniss, R. O. And W. T. Mcdonough. 1976. Yearly variation in germination in three subspecies of big sagebrush. *J. Range Manage*., 29:1678-168.

Hassan, M. A. And N. E. West. 1986. Dynamics of soil seed pools in burned and unburned sagebrush semi-deserts. *Ecology*, 67:269-272.

Leonard, K. M., K. P. Reese, And J. W. Connelly. 2000. Distribution, movements and habitats of sage grouse *Centrocercus urophasianus* on the Upper Snake River Plain of Idaho: Changes from the 1950s to the 1990s. *Wildlife Biol*., 6:265-270.

Maier, A. M., B. L. Perryman, R. A. Olson And A. L. Hild. 2001. Climatic influences on recruitment of 3 subspecies of *Artemisia tridentata*. *J. Range Manage.*, 54:699-703.

Meyer, S. E. 1994. Germination and establishment ecology of big sagebrush, p. 244-252 S. B. Monsen and S. G. Kitchen (eds.) Ecology and Management of Annual Rangelands. USDA Intermountain Research Station Report INT-GTR-313.

Mueggler, W. F. 1956. Is sagebrush seed residual in the soil of burns or is it wind borne? USDA Intermountain Forest Service and Range Experimental Station, Standard Research Note 35. 10pp.

Owens, M. K. And B. E. Norton. 1989. The impact of available area on *A. t. vaseyana tridentata* seedling dynamics. *Vegetatio*, 82:155-162.

Perryman, B. L., R. A. Olson, S. Petersburg, And T. Naumann. 2002. Vegetation responses to prescribed fire in Dinosaur National Monument. *West. N. Am. Naturalist*, 62:414-422.

Reichenberger, G. And D. A. Pyke. 1990. Impact of early root competition on fitness components of four semiarid species. *Oecologia*, 85:159-166.

Ratzlaff, T. And J. E. Anderson. 1995. Vegetal recovery following wildfire in seeded and unseeded sagebrush steppe. *J. Range Manage*., 48:386-391.

Schuman, G. E., D. T. Booth And J. R. Cockrell. 1998. Cultural methods for establishing Wyoming big sagebrush on mined lands. *J. Range Manage*., 51:223-230.

Seefeldt, S. S. And S. D. Mccoy. 2003. Measuring plant diversity in sagebrush steppe: influence of previous grazing management practices. *Environ. Manage*., 32:234-245.

Sneva, F. A. 1972 Grazing return following sagebrush control in eastern Oregon. *J. Range Manage*., 25:174-178

Tyler, C. M. 1996. Relative importance of factors contributing to postfire seedling establishment in maritime chaparral. *Ecology*, 77:2182-2195.

Wambolt, C. L., K. S. Walhof And M. R. Frisina. 2001. Recovery of big sagebrush communities after burning in southwestern Montana. *J. Range Manage*., 61:243- 252.

West, N. E. And M. A. Hassan. 1985. Recovery of sagebrush-grass vegetation following wildfire. *J. Range Manage*., 38:131-134.

West, N. E. And T. P. Yorks. 2002. Vegetation responses following wildfire on grazed and ungrazed sagebrush semi-desert. *J. Range Manage*., 55:171-81.

Williams, M. I., G. E. Schuman, A. L. Hild, And L. E. Wicklund. 2002. Wyoming big sagebrush density: effects of seedlings rates and grass competition. *Rest. Ecol*., 10:385-391.

Young, J. A. And R. A. Evans. 1978. Population dynamics after wildfires in sagebrush grasslands. *J. Range Manage*., 31:283-289.

Young, J. A., R. A. Evans And D. E. Palmquist. 1989. Big sagebrush (*Artemisia tridentata*) seed production. *Weed Sci.*, 37:47-53.

Young, J. A., R. A. Evans And D. E. Palmquist. 1990. Soil surface characteristics and emergence of big sagebrush seedlings. *J. Range Manage*., 43:358-367.

Measuring Early Vegetation Changes after Fire in Mountain Big Sagebrush (*Artemisia Tridentata* Nutt. *ssp. saseyana* [Rydb] Beetle) Rangelands

Steven S. Seefeldt, Rangeland Scientist, USDA, ARS, U.S. Sheep Experiment Station, Dubois, ID 83423.

Matthew Germino, Assistant Professor, Department of Biological Sciences, Idaho State University, Pocatello, ID 83209.

Katie DiCristina, Research Associate, Department of Biological Sciences, Idaho State University, Pocatello, ID 83209.

ABSTRACT
In rangeland fire research, before fire vegetation conditions have rarely been measured, although this information is necessary for predictions of after fire vegetation recovery. Multiple prescribed fires were lit 2002 and 2003 at the USDA-ARS United States Sheep Experiment Station in a mountain big sagebrush (*Artemisia tridentata* Nutt. ssp. *vaseyana* [Rydb] Beetle) steppe ecosystem that was relatively free of exotic plants. Measurements of cover components and plant species frequencies were taken before and for several years after the fires. Cover of forbs, grasses and bare ground returned to before fire levels after two yr. Shrub cover declined from 36 to 6%. Fire reduced the frequencies of three species (*A. tridentata* ssp. *vaseyana*, *Festuca Idahoensis*, and *Cordylanthus ramosus*). The fire also increased the frequencies of four species (Hesperostipa comata, Polygonum douglasii, Chenopodium fremontii and Chenopodium leptophyllum), but only P. douglasii increase was for more than a year. This study demonstrates that in a mountain big sagebrush steppe ecosystem, without significant non-native species or anthropogenic disturbances, cover components and plant species frequencies are only minimally altered and the plant community that develops after fire is similar to the one before fire and will most likely result in a return to a sagebrush dominated community.

Keywords: rangelands, vegetation, measurement, fire

INTRODUCTION

Wildfire is a natural part of the sagebrush steppe ecosystem (Blaisdell et al. 1982) with fire-free intervals before European settlement varying from 20 to 25 yr in higher elevation *Artemisia tridentata* ssp. v*aseyana* (Burkhardt and Tisdale 1976). In a Clementsian model developed in west-central Utah (Barney and Frischknecht 1974), fire in the sagebrush steppe restarts plant succession, which begins with an annual weedy stage that is followed by a perennial grass/forb stage 3 or 4 yr after a fire. Following stages of succession include dense sagebrush potentially followed by climax juniper woodland. Dense sagebrush stands are associated with declines in plant diversity and increased fire risk (Johnson et al. 1996). Additionally, dense sagebrush stands typically have decreased forage production of perennial grasses and forbs (Harniss and Murray 1973; Bork et al. 1998). We hypothesize that, as sagebrush stands increase in age, the succession of plants after fire will be altered.

Recent research has measured altered succession after fire due to the influence of exotic, invasive weeds resulting in increased fire frequency (Pellant 1990; Whisenant 1990). This and other observed alterations have resulted in the development of state and transition models of plant succession (reviewed by Stringham et al. 2003). To predict plant succession after fire, it is important to know the state of the vegetation before the fire. Most research conducted on vegetation recovery after fire has been initiated after the fire with little or no information on before fire vegetation (Harniss and Murray 1973; Barney and Frischknecht 1974; Wambolt et al. 2001; Wrobleski and Kauffman 2003). To properly test state and transition models, knowledge of vegetation conditions before disturbance is critical.

There are few areas of sagebrush steppe in Eastern Idaho are relatively free of exotic plants and available for prescribed fires. At the USDA-ARS United States Sheep Experiment Station (USSES) two areas that have only been lightly grazed by sheep and have a very low density of exotic plants (small patches of *Verbascum thapsus* on rock outcrops and trace amounts of *Taraxacum officinale*) were selected to measure influence of before fire vegetation on plant recovery after fire.

The objectives of this study were to determine vegetation change after fire in an ecosystem relatively free of exotic plants and to determine whether time since last fire influenced after fire vegetation. The results of this study will provide a baseline for subsequent prescribed fires in areas of the sagebrush steppe with vegetation communities that have larger invasive plant components.

METHODS

In the summer of 2001, an area in the Northeast corner of the USSES spring-fall range (lat 44º14’44” N, long 112º12’47” W) with a 34 to 42% shrub cover was selected for a prescribed burn (Figure 1). The site, at an elevation of 1,800 m, is in the northeastern part of the sagebrush steppe region (West 1983). Soils are fine-loamy, mixed, frigid Calcic Argixerolls derived from wind-blown loess, residuum, or alluvium on slopes ranging from 0 to 12% (Natural Resources Conservation Service 1995). Climate is semiarid with cold winters, several months have mean temperatures below freezing, and warm summers with daily highs averaging 27 C. During the study precipitation amounts were below the long term average from 2001 to 2003 (Table 1). Annual precipitation averages 330 mm, with up to 60% falling in the winter as snow. Mountain big sagebrush (*Artemisia tridentata* ssp. v*aseyana*), antelope bitterbrush (*Purshia tridentata*), Montana wheatgrass (*Elymus albicans*), Idaho fescue (*Festuca idahoensis*), Sandberg bluegrass (*Poa secunda*), rosy pussytoes (*Antennaria rosea*), longleaf fleabane (*Erigeron corymbosus*), and common yarrow (*Achillea millefolium*), dominate the vegetation.

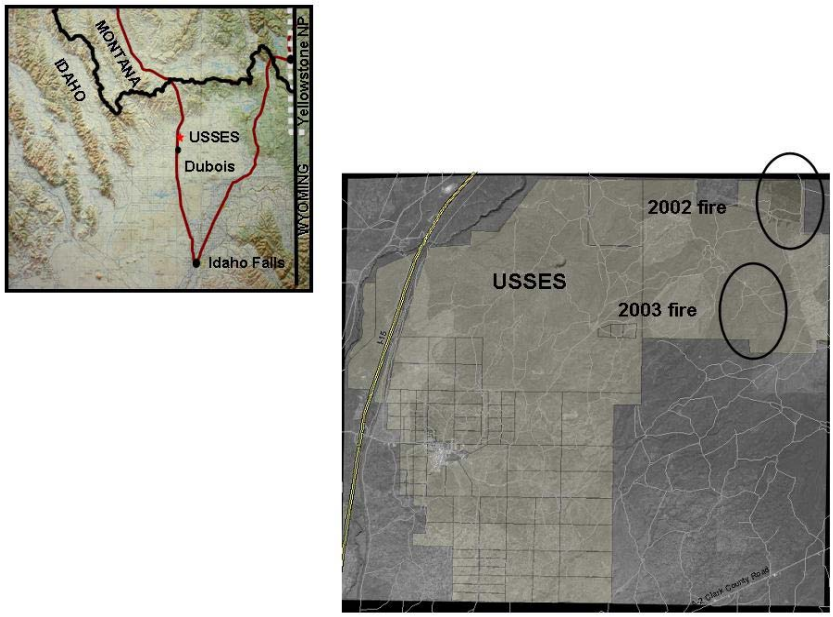

Figure 1. The U.S. Sheep Experiment Station is located in Eastern Idaho in the Upper Snake River Plain.

Table 1. Precipitation at the U.S. Sheep Experiment Station during the study and the 30 yr average

Month	2001	2002	2003	2004	2005	30-yr avg
				cm		
January	1.35	1.70	0.74	1.93	1.91	1.93
February	0.91	0.43	1.96	2.90	0.28	1.73
March	1.19	0.89	1.27	1.27	2.79	2.36
April	2.67	2.03	8.94	3.00	4.04	2.82
May	0.30	2.26	3.96	3.66	7.14	4.90
June	2.51	3.28	0.71	4.39	5.03	4.27
July	2.31	0.71	0.13	1.88	0.18	2.69
August	1.96	0.61	0.38	2.31	1.22	2.49
September	0.43	1.91	0.84	2.36	3.71	2.51
October	2.41	0.97	0.10	7.09	5.11	2.16
November	3.43	1.80	0.66	0.00	2.44	2.74
December	3.68	2.24	3.89	3.00	5.31	2.36
Total	23.16	18.82	23.57	33.78	39.14	32.97

The fires (2002 and 2003) were located on land (260 ha) that was typically sheep grazed for the last 20 yr. Sheep grazing usually occurred for 1 wk each spring and fall with an average yearly stocking density of 40 sheep d ha^{-1}. The land was not grazed the year before each fire. The southern two thirds of the 2002 site and the entire 2003 site burned in 1981 whereas the northern third of the 2003 site last burned in 1960. In June of the burn yr, two fire lines were constructed using a road grader. One encompassed a 250 ha area and the other fire line isolated approximately 100 ha within the larger area. The interior areas were burned in September using standard prescribed fire techniques for the sagebrush steppe. Initially, the graded fire lines on the north and east sides were widened using successive strips of fire (1, 3, 10, 20 m) from the graded fire line, creating a 20 m wide black line. Then, starting on the northwest and southeast corners,

lines of fire were ignited approximately 20 m east or north of the interior fire line towards the southwest corner. The black line was started when fire conditions were adequate for fire spread (typically around 10 am). In both years, the first and largest prescribed fire was completed at 4:30 pm. In 2002, 10 additional fires were ignited in the area south and east of the first fire. In 2003, three additional fires were ignited in an area north and east of the first fire (Table 1). Fires less than 4 ha were ignited from a point and allowed to burn until a certain size was achieved or the fire reached interior fire line. Fire crews suppressed fires using water and trying not to enter the burned area. Fires greater than 4 ha were ignited with a specific length of fire the length that was estimated to result in a pre-determined size of fire. In the largest four fires, some areas within the boundaries of the fire were not burned. These areas were ignited during the second day. In 2002, the last fire of the second day was planned to burn 30 ha in the northwest corner of the burn area. However, decreasing temperatures and solar radiation prevented the fire from spreading throughout the desired area.

Measurements of plant frequency, ground cover and, soil movement were taken at 100 permanent plots before and after the fire in 2002 and at 25 plots in 2003. The plots were located on a GIS database map of the site using a stratified random design. In 2002, 10 plots were outside the fire line, 10 plots were in the area that would be black lined, 25 plots were in the area of the large fire, 5 plots were in the green strip between the large fire and the interior fire line, and 50 plots were in the area where the small fires were ignited. In 2003, 5 plots were located outside the intended burn area, 20 in the large burn area. After the 2003 fire, only 1 plot of the 20 was in a small fire area, the other 19 were in large fire area. In the field, GPS units were used to locate each plot. At each plot a nested frequency quadrat frame was placed in a spot that was representative of the area vegetation. Two red, 24 penny nails were used to mark opposite corners of the frame for precise measurements after the fire. Cover of shrubs, grasses, forbs, litter, bare ground, and rock were estimated visually. Soil movement was measured using a piece of rebar that was placed at a third corner of the nested frequency quadrat frame and pounded in until about 35 cm remained above ground. Height of the rebar above ground was measured to the nearest mm. Species frequency, cover estimates, and soil movement were measured in July of 2002, 2003, 2004, and 2005.

Data from each fire were analyzed separately. The data were determined to be normally distributed using a UNIVARIATE procedure on model residuals with the Shapiro-Wilk statistic (SAS Inst. Inc., Cary, NC). For the cover analysis, repeated measures analyses of variance (ANOVA) were used to examine the relationship between time since fire and percent cover of each class (forb, grass, shrub, soil, litter, and rock) in burned and unburned plots within each year. An ANOVA with paired contrasts between each set of consecutive years was used to determine changes in percent cover between years for burned and unburned plot separately (SAS Inst. Inc., Cary, NC). The same analyses were used within burned plots from the 2002 fire to determine if time before last historic fire (21 or 42 yr) impacted vegetation recovery.
In order to analyze for differences in plant species frequency in 2002, only species that were in 30% or more of all sample plots (burned and unburned plots combined) could be used (19 of 70 species) to satisfy assumptions of normality. The greatest sensitivity to change is found when plant frequencies are near 50% of the plots (Stephen Bunting, personal communication). Therefore, we selected quadrat sizes (110, 870, 2210, or 4420 cm^2) independently for each species based on frequency percentages consistently nearest 50% for all years in burned and unburned plots. Presence/absence data were tallied for the chosen quadrat size for each species. For each species, 2x2 chi-square analyses with McNemar's test (SAS Inst. Inc., Cary, NC) were used to detect differences in frequencies between pairs of consecutive years for burned and unburned plots. If species were absent from at least one yr of the paired comparisons, a statistical determination could not be made (Table 2), however, the loss of a species was noted. Differences

were considered significant when the F-test probability was ≤ 0.05. The 2003 plant species frequency analyses could not be conducted. The small number of plots (25) biased the chi-square test statistic because the minimum frequency for each cell was not at least 5 for each 2x2 chi-square analysis (Zar 1974).

Table 2. Fire sizes in the 2002 prescribed fires on the spring-fall grazing property of the U. S. Sheep Experiment Station before grazing initiated

Fire	Size	Vegetation age
	ha	——yr——
1	104	21 and 42
2	10.2	42
3	2.63	21
4	1.55	21
5	1.29	21
6	1.23	21
7	0.51	21
8	0.46	21
9	0.20	21
10	0.09	21
11	0.001	21
12	0.001	21

RESULTS

COVER COMPONENTS

There were differences in many of the cover components (grass, forb, shrub, bare ground, litter, and rock) due to fire, time, and the interaction of fire and time. Before the fire in 2002, all cover components were similar except for bare ground (P = 0.04) where the area to be burned averaged 13% and the area that was not burned averaged 19%. Before the fire in 2003, all cover components were similar except for forbs (P = 0.01) where the area to be burned averaged 16% and the area that was not burned averaged 4%. There was no soil movement over the course of the study in the burned and unburned plots.

In the 2002 fire over the course of the experiment, grass cover (Figure 2a) was greater overall in the burned area compared to the unburned (P = 0.03) and there was an interaction of time and burn (P <0.0001). Grass cover in the burned area declined in the yr following fire and increased to before fire amounts in second and third yr after the fire. In the unburned area, grass cover did not change the first yr after fire, declined in the second yr and did not recover in the third yr. There was more grass cover in the unburned area the yr after the fire compared to the burned, but there was more grass cover in the burned area in second and third yr compared to the unburned. In the 2003 fire, grass cover did not differ between burned and unburned areas (Figure 3a). However, grass cover declined (P=0.006) the first year after the fire and increased (P = 0.05) in the second year after the fire.

The 2002 fire did not change forb cover (P = 0.88) over the course of the experiment (Figure 2b). However, forb cover changed with time (P < 0.0001) and there was an interaction with time and fire (P = 0.0003). In the first yr after the fire there were more forbs in the unburned area (P = 0.03) compared to the burned area. In first yr after the fire, forb cover declined in both burned (P = 0.0005) and unburned areas (P = 0.02). Forb cover increased (P < 0.0001) in the burned area in the second yr compared with the first yr after fire and forb covers decreased in burned (P = 0.0002) and unburned (P = 0.003) areas in the third yr after the fire. In the 2003 fire, forb cover

the yr after the fire was similar in the burned and unburned areas, and forb cover increased (P = 0.01) in the unburned area (Figure 3b). In the second yr following fire, forb cover declined in the unburned area (P = 0.03) and was less than in the burned area (P = 0.01). Over the course of the study forb cover was greater (P = 0.01) in the burned compared to the unburned area and forb cover in the burned area did not change.

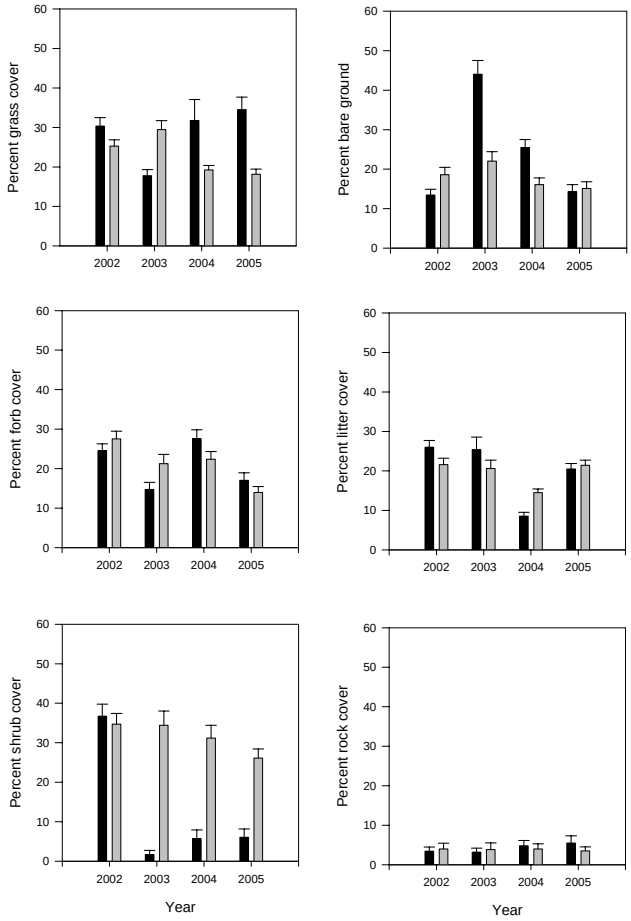

Figure 2. Cover components of burned (dark bars) and unburned (light bars) areas before and three yr after the 2002 prescribed fire at the U. S. Sheep Experiment Station.

Fire reduced (P < 0.0001) shrub cover in both the 2002 and 2003 fires (Figures 2c and 3c). The fire reduced shrub cover from 37 to 2% in the 2002 fire and 35 to 9% in the 2003 fire the yr after the burns. In the 2002 fire, each yr after the fire, shrub cover was less in the burned than unburned areas (P < 0.0001). In the 2003 fire, shrub in the burned and unburned areas was not different until the second yr after the fire (P < 0.0001). Shrub cover did not change in the unburned areas during the course of the study in both the 2002 and 2003 fires. Shrub cover in the burned area did not change after the initial decline caused by the fire for both 2002 and 2003 fires.

In the 2002 fire, bare ground differed due to burning (P = 0.007) and time (P = 0.0001), and there was an interaction (P < 0.0001) of time and burning (Figure 2d). In the year after the fire, the burned areas increased (P < 0.0001) in bare ground and there was more (P < 0.0001) bare ground in the burn area compared to the unburned area. In the burn area, bare ground decreased from 2003 to 2004 and from 2004 to 2005 (P < 0.0001 and = 0.0009, respectively). There was more (P

= 0.0004) bare ground in the burned area than the unburned area in second yr after the fire, but not in the third. In the unburned area, bare ground declined in second yr after the fire (P = 0.03) and stayed at that amount in the third yr after fire. In the 2003 fire, bare ground did not change in the unburned area over the course of the study (Figure 3d). In each yr of the study, there was no difference in bare ground between the burned and unburned areas. However, bare ground in the burned plots increased (P = 0.003) the yr after the fire and decreased (P = 0.002) to before fire levels the following yr.

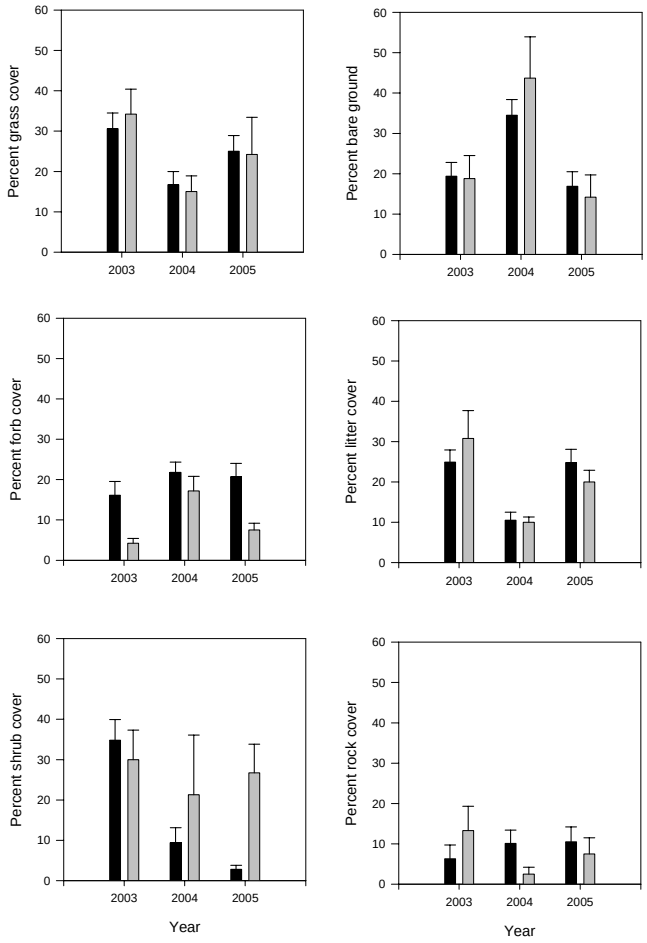

Figure 3. Cover components of burned (dark bars) and unburned (light bars) areas before and 2 yr after the 2003 prescribed fire at the U. S. Sheep Experiment Station.

Over the course of the experiment, burning did not alter (P = 0.74) litter cover (Figure 2e) in the 2002 fire. There was a time effect (P < 0.0001) and a time by burn interaction (P = 0.002). Litter did not change the yr after the fire, but in 2004 litter cover declined in both the burned (P < 0.0001) and unburned (P = 0.005) areas and increased to before fire conditions in 2005 in the burned (P < 0.0001) and unburned (P = 0.002) areas. In the second yr after the fire there was more litter in the unburned than the burned areas (P < 0.0001). In the 2003 fire, burning did not alter (P = 0.82) litter cover (Figure 3e) over the course of the experiment. There was a time effect (P < 0.0001) with litter declining the yr after the fire in both the burned (P = 0.0001) and unburned (P = 0.002) areas and increasing the second yr after the fire in the burned (P = 0.0001) and unburned (P = 0.05) areas.

Rock cover did not change over the course of the experiment in either the 2002 or 2003 fire, and there were no differences between burned or unburned areas (Figure 2f and 3f).

Time since the last historic fire (21 or 42 yr) did not appear to affect cover components after the 2002 fire. However, before the fire, bare ground was greater (P = 0.05) in the younger stand compared to the older (15.6 and 9.3%, respectively).

PLANT SPECIES FREQUENCIES

Based on the frequency plots analyzed at 870 cm^2 nested area, the two most common species were *Poa secunda* and *Elymus albicans*, both perennial grasses. Plants analyzed at 2210 cm^2 nested area were perennial grasses *Festuca idahoensis* and *Koeleria macrantha*, perennial forb *Erigeron corymbosus*, and annual forb *Polygonum douglassii*. The remaining plants were analyzed at the 4420 cm^2 area.

Of the 19 plant species analyzed for frequency, three (*Artemisia tridentata spp. vaseyana*, *Festuca idahoensis*, and *Cordylanthus ramosus*) declined and two (*Hesperostipa comata* and *Polygonum douglassii*) increased in the burned area (Figure 4a-e). Except for *Elymus albicans* (Figure 4f), the frequencies of the other plant species varied similarly during the course of the study (Figure 4g-s). *Viola nuttallii* and *Microseris nutans*, two perennial forbs, were only observed in abundance in 2004 in the burned and unburned plots and *Mertensia oblongifolia*, another perennial forb, disappeared in both the burned and unburned areas in 2005 (Figure 4g-i). Frequencies of *Poa secunda* and *Koeleria macrantha* increased over time (figure 4j-k). Frequencies of *Allium acuminatum*, a perennial forb, and *Gayophytum racemosum*, an annual forb, increased in 2004 (Figure 4l-m). The remaining plant species remained relatively stable over the course of the study (Figure 4n-s). Frequencies of analyzed and unanalyzed species at the 4420 cm^2 area are listed in Appendix A for the 2002 fire and Appendix B for the 2003 fire.

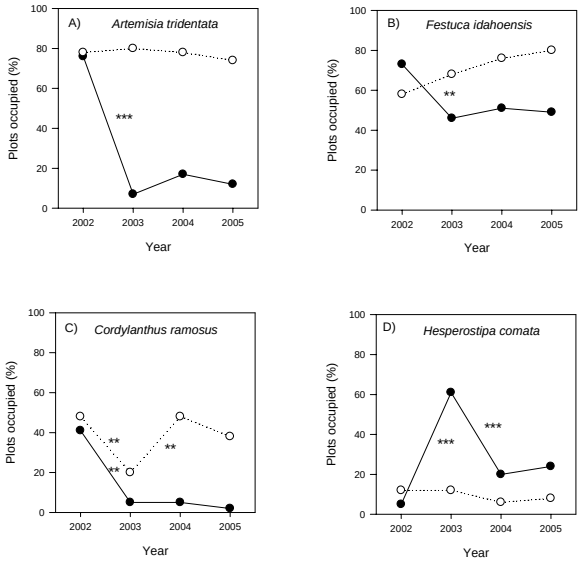

Figure 4. Plant species frequencies in burned (solid line) and unburned (dashed line) areas before and 3 yr after the 2003 prescribed fire at the U. S. Sheep Experiment Station.

DISCUSSION

Both 2002 and 2003 fires burned more than 95% of the area and removed more than 95% of the vegetation biomass in the burned areas (visual observation). The fires were classified as low

severity as the surface was largely black with some isolated pockets of gray ash and, in the 2003 fire, soil temperatures remained below 50 C at 0.5 cm depth (Hungerford 1996).

COVER COMPONENTS

Although vegetation decreased initially in the yr following fire, forbs, grass, and bare ground returned to or exceeded before fire levels after 2 yr. These results are consistent with previous studies (Harniss and Murray 1973; Barney and Frischknecht 1974) that reported vegetation in the first years after a fire being dominated by grasses and forbs.

An objective of this study was to determine whether time since last fire impacted subsequent vegetation. Time since the last fire (21 or 41 yr) did not have an impact on recovery of vegetation cover after fire.

PLANT SPECIES FREQUENCIES

Another objective of this study was to determine the response of plant species to fire in the sagebrush steppe. Plant populations respond to a variety of biotic and abiotic influences such as grazing (West et al. 1979), drought (Pechanec et al. 1937), and fire (Harniss and Murray 1973) and each plant species response may be independent or dependent on the other species around it (West et al. 1979). Although fire was the treatment applied in this study, the responses of plant species to the fire were affected through interactions with other biotic and abiotic factors such as neighboring vegetation, moisture, and aspect.

Within two yr, overall forb and grass cover had returned to before fire levels in both the 2002 and 2003 fires. However, in this relatively healthy and diverse sagebrush steppe community, the fire did result in some increases and decreases in the frequencies of some grass and forb species.

Artemisia tridentata spp. vaseyana, *Festuca idahoensis*, and *Cordylanthus ramosus* were the only three species that had decreased frequencies as a result of the 2002 and 2003 prescribed burns (Figure 4 a-c and Appendices A and B). *A. tridentata spp. vaseyana*, the dominant shrub in this ecosystem, does not sprout back after a fire and few seedlings were observed. Over the next 15 to 20 yr this shrub species will most likely re-establish and dominate the site (Harniss and Murray 1973). Over one third of the *F. idahoensis* plants, a perennial grass species, were killed during the 2002 and 2003 prescribed burns. This decline in frequency has also been observed in others studies (Blaisdell 1953; Conrad and Poulton 1966; Schwecke and Hann 1989; Wamboldt et al. 2001). *F. idahoensis* frequency did not increase in the second and third yr after the fire and may take several decades to fully recover (Harniss and Murray 1973). *C. ramosus*, a perennial forb common in the region, nearly disappeared in the burned areas after the 2002 and 2003 burns.

Hesperostipa comata and *Polygonum douglassii* increased as a response to the 2002 fire (Figures 4d and e). *H. comata*, a perennial grass, is known to be resistant to fire, especially when the fire occurs after August (Wright and Klemmedson 1965). *H. comata* frequencies increased to 60% in the yr following the 2002 fire in the burned plots representing a flush of new plants, but then declined in 2004. In the 2003 burn, *H. comata* frequencies were not altered in both the burned and unburned areas over the course of the experiment (Appendix B). *P. douglassii*, an annual forb, increased in second yr and declined the third year after the burn in both burned and unburned areas in after the 2002 fire. The size of the increase, however, was larger in the burned plots. In the 2003 fire, *P. douglassii* appeared in both burned and unburned areas after the fire. Two other annual forb species (*Chenopodium fremontii* and *Chenopodium leptophyllum*) that could not be analyzed due to lack of sufficient numbers each year, apparently increased as a response to the burn (Appendices A and B). *C. fremontii* appeared in 2004 in both burn areas and then declined in 2005. *C. leptophyllum* appeared the year after each fire and then declined the following year. In the 2003 fire, 3 of the 5 plots in the unburned area had *C. leptophyllum*. Other

studies have measured similar short-duration positive responses of *Chenopodium* species to fire (Bartos and Mueggler 1981; Bartos et al. 1994).

Elymus albicans was abundant before the 2002 burn (Figure 4f and Appendix A). Two yr after the 2002 fire, the frequency increased in the burned areas. Three yr after the 2002 fire, the frequency decreased in the unburned areas. In the 2003 burn, there were no *E. albicans* plants in the plots (Appendix B). The year after the fire, frequencies increased in the burned and unburned areas to 80%. *E. albicans* is a rhizomatous species that typically responds positively after fire (Harniss and Murray 1973; Akinsoji 1988). However, in this study the response was mixed. In the 2002 fire burn area *E. albicans* response was delayed a year and in the 2003 fire, the positive response was similar in the burned and unburned areas.

Responses to the 2002 fire were similar in the burned and unburned areas for *Viola nuttallii*, *Microseris nutans*, *Mertensia oblongifolia*, *Poa secunda*, *Koeleria macrantha*, *Allium acuminatum*, *Gayophytum racemosum*, *Carex filifolia*, *Astragalus miser*, *Antennaria rosea*, *Astragalus convallarius*, *Eriogonum heracleoides*, and *Erigeron corymbosus* (Figure 4g-s). Any responses in these species were possibly due to some other biotic or abiotic factor or, more probably, an interaction of factors. Generally, responses of the above plant frequencies in the 2003 fire are similar to the 2002 fire, but there were some exceptions. *A. convallarius*, *C. filifolia*, and *A. miser* all had potentially significant increases in frequency in the burned area compared to the unburned (Figures 4l, 4n, and 4o). Although frequencies of *Eriogonum heracleoides*, and *Erigeron corymbosu* did not vary in this study or in a 1952 fire in southeast Idaho, there was a reported increase in the biomass of these two species three yr after the fire (Mueggler and Blaisdell 1958).

Many increases and decreases of plant species followed earlier studies; many more species have not been reported in the scientific literature. Of particular interest are the perennial grasses *P. secunda* and *K. macrantha* (Figure 4j and 4k and Appendix B), which both increased in frequency after the 2002 and 2003 fires. The increases in frequency were dependent of year, 2004 for *P. secunda* and 2005 for *K. macrantha* and apparently independent of fire. These results for *P. secunda* are consistent with the measurements of Wright and Klemmedson (1965). However the results for *K. macrantha* are different from Antos et al. (1983) which showed increases restricted to burned areas.

There were 70 and 53 species observed in the 2002 and 2003 studies, respectively. Of these, only 3 species had decreased and 3 had increased frequencies. The first year after both fires there were decreases in grass and shrub cover. In the second year after the fires, grass cover had increased to before fire levels in the burned areas, whereas shrub cover would take years to return to before fire amounts. Except for the shrub *A. tridentata spp. vaseyana*, these two mid-September prescribed fires had only transient impacts on plant cover. Wildfire is a natural part of the sagebrush steppe ecosystem (Blaisdell et al. 1982). This study demonstrates that in a sagebrush steppe ecosystem, without significant non-native species or anthropogenic disturbances, plant species frequencies are only minimally altered and the plant community that develops after fire is similar to the one before fire and will most likely result in a return to a sagebrush dominated community (Harniss and Murray 1973; Barney and Frischknecht 1974; Wambolt et al. 2001).

ACKNOWLEDGMENTS

This study was made possible by a grant from the National Aeronautics and Space Administration Goddard Space Flight Center. ISU would also like to acknowledge the Idaho Delegation for their assistance in obtaining this grant. The authors express their appreciation to Scott McCoy, Ada

Williamson, Brad Eddins, Jack Hensley, and fire crews from the USDA Forest Service and the Bureau of Land management for their technical assistance.

LITERATURE CITED

Akinsoji, A. 1988. Postfire vegetation dynamics in a sagebrush steppe in southeastern Idaho, USA. *Vegetatio*. 78:151-155.

Antos, J. A., B. McCune, and C. Bara. 1983. The effect of fire on an ungrazed western Montana grassland. *The American Midland Naturalist*. 110:354-364.

Barney, M. O. and N. C. Frischknecht. 1974. Vegetation changes following fire in the pinyon-juniper type of west-central Utah. *Journal of Range Management*. 27:91-96.

Bartos, D. L. and W. F. Mueggler. 1981. Early succession in aspen communities following fire in western Wyoming. *Journal of Range Management*. 34:315-318.

Bartos, D. L., J. K. Brown, and G. D. Booth. 1994. Twelve years biomass response in aspen communities following fire. *Journal of Range Management*. 47:79-83.

Blaisdell, J. P. 1953. Ecological effects of planned burning of sagebrush-grass range on the Upper Snake River Plains. Tech. Bull. 1975. Washington, DC: U.S. Department of Agriculture. 39 p

Blaisdell, J. P., R. B. Murray, and E. D. McArthur. 1982. Managing intermountain rangelands – sagebrush-grass ranges. General Technical Report INT-134., U. S. Department of Agriculture Forest Service, Intermountain Research Station 41p.

Bork, E. W., N. E. West, and J. W. Walker. 1998. Cover components on long-term seasonal sheep grazing treatments in three-tip sagebrush steppe. *Journal of Range Management*. 51:293-300.

Burkhardt, J. W. and E. W. Tisdale. 1976. Causes of juniper invasion in southwestern Idaho. *Ecology*. 76:472-484.

Conrad, C. E. and C. E. Poulton. 1966. Effect of a wildfire on Idaho fescue and bluebunch wheatgrass. *Journal of Range Management*. 19:138-141.

Harniss, R. O. and R. B. Murray. 1973. 30 years of vegetal change following burning of sagebrush-grass range. *Journal of Range Management*. 26:322-325.

Hungerford, R. D. 1996. Soils. Fire in Ecosystem Management Notes: Unit II-I. USDA Forest Service, National Advanced Resource Technology Center, Marana, Arizona.

Johnson, K. H., R. A. Olson, and T. D. Whitson. 1996. Composition and diversity of plant and small mammal communities in tebuthiuron-treated big sagebrush (*Artemisia tridentata*). *Weed Technology*. 10:404-416.

Mueggler, W. F. and J. P. Blaisdell. 1958. Effects on associated species of burning, rotobeating, spraying, and railing sagebrush. *Journal of Range Management*. 11:61-66.

NRCS. 1995. Soil investigation of Agriculture Research Service, United States Sheep Experiment Station headquarters range, U. S. Department of Agriculture, Natural Resource Conservation Service, Rexburg, Idaho.

Pechanec, J. F., G. D. Pickford, and G. Stewart. 1937. Effects of the 1934 drought on native vegetation of the Upper Snake River Plains, Idaho. Ecology. 18:490-505.

Pellant, M. 1990. The cheatgrass-wildfire cycle – are there any solutions? Pages 11-18, *in* E.D. McArthur, E.M. Romney, S.D. Smith, and P.T. Tueller (eds.), Proceedings of the symposium on cheatgrass invasion, shrub die-off, and other aspects of shrub biology and management. United States Department of Agriculture, Forest Service General Technical Report INT-276.

Schwecke, D. A. and W. Hann. 1989. Fire behavior and vegetation response to spring and fall burning on the Helena National Forest. In: Baumgartner, D. M., D. W. Breuer, B. A. Zamora, [and others], compilers. Prescribed fire in the Intermountain region: Symposium proceedings. 1986 March 3-5. Spokane, WA. Pullman, WA, Washington State University, Cooperative Extension: 135-142.

Stringham, T. K., W. C. Krueger, and P. L. Shaver. 2003. State and transition modeling: An ecological process approach. *Journal of Range Management*. 56:106-113.

Wambolt C. L., K. S. Walhof, and M. R. Frisina. 2001. Recovery of big sagebrush communities in south-western Montana. *Journal of Environmental Management*. 61:243-252.

West, N. E. 1983. Western intermountain sagebrush steppe. *In:* N. E. West [EDS.]. Ecosystems of the World 5: Temperate Deserts and Semi-deserts. Elsevier Science Publishing. New York, NY. p. 351-397.

West, N. E., K. H. Rea, and R. O. Harniss. 1979. Plant demographic studies in sagebrush-grass communities of Southeastern Idaho. Ecology. 60:376-388.

Whisenant, S. G. 1990. Changing fire frequencies on Idaho's Snake River Plain: Ecological and management implications. Pages *in* E.D. McArthur, E.M. Romney, S.D. Smith, and P.T. Tueller (eds.), Proceedings of the symposium on cheatgrass invasion, shrub die-off, and other aspects of shrub biology and management. United States Department of Agriculture, Forest Service, Intermountain Research Station, General Technical Report INT-276.

White, R. S. and P. O. Currie. 1983. Prescribed burning in the Northern Great Plains: yield and cover responses of 3 forage species in the mixed grass prairie. *Journal of Range Management*. 36:179-183.

Wright, H. A. and J. O. Klemmedson. 1965. Effects of fire on bunchgrasses of the sagebrush-grass region in southern Idaho. Ecology. 46:680-688.

Wrobleski, D. W. and J. B. Kauffman. 2003. Initial effects of prescribed fire on morphology, abundance, phenology of forbs in big sagebrush communities in southeastern Oregon. Restoration Ecology. 11:82-90.

Zar, J. H. 1974. Biostatistical analysis. Prentice-Hall, Englewood Cliffs, NJ. 931 p.

Appendix A. Plant species frequencies in the 2002 burn area and percent of all plots with each species.

Species	Treatment	2002	2003	2004	2005	2002	2003	2004	2005
						----------%			----------
Annual forbs									
Amsinckia menziesii	Burned	0	1	0	0	0	2	0	0
Chenopodium fremontii	Burned	0	0	8	1	0	0	20	2
Chenopodium leptophyllum	Burned	0	17	4	0	0	41	10	0
Collinsia parviflora	Burned	7	5	7	0	17	12	17	0
	Unburned	9	7	8	0	18	14	16	0
Cordylanthus ramosus	Burned	17	2	2	1	41	5	5	2
	Unburned	24	10	24	19	48	20	48	38
Gayophytum racemosum	Burned	0	4	19	1	0	10	46	2
	Unburned	2	2	10	3	4	4	20	6
Lepidium densilorum	Burned	0	0	0	2	0	0	0	5
Polygonum douglassii	Burned	8	18	34	26	20	44	83	63
	Unburned	7	4	21	14	14	8	42	28
Tragapogon dubius	Burned	0	0	1	0	0	0	2	0
	Unburned	2	1	1	2	4	2	2	4
Perennial forbs									
Achillea millefolium	Burned	7	6	7	9	17	15	17	22
	Unburned	12	15	17	15	24	30	34	30
Agoseris glauca	Burned	2	0	1	0	5	0	2	0
	Unburned	1	0	2	0	2	0	4	0
Allium acuminatum	Burned	13	7	19	16	32	17	46	39
	Unburned	18	1	14	12	36	2	28	24
Antennaria dimorpha	Burned	0	0	1	0	0	0	2	0
	Unburned	0	0	1	0	0	0	2	0
Antennaria rosea	Burned	21	16	19	12	51	39	46	29
	Unburned	30	30	29	29	60	60	58	58
Antennaria umbrinella	Burned	0	0	1	0	0	0	2	0
	Unburned	0	0	1	0	0	0	2	0
Arabis holboelli	Burned	1	0	0	0	2	0	0	0
Arenaria kingii	Burned	0	0	1	0	0	0	2	0
	Unburned	1	0	3	0	2	0	6	0
Arnica fulgens	Burned	6	2	5	0	15	5	12	0
	Unburned	6	6	9	1	12	12	18	2
Astragalus convallaris	Burned	14	16	11	16	34	39	27	39
	Unburned	15	14	13	7	30	28	26	14
Astragalus filipes	Burned	0	3	0	0	0	7	0	0
	Unburned	0	1	0	0	0	2	0	0

Astragalus lentiginosus	Burned	1	1	2	0	2	2	5	0
Astragalus miser	Burned	9	10	13	6	22	24	32	15
	Unburned	9	4	10	6	18	8	20	12
Calochortus macrocarpus	Burned	0	0	0	1	0	0	0	2
	Unburned	0	0	0	1	0	0	0	2
Cirsium undulatum	Burned	4	1	1	1	10	2	2	2
	Unburned	3	2	2	2	6	4	4	4
Comandra umbellata	Burned	0	0	3	2	0	0	7	5
	Unburned	0	0	6	3	0	0	12	6
Crepis acuminata	Burned	1	0	5	2	2	0	12	5
	Unburned	0	0	2	1	0	0	4	2
Erigeron corymbosus	Burned	28	27	29	27	68	66	71	66
	Unburned	27	26	28	28	54	52	56	56
Erigeron filifolius	Burned	0	1	0	0	0	2	0	0
	Unburned	0	1	1	0	0	2	2	0
Eriogonum heracleoides	Burned	20	14	15	17	49	34	37	41
	Unburned	15	16	18	21	30	32	36	42
Erigeron pumilus	Unburned	0	0	1	0	0	0	2	0
Lomatium foeniculaceum	Burned	0	0	1	0	0	0	2	0
	Unburned	1	0	1	1	2	0	2	2
Lomatium triternatum	Burned	2	0	6	0	5	0	15	0
	Unburned	1	0	5	0	2	0	10	0
Lupinus caudatus	Burned	3	3	4	5	7	7	10	12
	Unburned	4	5	5	13	8	10	10	26
Mertensia oblongifolia	Burned	6	12	19	0	15	29	46	0
	Unburned	4	8	19	0	8	16	38	0
Microseris nutans	Burned	4	0	13	0	10	0	32	0
	Unburned	6	0	15	0	12	0	30	0
Penstemon deustus	Burned	0	1	0	0	0	2	0	0
	Unburned	0	1	1	0	0	2	2	0
Penstemon radicosus	Burned	2	1	3	3	5	2	7	7
	Unburned	0	0	1	0	0	0	2	0
Phlox hoodii	Unburned	0	0	3	1	0	0	6	2
Phlox longifolia	Burned	4	14	16	7	10	34	39	17
	Unburned	10	10	18	6	20	20	36	12
Potentilla gracilis	Unburned	2	2	2	2	4	4	4	4
Ranunculus glaberrimus	Unburned	0	1	0	0	0	2	0	0
Schoenocrambe linifolium	Burned	0	0	1	0	0	0	2	0
Senecio integerrimus	Burned	0	0	1	0	0	0	2	0
	Unburned	0	0	1	0	0	0	2	0
Sphaeralcea munroana	Burned	0	2	0	0	0	5	0	0
Stenotus acaulis	Unburned	1	1	0	0	2	2	0	0

Taraxacum officianale	Burned	0	0	1	1	0	0	2	2
	Unburned	0	0	1	0	0	0	2	0
Tragapogon dubius	Burned	0	0	1	0	0	0	2	0
	Unburned	2	1	1	2	4	2	2	4
Verbascum thapsus	Burned	0	0	1	1	0	0	2	2
	Unburned	1	1	0	0	2	2	0	0
Viola beckwithii	Burned	2	1	5	0	5	2	12	0
	Unburned	5	2	6	0	10	4	12	0
Viola nuttallii	Burned	0	0	12	0	0	0	29	0
	Unburned	1	0	20	0	2	0	40	0
Perennial grasses									
Achnatherum nelsonii	Burned	0	0	0	3	0	0	0	7
	Unburned	0	0	0	5	0	0	0	10
Calamagrostis montanensis	Burned	0	12	1	0	0	29	2	0
	Unburned	0	0	1	0	0	0	2	0
Carex filifolia	Burned	16	12	17	18	39	29	41	44
	Unburned	8	8	11	21	16	16	22	42
Elymus albican	Burned	29	20	36	36	71	49	88	88
	Unburned	43	40	38	24	86	80	76	48
Festuca idahoensis	Burned	31	22	23	25	76	54	56	61
	Unburned	36	39	43	46	72	78	86	92
Hesperostipa comata	Burned	2	25	8	10	5	61	20	24
	Unburned	6	6	3	4	12	12	6	8
Koeleria macrantha	Burned	0	2	3	25	0	5	7	61
	Unburned	4	6	4	22	8	12	8	44
Poa secunda	Burned	15	20	33	34	37	49	80	83
	Unburned	28	23	38	37	56	46	76	74
Pseudoroegneria spicata	Burned	0	0	4	6	0	0	10	15
	Unburned	3	1	5	3	6	2	10	6
Perennial shrubs									
Amelanchier alnifolia	Burned	0	0	0	1	0	0	0	2
	Unburned	0	0	0	1	0	0	0	2
Artemisia tridentata	Burned	31	3	7	5	76	7	17	12
	Unburned	39	40	39	37	78	80	78	74
Chrysothamnus viscidiflorus	Burned	2	4	5	5	5	10	12	12
	Unburned	2	2	1	3	4	4	2	6
Mahonia repens	Burned	2	1	1	1	5	2	2	2
	Unburned	3	3	3	3	6	6	6	6
Opuntia polycantha	Unburned	1	0	1	1	2	0	2	2
Purshia tridentata	Burned	6	3	7	6	15	7	17	15

	Unburned	2	4	3	3	4	8	6	6
Rosa woodsii	Unburned	1	1	1	0	2	2	2	0
Symphoricarpos oreophilus	Burned	1	2	1	1	2	5	2	2
	Unburned	2	3	1	0	4	6	2	0
Tetradymia canescens	Burned	3	6	4	5	7	15	10	12
	Unburned	5	6	5	7	10	12	10	14
Tree									
Larix occidentalis	Burned	1	0	9	0	2	0	22	0
	Unburned	0	0	2	0	0	0	4	0
Unknown									
ARHE	Unburned	0	0	1	0	0	0	2	0

Appendix B. Plant species frequencies in the 2003 burn area and percent of all plots with each species.

Species	Treatment	2003	2004	2005	2003	2004	2005
					----------%		----------
Annual forbs							
Chenopodium fremontii	Burned	0	4	1	0	20	5
Chenopodium leptophyllum	Burned	0	8	0	0	40	0
	Unburned	0	3	0	0	60	0
Collinsia parviflora	Burned	2	8	1	10	40	5
	Unburned	0	0	1	0	0	20
Cordylanthus ramosus	Unburned	2	2	3	40	40	60
Gayophytum racemosum	Burned	1	3	1	5	15	5
	Unburned	0	2	0	0	40	0
Lepidium densiflorum	Burned	0	2	3	0	10	15
Polygonum douglassii	Burned	0	10	13	0	50	65
	Unburned	0	4	3	0	80	60
Tragapogon dubius	Burned	0	1	0	0	5	0
Annual grasses							
Bromus tectorum	Burned	2	3	1	10	15	5
Perennial forbs							
Achillea millefolium	Burned	5	5	3	25	25	15
	Unburned	1	1	3	20	20	60
Agoseris glauca	Burned	0	1	0	0	5	0
	Unburned	0	1	0	0	20	0
Allium acuminatum	Burned	1	3	14	5	15	70
	Unburned	0	1	2	0	20	40
Antennaria dimorpha	Burned	0	1	0	0	5	0
	Unburned	0	1	0	0	20	0
Antennaria rosea	Burned	4	3	3	20	15	15
	Unburned	0	1	1	0	20	20
Arabis holboellii	Burned	0	1	0	0	5	0
Arenaria kingii	Unburned	0	0	1	0	0	20
Arnica fulgens	Burned	0	6	1	0	30	5
	Unburned	0	1	0	0	20	0
Astragalus convallarius	Burned	4	5	3	20	25	15
	Unburned	1	1	2	20	20	40
Astragalus filipes	Burned	2	0	0	10	0	0
Astragalus miser	Burned	0	5	3	0	25	15
	Unburned	0	2	1	0	40	20
Astragalus purshii	Burned	0	1	0	0	5	0
Calochortus macrocarpus	Burned	0	3	4	0	15	20
	Unburned	0	1	1	0	20	20
Cirsium undulatum	Burned	3	0	1	15	0	5
Collomia linearis	Burned	1	0	0	5	0	0
Comandra umbellata	Burned	3	5	6	15	25	30
	Unburned	1	2	1	20	40	20
Crepis acuminata	Burned	3	5	8	15	25	40
	Unburned	1	1	1	20	20	20

Erigeron corymbosus	Burned	8	4	8	40	20	40
	Unburned	4	2	3	80	40	60
Erigeron filifolius	Burned	0	0	1	0	0	5
Eriogonum heracleoides	Burned	16	9	9	80	45	45
	Unburned	4	5	3	80	100	60
Lomatium foeniculaceum	Burned	0	0	2	0	0	10
	Unburned	0	0	1	0	0	20
Lupinus caudatus	Burned	2	3	4	10	15	20
	Unburned	2	2	1	40	40	20
Mertensia oblongifolia	Burned	0	1	0	0	5	0
	Unburned	0	1	0	0	20	0
Penstemon radicosus	Burned	0	1	1	0	5	5
	Unburned	0	1	1	0	20	20
Phlox longifolia	Burned	11	8	8	55	40	40
	Unburned	3	2	2	60	40	40
Sphaeralcea munroana	Burned	0	1	0	0	5	0
Taraxacum oficinale	Burned	0	3	3	0	15	15
	Unburned	0	1	2	0	20	40
Viola nuttallii	Burned	0	1	0	0	5	0
Perennial grasses							
Achnatherum nelsonii	Burned	0	2	0	0	10	0
Calamagrostis montanensis	Burned	0	1	0	0	5	0
	Unburned	0	1	0	0	20	0
Carex douglasii	Burned	0	1	0	0	5	0
Carex filifolia	Burned	0	2	4	0	10	20
	Unburned	0	2	0	0	40	0
Elymus albican	Burned	0	17	16	0	85	80
	Unburned	0	4	4	0	80	80
Festuca idahoensis	Burned	10	7	2	50	35	10
	Unburned	1	3	1	20	60	20
Hesperostipa comata	Burned	9	5	6	45	25	30
	Unburned	3	1	3	60	20	60
Koeleria macrantha	Burned	1	2	13	5	10	65
	Unburned	2	0	2	40	0	40
Leymus cinereus	Burned	1	2	1	5	10	5
	Unburned	0	1	0	0	20	0
Poa secunda	Burned	10	9	12	50	45	60
	Unburned	3	3	5	60	60	100
Pseudoroegneria spicata	Burned	0	0	1	0	0	5
	Unburned	0	2	0	0	10	0
Perennial shrubs							
Atemisia tridentata	Burned	16	7	3	80	35	15
	Unburned	5	3	5	100	60	100
Chrysothamnum viscidiflorus	Burned	3	5	4	15	25	20
Opuntia polycantha	Burned	1	0	0	5	0	0
Purshia tridentata	Burned	1	0	0	5	0	0
Tetradymia canescens	Burned	4	1	3	20	5	15
	Unburned	1	1	1	20	20	20

Correlation of Neighborhood Relationships, Carbon Assimilation, and Water Status of Sagebrush Seedlings Establishing After Fire

Katherine DiCristina. Idaho State University, Department of Biological Sciences. Pocatello, Idaho 83209-8007.

Matthew Germino. Idaho State University, Department of Biological Sciences. Pocatello, Idaho 83209-8007. (germmatt@isu.edu)

ABSTRACT

Interactions of *Artemisia tridentata ssp. vaseyana* (mountain big sagebrush) and neighboring herbs may affect community development following fire in sagebrush steppe. Biomass, photosynthesis, and water relations were measured for seedlings of *A. t. vaseyana* occurring at different distances from neighboring herbs in the initial growing seasons following fire, when herbs dominate plant community cover. Biomass gain was nearly twice as great for *A. t. vaseyana* seedlings located furthest from neighboring herbs, compared to seedlings located adjacent to neighboring herbs. Similarly, carbon assimilation (Anet) was greater for *A. t. vaseyana* in microsites further from herbs, but only in early and not mid-late summer. Xylem pressure potentials (XPP) of seedlings were not correlated with their distances to neighboring herbs, on any sampling date. Moreover, supplemental watering had no effect on relationships between biomass of *A. t. vaseyana* seedlings and distances to neighboring herbs. In mid-late summer, when Anet, stomatal conductance, and XPP of seedlings decreased markedly as soils dried, Anet was no longer correlated with distances to neighboring herbs. Longer-term responses of *A. t. vaseyana* to neighboring herbs following fire may result largely from interactions between them in early summer, before the seasonal onset of water limitations. Although soil-plant water relations could explain much of the seasonal variability in Anet and growth of seedlings, correlations of Anet or biomass and proximity to neighboring herbs were not likely to result from water limitations in microsites near herbs.

Keywords: sagebrush; seedling establishment, photosynthesis, plant-soil water relations, fire, *Artemisia tridentata spp. Vaseyana.*

INTRODUCTION

Management of fire regimes, including prescribed burning and fire suppression, is common in sagebrush steppe ecosystems. Fire is applied in sagebrush steppe to promote forage production, reduce fuel loads, or restore disturbance for wildlife habitat. Whether, and to what extent application of fire achieves these ecological goals is currently debated, as indicated by much lower levels and higher variability of sagebrush cover (*Artemisia tridentata*) up to 30 years following fire (Wambolt et al. 2001) compared to expectations based on previous studies (Harniss and Murray 1973). Lack of sagebrush recovery following fire is a major concern for sustaining sage grouse (*Centrocercus urophasianus*) and other wildlife (Leonard et al. 2000). Altered rates of sagebrush reestablishment may result from changes in floristics of herb communities that are resulting from exotic plant invasions (Brooks and Pyke 2001).

Resprouting and rapidly-colonizing herbs, as well as a few shrubs, tend to dominate burned sagebrush steppe in the decade or so following fire, while the slower-growing shrub, Artemisia tridentata, reestablishes (Harniss and Murray 1973). Direct observations of interactions between sagebrush seedlings and other plant species are rare in the literature (e.g., Daubenmire 1975, Owens and Norton 1989; Berlow et al. 2002), especially for post-fire conditions. Seed dispersal and germination have been studied for *A. tridentata* and other aridland shrubs in undisturbed and post-fire situations (e.g., West & Hassan 1985; Young et al.1990; Tyler 1996, Chambers 2000), but less is known about factors affecting seedling success. New establishment of *A. t. vaseyana* seedlings was detected in sites burned 1-3 years prior to sampling and in sites in later stages of succession (i.e., having mature shrubs), but not in sites at intermediate stages of succession that had denser herb layers (DiCristina et al, in review, Harniss and Murray 1973, Young and Evans 1978). These temporal patterns of *A. t. vaseyana* establishment are nearly opposite of typical changes in herb cover during disturbance-succession cycles (eg. Harniss and Murray 1973), and indicate a potentially negative effect of herbs on *A. t. vaseyana* reestablishment following fire. The objective of this research was to determine how physiological performance of *A. t. vaseyana* seedlings is affected by their proximity to neighboring herbs, following fire and within the natural range of neighborhood spacing. We hypothesized that seedlings in microsites closest to neighboring herbs would exhibit less biomass accumulation, photosynthetic carbon uptake, and water status; and that growth limitations near herbs would result from water limitations. Moreover, we predicted that responses of *A. t. vaseyana* seedlings to neighboring herbs would be most negative in mid-late summer, when water availability reaches yearly minima. Seedling biomass was measured in response to experimental manipulations of distances to herbs, with and without supplemental water additions. We focused our sampling efforts on a site burned 1-2 years prior, when herb cover constitutes most of the plant community biomass.

METHODS

Research was conducted during the snow-free season of 2003 and 2004 in a site burned in September 2002 at the USDA, ARS, U.S. Sheep Experiment Station (USSES; 44°14’44” N Latitude, 112°12’47” W. Longitude; 1650 m a.s.l.), near Dubois, Idaho. The dominant shrub in this community is *Artemisia tridentata ssp. vaseyana* Nutt. Other, less abundant shrubs are *Chrysothamnus viscidiflorus* Nutt., *Tetradymia canescens* DC., and *Purshia tridentata* (Pursh) DC. Perennial bunchgrasses such as *Agropyron dastychium* (Hook.) Scribn., *Festuca idahoensis* Elmer and *Poa sandbergii Vasey* were common, as were numerous short-lived perennials such as *Achillea millefolium* L., *Antennaria sp.* Gaertn., *Erigeron sp.* L. and *Phlox sp*. L. Ground cover on 40- 1 m2 plots in 2003 and 2004 was 5 and 26% grass, 15 and 29% forb, 35 and 22 % soil, respectively, in addition to some litter and rock (DiCristina et al, in review). Soils are fine, loamy, mixed, frigid Calcic Argixerolls derived from wind blown loess or residuum (Natural Resources Conservation Service 1995). Total annual precipitation averaged 297 mm over the last 78 years, with 131 mm accumulating from May through August (Western Regional Climate

Center, Desert Research Institute, Reno NV). Precipitation during our study period of January through September 2003 and 2004 was 140 and 190 mm, respectively, compared to 240 mm for mean precipitation over these months over the previous 80 years. There has been light grazing (21.3 sheep days/ha) on the site from 1968-2002.

Biomass responses to experimental manipulations

Seedling responses to manipulated distances to neighboring herbs and water availability (+ or – supplemental water) were examined in 2003, on seedlings that had just recently emerged (within a week or so) during the first growth season following the 2002 fire. Five replicate plots having about 20 *A. t. vaseyana* seedlings within about 6 m2 of each other were identified within different burns in a < 2 km area. Herbs were removed from *A. t. vaseyana* seedlings that had naturally established within 10 cm of herbs, to generate a range of distances of seedlings to herbs. Distances from the base of each *A. t. vaseyana* seedling were then measured to the base of the nearest herb in each of four quadrants around seedlings (NW, NE, SE, SW), for a total of four distances per seedling. The four measured distances were added together and are hereafter referred to as the 'sum distance' of each *A. t. vaseyana* seedling to surrounding vegetation. Removal of surrounding herbs was accomplished by clipping aboveground structures at least once every two weeks from July through October. We randomly selected half of each replicate plot to receive supplemental watering. Water stored in 113-liter cisterns was applied to the root zones of seedlings using electric timers (Model 3020, Melnor USA) and drip irrigation lines. Seedlings in plots with supplemental water received about 300 ml of water in early morning and late evening every day from late July through September. Validation of effects of water additions on soil water content was accomplished by measuring volumetric water content (VWC, m3/m3) of soils under all seedlings using a handheld time domain reflectometer unit (Model CS616, Campbell Scientific Logan, UT) with 12 cm probes. Soil texture and bulk density were similar among the sites (sandy loam, Germino and Seefeldt, unpublished). VWC was measured four times throughout the watering treatments: August 1 and 13, September 3, and October 3. After September, all experimental seedlings were carefully excavated, rinsed in de-ionized water, and dried in an oven at 21°C for 24 hours. Seedling biomass was then measured to 0.001 g, and there were 59 and 33 seedlings among the five replicate watered and unwatered plots, respectively. We used regression and two-way ANOVA to determine significance of differences in biomass of seedlings with different sum distances to neighboring herbs, with and without watering. Seedlings selected for this experiment were initially similar in size (< 2 cm height) and age (emerged within about one week of each other), and we assumed that their biomasses at the beginning or the experiment were comparable.

Ecophysiological responses to neighboring herbs

Photosynthesis, water relations, and distance to neighboring herbs were measured in 2004 on seedlings of *Artemisia tridentata ssp. vaseyana* that we detected within three, separate, belt transects that were each 5 m wide by 25 m long, positioned in one ~ 100 ha burn patch. Data were collected on three separate sampling periods in 2004: 24-25 June, 17-18 July, and 4-5 September. Thirty seedlings were harvested at each sampling date, requiring selection of 30 new seedlings for each subsequent sampling. Seedlings were in their first or second season of growth and were between 1.5 and 10 cm in height, and consisted of between 7 and 20 leaves per plant. Sum distance to neighboring herbs (see methods above), photosynthetic gas exchange, and water status were measured for each seedling. We measured net photosynthetic carbon assimilation (Anet) and gs with a portable gas exchange system (LI-6400, LICOR Inc., Lincoln, Nebraska, USA) equipped with an artificial LED light sources and CO2 controller. Relative humidity, temperature, and CO2 were maintained near ambient values during measurements. Measurements were made during mid-morning to midday during the hours of maximal photosynthesis, and no daily time effects were evident in our data. Light intensity was 1000

µmol m-2s-1 for all measurements. All values were reported on silhouette leaf area basis according to recommendations of Smith et al. (1991). We quantified silhouette leaf area of each seedling by taking a digital photo of leaf area as it was naturally configured in the measurement chamber, perpendicular to the artificial light source and with objects of known size in view for calibration. Leaf areas and calibration objects in photos were traced onto paper and scanned into a computer-imaging program (Image J, version 1.23p) for calculation of leaf area.

Pre-dawn and midday xylem pressure potentials (PDXPP and MDXPP, respectively) were measured in the field immediately after excising shoots at the root interface, using a Scholander-type pressure chamber (Model 1000, PMS Instrument Co., Corvallis, Oregon, USA). We measured PDXPP between 0530 and 0630 on all sampling dates for half (n=15) of each sample population, except in June, when we measured the entire sample population (n=30) before dawn. We measured MDXPP between 1130 and 1400 for half (n=15) of each sample population in July and September only.

Time domain reflectometer (TDR) probes and data loggers (models CS616 and CR10, respectively, Campbell Scientific, Logan UT, USA) were used to measure and record VWC at one central location in the burn area. VWC was recorded at 4-hour intervals from June through September on two sets of 30 cm length probes inserted horizontally at 5 cm and at 50 cm soil depths. Soil water contents can vary considerably in space, and the TDR data were therefore used only to estimate how the timing of our physiological measurements corresponded to general seasonal trends in drying, or summer rains that led to soil wetting.

We used analysis of covariance (ANCOVA) to determine if month (main effect) affected the relationship between physiological responses of *A. t. vaseyana* and distances to neighbors (covariate). PDXPP values were log-transformed for statistical calculations. Statistical differences of VWC between months were not tested due to low replication, and we report only mean ± SD for monthly values for each soil depth. Least-square regressions were used to analyze relationships between Anet or gs and PDXPP over all sampling dates. Significant differences between specific means were determined with Tukey-Kramer tests at the $P < 0.05$ level. All analyses were conducted using SAS version 8, and JMP version 3.1 statistical software (SAS Institute Inc., Cary, North Carolina, USA).

RESULTS

Biomass responses to neighboring herb proximity and water additions

Biomass of *A. t. vaseyana* seedlings in unwatered plots was negatively correlated to proximity of neighboring herbs, though distances to herbs could explain only a small amount of the variation in seedling biomass (slope = 0.006 g/cm, r2 = 0.12, $F_{1,57} = 7.6$, $P < 0.001$; Fig. 1). Supplemental watering led to a more negative but less significant correlation of seedling biomass and proximity to herbs (slope = 0.009, r2 = 0.09, $F_{1,31} = 3.16$, $P = 0.08$; Fig. 1). Supplemental watering thus did not appear to ameliorate the negative relationship of seedling growth and distance to herbs, even though watering led to nearly a doubling of biomass ($F_{1,88} = 4.03$, $P<0.001$).

Volumetric water contents (VWC) in plots with supplemental water were 8-48% greater than in unwatered plots, on all dates measured ($F_{1,335} = 92.43$, $P < 0.0001$). Mean VWC of unwatered plots for monthly sampling dates from June to September 2003 were 11.0 ± 1.0, 9.8 ± 0.3, 10.3 ± 0.6 and 13.9 ± 0.4; whereas mean VWC of watered plots were 17.9 ± 1.0, 16.2 ± 1.4, 20.0 ± 1.3, and 15.1 ± 0.5, respectively. There were about 13 mm of precipitation during the month of September, compared to a mean of 6.3 mm for each of the previous three months.

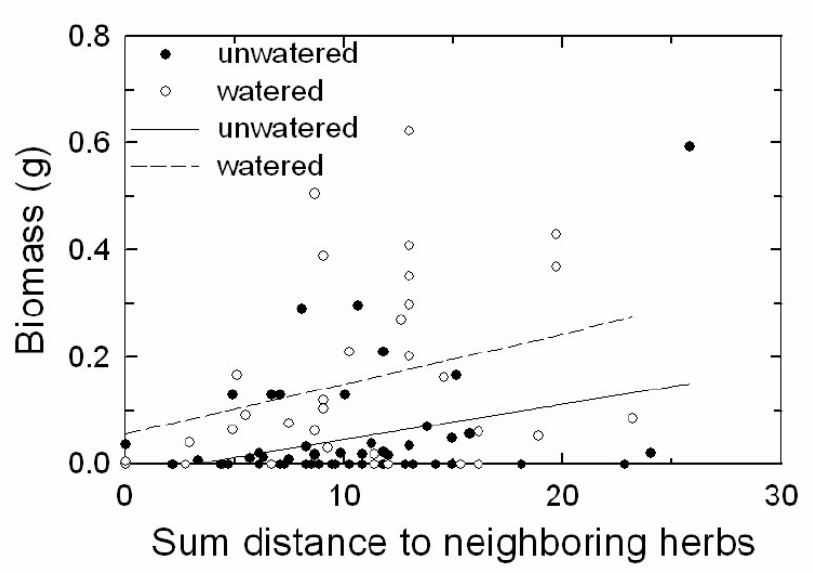

Figure 1. Correlation of biomass of *A. t. vaseyana* seedlings and sum distance to neighboring herbs in watered and unwatered plots in 2003. N = 59 seedlings in the watered and 33 in the unwatered plots.

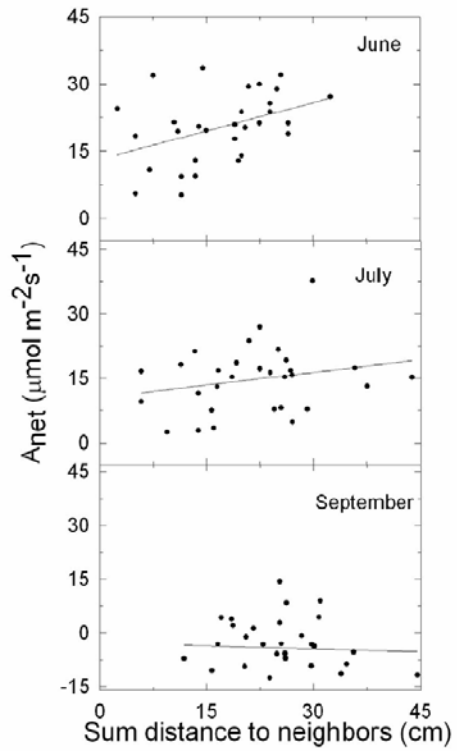

Figure 2. Relationship of distance to herbs and photosynthesis in *A. t. vaseyana* seedlings in June, July, and September 2004.

In June, there was a positive relationship (r2 = 0.14, F1,29 = 5.6, P = 0.03, Fig. 2) between net photosynthesis (Anet) and distance from *A. t. vaseyana* seedlings to neighboring plants. We did not detect any significant effect of sum distance on Anet in July or September (Fig. 2). The

percent of *A. t. vaseyana* seedlings having sum distances to neighboring herbs of 12 cm or less was 33% in June, 10% in July, and 0% in September, respectively (Fig. 2). Mean sum distances from *A. t. vasayana* seedlings to surrounding herbs increased about 35% from June to September ($F_{2,89} = 8.7$, $P < 0.001$, Fig. 2). No correlations of gs, or XPP and sum distances of seedlings to neighboring herbs were detected on any sampling dates, and therefore are not presented.

By September, Anet ($F_{2,89} = 71.7$, $P < 0.0001$), stomatal conductance (gs) ($F_{2,89} = 60.0$, $P < 0.0001$), pre-dawn xylem pressure potential (PDXPP) ($F_{2,56} = 112.7$, $P < 0.0001$), and mid-day xylem pressure potential (MDXPP) ($F_{1,20} = 19.4$, $P < 0.001$) were considerably lower than measurements in June (Fig. 3). At 5 cm soil depth, volumetric water content (VWC; m3 water/m3, reported as a percentage) in 2004 were highest in June (19.0% ± 4.2% SD) but decreased to 15% on 24-25 June, 12% on 17-18 July, and 8% on 4-5 September, which were days in which physiology was measured (Fig. 4). VWC was relatively more abundant at 50 cm depth, but also decreased from June (33.4% ± 0.6% VWC) to September (20.1% ± 0.5%, Fig. 4).

For all months combined, Anet ($r^2 = 0.61$, $P < 0.0001$) and gs increased ($r^2 = 0.80$, $P < 0.0001$) considerably with PDXPP (Fig. 5). Maximum levels of Anet and gs occurred when PDXPPs were above about –0.5 MPa (Fig. 5). Anet decreased less than gs as PDXPP decreased below about 0.5 MPa in the latter sampling dates (linear decline for Anet compared to exponential decrease in gs), reflecting increases in water use efficiency (A/gs) as soils dried in mid-late summer.

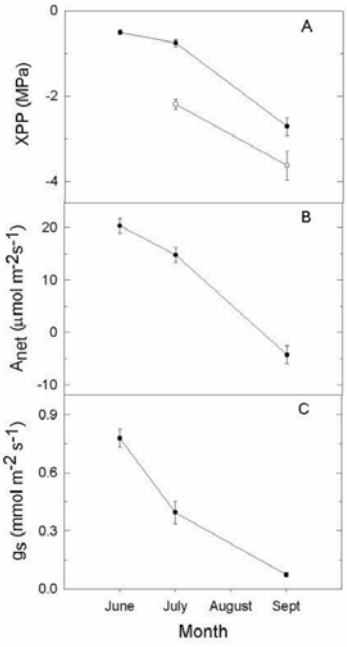

Figure 3. Mean (+/- 1 SE) pre-dawn (solid circles) and mid-day (open circles) xylem pressure potential (XPP) (A), photosynthesis (B), and stomatal conductance (C) of *A. t. vaseyana* in each of 3 months sampled in 2004.

DISCUSSION

Seedlings of *A. t. vaseyana* had less biomass at the end of their first growth season in microsites closest to neighboring grasses, but less carbon assimilation (Anet) near neighboring herbs in June only, and not in subsequent, drier months (Figs. 1 and 2). Relatively greater distances of *A. t. vaseyana* to neighboring herbs also occurred in months following June (Fig. 2), which could have resulted from mortality of *A. t. vaseyana* seedlings or senescence of herbs. Seasonal changes in neighborhood spacing could contribute to - but not completely explain – seasonal decreases in photosynthetic responses of *A. t. vaseyana* seedlings to proximity of neighboring herbs, because

sum distances >15 cm were observed on all sampling dates (Fig. 2). Thus, photosynthetic and growth responses of *A. t. vaseyana* to proximity of neighboring herbs could possibly reflect growth limitations in microsites adjacent to herbs.

The intensity of plant interactions in communities with low water availability and productivity is expected to be greatest during brief periods of increased resource availability, rather than when resource scarcity leads to reductions in background growth levels (Goldberg and Novoplansky 1997, see also Bilbrough and Caldwell 1997). Availability of soil water is typically greatest in sagebrush steppe during spring and early summer, following snowmelt and spring rain (Fig. 4). Although drought-adapted species might be capable of extracting water from drier soils, water potentials near –1.5 MPa are typical thresholds for water uptake in many plant species (Lambers et al. 1998). Comparisons of VWCs (Fig. 4) with water retention curves (Germino and Seefeldt, unpublished) indicated that VWCs around our TDR probes likely became less than –1.5 MPa (10-12% VWC), at the end of July and only at 5 cm soil depths. Although we did not measure VWC directly under seedlings, sharp reductions in stomatal conductance in seedlings occurred as plant water potentials at predawn decreased to and below –1.5 MPa, and were also somewhat synchronous with decreases in water content to below 10-12% VWC and –1.5 MPa in soils around our TDR probes (Figs. 3-5). Despite apparent increases in water use efficiency, stomatal limitations likely led to appreciable decreases in Anet as water potentials of plants and soils around TDR probes decreased to below about –1.5 MPa (Figs 3-5). Anderson et al. (1987) found that water consumption ceased at 10-12% VWC in older *A. t. wyomingensis* in a nearby site with similar soil textures (Anderson et al. 1987), and *A. t. wyomingensis* typically occurs in drier sites than *A. t. vaseyana* (reviewed in Smith et al. 1997). Responses of Anet in *A. t. vaseyana* seedlings to proximity of neighboring herbs in June, but not in subsequent months, corresponds with drought-induced reductions in Anet in the later months (Figs. 3 and 5; see Gillespie and Loik 2004 for drought responses in seedlings of other subspecies of Artemisia), and therefore matches the predictions of Goldberg and Novoplansky (1997). Community relationships of A. t. vaseyana seedlings and neighboring herbs may result largely from their interactions before the onset of seasonal water limitations to photosynthesis and growth.

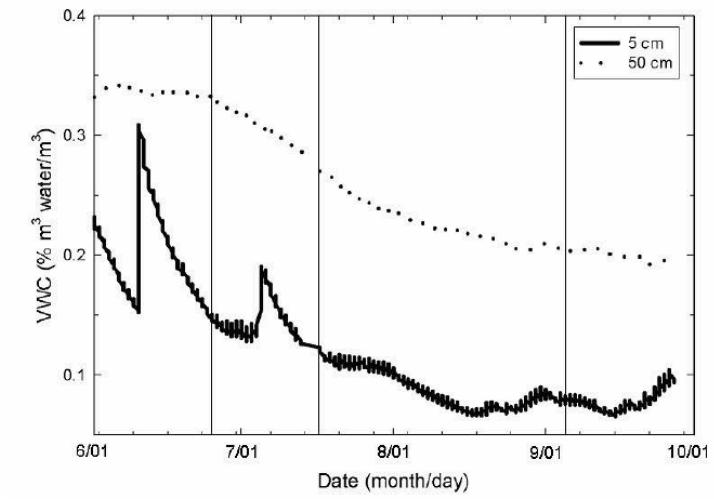

Figure 4. Volumetric soil water content from 1-June through 30-September 2004 at 5 and 50cm depths in soil. Data are plotted as recorded, in 4-hr intervals. Minor ticks on X-axis represent 7-day intervals. Vertical lines indicate sampling dates.

Differences in photosynthesis (when normalized for area and time) result from increases in diffusive supply of CO2 through stomata, or physiological demand for CO2 in carboxylation

reactions. Although water availability strongly affected biomass and temporal patterns of gs and Anet in *A. t. vaseyana* seedlings (Figs. 1 and 2), plant water status and gs were not correlated with proximity of neighboring herbs on any sampling date, and were therefore unlikely to explain lower Anet in seedlings nearest herbs, in June (Fig. 2). Moreover, negative relationships of biomass and proximity of neighboring herbs were not alleviated by supplemental watering (Fig. 1). Less Anet and growth of *A. t. vaseyana* in microsites closest to neighboring herbs were therefore not likely to have resulted from preemption of soil water for seedlings by neighboring herbs. Alternative explanations for reduced Anet in *A. t. vaseyana* seedlings near herbs could include factors that affect photosynthetic demand for CO2, such as less sunlight or soil nutrient availability in microsites closer to herbs. Seedlings we studied were only rarely overtopped by neighboring herbs, and often did not appear located closely enough to herbs to be shaded by them (dividing sum distances in Figs. 1 and 2 by four gives mean proximities). Moreover, DiCristina et al. (in review) found distances of *A. t. vaseyana* seedlings to neighboring herbs were not affected by whether seedlings were located on the north or south sides of herbs, which would otherwise indicate shading effects.

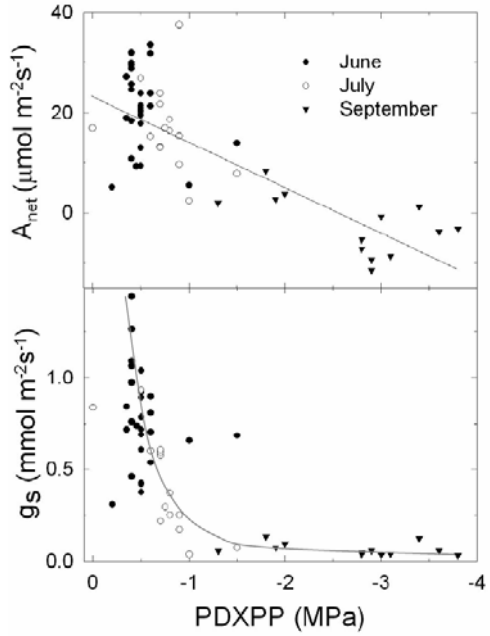

Figure 5. Relationship of pre-dawn xylem pressure potential (PDXPP) to photosynthesis (top) and stomatal conductance (bottom) of *A. t. vaseyana* seedlings in 2004.

High nutrient levels commonly occur after fires and could diminish the role of nutrients in plants interactions. However, nitrogen levels returned to pre-fire levels after about 10 months following fire in sagebrush (Hobbs and Schimel 1984), leading us to speculate that nutrient availability was not unusually high during years of our study. Several studies indicated greater nutrient uptake during moisture pulses in semiarid communities (Cui and Caldwell 1997; Ivans et al. 2003), and high uptake rates in June by herbs, and corresponding depletion of soil nutrients near herbs, would be consistent with our results. Our study was not designed to experimentally isolate the importance of specific resources on seedling Anet, but we speculate that nutrient limitations could be an important factor contributing to less Anet and growth of *A. t. vaseyana* seedlings located near herbs.

Summary and implications

Biomass gain and early-season photosynthesis in *A. t. vaseyana* establishing following fire was negatively correlated with proximity to neighboring herbs. Nearly inverse relationships of *A. t.*

vaseyana establishment and herb cover during disturbance-succession cycles, and much larger distances of *A. t. vaseyana* seedlings to neighboring herbs after fire than could occur randomly (DiCristina et al. in review), may therefore be partly attributable to physiological responses of *A. t. vaseyana* to herbs. Interactions between *A. t. vaseyana* and herbs in early season may be particularly important to post-fire establishment of *A. t. vaseyana*, and are more likely to be mediated by factors such as nutrients than soil water, in contrast to our initial predictions. Studies have investigated competitive relationships between adult sagebrush and herbs, but our study indicates a potential for competitive effects of lush, post-fire herb cover on establishment of young *A. t. vaseyana*, that is worthy of further experimental verification. The composition and abundance of herb communities following fire in sagebrush steppe is sensitive to management actions such as grazing, seeding, and herbicide applications (eg. Seefledt et al. 2002), and how changes in herb communities affect longer-term community development through their effect on sagebrush establishment should received greater consideration.

ACKNOWLEDGEMENTS

This study was made possible by a grant from the National Aeronautics and Space Administration Goddard Space Flight Center. ISU would also like to acknowledge the Idaho Delegation for their assistance in obtaining this grant. Steve Seefledt provided commentary and access to study sites.

LITERATURE CITED

Bilbrough, C.J., and Caldwell, M.M. 1997. Exploitation of springtime ephemeral N pulses by six Great Basin plant species. Ecology 78:231-243.

Cui, M., and Caldwell, M.M. 1997. A large ephemeral relearse of nitrogen upon wetting of dry soil and corresponding root responses in the field. Plant and Soil 191:291-299.

Gillespie, I.G., and Loik, M.E. 2004. Pulse events in Great Basin Desert shrublands: physiological responses of Artemisia tridentata and Purshia tridentata seedlings to increased summer precipitation. Journal of Arid Environments 59:41-57.

Goldberg, D.E., and Novoplansky, A. 1997. On the relative importance of competition in unproductive environments. Journal of Ecology 85:409-418.

Harniss, R.O., and Murray, R.B. 1973. 30 years of vegetal change following burning of sagebrush-grass range. Journal of Range Management 26:322-325.

Hobbs, N.T., and Schimel, D.S. 1984. Fire effects on nitrogen mineralization and fixation in mountain shrub and grassland communities. Journal of Range Management 37:402-405.

Ivans, C.Y., Leffler, A.J., Spaulding, U., Stark, J.M., Ryel, R.J., and Caldwell, M.M. 2003. Root responses and nitrogen acquisition by Artemisia tridentata and Agropyron desetorum following small summer rainfall events. Oecologia 234:17-324.

Lambers, H. Chapin , F.S. III, and Pons, T.L. 1998. Plant Physiological Ecology. Springer, New York.

Natural Resources Conservation Service. 1995. Soil investigation of Agriculture Research Service, United States Sheep Experiment Station headquarters range. United States Department of Agriculture, Natural Resource Conservation Service, Rexburg, Idaho.

Seefeldt, S.S., and McCoy, S.D. 2003. Measuring plant diversity in the tall threetip sagebrush steppe: influence of previous grazing management practices. Environmental Management 32:234-245.

Smith, S.D., Monson, R.K., and Anderson J.E. 1997. Physiological Ecology of North American Desert Plants. Springer, Berlin.

Smith, W.K., Schoettle, A.W., and Cui, M. 1991. Importance of the method of leaf area measurement to the interpretation of gas exchange of complex shoots. American Journal of Botany 75:496-500.

Wambolt, C.L. Walhof, K.S., and Frisina, M.R. 2001. Recovery of big sagebrush communities after burning in southwestern Montana. Journal of Environmental Management 61:243-252.

West, N.E., and Hassan, M.A. 1985. Recovery of sagebrush-grass vegetation following wildfire. Journal of Range Management 38:131-134.

Young, J.A., and Evans, R.A. 1978. Population dynamics after wildfires in sagebrush grasslands. Journal of Range Management 31:283-289.

Young, J.A., Evans, R.A., and Palmquist, D.E. 1990. Soil surface characteristics and emergence of big sagebrush seedlings. Journal of Range Management 43:358-367.

Analysis of LiDAR-Derived Topographic Information for Characterizing and Differentiating Landslide Morphology and Activity

Nancy F. Glenn, Department of Geosciences, IdahoStateUniversity- Boise, 12301W. Explorer Dr., Suite102, Boise, ID 83713 (glennanc@isu.edu)

David R. Streutker , Department of Geosciences, IdahoStateUniversity- Boise, 12301W. Explorer Dr., Suite102, Boise, ID 83713

D. John Chadwick, Department of Geosciences, Idaho State University, Campus Box 8072, Pocatello, ID83209-8072

Glenn D. Thackray, Department of Geosciences, Idaho State University, Campus Box 8072, Pocatello, ID83209-8072

Stephen J. Dorsch, Department of Geosciences, Idaho State University, Campus Box 8072, Pocatello, ID83209-8072

ABSTRACT

This study used airborne laser altimetry (LiDAR) to examine the surface morphology of two canyon-rim landslides in southern Idaho. The high resolution topographic data were used to calculate surface roughness, slope, semivariance, and fractal dimension. These data were combined with historical movement data (Global Positioning Systems (GPS) and laser theodolite) and field observations for the currently active landslide, and the results suggest that topographic elements are related to the material types and the type of local motion of the landslide. Weak, unconsolidated materials comprising the toe of the slide, which were heavily fractured and locally thrust upward, had relatively high surface roughness, high fractal dimension, and high vertical and lateral movement. The body of the slide, which predominantly moved laterally and consists mainly of undisturbed, older canyon floor materials, had relatively lower surface roughness than the toe. The upper block, consisting of a down-dropped section of the canyon rim that has remained largely intact, had a low surface roughness on its upper surface and high surface roughness along fractures and on its west face (unrelated to landslide motion). The upper block also had a higher semivariance than the toe and body. The topographic data for a neighboring, older and larger landslide complex, which failed in 1937, are similarly used to understand surface morphology, as well as to compare to the morphology of the active landslide and to understand scale-dependent processes. The morphometric analyses demonstrate that the active landslide has a similar failure mechanism and is topographically more variable than the 1937 landslide, especially at scales N20 m. Weathering and the larger scale processes of the 1937 slide are hypothesized to cause the lower semivariance values of the 1937 slide. At smaller scales (b10 m) the topographic components of the two landslides have similar roughness and semivariance. Results demonstrate that high resolution topographic data have the potential to differentiate morphological components within a landslide and provide insight into the material type and activity of the slide. The analyses and results in this study would not have been possible with coarser scale digital elevation models (10m DEM). This methodology is directly applicable to analyzing other geomorphic surfaces at appropriate scales, including glacial deposits and stream beds.

Keywords: Laser altimetry; LiDAR; Landslide; Surface morphology

INTRODUCTION

Landslides cause substantial economic, human, and environmental losses throughout the world. They are often triggered by other natural disasters, such as earthquakes and floods, and are difficult to predict. One of the greatest limiting factors in predicting and mapping landslide activity is the lack of understanding of scale-dependent processes, such as erosion, weathering, and fracturing. The literature on this topic is predominantly theoretical, although several uses of remote sensing and statistics to describe scale and morphometric parameters have been proposed (Bishop et al., 1998, 2003; Bonk, 2002; Phillips, 2005; Wallace et al., 2004). Previous studies have linked landslide processes with morphology and slide components (Smith, 2001; Korup, 2004; McKean and Roering, 2004).

Topographic data with a resolution relevant to the scale of morphological features of the landslide are necessary to understand the space-and time-depen-dent processes manifested in the slide morphology. Though 10-m digital elevation models (DEMs) are widely available in the U.S., they are not always of sufficiently fine scale for landslide mapping, nor are they widely available for many countries. Numerical analyses of fine scale topography can provide preliminary insight into landslide-scale mechanics and surface deformation (McKean and Roering, 2004). For example, relationships between topographic data and the surface expression of processes may provide insight into landslide activity, age, and material type. Previous studies have linked scale and morphology to weathering (Phillips, 2005), but addressing the problem of spatially and temporally dependent geomorphological mapping of landslides has been challenged by the lack of high-resolution topographic data.

Several techniques have been used to study landslide morphological elements and deformation. Interferometric synthetic aperture radar (InSAR) can provide information on spatial patterns and mechanics of individual landslide blocks, leading to modeling of slide failure (Kimura and Yamaguchi, 2000). Though InSAR has promising potential for understanding temporal deformation of landslides, it is subject to several complicating factors including landslide scale and satellite viewing geometry (Catani et al., 2005).Global Positioning System (GPS) and other point data (e.g., from extensometers) can provide temporal patterns of slide velocity for landslide modeling (Coe et al., 2003). While GPS and InSAR can elucidate slide mechanics and constrain slide models, currently only high resolution laser altimetry topographic data allow for the quantitative geomorphometric analyses necessary to understand spatial scale-dependent processes. Data from small-footprint airborne laser altimetry (light detection and ranging, LiDAR) can provide high resolution topographic information (1 m horizontal and 15 cm vertical accuracy) for geomorphometry (Gold, 2003; Rowlands et al., 2003; Hsiao et al., 2004; McKean and Roering, 2004).

The use of LiDAR for these types of quantitative analyses is relatively new; however, previous studies have used DEM-based geomorphometry for landslide delineation and risk (Gritzner et al., 2001), discriminating zones of surficial processes in mountainous terrain (Bishop et al., 2003),and mapping landforms for structural interpretations(Ganas et al., 2005) and regional analysis (Bolongaro-Crevenna et al., 2004).These analyses typically included first-and second-order derivatives of elevation such as slope angle, slope aspect, profile curvature, tangential curvature, etc. A few studies have used statistical measures such as semivariograms and spatial autocorrelation for geomorphometry, which can provide information about topographic variability and surface roughness (Bishop et al., 1998, 2003; Walsh et al., 2003; Miska and Hjort, 2005).

The purpose of this research is to demonstrate local topographic variability for landform mapping and characterization of two landslides (0.22 and 0.85 km2 in size) in southern Idaho using LiDAR data.

We examine local topographic variability through measures of topographic roughness (referred to hereafter as surface roughness), slope semivariance and fractal dimension. Specifically, our objectives are to (i) develop the use of surface roughness and slope maps, semivariograms, and fractal dimensions using vector point LiDAR elevation data for identifying patterns in morphology, movement history, and material types for the active, smaller Salmon Falls landslide; and (ii) use these same morphometric parameters (surface roughness, semivariance, fractal dimension) to compare the active slide with the older and larger 1937 landslide. We hypothesize that those components of the currently active landslide that have undergone high degrees of deformation also have high topographic variability and that the landslide morphological components have higher topographic variability than the comparable components of the older landslide.

STUDYAREA

The Salmon Falls landslide is a canyon-rim landslide along Salmon Falls Creek, a tributary to the Snake River in southern Idaho (Fig. 1).The slide is located ~11 km upstream from the confluence of the Snake River and is ~0.22 km2 in area. The slide is part of a larger slide complex along Salmon Falls Creek, an area known as Sinking Canyon. Just north of the currently active landslide within Sinking Canyon is another slide, larger in scale (~0.85 km2) and which failed in 1937.

The Salmon Falls landslide is hypothesized to be a hybrid of a rotational–translational-style slide (Dorsch, 2004) of Lucerne School basalt overlying weak lacustrine and fluvial sediments, both of the Tertiary Glenns Ferry Formation. Movement of the slide was first observed in 1999 and was monitored with laser-theodolite data from 2001 to 2004; GPS data were also used to monitor the slide in 2003 and 2004 (Chadwick et al., 2005).

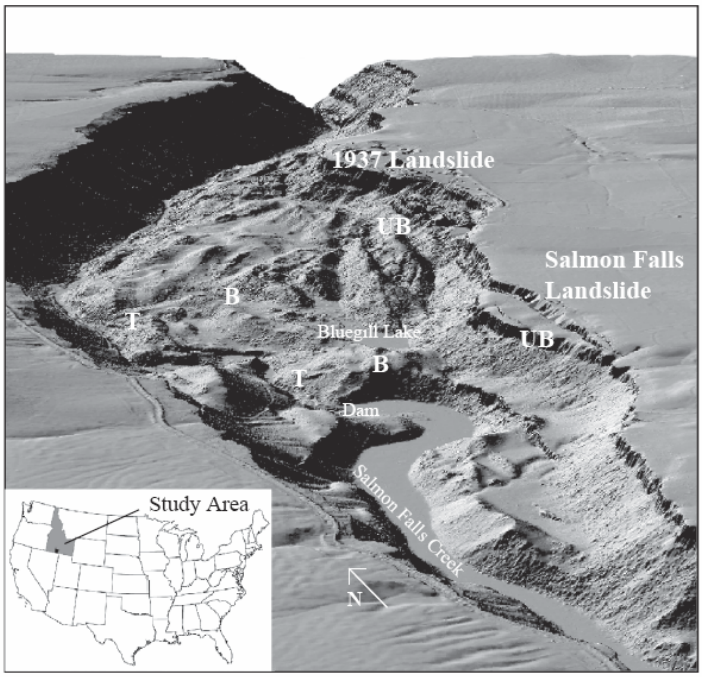

Figure 1. LiDAR perspective view of Sinking Canyon. UB=Upper block, B=Body, T=Toe.

The Salmon Falls landslide consists of three main morphological components defined in this study: the upper block (~130,000 m2), main body (~60,000 m), and toe (~25,000 m2)(Fig. 1). The upper block is a portion of the canyon rim and wall that has detached and moved downward and westward into the canyon, and consists of Lucerne School basalt with a series of fractures on the east and west sides. Basalt blocks have littered the slope below, contributing to a steep talus slope on the western side of the upper block. The main body of the slide consists of older landslide debris and canyon floor materials, mostly Lucerne School basalt underlain by Glenns Ferry Formation lacustrine and fluvial sediments. The toe of the slide, also consisting of these weak, unconsolidated materials, has uplifted ~1.25 m and partially dammed Salmon Falls Creek in two locations (Dorsch, 2004). The southernmost dam has resulted in the formation of a ~2-km long lake.

Dorsch (2004) utilized Quickbird multispectral satellite imagery and digitized aerial photographs to perform a change detection analysis between 1990 and 2002 for the Salmon Falls landslide; this study also developed a fracture map showing the pattern of surface deformation of the landslide. The fracture map showed significant fractures at the toe, upper block, and southern boundary of the landslide. The study concluded that the Salmon Falls landslide moved significantly (e.g., 8-m lateral toe movement) prior to the commencement of theodolite monitoring in 2001 and GPS monitoring in 2003. Theodolite monitoring was performed on the landslide by the Bureau of Land Management (unpublished data) and Dorsch (2004) between 2001 and 2004. The theodolite data indicate that the toe of the Salmon Falls landslide had the largest amount of lateral and vertical movement (1 m westward and 1.25 m upward, respectively), the main body had large lateral movement (1.75 m westward) but less vertical movement (5 cm downward), and the upper block had large amounts of lateral and vertical movement (75 cm westward and 1 m downward, respectively) (Dorsch, 2004). Chadwick et al. (2005) utilized five GPS stations to obtain information about subtle changes in movement between February 2003 and March 2004, and converted two-dimen-sional historical (1990–2002) velocities derived from the Quickbird-air photo analyses to three-dimensional velocities. While the GPS data were collected over a shorter time period, they indicated similar movements to the theodolite data over the corresponding time frame (Chadwick et al., 2005).Ellis et al. (2004) assessed the hazard of further failures of the Salmon Falls landslide and of dam breaching and potential flooding of Salmon Falls Creek. They indicated that catastrophic breaching of the major landslide dam is unlikely given current conditions.

The 1937 slide adjacent to the Salmon Falls slide has not been studied in detail; however, the morphology and failure patterns are similar for both. Lee (1938) proposed that the 1937 slide was caused by Salmon Falls Creek deepening its channel and undercutting the toe. Like the Salmon Falls landslide, fractures are present along the upper portion of the landslide; several basalt masses broke away from the canyon rim at those fractures and slid into the canyon (Fig. 1). These basalt masses are equivalent to the upper block of the Salmon Falls slide in this study. The body consists of weathered basalt blocks and upturned Glenns Ferry Formation lacustrine and fluvial sediments. The toe of the slide consists of the Glenns Ferry Formation lacustrine and fluvial sediments.

METHODS

LIDAR DATA

LiDAR vector point data were collected over ~17 km2 of the Salmon Falls landslide and adjacent areas of Sinking Canyon in October 2002. The data were collected with a small-footprint (~25-cm diameter at nadir), 25-kHz infrared laser at a horizontal spacing of ~1 m, resulting in nearly 20 million data points. First and last laser pulse readings were recorded with an elevation, time stamp, and return intensity. The last pulse data were then divided by the vendor into separate bald

earth and vegetation classes, with the bald earth vector point data used for subsequent analysis in this study. The absolute vertical accuracy of the LiDAR data, with respect to a standard geographic coordinate system, is 16 cm (95% confidence level), as measured by the vendor using a ground survey of 828 GPS points. The relative or point-to-point vertical accuracy of the elevation data was found to be on the order of 5 cm. Relative accuracy is determined by measuring the standard deviation of a group of points that are known to form a flat surface. In the case of this study, such calculations were made using the lakes and ponds found within Sinking Canyon. Though infrared lasers generally reflect poorly from water surfaces, the number of returns in the data set was adequate to perform this analysis.

GEOMORPHOMETRY

Several techniques are used in this study to examine the landslide morphology expressed in the topographic data within the different landslide components and to evaluate the relationship between surficial expression of landslide morphology, movement rates, and material type. Specifically, the bald earth LiDAR data were used to generate maps of local topographic roughness (surface roughness) and slope, semivariograms for understanding the morphological and scale dependent characteristics of the topography, and fractal dimensions as a tool for comparing scale-dependent topographic variability of different landslide components. These analyses used the vector point data from the bald earth data set and were performed for both landslides. The vector point data were used in lieu of a DEM in order to preserve the high accuracy of the original data by avoiding the interpolation errors that accompany raster DEM generation.

As stated above, the great value of LiDAR data lies in its high spatial resolution. As such, the focus of this study is topographic variability at fine length scales, such as those of a few meters. This focus led to the development of an algorithm which determines the local topographic variability, or surface roughness, of the LiDAR data. To accomplish this, it was necessary to separate the large scale topography from the fine scale variability. The vector point data were divided into 5_5 m grid cells, each containing 5 to 50 data points, depending on the local density of the data points. Within each cell, the point of lowest elevation was selected. These locally low elevation points, with an average spacing of 5 m by virtue of the cell size, were used to interpolate the baseline elevation surface. The interpolation was performed using a thin-plate spline. The height of each remaining data point above this surface was then calculated. The surface roughness of each cell was determined by calculating the standard deviation of these heights above the underlying surface. Such a calculation provides a measure of local surface roughness independent of large-scale topographic variability. The one-dimensional analogue of this process is shown in Fig. 2. Fig. 2a shows a cross-section of the elevation data, where the solid black line represents the vector point data, and the dashed line is the resulting interpolated underlying surface. Fig. 2b shows the local variability (the large-scale topography having been removed), where the grey line represents the heights of the vector point data above the underlying surface, and the black line shows the surface roughness, calculated as the standard deviation over the 5-m intervals. The 5-m width was chosen for the grid cells in order to include a sufficient number of data points for the calculation while maintaining a relatively high spatial resolution. The resulting surface roughness value (Fig. 3)of each grid cell is thus the average topographic variability over length scales from approximately one meter (the horizontal spatial resolution of the LiDAR data) to 5 m (the size of the cell).

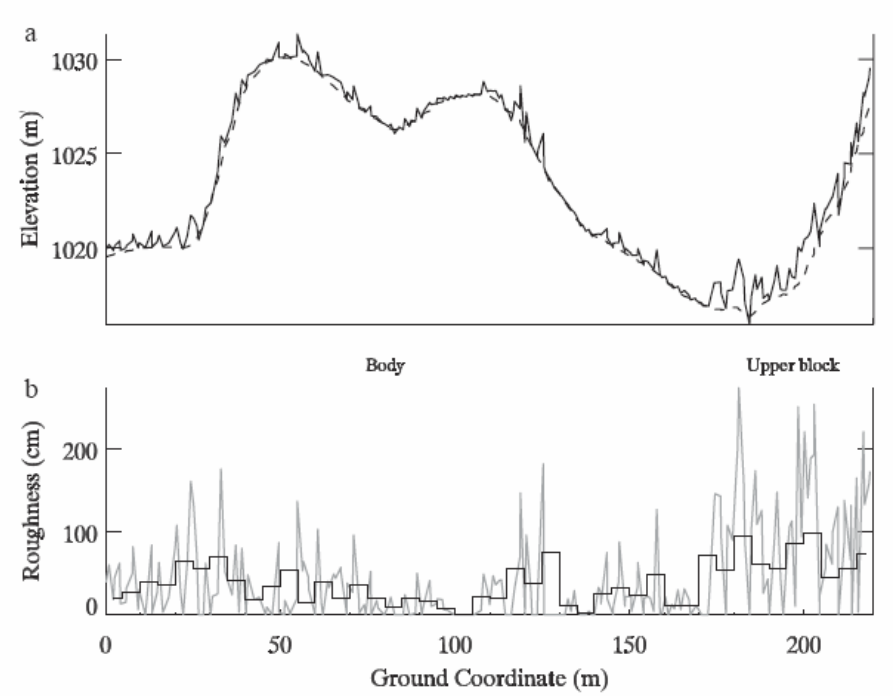

Figure 2. (a) One-dimensional elevation profile of Salmon Falls landslide. Solid line is bald earth LiDAR data and dashed line is interpolated underlying surface. (b) Grey line is elevation (height) of the data points above the interpolated underlying surface. The black line is the one dimensional profile of surface roughness, calculated over the 5-m cell intervals.

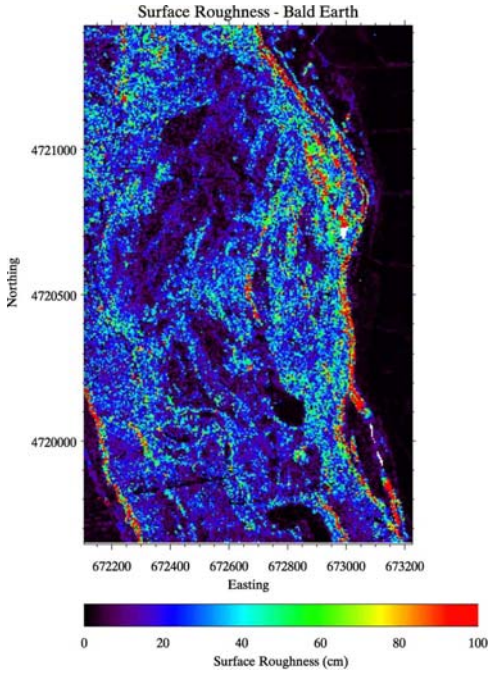

Figure 3. Surface roughness of Sinking Canyon area. White areas indicate no available data.

The map of slope values (Fig. 4) was calculated in a manner similar to the surface roughness map. The point vector LiDAR data were again divided in 55 m grid cells. The overall gradient (in both the x-and y-directions) of the points in each cell was calculated, and the slope value of each cell was found by summing the two gradient components.

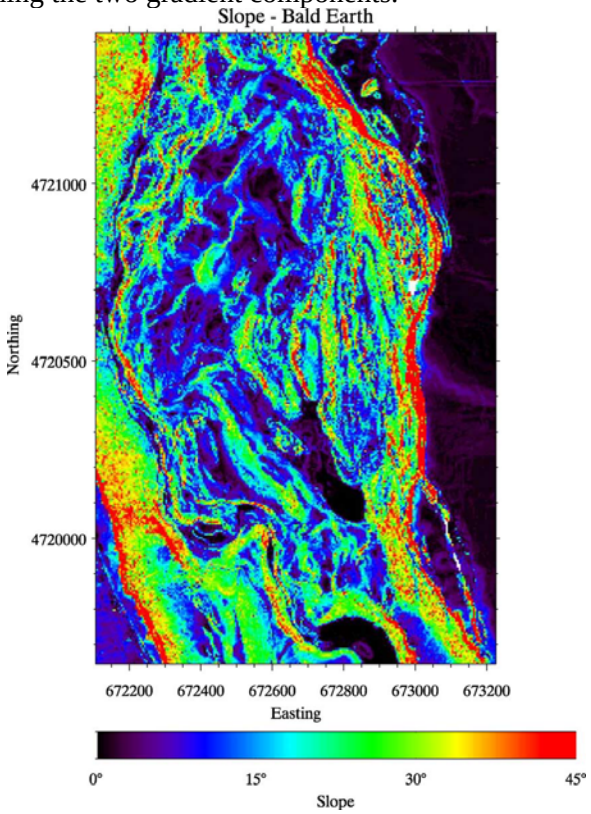

Figure 4. Slope of Sinking Canyon area. White areas indicate no available data.

Two-dimensional semivariograms were generated for sample locations (Fig. 5) in each of the main landslide components to examine relative spatial variability of the topography. Following Carr (1995), the two-dimensional semivariogram is expressed as

$$\gamma(h) = (1/2n)\sum [Z(x_i, y_i) - Z(x_{i+h}, y_{i+h})]^2 \qquad (1)$$

where y(h)= semivariance at lag distance h; Z(xi, yi)= data value at location i; Z(xi+h, yi+h)= data value at location i plus distance h; and n= number of samples in the data set. In this study, Z represents the vector point elevation obtained from the bald earth data set.

The shape of the semivariogram plot describes the spatial dependence between samples Z as a function of distance h. If there is spatial dependence within the data, y(h) typically increases with separation distance h, and may level off or even decrease after a certain distance. The range of the semivariogram is the lag distance at which the semivariance reaches a plateau and spatial autocorrelation between samples no longer exists (Fig. 6). This range corresponds to the ceiling of the semivariogram, called the sill, and is often equal to the statistical variance of Z. The nugget is the value of the semivariance at zero lag distance and is obtained by extrapolating the plot back to the origin. A nonzero nugget value provides an indication of the amount of noise in the data set or an indication of a microspatial autocovariance at a scale below the sampling resolution (Carr,

1995). In essence, the semivariograms are used to show spatial trends in the topographic data (variability in relief) over different spatial scales (lag distances).

The semivariograms were computed for the toe, body, and upper block of both landslides using Visual_Data, a Windows-based Visual Basic program (Carr, 2002). The number of samples (elevation postings) included 5322 for the toe, 32,223 for the body, 20,781 for the upper block of the currently active slide and 32,974 for the toe, 32,653 for the body, and 79,222 for the upper block of the 1937 landslide. The largest possible number of samples was included in each data set in order to characterize the overall topography without sample size bias. The sample locations used for the semivariogram and fractal analyses for the 1937 slide were chosen to best represent equivalent features in the currently active slide. The semivariograms were plotted to a lag distance equal to ~50% of the smaller size dimension of the sample. Two-dimensional omni-directional semivariograms were computed, averaging over all spatial directions, for each of the landslide components. Omnidirectional semivariograms were chosen over directional semivariograms in order to compare the relative average spatial patterns within each landslide component. The range, mean and variance of each of the subsets were also computed to compare to the semivariograms (Table 1).

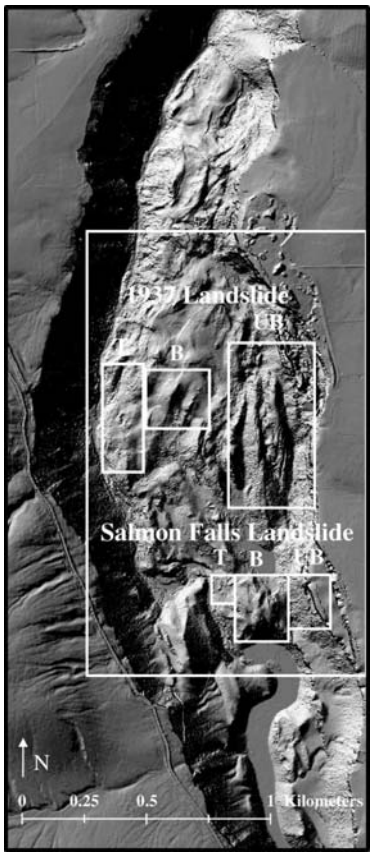

Figure 5. Subsets of 1937 and Salmon Falls landslides for semivariogram and fractal anlaysis. Outer box is area used for surface roughness and slope in Figs. 3 and 4, respectively. UB=Upper block, B=Body, T=Toe.

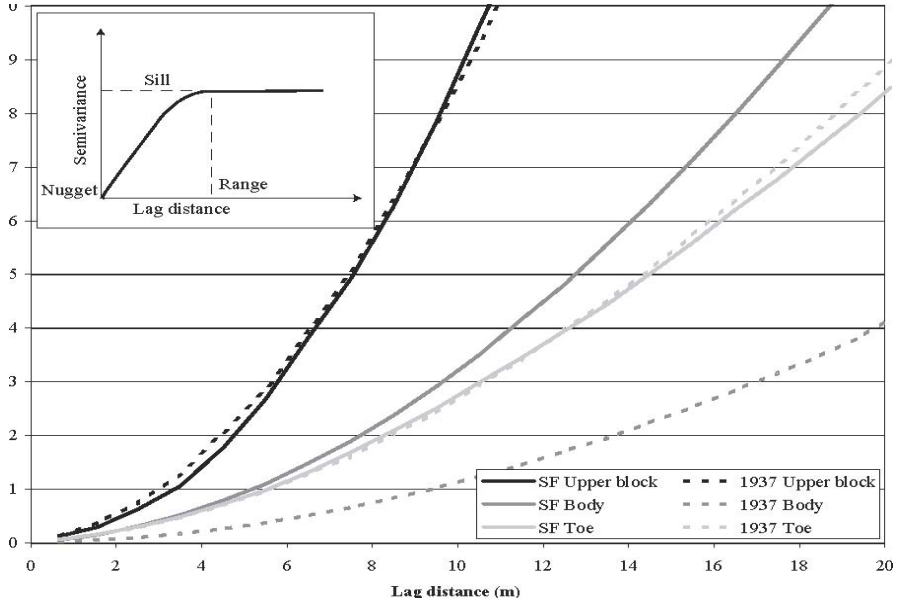

Figure 6. Semivariograms for Salmon Falls and 1937 landslides at lag distances b20 m. Inset is a graphical display of a spherical semivariogram model.

Table 1. Statistical moments of landslide components.

	Toe	Body	Upper block
Salmon Falls Landslide			
Number of LiDAR Samples	5322	32,223	20,781
N–S dimension (m)	113	273	216
E–W dimension (m)	94	240	169
Elevation minimum (m)	981.45	986.38	1011.21
Elevation maximum (m)	1014.13	1047.34	1098.10
Elevation range (m)	32.68	60.96	86.89
Elevation mean (m)	997.10	1016.16	1068.01
Elevation variance (m^2)	44.50	104.46	822.61
1937 Landslide			
Number of LiDAR Samples	32,974	32,653	79,222
N–S dimension (m)	185	236	659
E–W dimension (m)	187	257	345
Elevation minimum (m)	950.78	986.33	1003.07
Elevation maximum (m)	1001.72	1021.15	1104.08
Elevation range (m)	50.94	34.82	101.01
Elevation mean (m)	979.94	1005.83	1035.31
Elevation variance (m^2)	119.16	74.46	368.68

Topographic data can be described as self-affine random fractals (Turcotte, 1997), allowing fractal dimension to be used to understand the topographic roughness. In general, the greater the fractal dimension of the surface, the brougherQ the surface is. The fractal dimensions were computed in this study for understanding the degree of complexity and spatial autocorrelation in

the topography. Fractal dimensions were computed using the semivariogram method where the fractal dimension D is estimated by

$$D = 3 - m/2 \qquad (2)$$

where m=the slope derived from the log(c(h)) versus log(h) plot. The log–log plots were examined for multi-fractality, as signified by scale-breaks (changes in the slope, and therefore in fractal dimension). In order to verify linearity in the log–log plots, R2 values were computed. Fractal dimension was computed from the slope between each data point, starting at the lowest lag and ending at the lag distance where the first break in slope occurred (R2 value lower than 0.99). The fractal dimension was not computed beyond a lag distance of ~20 m for the body of the currently active landslide and 90 m and 30 m for the body and upper block, respectively, for the 1937 landslide because of scale-breaks. More information detailing methods on computations of fractal dimension can be found in Carr (2002) and Carr and Benzer (1991).

RESULTS

SURFACE ROUGHNESS AND SLOPE

Although the absolute accuracy of the LiDAR data is 16 cm, relative accuracies of a few centimeters allow for the computation of surface roughness values that are less than the absolute accuracy. The surface roughness values for the Salmon Falls and 1937 landslides range from b5cmto N1 m with higher surface roughness near the toes of the slides and the fractured edges of the upper blocks. Lower surface roughness is exhibited in the relatively un-deformed body of each slide and the upper surface of the upper block of the currently active landslide (Fig. 3). Within the active landslide, surface roughness ranges from b5 to 100 cm for the upper block (reflecting the inclusion of both the flat, un-deformed surface and the talus slope at the western edge), 5 to 50 cm for the main body (with localized areas up to 100 cm), and ~40 to 100 cm for the toe. In the 1937 slide area, the numerous ridges that comprise the upper block region have high surface roughness values (20–100 cm), grading to lower surface roughness values in the main body of the landslide debris (b40 cm). Surface roughness increases near the toe of the slide, with values up to 100 cm (Fig. 3).

The slope calculation (Fig. 4) resulted in high slopes for several portions of the upper block region and, to a lesser degree, toe area comprised of Glenns Ferry sediments in both landslides. The failed upper blocks of the 1937 slide and the upper block of the currently active landslide have slopes up to 458. Failed basalt blocks in the body of the 1937 slide also form ridges of high slopes (308to 458) that are oriented to the NW in the northern portion, to the west in the main portion, and to the SW in the southern portion of the slide. The toes of both slides have high slopes (up to 458) consisting of over-steepened sediments.

SEMIVARIOGRAMS

The shape of the semivariograms for the toe, body, and upper block of the currently active landslide are similar to a parabolic form, indicative of continuity of the elevation variable (Figs. 6 and 7).At short lag distances (b20 m) the semivariance of the upper block is larger than that of the body and toe. At lag distances N20 m the semivariance of the upper block appears to have no limit: the elevation properties have no finite variance (the semivariogram is unbounded). Overall the semivariance of the upper block indicates high variability in the topographic data over spatial scales of ~50 m. The body semivariance is slightly larger than that of the toe, with increasing difference between the two with increasing lag distance; however, the semivariance of the toe supersedes that of the body at a lag distance of ~70 m and rises to a sill at a range of ~85 m. This indicates that beyond ~85 m there is no longer a spatial relationship between the topographic data. Note that the toe semivariogram is plotted at lag distances over the 50% break-point of data

pairs (~50 m) for comparison with the other data sets. The semivariance of the body nearly reaches a sill at a lag distance of ~130 m, indicating that beyond this distance there is little spatial autocorrelation in the topographic data.

The semivariograms of the 1937 landslide also have a parabolic form at short lag distances (<20 m) and none reach a sill (Figs. 6 and 7).The upper block has the largest semivariance of the 1937 plots and is very similar to the semivariogram for the upper block of the currently active landslide at lag distances <20 m. At lag distances larger than ~20 m, the semivariance of the 1937 upper block is lower than that of the currently active landslide indicating that at this spatial scale, the topography of the 1937 upper block is more uniform. The semivariance of the toe of the 1937 slide is very similar to that of the toe of the active landslide; however, it does not reach a sill and appears to continue to rise with larger lag distances. The semivariance of the 1937 body is the lowest, indicating similar topographic data at a larger spatial scale (lag distance) than the other data sets.

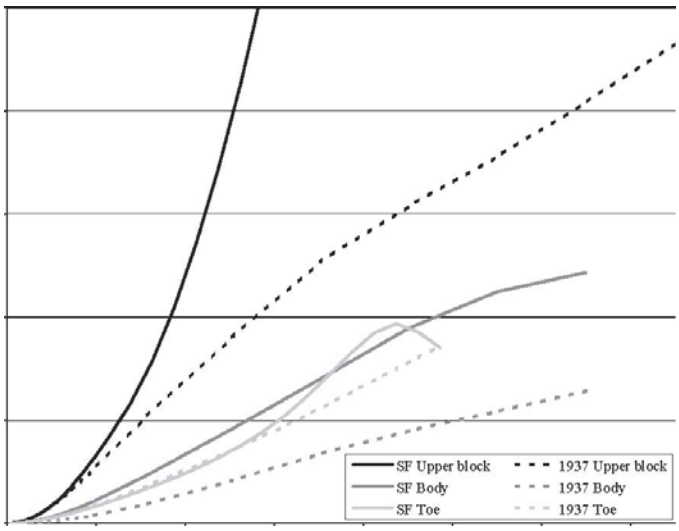

Figure 7. Semivariograms for Salmon Falls and 1937 landslides.

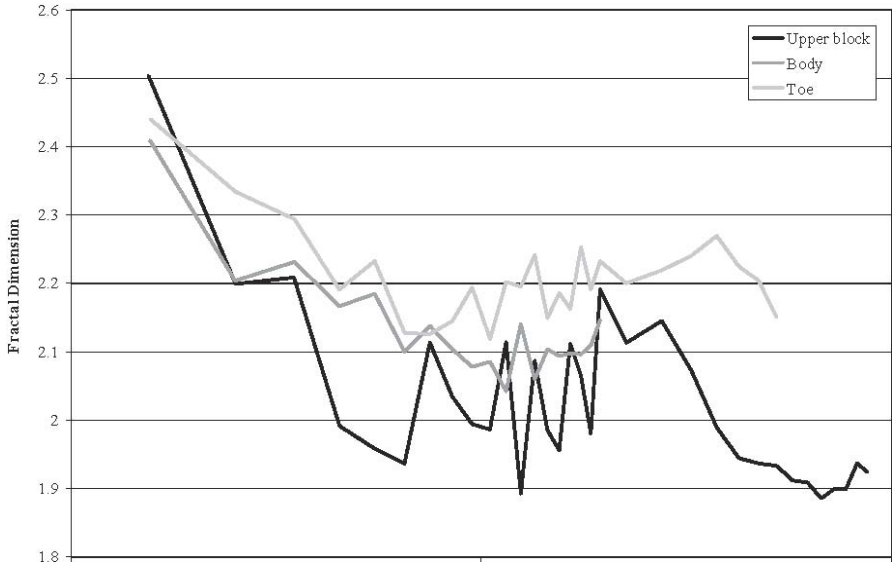

Figure 8. Fractal dimensions for the Salmon Falls landslide.

FRACTAL DIMENSION

Fractal dimensions were plotted against *h* (Figs. 8 and 9). In general, the fractal dimension of the toe is higher than that of the body and upper block of the currently active landslide, ranging from approximately 2.45 to 2.15. The fractal dimension of the upper block dips below 2.0 (fractal dimensions of surfaces are expected to be between 2 and 3) at several lag distances (e.g., 5 and 50 m). This result is not surprising because the calculation of fractal dimensions using the semivariogram method is a function of slope and the log–log semivariogram is steep (over 2) in these areas. These values are retained herein for descriptive purposes; further discussion of fractal values beyond expected limits can be found in Carr and Benzer (1991). Similar to the active landslide, the fractal dimension of the toe is greater than that of the body and upper block of the 1937 landslide; however, at hof ~10 m, the fractal dimension of the upper block increases and is higher than both the toe and body. The fractal dimension varies widely with lag distance; however, in both data sets, lower fractal dimensions occur near *h* of ~10 m.

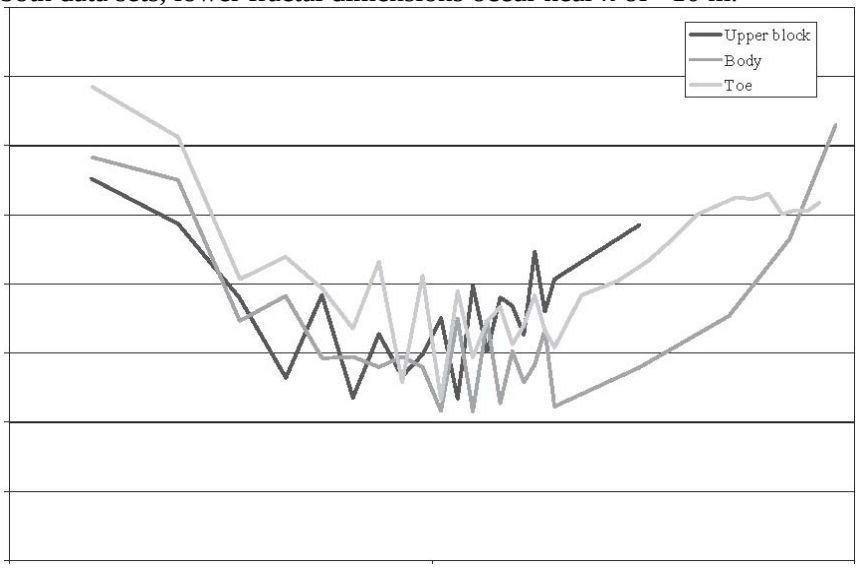

Figure 9. Fractal dimensions for the 1937 landslide.

DISCUSSION

COMPARISONS BETWEEN CURRENTLY ACTIVE AND 1937 LANDSLIDES

The surface roughness calculations and field observations of the currently active landslide indicate that the upper block and toe have relatively higher topographic variability than the body at scales relevant to the landslide components (~5 to 130 m). The semivariograms indicate a higher semivariance (and lower spatial autocorrelation) for the upper block than for the body and toe at the modeled lag distances of the active slide. While the high semivariance isn't a direct measurement of surface roughness, it does indicate a lack of similarity between topographic values in the upper block. The upper block is defined by the stark differences between the west talus slope and the smooth, but fractured upper surface. The semivariance of the toe is lower than the body of the active slide, consistent with the comparison of statistical variance; however, at a scale of ~85 m, the toe semivariance exceeds that of the body, indicating a lower spatial autocorrelation in the toe topographic data. While the high surface roughness from the LiDAR imagery and field observations of upturned sediments in the toe indicate deformation and roughness at small scales (~5 m), the semivariance is lower than that of the smoother body. The semivariogram of the body has a larger range and sill than the toe, indicating lower spatial autocorrelation at larger lag distances. This is interpreted as higher spatial variability as a function

of distance in the topographic data and shouldn't be correlated to simply higher surface roughness. Field, theodolite, and GPS observations show little vertical movement or fracturing on this part of the slide, yielding lower surface roughness values.

The fractal dimensions can also be considered a measure of the "roughness"of the topography (Klinkenberg, 1992; Lifton and Chase, 1992; Carr, 1995). The highly variable fractal dimension data set in this study is somewhat ambiguous; yet still useful for relative comparisons between landslide components. For example, while the fractal dimension of the toe is larger than the body and upper block for both landslides (indicating a "rougher"surface), the fractal dimension of the body is also higher than that of the upper block in the currently active slide. The steep slope of the upper block semivariograms result in low fractal dimensions for both slides. The smoother upper surface of the upper block in the active slide may outweigh the influence of the rough west-facing talus slope when comparing to the body. These results indicate that though relative comparisons may be made between data sets, caution should be exercised in correlating fractal dimension to a "rough" or "smooth" topography.

The weak unconsolidated toe material has a higher surface roughness than many areas of the body in the active slide. This portion of the landslide also demonstrated the highest vertical and lateral motion during the time of monitoring, resulting in greater disruption of the surface. The surface roughness is inherently linked to the material type and type of motion (upward thrusting versus lateral sliding). As the upper block drops down and away from the canyon wall, the body and the toe are pushed westward. The material of the toe is confined by the west canyon wall, which causes the slide to be thrust upward there. The sediments in the toe are weak, and as this motion is inherently disruptive to the surface, it results in large cracks and a rough, uneven surface. The main body, composed of canyon floor and canyon wall materials that have remained largely intact because of the primarily lateral motion of this part of the slide, has a smoother surface than the toe and the upper block. The steep talus slope of basalt on the western unconfined side of the upper block and the fractures within the upper block result in high surface roughness. However, the high surface roughness on the west face is related to rockfall processes independent of the landslide motion. Though not instrumented, this area of the upper block likely had similar movement patterns as the flat, instrumented surface. The low fractal dimension of the upper block is likely the result of the difference between the disaggregated canyon wall basalt and the upper intact surface of the block. The upper block exhibited significant downward motion and slightly less lateral motion. The motion and the unconfined west face of the upper block resulted in high topographic variability along the west face and in highly fractured areas (Fig. 10).

The fracture patterns of the active landslide (Dorsch, 2004) are consistent with the surface roughness maps, as areas with tension cracks and fractures (specific locations on the toe and upper block) also have high surface roughness (Fig. 10).The unconsolidated material of the toe leads to large cracks and high surface roughness. The fractures in the basalt of the upper block also result in localized high surface roughness. The tension cracks and fractures near the southern edge of the landslide are less distinct in the surface roughness map, likely because of the small size of the cracks and the lack of vertical offset on these primarily strike-slip fractures.

The data from the 1937 slide reveal similar patterns to those from the active landslide; however, movement data are not available to correlate to surface roughness and spatial patterns in the topographic data. Furthermore, the 1937 slide is approximately four times as large, resulting in larger spatial characteristics and patterns that make comparisons challenging. This example of scale dependency is one of the most important aspects in linking landslide processes to morphology. And while this study uses the 1937 landslide as a comparative feature to the active

slide, the comparative parameters (e.g., surface roughness) can be used as first-step mapping tool (Fig. 11).

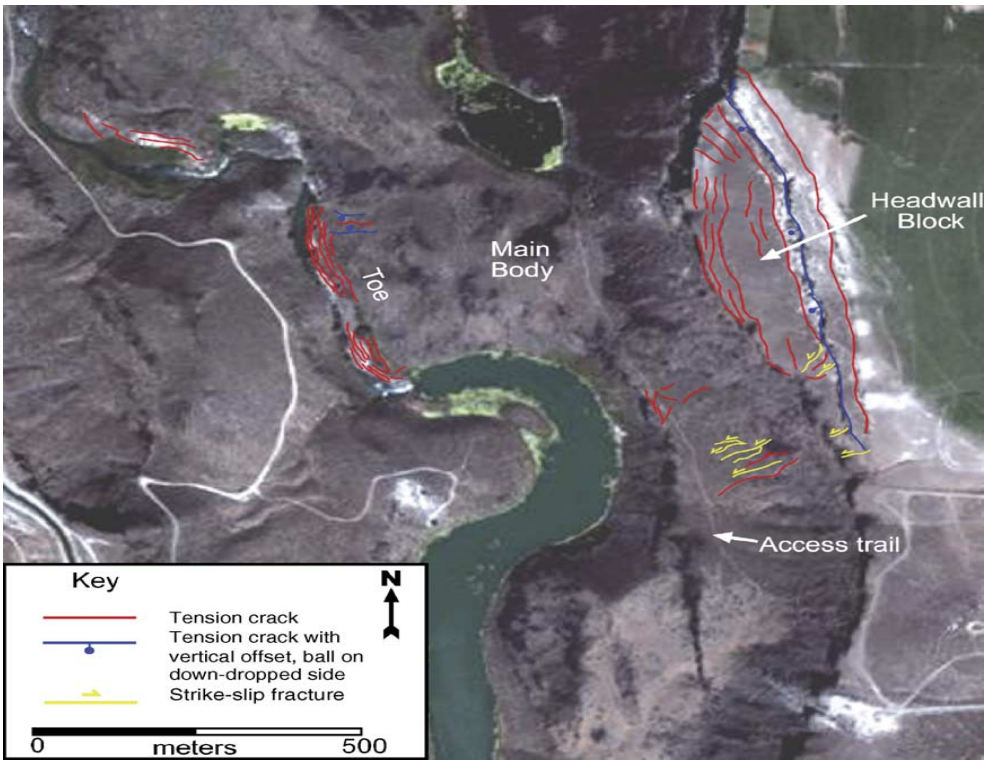

Figure 10. Fracture map from Dorsch (2004). Tension cracks and fractures on upper block and toe correspond to high surface roughness areas in Fig. 3. Cracks and fractures near access trail are not as easily identified in Fig. 4.

In comparison to the active landslide, the 1937 toe has a similar surface roughness and semivariance at short lag distances. At larger lag distances the semivariogram of the toe has a shallower slope, demonstrating slightly higher spatial autocorrelation at larger scales (60–100 m). The broader toe (and topographic expression) of the 1937 slide is likely from secondary slumping in the toe sediments. The LiDAR derived surface roughness of the body of the 1937 slide is lower and more uniform than that of the active slide. For example, the surface roughness of the 1937 slide's body is consistently b40 cm, while some areas of the body of the active landslide have surface roughness values as large as 100 cm. The higher surface roughness values of the active landslide are expected, given the younger age of the slide, and likely result from less weathering and surface erosion as well as less dust deposition and organic accumulation. This implies that surface roughness may be one method to assess relative ages between slides that have similar material types. The semivariogram of the body of the 1937 slide demonstrates lower spatial autocorrelation than the active landslide at all modeled scales, indicative of low spatial variability of the topographic data. As expected, the elevation variance of this subset is also smaller than that of the toe and upper block (Table 1). The repetitive down-dropped blocks of the canyon wall in the 1937 slide display similarly high surface roughness in the LiDAR-derived data as the upper block (largely still intact) of the active slide.

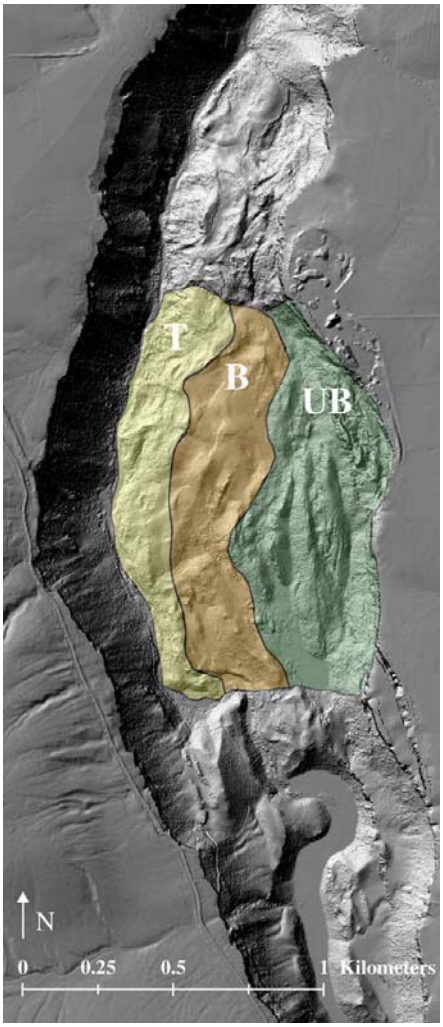

Figure 11. Mapped boundaries of the toe, body, and upper block regions of the 1937 slide. UB=Upper block, B=Body, T=Toe.

The 1937 upper blocks detached and moved rapidly away from the canyon wall, resulting in larger-scale rock fall and more extensive fracturing than in the Salmon Falls slide. The repetitive pattern of down-dropped upper blocks was captured in the sample used for the semivariogram. However, samples used in the semivariogram calculations that were taken near the canyon wall where the topography has higher variability resulted in nested semivariograms (not shown) and are examples of the location-and scale-dependency of semivariograms. As the fractures in the upper block and canyon rim of the active slide continue to cut back towards the east, we expect the upper block will attain a statistically similar morphology to that of the 1937 slide. This type of spatial information, especially over time, can provide inferences about the age and movement activity of landslides. The challenge is quantitatively relating changes in properties of topography with landslide age and rates of motion. These relationships hold promising information for understanding landscape development on both a “local” and “regional” level for landslide and other geomorphic processes (e.g., erosion, weathering; see Phillips, 2005).However, comparative analysis is complicated by the scale-dependent processes.

As with the active landslide, the fractal dimensions of the 1937 slide are higher in the toe than in the body. Furthermore, the fractal dimensions for the toe and body are slightly smaller than those for the active landslide. The fractal dimension of the upper block does exceed that of the body

and toe at high lag distances (>10 m) in the 1937 slide. This result can be observed in Fig. 5, where the upper block consists of at least three down-dropped blocks with rough west faces in comparison to the smoother, lower frequency ridges of the body.

The surface roughness, semivariance, and fractal dimension results indicate that the active landslide is similar in topographic expression to the older landslide. The surface roughness values for each of the landslide components are comparable between the two slides. Even visual interpretation of the surface roughness (Fig. 3) of both slides distinguishes between the rougher upper blocks, smoother areas in the main bodies, and rougher toes. The high surface roughness ridges in the older slide are equivalent to westerly rotated versions of the upper block in the active slide. These segments were originally flat with The 1937 upper blocks detached and moved rapidly rough west talus faces, but were then rotated on a away from the canyon wall, resulting in larger-scale listric plane. The western edges of these ridges are rock fall and more extensive fracturing than in the equivalent to the west face of the upper block on the active slide and the smoother east sides of these ridges are equivalent to the surface of the upper block. From this we can expect the upper block of the active slide to rotate and form a tilted ridge. Likewise from studying the 1937 slide and understanding the motion of the active slide, we can expect the body of the active slide to remain intact and smooth with increased weathering, erosion and dust deposition. The slope-gener-ated data (Fig. 4) indicate that failed basalt rims in the 1937 slide, and to a lesser degree Glenns Ferry sediments in both slides, have steep slopes. The basalt rims in the 1937 slide provide information about the scale of fracturing and failure. The rims are oriented NW and W, indicating the orientation of fractures in the basalt on which motion initiated. These rims are ~400 m in length from north to south. This is comparable to the upper block of the active landslide (500 m), further indicating that the younger landslide is likely demonstrating similar failure mechanics as the 1937 slide.

Results of semivariogram analyses indicate that, in general, the active slide has a higher semivariance and lower degree of spatial autocorrelation than the older slide. While there are some exceptions to this (e.g., at lag distances b8 m in the upper blocks and lag distances between 12 and 50 m for the toes), the differences in semivariance between the slides at these lag distances are very small. These findings indicate that the active slide has higher topographic variability as a function of distance. This can be explained by the smaller scale processes of the landslide and the younger age in comparison to the 1937 slide. These results indicate that the semivariograms can be useful for relative assessments of processes and age between landslides.

The fractal dimension results also indicate potential for classifying between landslide scales and ages. As previously stated, fractal dimensions of the body and toe of the 1937 slide are smaller than comparable components of the active slide at a scale near 10 m. Yet this doesn't hold true for the upper block where the steep semivariance results in extremely low fractal dimensions in the active slide. We may expect the fractal dimensions to become more similar between the two slides over time at small scales (~10 m), as the semivariograms of the active slide become closer to those of the 1937 slide. Because our analysis of fractal dimension was based on our 2-D semivariograms, the fractal dimensions represent a surface (rather than a profile). For our purposes, using fractal dimension to demonstrate the relative difference in topographic relief patterns (in space) between landslide components and between older and younger landslides, the semivariogram analyses were sufficient. Alternative methods, such as using the spectral-wavelength plot of a two-dimensional spectral analysis to discern smooth, unfailed terrain from relativel y rougher failed terrain, could also be useful (McKean and Roering, 2004).

LINKAGES BETWEEN MOTION, MATERIAL, AND TOPOGRAPHY

Our first hypothesis, that the high motion areas of the active landslide were linked to high surface roughness, was valid for the toe. Additionally, portions of the upper block have a high surface roughness due to landslide related fracturing. However, the west talus face of the upper block has the highest surface roughness in the landslide area, but its roughness is a result of rockfall rather than landslide motion. With this important exception, the study indicated that both type of motion and type of material play key roles in the surface expression and resulting surface roughness. Our second hypothesis, that the 1937 slide had a lower or bsmootherQsurface roughness than the active slide, was proven correct through the surface roughness calculations. Further, because we found that material type, motion, and surface roughness were linked, the comparisons between the landslide data sets are significant for mapping the 1937 slide. The lithology and canyon rim slopes of the 1937 slide are similar to the active slide. These similarities, coupled with the results of the numerical analyses of the topography, allowed us to provide a provisional map of the toe, body, and upper block boundaries of the 1937 slide (Fig. 11). Note that the upper block comprises many of the failed basalt blocks originating from the canyon wall. The northern boundary of the slide is difficult to discern because of another canyon rim slope failure just to the north. Likewise, the southern boundary of the 1937 slide in relation to the northern boundary of the active slide is obscure. More detailed analyses such as edge and linear effects in the topographic data could be explored to help map these boundaries with more confidence.

CONCLUSIONS

High spatial resolution, bald earth LiDAR data provide new opportunities for mapping landslide morphology through visual interpretation and numerical analysis. Surface roughness and slope calculations, semivariogram analysis, and fractal dimension all provide insight into the landslide morphology and linked slide processes. The results of this study show that topographic data with postings of 1 m or less are appropriate to conduct these analyses on landslides similar in size to the active Salmon Falls landslide. Vertical resolution on the order of 5 cm must be available to depict subtle changes in surface roughness of landslide components. Caution must be exercised when using semivariance and fractal dimensions to understand topographic variability because sample location and scale affect results. However, these tools provide useful relative comparisons of topographic expression in order to understand scale-dependent processes. Our topographic analyses indicate that different morphological components of the currently active landslide have different measurable, but comparable, surface characteristics, likely because of the type of material (e.g., weak sediments vs. intact basalt) and type of motion (e.g., disruptive thrusting and fracturing in the toe vs. the coherent down-drop-ping of the upper block). High rates of vertical and lateral motion were correlated with both the weak, unconsolidated toe materials having high surface roughness, as well as with the basalt upper block having both low (e.g., upper surface) and high (e.g., fractures and talus slope)surface roughness. However, the high surface roughness of the talus slope is not a function of landslide motion or activity. While the upward motion of the weak toe resulted in a rough disruptive surface, the downward motion of the upper block resulted in a smooth surface with rough fractures. Smaller vertical motion and less surface disruption were associated with a relatively smoother topography in the body. The topographic analysis also indicates that the active landslide has a similar failure mechanism to that of the 1937 slide. Though in situ movement data are not available for the 1937 slide, the statistical analysis for the toe and main body produced similar results as those for the active landslide. The blocks of the 1937 slide that dropped from the canyon rim provided a rougher morphology than the upper block of the active landslide. This information allowed us to map the toe, body, and upper blocks of the 1937 slide without large amounts of field reconnaissance and ground instrumentation. Though the 1937 slide is much larger in scale, the topographic expression provided by the LiDAR data helps to link related processes between the two landslides. High resolution topographic data have the potential to differentiate failure zones within a landslide and provide insight into the

material type and movement. This type of analysis is also relevant to other geomorphic applications, such as understanding stream bed topography, fluvial terrace morphology, and glacial landform degradation.

ACKNOWLEDGEMENTS
This study was made possible by a grant from the National Aeronautics and Space Administration Goddard Space Flight Center. ISU would also like to acknowledge the Idaho Delegation for their assistance in obtaining this grant.

Research funded by NASA Idaho Space Grant Consortium EPSCoR (FPK302-02), NOAA Environmental Technology Laboratory, and NASA Goddard (NAG5-12301). LiDAR data was provided in part by the Bureau of Land Management, Idaho (Ms. Karen Shilling). Ralph Wheeler, Claire Chadwick, and Kaleb Scarberry assisted with field investigations. We would like to thank Dr. J.R. Carr for help with Visual_Data.

LITERATURE CITED
Bishop, M., Shroder, J., Hickman, B., Copland, L., 1998. Scale-dependent analysis of satellite imagery for characterization of glacier surfaces in the Karakoram Himalaya. Geomorphology 21, 217 – 232.

Bishop, M., Shroder, J., Colby, J., 2003. Remote sensing and geomorphometry for studying relief production in high mountains. Geomorphology 55, 345 – 361.

Bolongaro-Crevenna, A., Torres-Rodrı´guez, V., Sorani, V., Frame, D., Ortiz, M.A., 2004. Geomorphometric analysis for characterizing landforms in Morelos State, Mexico. Geomorphology 67, 407 – 422.

Bonk, R., 2002. Scale-dependent geomorphometric analysis for glacier mapping at Nanga Parbat: GRASS GIS approach. Proceedings of the Open Source GIS -GRASS Users Conference 2002, Trento, Italy, pp. 1– 4.

Carr, J.R., 1995. Numerical Analysis in the Geological Sciences. Prentice-Hall, New Jersey.

Carr, J.R., 2002. Data Visualization in the Geosciences, Accompanied by Visual _Data CD-Rom. Prentice-Hall, New Jersey. Carr, J.R., Benzer, W.B., 1991. On the practice of estimating fractal dimension. Mathematical Geology 23 (7), 945 – 958.

Catani, F., Farina, P., Moretti, S., Nico, G., Strozzi, T., 2005. On the application of SAR interferometry to geomorphological studies: estimation of landform attributes and mass movements. Geomorphology 66, 119– 131.

Chadwick, J., Dorsch, S., Glenn, N., Thackray, G., Shilling, K., 2005. Application of multi-temporal high resolution imagery and GPS in a study of the motion of a canyon rim landslide. ISPRS Journal of Photogrammetry and Remote Sensing 59, 212 – 221.

Coe, J., Ellis, W., Godt, J., Savage, W., Savage, J., Michael, J., Kibler, J., Powers, P., Lidke, D., Debray, S., 2003. Seasonal movement of the Slumgullion landslide determined from Global Positioning System surveys and field instrumentation, July 1998–March 2002. Engineering Geology 68, 67 – 101.

Dorsch, S., 2004. The geologic framework, movement history and mechanics of the Salmon Falls landslide, Twin Falls County, Idaho. M.S. Thesis, Idaho State University, Pocatello, Idaho.

Ellis, W.L., Schuster, R.L., Schulz, W.H., 2004. Assessment of Hazards Associated with the Bluegill Landslide, South-central, Idaho. U.S. Geological Survey Open File Report 2004–1054. USGS, Denver, CO.

Ganas, A., Pavlides, S., Karastathis, V., 2005. DEM-based morphometry of range-front escarpments in Attica, central Greece, and its relation to fault slip rates. Geomorphology 65, 301 – 319.

Gold, R.D., 2003. A comparative study of aerial photographs and LiDAR imagery for landslide detection in the Puget Lowland, Washington. Geological Society of America, Cordilleran Section, 99th Annual Meeting, Geological Society of America, vol. 35 (4), p. 12.

Gritzner, M., Marcus, A., Aspinall, R., Custer, S., 2001. Assessing landslide potential using GIS, soil wetness modeling and topographic attributes, Payette River, Idaho. Geomorphology 37, 149 – 165.

Hsiao, K.H., Liu, J.K., Yu, M.F., Tseng, Y.H., 2004. Change detection of landslide terrains using ground-based LiDAR data. XXth ISPRS Congress, Istanbul, Turkey, Commission VII, WG VII/5.

Kimura, H., Yamaguchi, Y., 2000. Detection of landslide areas using satellite radar Interferometry. Photogrammetric Engineering and Remote Sensing 66 (3), 337 – 344.

Klinkenberg, B., 1992. Fractals and morphometric measures: is there a relationship? Geomorphology 5, 5– 20.

Korup, O., 2004. Landslide-induced river channel avulsions in mountain catchments of southwest New Zealand. Geomorphology 63, 57 – 80.

Lee, C.A., 1938. Recent landslides in Salmon Creek canyon, Idaho. Journal of Geology 46 (4), 660 – 665.

Lifton, N., Chase, C., 1992. Tectonic, climatic and lithologic influences on landscape fractal dimension and hypsometry: implications for landscape evolution in the San Gabriel Mountains, California. Geomorphology 5, 77 – 114.

McKean, J., Roering, J., 2004. Objective landslide detection and surface morphology mapping using high-resolution airborne laser altimetry. Geomorphology 57, 331 – 351.

Miska, L., Hjort, J., 2005. Evaluation of current statistical approaches for predictive geomorphological mapping. Geomorphology 67, 299 – 315.

Phillips, J., 2005. Weathering instability and landscape evolution. Geomorphology 67, 255 – 272.

Rowlands, K., Jones, L., Whitworth, M., 2003. Landslide laser scanning: a new look at an old problem. Quarterly Journal of Engineering Geology and Hydrogeology 36, 155 – 157.

Smith, L., 2001. Columbia Mountain landslide: late-glacial emplacement and indications of future failure, Northwestern Montana, USA. Geomorphology 41, 309 – 322.

Turcotte, D., 1997. Fractals and Chaos in Geology and Geophysics, 2nd ed. Cambridge University Press, New York.

Wallace, J., Morris, B., Howarth, P., 2004. The effects of scale on fractal dimension of topography: a case study from Sudbury, Ontario, Canada. Proceedings Geoscience and Remote Sensing Symposium, IEEE International, vol. 5, pp. 2845 – 2848.

Walsh, S.J., Bian, L., McKnight, S., Brown, D.G., Hammer, E.S., 2003. Solifluction steps and risers, Lee Ridge, Glacier National Park, Montana, USA: a scale and pattern analysis. Geomorphology 55, 381 – 398.

Advantages in Water Relations Contribute to Greater Photosynthesis in *Centaurea maculosa* Compared with Established Grasses

Judson P. Hill, Department of Biological Sciences, Idaho State University, Pocatello, Idaho 83209-8007

Matthew J. Germino, Department of Biological Sciences, Idaho State University, Pocatello, Idaho 83209-8007

John M. Wraith, Department of Land Resources and Environmental Sciences, Montana State University, Bozeman, Montana 59717-3120.

Bret E. Olson, Department of Animal and Range Sciences, Montana State University, Bozeman, Montana 59717-2900.

Megan B. Swan, Department of Land Resources and Environmental Sciences, Montana State University, Bozeman, Montana 59717-3120.

ABSTRACT
Semiarid steppe communities in North America appear particularly vulnerable to persistent infestations by exotic, taprooted forbs, such as European spotted knapweed (*Centaurea maculosa*). We determined whether species differences in ecophysiological response to water availability could help link traits of *Centaurea* with invasibility of steppe communities. Plant–soil water relations and photosynthesis were measured under three water levels in a greenhouse and at two sites over two years in the field for *Centaurea* and dominant rangeland species of southwestern Montana: *Pseudoregneria spicata*, *Pascopyron smithii*, and *Bromus inermis*. *Centaurea* had greater and more seasonally persistent photosynthesis than the other species under field conditions but not in the greenhouse, where water availability was similar for the species. *Centaurea*had no greater water use efficiency, except under unusually dry conditions, but maintained greater water potentials despite greater transpiration than the grasses. Changes in soil water indicated uptake from deeper and wetter soils in *Centaurea*than in grasses. Greater photosynthesis in *Centaurea*compared with grasses may result from uptake of deeper soil water and corresponding drought avoidance. Interspecific differences in resource use may therefore contribute to the success of *Centaurea*, and *Centaurea*'s ecological requirement for water matches an available resource niche in the communities we examined.

Keywords: exotic plants, grasslands, photosynthetic gas exchange, water relations.

INTRODUCTION

Replacement of native species by exotic annual grasses and perennial forbs has occurred in many areas of semiarid steppe in western North America, especially in areas converted to steppe through exclusion of woody species. The persistence of *Bromus tectorum* and similar invasive grasses in these semiarid rangelands has been attributed to differences in their phenology and soil resource use compared to native species, which, along with altered fire frequencies, can lead to site modifications that favor traits of invasive over those of native species (Booth et al. 2003). However, less is known about factors contributing to the invasiveness of the numerous species of exotic perennial forbs (e.g., thistles, *Centaurea* sp.) that are commonly taprooted members of the Asteraceae and are noxious invaders of semiarid grasslands and disturbed shrublands (Taylor 1992; Pyke 1999). These species can both colonize and persistently dominate sites for decades or longer. *Centaurea maculosa* Lam. (European spotted knapweed) is a particularly noxious, taprooted, and exotic forb that was introduced to the San Juan Islands in the late 19th century and has since expanded its range to much of North America, especially grasslands of the Pacific Northwest (Sheley et al. 1998).

Soil resource availability may contribute to invasions, provided that interspecific variation in soil resource use leads to selective advantages for exotic invaders compared to native species (e.g., Lonsdale 1999; Davis et al. 2000). *Centaurea maculosa* did not appear to use nitrogen more efficiently than native grasses it competes with (Olson and Blicker 2003) and did not appear to alter soil physical characteristics (Sperber et al. 2003). However, *C. maculosa* and other exotic forbs frequently have deeper roots and can emerge earlier and persist longer during seasonal drought than native or naturalized (hereafter ‘‘established’’) steppe herbs. Soil water within steppe is usually replenished by snowmelt and spring rain but then becomes depleted to low levels during warm summers, particularly in the shallow root zones of grasses (Smith et al. 1997). While several studies have addressed allelopathy as a factor contributing to invasiveness of *C. maculosa* (Ridenour and Callaway 2001; Bais et al. 2003), differential use of soil water during seasonal drought could also be a key factor affecting the success of *C.maculosa*.

Invasive species in forests and grasslands that are more productive than semiarid steppe typically had greater growth and photosynthesis or photosynthetic efficiency than native plants, and these advantages were frequently related to properties that enhance sunlight use (e.g., Williams and Black 1993; Williams et al. 1995; Pattison et al. 1998; Baruch and Goldstein 1999; Durand and Goldstein 2001; Myers and Anderson 2003; Nagel and Griffin 2004). Surveys of traits related to resource utilization and carbon gain across groups of exotic invasive and native species have not always revealed differences (e.g., Smith and Knapp 2001). Matching differences in resource use between exotic and native species to the specific ways that resources become available in time and space may lead to more comprehensive linkages between species invasiveness and community invasibility. Photosynthetic differences among species in semiarid steppe can result from variation in plant–soil water relations, and greater photosynthesis might increase plant fitness. Determining whether suites of traits in exotic forbs such as *C. maculosa* reflect relatively greater drought avoidance, tolerance, or water conservation than native plants could yield important insight on the invasiveness of *C. maculosa* as well as the susceptibility of steppe communities to invasion.

The objective of this study was to determine whether inter-specific differences in net carbon assimilation rates (A_{net}) and soil-plant water relations between *C. maculosa* and established species exist, and could contribute to the success of *C. maculosa* in semiarid steppe. We hypothesized that *C. maculosa* would have greater A_{net} than grasses that otherwise dominate sites frequently invaded by *C.maculosa*. Moreover, we predicted that the greater A_{net} in *C. maculosa* would be the result of persistent water acquisition and flexibility in the utilization of water as

water availability decreased from early to late season. Greater flexibility or plasticity in ecophysiological characteristics in exotic plants can contribute to their success in different environments (Williams et al. 1995). From its widespread distribution and relatively extended phenology, we also hypothesized that *C. maculosa* would be more flexible in its carbon assimilation and water relations among sites and times, compared with established species.

METHODS

Photosynthesis and water relations were measured under controlled soil water levels in a greenhouse experiment in the summer of 2001 and under natural field conditions in the summers of 2002 and 2003. Measurements were performed on *Centaurea maculosa* and the dominant native rangeland grasses *Pascopyron smithii* Rydb. (western wheatgrass), *Pseudoregneria spicata* Pursh A. Love ssp. *spicata*(bluebunch wheatgrass), and the nonnative but established *Bromus inermis* Leyss. (smooth brome).

FIELD OBSERVATIONS

Plants were monitored in monocultures at two sites: in Leverich Canyon, 10 km south of Bozeman, Montana, and another site ca. 16 km east of Helena, Montana. Four 2 3 2-m monocultures were created for each species at each site by painting glyphosphate herbicide (Roundup, Monsanto, Columbus, OH) onto leaves of other species in each plot during the year before the experiment. Ground litter was removed from the plots once the nontarget species had died to prevent the species from receiving extra nutrients. Soils at Bozeman were a silty loam overlaying gravelly and sandy loams below ca. 25 cm. Soils at Helena were silty clay loam overlaying clay below ca. 25 cm, as described in Swan (2004).

MICROCLIMATE

Field microclimate conditions were continuously recorded at both sites using dataloggers (CR10X, Campbell Scientific, Logan, UT) throughout both growth seasons. Air temperatures were measured with fine-wire, radiation-shielded thermocouples positioned at 5 cm (n= 4) and 100 cm (n= 2) above ground, and averages of readings made at 5-min intervals were recorded every 30 min (24-gauge, Omega, Stamford, CT). The different heights were chosen for their comparability to rosette foliage and regional weather stations, respectively. Long-term maximum and mean temperatures during the summer months were determined for both sites from the three Western Regional Climate Center (WRCC; Desert Research Institute, Reno, NV) monitoring stations located closest (<20 km) to each site. These climate stations have reported monthly averages of daily minimum, maximum, and mean temperatures over the past 40–60 yr.

During the 2003 season, 32 time-domain reflectometry (TDR) probes (model TDR 100, Campbell Scientific) were permanently inserted vertically into soil, from the surface to 30 cm deep, to provide continuous monitoring of soil water. TDR was measured every 6 h at the Bozeman and Helena field sites from June through August. Volumetric soil water contents were also determined under four monospecific stands of *C. maculosa* or four plots of grasses only at each site, at incremental depths of 20 down to 120 cm at Bozeman and to 100 cm at Helena, during the 2002 and 2003 seasons using a neutron moisture meter (503DR, California Pacific Nuclear, Martinez, CA). Neutron probe readings were made in one PVC-lined access hole per plot at midday on one day in the second week of each summer month.

Soil water retention curves (plots of soil water potential and water content) were determined for the two different soils found at the two different sites. Three soil cores were extracted at each site, and samples were collected at 10-cm intervals to the 50-or 70-cm depth. Each 10-cm sample increment was saturated in the lab with distilled water, and a subsample of ca. 8–10 g of soil was taken for measurement. Water potential was measured using a WP4-T model dew point

potentiometer (Decagon, Pullman, WA), and water content was determined using the mass-based gravimetric method on each subsample at 15–30-min intervals as samples dried at room temperature. After ca. 8 h of drying, soil samples were then dried in an oven for 24 h and weighed. We then calculated (gH_2O)/(gdrysoil) and (mLH_2O)/(mLdrysoil) for each interval measurement during the dry-down. Additional subsamples were taken from the 10-cm incremental samples and used to determine soil bulk density (m^3 m^{-3}).

GAS EXCHANGE MEASUREMENTS

Leaf-level gas exchange measurements were made at both sites on *C. maculosa*, on *P.spicata* at the Helena site, and on *B. inermis* at the Bozeman site, in 2002 and 2003. Bromus inermiswas also measured in 2003 at the Helena site. *Pascopyron smithii* was a relatively less abundant species at the sites, and although we examined it in our greenhouse study, we did not generate enough field data for meaningful statistics or presentation. Measurements were made at each site three times during the growing season, at ca. 6-wk intervals, to evaluate temporal variations in carbon assimilation as soil water decreased from seasonal maximum to minimum availability by late summer. Seasonal variation in water results from high water inputs during snowmelt and early spring rain, when plants are dormant, followed by little precipitation as temperatures and vapor deficits increase during the summer growing season. Gas exchange measurements were made on representative leaves of five arbitrarily selected individuals of each species starting at 0800 hours on days with clear skies. Different individuals were measured for each sampling. Carbon assimilation (A_{net}) and stomatal conductance to water vapor (g_{st}) were determined with a portable closed-flow gas exchange system (LI-6400, LI-COR, Lincoln, NE), equipped with a CO_2 controller, and an artificial red-blue light source. All measurements were made with CO_2 concentration at 370 ppm and under saturating light conditions (>1500 mmol m2s1, 400–700 nm). Transpiration (E) was calculated from the product of conductance and leaf-air vapor deficit (von Caemmerer and Farquhar 1981). Leaf-air vapor pressure deficit was determined from separate measurements of relative humidity and leaf and air temperatures taken before inserting leaf into measurement chamber (Hygro-Thermo-Anemometer, Extech, Waltham, MA; PM Plus infrared thermometer, Raytek, Santa Cruz, CA). Water use efficiency (WUE) was calculated as A_{net} / E($\mu molCO_2/mmolH_2O$). Gas exchange parameters were calculated on a projected leaf area basis, which was determined from digital photographs using the following procedure. After the measurement of photosynthesis, the measurement lid was opened without disturbing the arrangement of leaves resting on the chamber bottom. A spare chamber gasket was then pressed against the leaf, in alignment with the bottom gasket of the chamber. The leaf and spare gasket were then carefully removed as one unit and laid flat for photographing. The resulting image showed the display of leaves bound by the 2 3 3-cm gasket (which matched the chamber dimensions), and leaf area in the gasket area was determined to 0.05-cm^2 resolution using image-processing software (Scion, Frederick MD).

PLANT WATER STATUS

Plant water potential (Ψ_{plant}) was measured before dawn and between 1600 and 1700 hours using a Scholander-type pressure chamber (Plant Moisture Stress Instruments, Albany, OR) on several of the same days as plant gas exchange measurements. Five representative terminal shoots, ca. 4–8 cm long, were collected from the midcrown of different individuals of each species at each measurement period. Each sample was excised and immediately placed into the pressure chamber for measurement of Ψ_{plant} (MPa).

GREENHOUSE EXPERIMENT

Carbon assimilation and WUE were compared in *C. maculosa, P. spicata,* and *P. smithiiacross* three tightly controlled soil water regimes in the greenhouse during the summer of 2001, before the field observations. All species were grown from seed in a greenhouse with constant light and

temperature under three different soil water matric potentials: 1.0, 0.1, and 0.01 MPa (hereafter referred to as the dry, mesic, and wet levels, respectively). Seeds of each species were planted in 18 columns, each 0.1 m in diameter and 0.4 m tall, with six columns assigned to each of the three water treatments, for a total of 54 columns. These columns were randomly assigned to one of six blocks. Water treatments were maintained three times each week by adding enough water to attain target soil matric potentials that were previously determined from soil water retention curves of the columns (Or and Wraith 1999). Actual soil water potentials were somewhat less because of drying between water additions, though the tall, narrow column design minimized water loss. After 4 mo of growth during the summer under natural light, leaf-level gas exchange measurements were made for four consecutive days on three randomly chosen individuals of each species under each soil water treatment. Leaf-level gas exchange measurements were made to determine A_{net}, g_{st}, E, and WUE.

STATISTICS

The significance of differences in A_{net} and WUE throughout the study was determined with separate one-way ANOVAs using JMP software (SAS Institute, Cary, NC), with the years, sites, times of year, or species as factors. Gas exchange plant data were natural log–transformed when assumptions of normality were not met. A multifactor design was precluded because of differences in species composition among sites and the different phenology of the species. Least squares linear regression was used to determine the relationship between the natural logs of A_{net} and Ψ_{plant} of each species, and MANOVA was used to determine whether the slopes of A_{net} and Ψ_{plant} were significantly different among the species.

RESULTS

FIELD MICROCLIMATE

Mean growing season temperatures were 1°–2°C higher in 2003 than in 2002, and Helena was generally warmer than the Bozeman site in both summers (table 1). The maximum air temperature at 5 cm, the height of rosettes, was up to 7°C warmer at the drier Helena site than at the Bozeman site, as in 2003. Mean temperatures at 1 m of both sites were similar, 1° and 2°C higher than the long-term averages in 2002 and 2003, respectively. Maximum temperatures at 1 m were 2°–3°C higher in both summers, compared to long-term averages.

Table1. Average Daily Mean and Maximum Air Temperature (°C; ±1SE) at the Bozeman and Helena Field Sites during June, July, and August of 2002 and 2003.

	2002		2003		Long-term average	
Temperature, height	Bozeman	Helena	Bozeman	Helena	Bozeman	Helena
Mean:						
1 m	17.7 ±0.4	18.6 ± 0.4	18.6 ± 0.5	20.2 ± 0.5	17.4	18.5
5 cm	18.1 ± 0.4	19.7 ± 0.4	19.4 ±0.5	21.8 ± 0.5		
Maximum:						
1 m	27.9 ± 0.6	29.4 ± 0.6	29.1 ± 0.7	30.7 ± 0.6	26.1	26.6
5 cm	34.2 ± 0.6	37.4 ± 0.6	34.8 ± 0.7	42.0 ± 0.8		

Note. Temperatures were determined with shaded fine-wire thermocouples at 1 m (n= 2) and 5 cm (n= 4) above soil surface. Long-term (40–60-yr) averages were obtained from three climate monitoring stations closest to each site (from WRCC).

Mean annual precipitation since ca. 1950 was 452 ± 45 and 276 ± 13 mm yr1 at weather stations closest to the Bozeman and Helena sites, respectively, with long-term precipitation totals of 255 ±

20 and 181 ± 6 mm for the respective sites from May through September. During the May–September growing season, Bozeman received 362 and 161.5 mm and Helena received 263.4 and 120.4 mm precipitation in 2002 and 2003, respectively (WRCC). During 2002, both sites received almost double the long-term average precipitation for the month of June.

Soil water potential (Ψ_{soil}), determined from volumetric water content (VWC) in the top 30 cm of soil, decreased twofold from June to August at the Helena site, and more than threefold from June to August at the Bozeman site (fig. 1). The Ψ_{soil} was greater (by 32% initially) at the Bozeman compared to the Helena site earlier in the 2003 season and remained greater throughout August (fig. 1). Soil water potentials that are less than or equal to 1.5 MPa are generally considered to be difficult for plants to extract water from, although species can differ in this respect. Water was more readily available to plants when Ψ_{soil} was greater, particularly above ca. 1.5 MPa (fig. 2). At both sites, VWCs under *Centaurea* maculosa and the grasses were in the typical range of plant-available water at all of the measured depths during the early part of the season, but during later months of summer, only soils deeper than ca. 40–50 cm had Csoil greater than 1.5 MPa (fig. 2). Mean VWC in 60–120-cm soil depths decreased significantly more under *C. maculosa* (43%), compared to soils under grasses (27%), from June to August for both years, at the Bozeman site ($F_{1, 15}$ = 7:64, P = 0.015). At the Helena site, there was less statistical support for greater decreases in mean VWC of soils between 60 and 100 cm under *C. maculosa* (21%), compared to soils under grasses (9%), from June to August ($F_{1, 11}$ = 1:28, P = 0.28). No differences in VWC were evident in soils shallower than 40 cm under the different species.

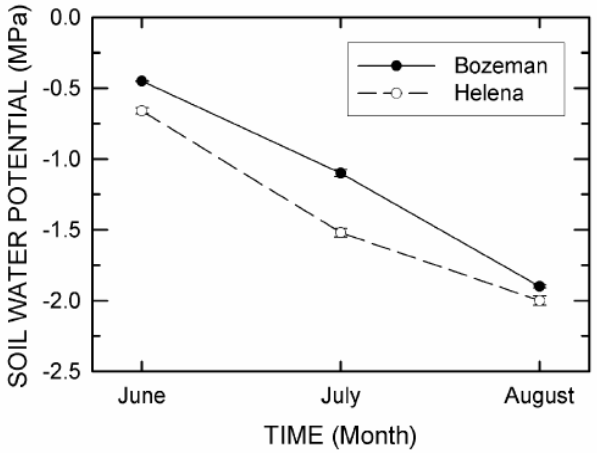

Figure 1. Monthly average (±1 SE; error bars are smaller than symbols) of soil water potential for the top 30 cm of soil under all vegetation types at Bozeman (filled circles) and Helena (open circles) field sites, as determined from soil water content measurements made with time domain reflectometry probes during the 2003 season (n = 24) and converted to MPa with soil water retention curves.

GAS EXCHANGE MEASUREMENTS

Leaf-level carbon assimilation (A_{net}) of all of the species was twofold greater in 2002 than in the drier summer of 2003 at both the Helena ($F_{1, 51}$ = 32:98, P< 0.0001) and Bozeman sites ($F_{1, 44}$ = 7:01, P= 0.012). Mean A_{net} of all species combined at Bozeman was 48% greater than at the Helena site in both years ($F_{1, 96}$ = 11.97, P= 0.0008). *Centaurea maculosa* had greater A_{net} than the co-occurring dominant rangeland grasses during both seasons at the Helena site ($F_{2, 51}$ = 3.60, P= 0.035) and the Bozeman site ($F_{1, 44}$ =19:0, P< 0:0001; fig. 3). In addition, A_{net} was measured later into the growth season for *C.maculosa* during the wetter 2002 season. Rosette leaves of *C.maculosa* senesced earlier (by mid-August) in 2003 than in 2002 at both sites (fig. 3). Mean E for both sites throughout both growth seasons was more than twofold greater for *C.maculosa*(5.4

± 1.3 mmol H_2O $m^{-2}s^{-1}$) than for any of the grasses (2.5 ±0.4 mmol H_2O $m^{-2}s^{-1}$; $F_{2, 95} = 6.32$, P= 0.03; fig. 3).

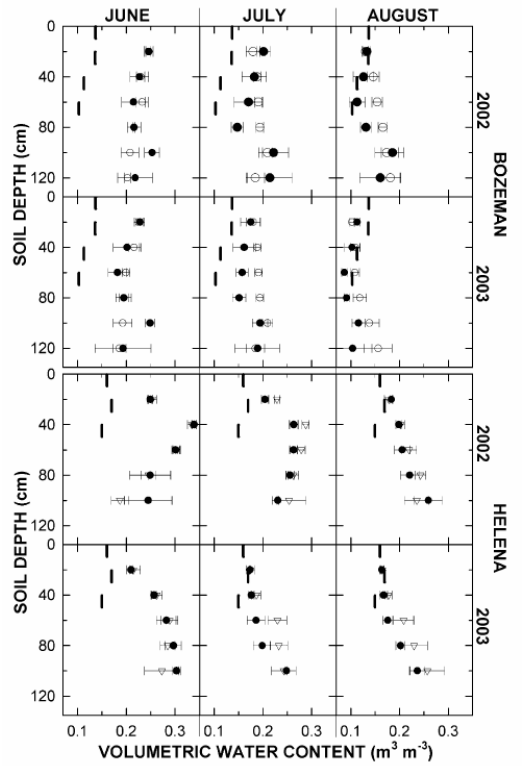

Figure 2. Mean volumetric soil water content (VWC; ±1 SE), as determined with neutron probe, at multiple depths under monospecific stands of *Centaurea maculosa* (filled circles) at both field sites, as well as *Bromus inermis* (open circles) at the Bozeman site and *Pseudoregneria spicata* (triangles) at the Helena site (*n*=4). Solid vertical bars show the VWC values for 10-cm soil depth intervals that correspond to the approximate soil water potential of _1.5 MPa (*n*=3 water retention curves). Soil water would typically be scarce for most plants at VWCs less than the VWC values shown by the bars.

WUE of *C. maculosa* was similar to that of the grasses during June and July 2002 at both sites but greater than that of the grasses for all 2003 sampling dates at Helena and during late summer of 2003 at Bozeman (fig. 3). WUE of *C. maculosa* was 102% greater than that of *Pseudoregneria spicata* ($F_{1, 19} = 29.63$, P< 0:0001) and 32% greater than that of *Bromus inermis* ($F_{1, 17} = 3.07$, P= 0.099) at the Helena site during 2003. At the Bozeman site during July 2003, WUE of *C. maculosa* was 75% greater than WUE of *B. inermis* ($F_{1, 9} = 5.97$, P= 0.040; fig. 3). WUE also varied considerably more among sampling dates in *C. maculosa* than in the grasses. WUE in C. maculosa in 2002 was 93%–252% greater in August than in July at the Bozeman ($F_{2, 14} = 6.80$, P= 0.011) and Helena ($F_{2, 13} = 38.80$, P< 0:0001) sites, respectively (fig. 3). WUE in *C. maculosa* was 82% greater in 2003 than in 2002 at Helena during June and July ($F_{1, 19} = 22.80$, P=0.0002). Seasonal variations in WUE for grasses were relatively smaller, and the greatest changes were decreases in WUE of 42% for *B. inermis* and 21% for *P. spicata* as soils dried during 2003 (fig. 3).

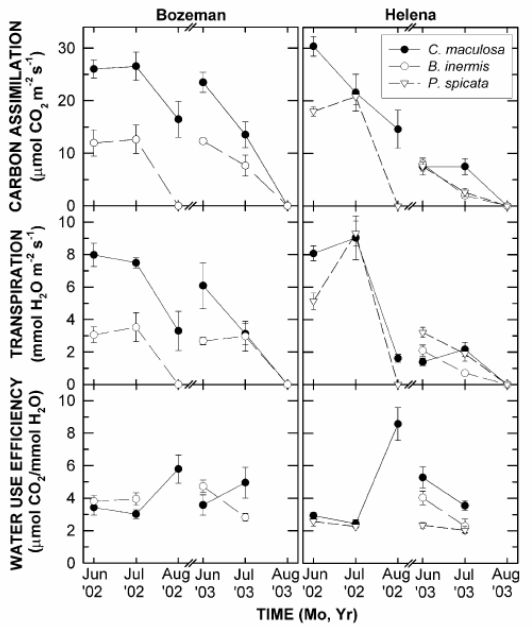

Figure 3. Daily maximum carbon assimilation rate, transpiration, and corresponding water use efficiency (A_{net}=E) of rosette leaves of *Centaurea maculosa* (filled circles), *Bromus inermis* (open circles), and *Pseudoregneria spicata* (triangles) in natural communities across 2002 and 2003 at two field sites in SW Montana (±1 SE); *n* = 5 plants.

PLANT WATER STATUS

Centaurea maculosa did not always have the greatest predawn Ψ_{plant}, but midday Ψ_{plant} measurements of C. maculosa were relatively higher and closer to predawn observations, compared to the other species ($F_{2, 14}$ = 8.46, P= 0.004; fig. 4). For example, at the Helena site in June 2003, mean Ψ_{plant} of *C. maculosa* decreased only 18% from predawn to midday measurements in June (-0.94 ± 0.09 to -1.12 ± 0.1 MPa) and only 19% in late July (-3.32 ± 0.27 to -3.95 ±0.17 MPa). At the Bozeman site during the same two months, Ψ_{plant} of *C. maculosa* decreased only 58% from predawn to midday in June (-0.58 ±0.02 to -0.92 ±0:.0 MPa) and decreased 194% in July (-0.78 ±0:08-2.28 ±0.09 MPa at midday). In comparison, Ψ_{plant} of *P.spicata* at the Helena site decreased 108%, from -1.69 ±0.9 MPa at predawn to -3.45 ±0.12 MPa at midday, in June and well over 100%, from -3.97 ±0.6 MPa at predawn to <-8 MPa at midday, in July (beyond the maximum scale of the pressure chamber). In 2003, diurnal decreases in Ψ_{plant} of *B.inermis* at the Bozeman site were 292% in June (-0.40 ±0.03 to -1.55 ±0:11 MPa) and 207% in July (-0.93 ±0:09 to -2.88 ±0:20 MPa). Over the course of the study, Ψ_{plant} of *C. maculosa* decreased an average 77% ±23% from predawn to midday, compared with decreases of 104% ±2% and 408% ±84% in *P. spicata* and *B. inermis*, respectively (fig. 4). Accordingly, throughout the study, *C.maculosa* also had midday water potentials that were 183% and 110% greater than those of *P. spicata* and *B .inermis*, respectively.

All three species exhibited a decrease in photosynthesis at lower Ψ_{plant} (fig. 5). A positive correlation was observed between ln A_{net} and Ψ_{plant} for *C. maculosa* (slope = 0.41 [μmol CO_2 m^{-2} s^{-1} Ψ^{-1}], $F_{1, 17}$ = 5.59, P= 0.030, r^2 = 0.25), *B. inermis* (slope = 0.24, $F_{1, 9}$ = 10:50, P= 0.010, r^2 = 0.54), and *P. spicata* (slope = 0.55, $F_{1, 4}$ = 16.16, P= 0.057, r^2 =0:89), and there was marginal statistical support for differences in slopes among the species (MANOVA: $F_{2, 32}$ = 2:98, P= 0.07). The most notable difference among species was greater photosynthesis in *C.maculosa* than in the grasses at water potentials above ca. -1 MPa..

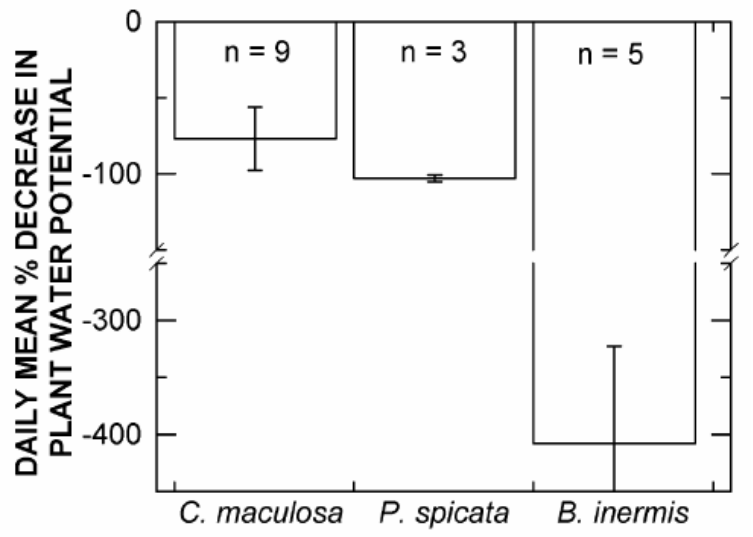

Figure 4. Mean percent change in plant water potential between predawn and midday measurements (±1 SE) at two field sites in southwestern Montana during the 2002 and 2003 growth seasons for *Centaurea maculosa, Pseudoregneria spicata,* and *Bromus inermis*. Number of replicates (daily means) is shown in each bar.

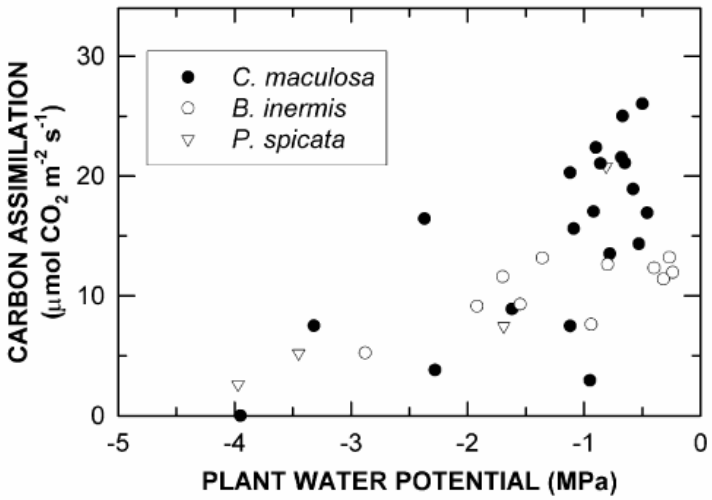

Figure 5. Relationship between photosynthesis and plant water potential for *Centaurea maculosa* (filled circles), *Bromus inermis* (open circles), and *Pseudoregneria spicata* (triangles) at two field sites in southwestern Montana during the 2002 and 2003 growth seasons.

GREEN HOUSE EXPERIMENT

Mean A_{net} in the greenhouse increased among all species with greater water availability ($F_{2, 99}$ = 17.08, P< 0.0001). Mean A_{net} was not greater at any water level in *C. maculosa*, and there was no statistical support for differences in A_{net} between any of the species ($F_{2, 99}$ = 1.96, P= 0.147; fig. 6). WUE decreased with increasing water levels for all of the species ($F_{2, 99}$ = 8.35, P= 0.0005; fig. 6), but no differences were observed between the species ($F_{2, 99}$ = 0.21, P= 0.810).

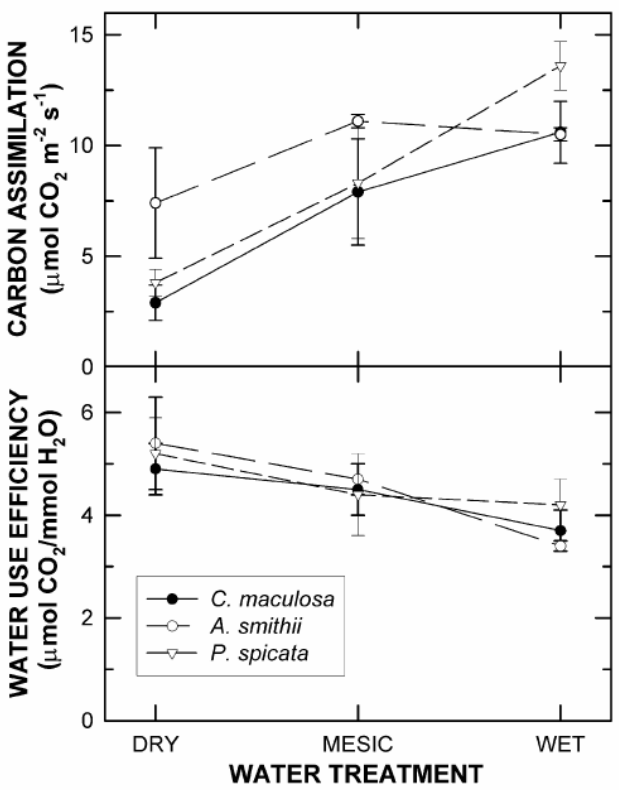

Figure 6. Mean carbon assimilation rate (±1 SE) and water use efficiency (Anet=E; 61 SE) of *Centaurea maculosa* (filled circles), *Pascopyron smithii* (open circles), and *Pseudoregneria spicata* (triangles) in a greenhouse under three target soil water matric potentials: dry (-1.0 MPa), mesic (-0.1 MPa), and wet (-0.01 MPa); *n*=4 daily means.

DISCUSSION

Centaurea maculosa had greater carbon assimilation (A_{net}) and Ψ_{plant} at midday than established grasses during two years that were considerably drier than average. Photosynthetic WUE was greater in *C. maculosa* than in grasses only under the most unusually dry conditions. Greater A_{net} of *C.maculosa*, combined with several-fold greater leaf area per individual and a longer season for carbon assimilation, likely led to much greater annual carbon assimilation for individuals of *C. maculosa* than for established grasses. Active photosynthetic tissue in the form of green stems and cauline leaves persisted later in the season than the rosette leaves of *C. maculosa* we measured (Hill and Germino, forthcoming). Our emphasis on rosette leaves therefore potentially underestimates the amount of carbon gain for *C. maculosa* relative to grasses during dry periods but does not alter our general findings of superior net carbon gain in *C. maculosa*. Therefore, greater yearly carbon assimilation could potentially contribute to greater growth and reproductive output in *C. maculosa* than in the perennial grasses.

RELATIONSHIPS OF WATER RELATIONS AND PHOTOSYNTHESIS AMONG SPECIES

Correspondence between greater A_{net} and higher Ψ_{plant} in *C. maculosa* compared to established grasses indicated that greater A_{net} was related to traits that enhance water relations in these water-limited communities. Photosynthetic advantages for *C. maculosa*, compared to the grasses, were most evident at high Ψ_{plant} (fig. 5). *Centaurea maculosa* also had lower diurnal variation in Ψ_{plant} than established species (fig. 4), despite greater transpiration per unit leaf area (fig. 3), especially per whole plant (based on relatively greater leaf area in *C. maculosa* compared to grasses; data not shown). Maintenance of higher Ψ_{plant} during days, despite greater transpiratory water efflux,

was most likely to result from greater supply of water from roots to foliage. The lack of differences in A_{net} and $A_{net} = \Psi_{soil}$ relationships among the species under greenhouse conditions (fig. 6), where *C. maculosa* was rooted in soil with VWC levels similar to those for the grasses, suggests that photosynthetic advantages in *C. maculosa* in the field depend on *C. maculosa* having greater water availability than neighboring grasses. The greater water supply to foliage for *C. maculosa* than for grasses could result from a number of factors, including greater access to soil water sources, a greater ability to extract water from dry soils, and water storage in *C. maculosa*.

Roots of mature *C. maculosa* and other forbs are commonly observed growing more than 1 m deep, which may allow access to more abundant, less variable water supplies below typical rooting zones of grasses, which are from less than 25 to 40 cm deep (Jackson et al. 1996; Swan 2004). Similarities in seasonal trends of VWC at 20–40-cm depths under *C. maculosa* and grasses, where we ascertained roots of both species, did not support (or rule out) a greater ability of *C. maculosa* to extract water from dry soils. However, greater depletion of water from soils deeper than 40–60 cm under *C. maculosa* than under the grasses but similar soil water depletion patterns between the species at 20–40-cm depths (fig. 2) indicated greater uptake of deeper water in *C. maculosa*. California rangelands dominated by *Centaurea solstitialis* also had lower soil water contents in deep soils than nearby rangelands that did not have *C. solstitialis* (Gerlach 2004).

Site differences in photosynthesis and water relations further point to the potential significance of deeper soil water uptake in *C. maculosa* than in grasses. Water availability appeared to be scarce in soils above the 80-cm depth at Bozeman and the 40-cm depth at Helena in August 2002, when photosynthesis persisted in *C. maculosa* but not in the grasses. By August 2003, as gas exchange decreased below detection limits in all species, water decreased to (or below) -1.5 MPa at all depths at Bozeman and down to the 60-cm depth at Helena. Our estimates of water potential in deep soils rely on the assumption that water retention characteristics measured for soils from 50–70-cm depths were also representative of deeper depths. Soils also had more clay at Helena than at Bozeman, which may reduce root penetration to deeper soils, in addition to possibly enhancing water availability, water relations, and photosynthesis at Bozeman (see Rosenthal et al. 2005 for a similar scenario in *Helianthus*).

Although *C. maculosa* does not have the ability to store large amounts of water like some succulent arid plants, its large taproot may act in a limited capacity to store water taken up overnight for use during dry days. Taproots are commonly perceived as organs specialized more for storage than for assimilation, but our crude calculations (data not shown) suggest that taproots with a typical volume of 30 cm^3 could provide a few hours of water required for late-season transpiration, at best. These estimates are based on total leaf area, whole-plant sunlight interception, transpiration, tissue water contents, and pressure-volume curves (fig. 3; P. Schwarz, K. Harbuck, and M. J. Germino, unpublished data).

Thus, the greater persistence of photosynthesis in *C. maculosa*, compared to grasses, in mid-late summer appeared to be dependent on the availability of water from depths greater than typical rooting zones of grasses but apparently within the rooting depth of *C. maculosa*. Annual herbs with a greater ability to persist through seasonal drought had relatively deeper roots and deeper soil water uptake than less persistent herbs in California grasslands (Gulmon et al. 1983). Reliance of *C. maculosa* on soil water deeper than that available to grasses could be verified directly using stable-isotope tracers of water source.

PHYSIOLOGICAL ADJUSTMENT TO WATER AVAILABILITY

Plant species that persist under low soil water availability often have adaptations for greater WUE than species from mesic environments (e.g., Anderson et al. 1997). *Centaurea maculosa* did not use water more efficiently than other species in the greenhouse or in the field under relatively wet or average conditions. Similarly, *C.maculosa* did not use water more efficiently than *Pseudoregneria spicata* and *Festuca idahoensis*, based on carbon isotope discrimination (Blicker et al. 2003). Carbon isotopes of plant biomass provide a time-integrative measure of WUE that is unable to detect fine-scale fluctuations that may include potentially critical events. Indeed, the few cases where WUE was greater in *C. maculosa* than in established flora happened under the driest conditions of the study period, such as the unusually warm and dry days in the drought of 2003 (fig. 3).

Flexible WUE could allow plants to exploit favorable conditions while maintaining growth during drier conditions (Williams et al. 1995; Silim et al. 2001). Greater flexibility of WUE probably contributed to effects of deep-water uptake in extending *C. maculosa's* growing season beyond that of grasses, whose primary strategy for avoiding drought is dormancy. Flexibility in WUE may enable high A_{net} when water is abundant while possibly conserving soil water as it becomes scarce and consequently increasing the duration of *C. maculosa's* seasonal carbon assimilation as soils dry. Water conservation may not be advantageous to a species when competitors consume the otherwise conserved soil water. However, *C. maculosa's* greater WUE corresponded in time to an apparent reliance on deep moisture (or water stored in taproots), which grasses presumably could not access. Moreover, grasses appeared to enter dormancy as WUE increased in *C. maculosa* (fig. 3).

CONCLUSIONS

Most research on *C. maculosa* has emphasized escape from natural enemies (e.g., herbivores or pathogens) or novel weapons, such as soil allelopathogens, as factors contributing to its ecological success (Ridenour and Callaway 2001; Bais et al. 2003). Whether interspecific differences in soil resource use also contribute to the vulnerability of steppe to exotic forbs is a key issue, because such differences could point to the availability of niches open to invasive species. Availability of soil resource niches, in turn, is likely affected by land uses or disturbances that alter relative abundances of species or functional groups (e.g., Seefeldt and McCoy 2003). While our results indicate that several interspecific differences in resource use likely contribute to the success of *C. maculosa*, previous research shows that *C. maculosa* is unlikely to benefit from relatively greater acquisition or efficient use of nitrogen (Olson and Blicker 2003) or alteration of soil physical properties (Sperber et al. 2003). The ability to sustain high transpiration without significant lowering of Ψ_{plant} and the ability to adjust WUE to variation in water availability are potentially key factors that enable *C. maculosa* to have relatively greater and more persistent A_{net} than neighboring grasses. Superior water status, despite high transpiration in *C. maculosa*, appears to result from greater access to consistently available water in deep soils, which appears to represent an available niche within the steppe we examined (fig.2). Use of deeper soil water also contributed to the success of invasive shrubs and forbs, compared to native grasses, in other semiarid rangelands (Harrington 1991; Yoder et al. 1998). These findings illustrate how invasions in semiarid lands are affected by site conditions resulting from community resource use as they compare with resource requirements of invasive compared to established species.

Sixty percent of the 46 exotic plants considered to be invasive problems on rangelands are deep-rooted forbs in the Asteraceae like *C. maculosa* (Taylor 1992; Pyke 1999), whose phenology, rapid growth patterns, growth form, and other traits seem to contrast with growth strategies of established grasses that dominate rangelands (Whitson 2000). The rapid growth and extended phenology into seasonally dry periods commonly observed in these other exotic forbs might

result from ecophysiological mechanisms similar to those reported here for *C. maculosa*. Our findings provide empirical support for theoretical predictions that fluctuations in resource availability can contribute to the success of exotic invaders in grasslands (Tilman 1997; Davis et al. 2000). Whereas relatively undisturbed communities in sagebrush steppe use soil water relatively completely (Anderson et al. 1987), many rangelands experience disturbances (e.g., fire) that temporarily exclude deep-rooted native species that reestablish slowly by seed and thereby lead to corresponding increases in deep soil water (Harniss and Murray 1973; Link et al. 1990; Sturges 1993). *Centaurea maculosa* and other exotic forbs are particularly problematic in disturbed areas such as burns and roadsides. On the basis of relatively high water demands required for photosynthetic advantages of *C. maculosa*, we speculate that increases in deep soil water may be a key way that disturbances that select against deep-rooted species encourage site persistence by *C. maculosa* and possibly other deep-rooted exotic forbs. Variation in ecophysiological traits between native and invasive species may lead to better generalizations on factors contributing to invasiveness or invasibility, if ecophysiological advantages can be related to specific changes in resource availability and resource utilization by the native community.

ACKNOWLEDGMENTS

This study was made possible by a grant from the National Aeronautics and Space Administration Goddard Space Flight Center. ISU would also like to acknowledge the Idaho Delegation for their assistance in obtaining this grant. Paul Schwartz and Kristin Harbuck provided assistance with data collection in the field during the summers of 2002 and 2003. Funding was provided through grants received from the USDA National Research Initiative and NASA.

LITERATURE CITED

Anderson JE, ML Shumar, NL Toft, RS Nowak 1987 Control of the soil water balance by sagebrush and three perennial grasses in a cold-desert environment. Arid Soil Res Rehabil 1:229–244.

Anderson JE, J Williams, PE Kriedman, MP Austin, GD Farquhar 1997 Correlations between carbon isotope discrimination and climate of native habitats for diverse eucalypt taxa growing in a common garden. Aust J Plant Physiol 23:311–320.

Bais HP, R Vepachedu, S Gilroy, R M Callaway, J M Vivanco 2003 Allelopathy and exotic plant invasion: from molecules and genes to species interactions. Science 301:1377–1380.

Baruch Z, G Goldstein 1999 Leaf construction cost, nutrient concentration, and net CO_2 assimilation of native and invasive species in Hawaii. Oecologia 121:183–192.

Blicker PS, BE Olson, JM Wraith 2003 Water use and water-use efficiency of the invasive Centaurea maculosa and three native grasses. Plant Soil 254:371–381.

Booth MS, MM Caldwell, JM Stark 2003 Overlapping resource use in three Great Basin species: implications for community invisibility and vegetation dynamics. J Ecol 91:36–48.

Davis MA, JP Grime, K Thompson 2000 Fluctuating resources in plant communities: a general theory of invasibility. J Ecol 88: 528–534.

Durand LZ, G Goldstein 2001 Photosynthesis, photoinhibition, and nitrogen use efficiency in native and invasive tree ferns in Hawaii. Oecologia 126:345–354.

Gerlach JD 2004 The impacts of serial land-use changes and biological invasions on soil water resources in California, USA. J Arid Environ 57:365–379.

Gulmon SL, NR Chiariello, HA Mooney, CC Chu 1983 Phenology and resource use in three co-occurring grassland annuals. Oecologia 58:33–42.

Harniss RO, RB Murray 1973 30 years of vegetal change following burning of sagebrush grass range. J Range Manag 26:322–325.

Harrington GN 1991 Effects of soil moisture on shrub seedling survival in a semi-arid grassland. Ecology 72:1138–1149.

Hill JP, MJ Germino Forthcoming Coordinated variation in ecophysiological properties among life stages and tissue types in an invasive perennial forb of semiarid rangelands. Can J Bot.

Jackson RB, J Canadell, JR Ehleringer, HA Mooney, OE Sala, ED Schulze 1996 A global analysis of root distributions for terrestrial biomes. Oecologia 108:389–411.

Link S, GW Gee, ME Thiede, PA Beedlow 1990 Response of a shrub-steppe ecosystem to fire: soil water and vegetational change. Arid Soil Res Rehabil 4:163–172.

Lonsdale WM 1999 Global patterns of plant invasions and the concept of invasibility. Ecology 80:1522–1536.

Myers CV, RC Anderson 2003 Seasonal variation in photosynthetic rates influences success of an invasive plant, garlic mustard (*Alliaria petiolata*). Am Midl Nat 150:231–245.

Nagel JM, KL Griffin 2004 Can gas-exchange characteristics help explain the invasive success of *Lythrum salicaria*? Biol Invasions 6:101–111.

Olson BE, PS Blicker 2003 Response of the invasive *Centaurea maculosa* and two native grasses to N-pulses. Plant Soil 254:457–467.

Or D, JM Wraith 1999 Handbook of soil science. CRC, Boca Raton, FL.

Pattison RR, G Goldstein, A Ares 1998 Growth, biomass allocation and photosynthesis of invasive and native Hawaiian rainforest species. Oecologia 117:449–459.

Pyke DA 1999 Invasive exotic plants in sagebrush ecosystems of the intermountain west. Pages 43–54 in PG Entwistle, AM DeBolt, JH Kaltenecker, K Steenhof, eds. Proceedings: sagebrush steppe ecosystems symposium. Publication BLM/ID/PT-001001+1150. Bureau of Land Management, Boise, ID.

Ridenour WM, RM Callaway 2001 The relative importance of allelopathy in interference: the effects of an invasive weed on a native bunchgrass. Oecologia 126:444–450.

Rosenthal D M, F Ludwig, LA Donovan 2005 Plant responses to an edaphic gradient across an active sand dune/desert boundary in the Great Basin desert. Int J Plant Sci 166:247–255.

Seefeldt SS, SD McCoy 2003 Measuring plant diversity in the tall threetip sagebrush steppe: influence of previous grazing management practices. Environ Manag 32:234–245.

Sheley RL, JS Jacobs, MF Carpinelli 1998 Distribution, biology, and management of diffuse knapweed (*Centaurea diffusa*) and spotted knapweed (*Centaurea maculosa*). Weed Technol 12:353–362.

Silim SN, RD Guy, TB Patterson, NJ Livingston 2001 Plasticity in water-use efficiency of *Picea sitchensis, P. glauca* and their natural hybrids. Oecologia 128:317–325.

Smith MD, AK Knapp 2001 Physiological and morphological traits of exotic, invasive exotic, and native plant species in tallgrass prairie. Int J Plant Sci 162:785–792.

Smith SD, RK Monson, JE Anderson 1997 Physiological ecology of North American desert plants. Springer, New York.

Sperber TD, JM Wraith, BE Olson 2003 Soil physical properties associated with the invasive spotted knapweed and native grasses are similar. Plant Soil 252:241–249.

Sturges DL 1993 Soil-water and vegetation dynamics through 20 years after big sagebrush control. J Range Manag 46:161–169.

Swan MB 2004 Soil water use and root system characteristics of *C. maculosa* and sympatric plants. MS thesis. Montana State University, Bozeman.

Taylor RJ 1992 Sagebrush country: a wildflower sanctuary. Mountaineers, Seattle.

Tilman D 1997 Community invasibility: recruitment limitation, and grassland biodiversity. Ecology 78:81–92.

von Caemmerer S, GD Farquhar 1981 Some relationships between the biochemistry of photosynthesis and the gas exchange of leaves. Planta 153:376–387.

Whitson TD 2000 Weeds of the West. 9th ed. Western Society of Weed Science, Newark, CA.

Williams DG, RA Black 1993 Phenotypic variation in contrasting temperature environments: growth and photosynthesis in *Pennisetum setaceum* from different altitudes on Hawaii. Funct Ecol 7: 623–633.

Williams DG, RM Mack, RA Black 1995 Ecophysiology of introduced *Pennisetum setaceum* on Hawaii: the role of phenotypic plasticity. Ecology 76:1569–1580.

Yoder CK, TW Boutton, TL Thurow, AJ Midwood 1998 Differences in soil water use by annual broomweed and grasses. J Range Manage 51:200–206.

Comparing GPS Receivers: A Field Study

Kindra Serr, ISU GIS Training and Research Center, Campus Box 8130, Pocatello, Idaho 83209-8130 (giscenter@isu.edu)

Thomas Windholz, ISU GIS Training and Research Center, Campus Box 8130, Pocatello, Idaho 83209-8130

Keith Weber, ISU GIS Training and Research Center, Campus Box 8130, Pocatello, Idaho 83209-8130 (webekeit@isu.edu)

ABSTRACT
This paper compares the precision and accuracy of five current global positioning system (GPS) receivers—Trimble ProXR, Trimble GeoXT without WAAS, Trimble GeoXT with WAAS, Trimble GeoExplorer II, and an HP/Pharos receiver. Each of these receivers, along with other similar units, are frequently used today for data collection and integration within a geographic information system (GIS). To compare receivers, we conducted a field study of 15 established survey markers in the City of Pocatello, Idaho. The points were observed on ten different dates with equivalent settings (e.g., averaging and acceptable point dilution of precision—PDOP). Overall, the results indicate that the GeoXT is well suited where sub-meter accuracy is required while the Pharos receiver is a viable alternative for applications with accuracy requirements of +/- 10m and more.

Keywords: GPS, co-registration, high resolution imagery

INTRODUCTION

The use of GPS receivers has become wide spread over recent years. Many applications, from hunting to surveying, benefit greatly from these devices. The level of accuracy required from application to application varies greatly. It is important to recognize the grades of GPS receivers, namely consumer, mapping and survey grade, and their ability to accurately map features with or without differential correction. The accuracies of these receivers range from centimeter to several meters, making it necessary to evaluate how accuracy and precision can affect individual applications.

When using a GPS receiver to collect field data, accuracy can be very important, especially when collecting data for use with high-spatial resolution imagery. Quickbird multispectral imagery, for example, achieves a resolution of 2.4 meters per pixel. In order to co-register corresponding ground sample locations within the correct pixel(s), an accurate GPS receiver is required. To ensure that each field observation is co-registered with the correct pixel, a GPS receiver must achieve an accuracy <50% of the pixel size (e.g., +/-1.2m @ 95% CI where Quickbird imagery will be used). The increased availability of less expensive, consumer grade GPS receivers, such at the HP/Pharos receiver used in this study, that are compatible with common GPS software, such as ESRI's ArcPad or Trimble's TerraSync, has raised concern about data quality. Many such receivers collect data that cannot be differentially corrected, increasing the margin of positional errors in the data collected. Consumer grade receivers are also unable to control the quality of PDOP during data collection, further increasing positional error. To assess the validity of these concerns, a field study was designed to calculate and compare the accuracy and precision of several GPS receivers. The goal of this study was to identify the receivers most appropriate for various research, remote sensing, and GIS applications.

Similar studies have been conducted where GPS receiver accuracy has been investigated. Some studies compared receivers under various collection protocols. Studies conducted in Ridley State Park in Pennsylvania (McCullough 2002) and the Clackamas Test Network in Oregon (Chamberlain 2002) tested the capability of the Trimble GeoXT receiver in forested and clear areas with similar procedures and yielding comparable results in each study. Using internal and external receivers (antenna located within the receiver – internal, antenna attached externally to receiver – external), the studies experimented with WAAS and post-process differential correction techniques, but used higher PDOP masks (e.g., PDOP mask= 7.0) than used in this study (PDOP mask=5.0). Published studies comparing various GPS receivers are limited. One completed in the summer of 2000, compared the accuracy of five different GPS receivers under forest canopy cover with Selective Availability (SA) off (Karsky et.al. 2000). In this study, WAAS was not used because it was not yet available. Differential correction was performed on files that could be corrected and positions were taken at known points in forested areas with 1, 60, and 120 positions averaged for each point. None of the above studies mentions how often points were collected over time or how many times points were collected. Each study concluded the receiver tested was appropriate for their research purposes, whatever those may have been. Overall, previous studies have taken into account some of the aspects related to GPS receiver accuracy, but a comprehensive analysis was not completed.

A study done in McDonald Forest, located in western Oregon, investigated the accuracy and reliability of consumer-grade GPS receivers under differing canopy conditions. Six different GPS receivers were evaluated for accuracy under three different canopies: open sky, young forest, and closed canopy. Although the collected data was unable to be differentially corrected, points were averaged and compared relative to the known location, allowing for the receivers' accuracies to be compared to one another (Wing et. al. 2005). This evaluation did not include real-time correction, nor was it conducted over an extended period of time.

In this paper we describe a field study comparing different GPS receivers to determine optimum applicability for various uses.

METHODS

The study area was located in the City of Pocatello and environs (Figure 1). Fifteen points were selected from known locations in Pocatello, Idaho. These points were obtained from the City of Pocatello's ground control database. Each was referenced in the field with permanent survey markers so the exact location could be re-located easily. Each point was visited ten times over a period of one month at approximately the same time each day (+/- 1 hr.). The points were selected for their accessibility and visibility to GPS satellite signals (avoiding vegetation or building interference). These criteria were followed to provide uniformity and the best operating condition for each GPS receiver, thereby verifying the precision and accuracy reported by the manufacturer and eliminating as much environmental influence as is possible in a field-based study. Data collection occurred on days where PDOP was within acceptable limits ($\leq$5.0). This was determined using Trimble's QuickPlan software.

The location for each point was observed with the following GPS receivers:

1. Trimble GeoXT receiver with WAAS
2. Trimble GeoXT receiver without WAAS
3. Trimble GeoExplorer II
4. Trimble ProXR
5. HP iPaq with Pharos Navigation software and antenna

Points were collected in latitude/longitude (WGS84), the native reference system for GPS receivers. This was done to avoid any transformation errors that may occur during projection. Receivers did not collect data when the PDOP was >5.0 to reduce this type of error. Receivers averaged 120 positions per point each time a site was visited. The weather conditions on most collection dates were comparable and skies were relatively cloud free in all cases.

After collection, each point file was differentially corrected using files from Idaho State University (ISU) GIS Training and Research Center's (GIS TReC) GPS Community Base Station, with the exception of the those points collected with the HP/Pharos receiver (the Pharos receiver does not collect the necessary information for differential correction through a base station). The base station was located on the ISU campus in Pocatello. The location of each point ranged from 1.5km to 12.6km away from the base station. Seven of the fifteen original points were then revisited and their location collected using a Leica survey-grade GPS receiver (+/-0.1m @ 95% CI); corrected in real-time using the ISU College of Technology's GPS CORS station (NGS 2005), also located on the ISU campus. These seven locations were used to assess the accuracy of the GPS receivers; where as all 15 locations were used to assess precision.

In this study precision refers to the repeatability of a specific GPS receiver collecting locational estimates. The error value (i.e., precision) was based on a relative comparison among measurements (Equation 1 and 2) of the same unit on different days. Accuracy, however, is not a relative comparison, but an absolute comparison. In this case the error value (i.e., accuracy) was calculated (Equation 3) by comparing measurements of a single unit on different days to the known true location of the observed point. These points were collected independently (i.e., different observer, different base station, and well established GPS receiver accuracy) and corrected using the nearby (<12 km) CORS station in real-time. Thus, 150 samples were collected to calculate precision (15 points visited 10 times each) and 70 samples were collected to calculate accuracy (seven points visited 10 times each).

$$1.96 \cdot \sqrt{\frac{\sum_{i=1}^{n}\left(x_i - \bar{x}\right)^2}{n-1}} \quad \text{and} \quad 1.96 \cdot \sqrt{\frac{\sum_{i=1}^{n}\left(y_i - \bar{y}\right)^2}{n-1}} \qquad \textbf{Equation 1}$$

Accepted true location based on the mean of observations per sampling site.

$$1.96 \cdot \sqrt{\frac{\sum_{i=1}^{n}\left(x_i - \mu_x\right)^2}{n}} \quad \text{and} \quad 1.96 \cdot \sqrt{\frac{\sum_{i=1}^{n}\left(y_i - \mu_y\right)^2}{n}} \qquad \textbf{Equation 2}$$

Precision of observations at 95% confidence.

$$\bar{x} = \frac{\sum_{i=1}^{n} x_i}{n} \quad \text{and} \quad \bar{y} = \frac{\sum_{i=1}^{n} y_i}{n} \qquad \textbf{Equation 3}$$

While the accepted "true" location was based on independent, survey-grade GPS observations of control points, accuracy of tested GPS receivers was calculated as given above at 95% confidence

Spatial analysis of these points was conducted within the native WGS84 geographic reference system. Conversion from decimal degrees (WGS84) to meters was performed using ESRI's ArcGIS software. Resulting units are reported in meters.

RESULTS

The results of precision and accuracy calculations for the tested GPS receivers are given in Table 1.

There is a slight difference in the magnitude of errors between x and y coordinates. Sum of squares was used to assess positional accuracy (i.e., $\sqrt{\sum x^2, y^2}$). To assess the utility of each receiver for various applications we used sum of squares.

Extreme values of individual point observations (100% CI) varied between individual receivers (Table 2). The largest error observed was recorded with the HP/Pharos unit (8.41m).

Table 1- Results of GPS receiver precision and accuracy (in meters) at 95% confidence

	Precision		Precision Sum of Squares	Accuracy		Accuracy Sum of Squares
	x	y		x	y	
ProXR	**0.38**	**0.46**	**0.59**	**0.46**	**0.78**	**0.91**
GeoXT	**0.43**	**0.59**	**0.73**	**0.53**	**0.77**	**0.93**
GeoXT with WAAS	**0.36**	**0.66**	**0.75**	**0.43**	**0.96**	**1.05**
GeoExp II	**1.96**	**2.90**	**3.50**	**2.02**	**3.25**	**3.83**
Pharos	**1.68**	**2.32**	**2.86**	**3.73**	**4.21**	**5.62**

Table 2-- Proportion of extreme positional outliers (>0.5 and >1.0m thresholds) by receiver.

	Limit	Counts	Limit	Counts
ProXR	**>0.5**	**14%**	**>1**	**0%**
GeoXT	**>0.5**	**16%**	**>1**	**1%**
GeoXT with WAAS	**>0.5**	**20%**	**>1**	**3%**
GeoExp II	**>0.5**	**68%**	**>1**	**37%**
Pharos	**>0.5**	**78%**	**>1**	**67%**

DISCUSSION

The calculated accuracies were all within manufacturer specified ranges. Table 3 lists manufacturer stated accuracies with accuracies reported in the results of this paper. Also given is the cost of each receiver provided by the manufacturer. Selecting a GPS receiver that has acceptable accuracy and a reasonable price is important. Generally, increased accuracy comes at higher expense as was demonstrated by this study. While purchasing a low cost receiver, such as the Pharos iGPS 360, may create less expense for an organization but accuracy is compromised. The best accuracy was achieved using the Trimble ProXR (+/- 0.5m @ 95% CI), but this accuracy comes with increased expense. Based upon this information, we conclude that accuracy and cost are directly linked. Higher accuracy results in higher receiver costs.

Table 3-- Correlation between manufacturers stated accuracy, measured accuracy, and cost of receiver.

	Stated Accuracy (m)	Calculated Accuracy (m)	Cost
ProXR (Trimble 2005a)	**0.5**	**± 0.91**	**$8,490 (w/data logger)**
GeoXT (Trimble 2005b)	**<1.0**	**± 0.93**	**$4,295**
GeoExplorer II (Trimble 2005c)	**2.0-5.0**	**± 3.83**	**$3,995**
Pharos iGPS 360 (Pharos 2005)	**<10.0**	**± 5.60**	**$300**

In Table 1, we reported diminished accuracy when the wide area augmentation system (WAAS) was activated on the Trimble GeoXT receiver. We speculate that the cause for this performance decline was the lack of station coverage within our study area. WAAS uses approximately 25 ground reference stations that collect correction data for effects of the atmosphere, clock errors, and slight satellite orbit errors (ephemeris) (Figure 2). The closest ground station to our study area was the Elko, Nevada station, which is approximately 360 kilometers away (Figure 1). However, the Elko station was off-line at the time of this study, making the Great Falls, Montana station the closest active reference station (523 kilometers away). We assumed that the correction factor applied for the column of atmosphere near Great Falls departed from conditions in and around the study area therefore making the WAAS correction less reliable for our application. This was not anticipated nor is it expected for all applications.

In general, outliers, or extreme values were within vendor specified ranges. The Pharos receiver had the greatest extreme values. Thus, where accuracy and precision are concerned, the more expensive receivers outperformed less expensive receivers. It should be noted that Pharos GPS receivers cannot mask for PDOP and do not collect files suitable for differential correction. As indicated in Table 1 the lack of the ability to differentially correct the data is reflected in the relatively large decrease in accuracy compared to its precision. The results reported for the Pharos receiver were effectively best-case scenarios, inferring that accuracy and reliability will quickly deteriorate under more realistic conditions (i.e., poor PDOP, obstruction, etc.)

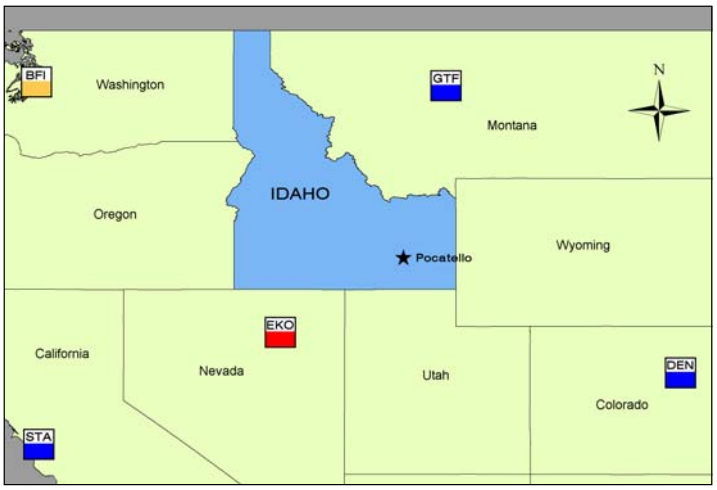

Figure 1- The location of the Pocatello study area and WAAS stations.

The achieved accuracy and precision may be attributed –at least in part-- to pre-collection planning. To better ensure field conditions would satisfy the PDOP mask, Trimble's QuickPlan software was used to determine the optimum collection window. This procedure virtually guaranteed that the Pharos receiver, as well as the other receivers tested, would also collect data under ideal conditions. The use of receivers with the ability to implement a PDOP mask allowed us to monitor PDOP, thereby assuring the Pharos receiver was collecting data within the same specified PDOP parameters. A more realistic scenario, however, often requires the user to collect data completely independent of other receivers and planning software/tools. For example, if the only available receiver was a Pharos, PDOP could not be observed or masked, which would lead to reduced accuracy. For these reasons, the Pharos receiver cannot be recommended for any tasks requiring <10m accuracy, yet it is definitely a viable alternative for other applications, such as data collection for lower resolution imagery (i.e., Landsat).

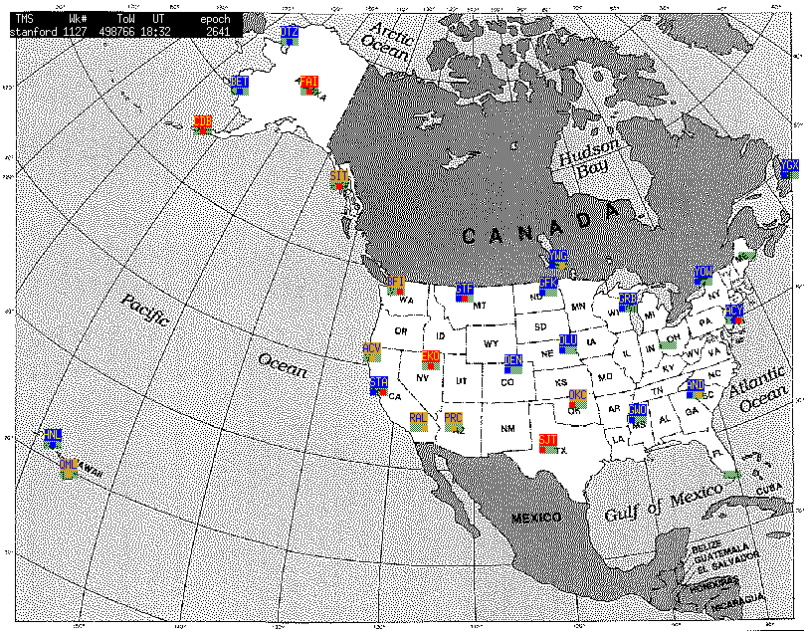

Figure 2- The location of WAAS stations across the United States. Blue indicates active, gold indicates passive, and red indicates communication failure.

A limitation of this study was that accuracy calculations were not based on continuously observed data, but rather on field sampling and revisiting a site over a period of time (i.e., one month). This study does, however, offer a comparison between various GPS receivers under similar research conditions.

Reliable accuracy and precision of GPS receivers has become increasingly important concomitant with advances in high spatial resolution imagery. GPS receivers with accuracies of 2 to 5 meters, such as the Trimble GeoExplorer II, are unable to collect data that will reliably co-register within the correct 2.4 meter pixel of Quickbird imagery (Table 3) or other similar imagery. Depending on these types of project-dependent considerations it may be necessary to use a GPS receiver capable of achieving superior accuracy and precision. The Trimble GeoXT tested in this study is a viable receiver for applications requiring high accuracy. Although the Trimble ProXR achieved better results, the GeoXT offers a user friendly interface and compatibility with common GPS software, such as ESRI's ArcPad or Trimble TerraSync, effectively lowering the total cost of ownership by decreasing the time it would take to learn to use the receiver.

Table 4—Suitability of various GPS receivers for use with remote sensing imagery and GIS mapping products.

	Precision	Accuracy	Applicable image resolution	Effective Map Scale
Trimble ProXR	**±0.59**	**±0.91**	**>1.8m**	**1:1,075**
Trimble GeoXT	**±0.73**	**±0.93**	**>1.9m**	**1:1,100**
Trimble GeoExplorer II	**±3.50**	**±3.83**	**>7.7m**	**1:4,524**
Pharos	**±2.86**	**±5.62**	**>11.2m**	**1:6,639**

CONCLUSIONS

This study assessed four GPS receivers and determined both precision and accuracy at 95% confidence. While selection of the optimal GPS receiver is a project-dependent consideration, the data we present are important for GIS managers to help them 1) understand the differences in horizontal positional accuracy obtained from various GPS receiver types, 2) ensure co-registration of GPS-acquired features and satellite or aerial imagery, and 3) determine the appropriate GPS receiver to use to satisfy mapping scale requirements.

LITERAURE CITED

Chamberlain, K., 2002, Performance Testing of the Trimble GeoXT Global Positioning System Receiver, *Draft Report – Global Positioning System*, United States Department of Agriculture – Forest Service, October 2002, http://www.fs.fed.us/database/gps/mtdc/geo_xt/trimble_geoxt.pdf.

Karsky, D., K. Chamberlain, S. Mancebo, D. Patterson, and T. Jasumback, 2000, Comparison of GPS Receivers under a Forest Canopy with Selective Availability Off, *Project Report - Technology and Development Program*, United States Department of Agriculture – Forest Service, December 2000, http://www.fs.fed.us/database/gps/mtdc/gps2000/gps_comparison.htm.

McCullough, M., 2002, Performance Testing of the Trimble GeoXT Global Positioning System Receiver, *Draft Report – Global Positioning System*, United States Department of Agriculture – Forest Service, November 2002, http://www.fs.fed.us/database/gps/mtdc/geo_xt/ridley_ck_geoxt_rich_mccollough.pdf.

NGS, 2005, National Geodetic Survey Continuously Operating Reference Stations (CORS), http://www.ngs.noaa.gov/cgi-cors/corsage.prl?site=idpo.

Pharos, 2005, Pharos Science and Applications—Bluetooth Navigation, http://www.pharosgps.com/products/bluetooth/PT200.htm.

Trimble, 2005a, GPS Pathfinder Pro XR, http://trl.trimble.com/docushare/dsweb/Get/Document-128930/.

Trimble, 2005b, Datasheet—GeoXT Handheld, http://trl.trimble.com/docushare/dsweb/Get/Document-128927/.

Trimble, 2005c, Trimble GeoExplorer II Specifications, http://trl.trimble.com/docushare/dsweb/Get/Document-10404/geo2_specs.pdf.

Wing, M.G., A. Eklund, and L.D. Kellogg, 2005, Consumer Grade Global Positioning System (GPS) Accuracy and Reliability, *Journal of Forestry*, 103(4), 169-173.

.

A Comparison Between Multi-Spectral and Hyperspectral Platforms for Early Detection of Leafy Spurge in Southeastern Idaho

Weber, K. T., GIS Director, Idaho State University, GIS Training and Research Center, Pocatello, Idaho 83209 (webekeit@isu.edu)

Glenn, N. F., Research Assistant Professor, Department. of Geosciences, Boise, Idaho 83702 (glennanc@isu.edu)

Mundt, J. T., Research Associate, Idaho State University, Department of Geosciences, Boise, Idaho 83702 (mundjaco@isu.edu)

Gokhale, B., GIS/RS Technician, Idaho State University GIS Training and Research Center, Pocatello, Idaho 83209 (gokhbhus@isu.edu)

ABSTRACT
Knowledge of the distribution of invasive plants and early detection of these species is critical for both short and long-term management of ecological systems. This study compared the quality of products derived from various multi-spectral (Landsat 7, SPOT, and Quickbird) and hyperspectral (HyMap) imaging platforms for early detection of the invasive plant leafy spurge. For each platform, the study compared: 1) detection accuracy, 2) ease of processing, and 3) cost effectiveness. We found that both SPOT multispectral and HyMap hyperspectral data were able to yield reliable detection accuracies (≥70%) with reasonable processing demands. SPOT imagery yielded results which were most cost-effective; however, HyMap data allowed researchers to reliably detect smaller infestations.

Keywords: invasive weeds, *Euphorbia esula*, remote sensing, GIS

INTRODUCTION

Rangelands are a diverse land type covering large amounts of the earth's surface. They support wildlife and vegetation and are used to graze domesticated livestock for the production of meat, wool, and other goods. Recent concerns have centered over the condition of rangelands and their appropriate use. Overgrazing, drought, and weeds have all been cited as causes of rangeland degradation (Du Toit and Cumming 1999). Regardless of cause, few will argue that the condition of rangelands worldwide has declined in the past 50 years, and invasive weeds such as leafy spurge are a common symptom of degraded rangeland condition.

Much previous work has considered the issue of rangeland condition. In 1994, the National Research Council defined rangeland health as "the degree to which the integrity of the soil and the ecological processes of rangeland ecosystems are sustained". In 2002, Pyke *et al.* stated that rangeland health could be determined "by evaluating an ecological site's potential to conserve soil resources and by a series of indicators for ecosystem processes and site stability." In both of these definitions, soil resources play a prominent role in the definition of rangeland health. Additionally, effective hydrologic function is considered an important indicator of healthy rangelands (Pellant *et al.* 2003, Pyke *et al.* 2002); however, it is frequently treated independent of soil stability. In reality, vegetation, the soil upon which it grows, and the water cycling through the system are all intimately linked to rangeland health.

When rangelands are impacted so that one of the elements (soil, vegetative cover, water cycling) is disturbed, the other elements are affected as well. For instance, if 50% of vegetation cover is removed, soil exposure increases. This decreases the potential for water infiltration and increases the potential for erosion (Holecheck *et al.* 2001). As a result, soil water and aquifer recharge is reduced (Thurow and Hester 1997, Kemble and Carroll 2005). Furthermore, the exposed ground is vulnerable to invasive plants, which are frequently highly competitive annuals with little value in rangelands ecosystems.

Invasive plants can be used as an indicator of disturbance and declining rangeland condition (O'Brien et al. 2003). Knowledge of the distribution of invasive plants is important to land stewards who are responsible for developing strategies to remedy the declining condition. In the state of Idaho, invasive plants impact the ecosystem and cost approximately $10 million per year for control treatments alone (Northwest Natural Resource Group, 2003). Because much of Idaho (~70 %) is comprised of large tracts of public land, weeds can invade and quickly spread without detection. For these reasons, the use of remotely sensed imagery to detect and monitor invasive species for proactive management of rangelands is ideal (Lass et al 2005).

This paper compares and contrasts two remote sensing-based invasive plant detection studies focusing on leafy spurge (*Euphorbia esula* L.). The first study used multispectral imagery for leafy spurge detection in the Oxford Resource Area, Idaho and the second study used hyperspectral imagery for leafy spurge detection in the Swan Valley, Idaho. Both study sites are located in southeastern Idaho (Fig. 1) and funded by NASA grants. We used the following evaluation metrics, which were determined through discussions with land managers intending to integrate remote sensing into operational land management practices, to compare the products of both studies:

1) Detection accuracy: The imagery must yield classification user accuracy >70% to be considered reliable for implementation by land managers.
2) Ease of processing: The ability to process the imagery in a timely and repeatable fashion.
3) Cost-effectiveness: Cost of the imagery per square km and considerations for the cost of processing.

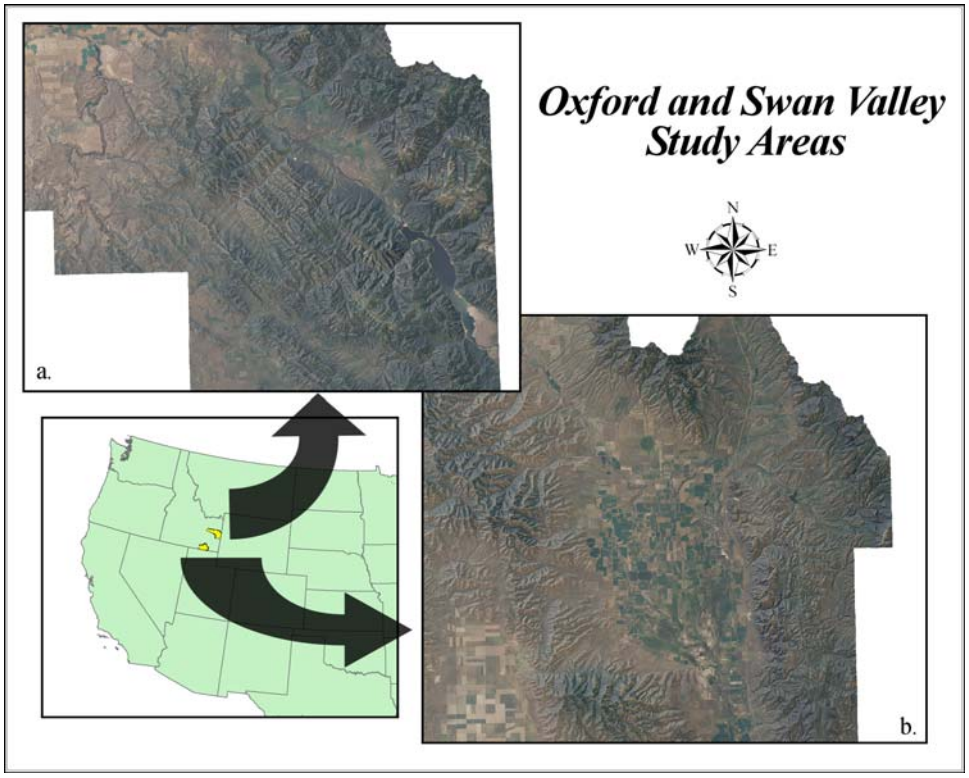

Figure 1. Location of Swan Valley (a) and Oxford Study Areas (b).

METHODS

We evaluated and compared multispectral and hyperspectral imagery for early detection of invasive plants using two discrete projects as case studies. The goal of the first project was to model small and patchy leafy spurge infestations in the Oxford resource area (USDA Forest Service) in southeastern Idaho using multispectral imagery (*i.e.*, Landsat 7, SPOT 5, and Quickbird). The goal of the second project was to model similar leafy spurge infestations using hyperspectral imagery (*i.e.*, HyVista's HyMap, Cocks et al., 1998) in remote areas of Swan Valley in southeastern Idaho to enable land managers to be proactive in weed treatments. In both studies, imagery and field samples were acquired during the summers of 2002 and 2003. Multispectral imagery were processed using Idrisi (Eastman 2003), whereas the hyperspectral imagery were processed using Environment for Visualizing Images (ENVI) version 4.0 software (Research Systems, Boulder, CO).

CASE STUDY 1: MULTISPECTRAL IMAGERY FOR THE OXFORD RESOURCE AREA

Study area

A model predicting the presence of leafy spurge was developed for the Oxford Resource Area in southeastern Idaho (Fig. 1), approximately 90 km southeast of Pocatello, Idaho (42° 5' 33" North, 112° 9' 44" West). These lands are managed by the USDA Forest Service as part of the Caribou-Targhee National Forest. This mountainous area has a mean elevation of 1800 m with peaks rising to 2294 m and is typified by Big Sagebrush (*Artemisia tridentata*), Balsamroot (*Balsamorhiza sagittata* (Pursh) Nutt.), Douglas-fir (*Pseudotsuga menziesii* (Mirbel) Franco), Mountain mahogany (*Cercocarpus spp.*), choke cherry (*Prunus virginiana* L.), and service berry (*Amelanchier alnifolia* (Nutt.). In this area, numerous leafy spurge infestations were relatively small (<100 m^2) but with 76-95% canopy cover.

Imagery Collected

Three Landsat 7 scenes were collected on 26-June-2002, 12-July-2002, and 28-July-2002, one SPOT scene (10 m) was collected on 12-July-2002, and two Quickbird scenes were collected on 8-August-2002 and 23-June-2003. All images used in this study were acquired during leafy spurge bloom in June 2002 and 2003 (save for the 2002 Quickbird imagery) with pre-processed georectification. Six of the seven Landsat 7 (28.5 meters per pixel (mpp)) bands were used in this study (band 6 was not used). Similarly, SPOT 5 (10 mpp) and Quickbird (2.4 mpp) imagery were acquired for the area, and subsequent processing utilized all multispectral bands. Prior to classification, we tested the image georectification and corrected as necessary using first order polynomial transformation. In all cases, imagery was co-registered with field global positioning system (GPS)-derived control points (18 locations with an accuracy of +/- 0.96 m (95% CI)) and verified using geographic information systems (GIS) datasets (*i.e.* 1:24,000 scale roads). From this, we calculated a root mean square (RMS) error of < 4 pixels in all cases (RMS = 94.80 m for Landsat imagery (approximately 3 pixels), RMS = 2.62 m for SPOT imagery (sub-pixel), and RMS = 4.78 m (approximately 2 pixels) for Quickbird imagery). These errors have the potential to affect classification accuracy, especially when modeling a patchy target. If the target training site is not properly co-registered, then extracted spectral signatures will represent non-target responses and thereby yield poor classification accuracy.

Field Sampling Methods

Initial field data (n = 47) were collected early in the summer of 2003 using a map of known leafy spurge infestations provided by the USFS. Thirty-nine sites were considered leafy spurge training sites with mean percent cover between 51-75% (note: while some sites had greater percent cover of leafy spurge, there were not enough sites to located to support a classification). In addition to these initial sites, an additional 151 training sites were collected in June 2003. Forty-one of these sites were considered leafy spurge training sites while the remainder (n= 110) were considered non-target training sites. The approach of this study was to: 1) iteratively collect field locations of leafy spurge target and non-target sites, 2) perform classification and validation, and 3) add new validation sites ($n \geq 100$ annually) into the training site dataset to increase sample size and better account for the variability within the spectral signature of leafy spurge. This was repeated over the 2003 and 2004 field seasons resulting in a dataset containing 320 sites (103 leafy spurge sites and 217 non-target training sites). At each site, a point location was recorded and attributed with percent cover (using the following cover classes: 0%, 1-5%, 6-15%, 16-25%, 26-35%, 36-50%, 51-75%, 76-95%, and >95%) of leafy spurge, bare ground, shrub, litter, and grass. Points were used because of the small size of many infestation sites. Validated leafy spurge infestations in the study area had an average percent cover class of 36-50% and median cover class of 51-75%. Each training site's cover assessment described land cover for a $100m^2$ area. The location of each training site was acquired using a Trimble GeoXT GPS receiver with WAAS reception turned on. All training sites were occupied for approximately 2 minutes, or until a minimum of 120 positions were acquired by the receiver. All points were post-process differentially corrected using the Idaho State University GIS Training and Research Center Community Base Station located approximately 90 km from the study area. Horizontal positional accuracy of points collected following this protocol was determined to be +/-0.96 m (95% CI). This accuracy statement was determined using repeated control point measurements (Serr et al 2005).

Image Processing Methods

All field training site data were entered into Idrisi (Eastman 2003) where spectral signatures were extracted for leafy spurge and non-target sites. The data used for signature extraction and classification included a stack of normalized difference vegetation index (NDVI), soil adjusted vegetation index (SAVI), and several principal component loaded images (PCA). The PCA

images used captured approximately 95% of the total variation within the original imagery bands (*i.e.*, bands 1-4 for Quickbird and SPOT imagery and bands 1-5 and 7 for Landsat imagery).

The extracted signatures were then purified using a threshold of 0.5 (McKay and Campbell 1982). Purification is a process whereby statistical outliers are identified and removed from the training site dataset. Because the multispectral platforms used in this study had different pixel sizes, the number of training sites used for classification also varied. Classification was performed using purified spectral signatures with Landsat imagery (n=69), SPOT imagery (n=85), and Quickbird imagery (n=111). Following purification, all images were classified using maximum likelihood supervised classifications, although minimum-distance to means, and various soft-classifiers were tested but failed to achieve better accuracy (Settle and Drake 1993, Sohn and McCoy 1997). Classification improvements were determined by examining overall, producer's and user accuracy estimates and by examining resulting Kappa statistics. Maximum likelihood has been used effectively by other researchers to classify leafy spurge (Casady et al 2005).

Validation Methods

Once the first modeling iteration was completed (using 47 leafy spurge training sites), researchers field validated the model using 151 independent validation sites (both leafy spurge and non-leafy spurge). The training and validation sites were then combined (n = 198) and used to produce a refined leafy spurge model during the fall/winter of 2003. The second iteration model was then field validated using 122 randomly located sites (within predicted leafy spurge and non-leafy spurge areas) in the summer of 2004. A final model was developed using all 320 sites for classification and validation. While this technique is sometimes considered invalid as it could introduce a bias of artificially inflated accuracies, this is true only when sample size is small. In our case, where the training site sample size was large, we detected no qualitative difference between model accuracies derived in this fashion versus the more traditional (but more time consuming) boot-strap technique (Efron 1979). Spectral signatures for the training sites were then purified and used to produce the final model which was validated using a standard error matrix and Kappa statistic (Titus et al 1984).

Classification Results

Using Landsat imagery, the results of accuracy assessments for leafy spurge presence indicate 82% overall accuracy, 93% producer's accuracy, and 52% user accuracy. In comparison, SPOT imagery produced 95%, 100%, and 74% accuracies (overall, producer's, and user accuracy, respectively) while Quickbird imagery produced 68%, 100%, and 25% accuracies (overall, producer's, and user accuracy, respectively) (Fig. 2). Kappa values were 0.54, 0.84, and 0.27 for Landsat, SPOT, and Quickbird imagery respectively.

CASE STUDY 2: HYPERSPECTRAL IMAGERY USE FOR THE SWAN VALLEY AREA

Study area

This study, beginning in Spring 2002, collected ground-based data and remote sensing imagery in Swan Valley, Bonneville County, Idaho (43° 20' to 43° 40' North, 111° 5' to 111° 35' West). The South Fork of the Snake River runs through the length of the valley (approximately 30 km), providing irrigation for farming and feeding riparian zones with abundant flora and fauna. The mountains bounding the Swan Valley are semi-arid, typified by sagebrush-steppe vegetation. The region provides an ideal environment for the spread of leafy spurge seed through water, anthropogenic and animal transportation vectors. In the Swan Valley, there are a few large (>1 ha) leafy spurge infestations; however, approximately 50% of infestations are smaller than 75 m^2. Leafy spurge infestations in the study area have an average cover of approximately 40% (derived from oblique field cover estimation methods).

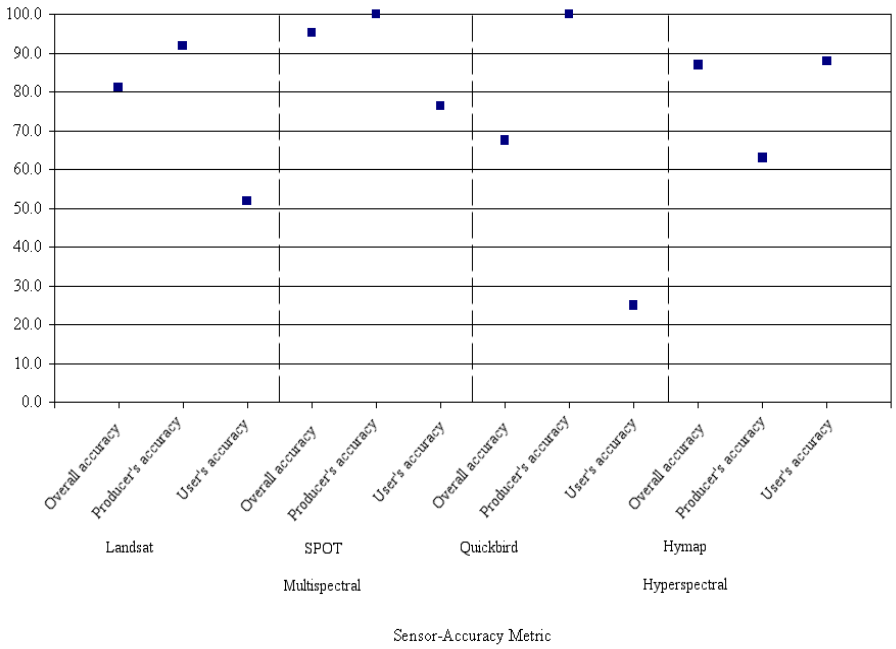

Figure 2. Accuracy of leafy spurge classification using various sensors (2003).

Imagery Collected

HyMap hyperspectral data were collected by the HyVista Corporation over the study area on June 30th, 2002, and again on June 29th, 2003 (Fig. 1), while leafy spurge was in full bloom. The HyMap data consists of 126 bands between 0.45μm and 2.5 μm with a pixel size of 3.5 m x 3.5 m (Cocks et al., 1998). Bandwidths ranged from 15 μm in the visible and near infrared to 20 μm in the shortwave infrared. In 2002, three 1.8 km wide hyperspectral flightlines (totaling approximately 40 km in length) were collected. In 2003, similar areas were collected, as well as an additional data flightline approximately 1.8 km wide and 20 km long.

Field Sampling Methods

The majority of the field sampling took place during the summer of 2003 (for both the 2002 and 2003 imagery datasets) with supplemental sampling during summer 2004. Because leafy spurge has not been observed to spread more than ~3 to 7m (1 to 2 pixels) over a 1 year period in Swan Valley, it is assumed for this study that the use of 2003 and 2004 field data is appropriate for imagery collected in 2002 and 2003 (Glenn et al., 2005). A total of 364 differentially corrected polygons (henceforth referred to as validation samples) were collected which included 323 polygons collected in 2003 and 41 polygons collected in 2004. Of the 364 polygons, 270 were located within the geographical bounds of the 2002 imagery and 214 were located within the geographical bounds of the 2003 imagery. The polygon data included leafy spurge presence/absence and ocular estimates of percent cover when leafy spurge was present. Bare ground, shrubs, and grass were also estimated. Polygon data were considered more desirable than point data in these surveys because in high spatial resolution images the size and shape of reference polygons can be visually compared to the size and shape of an infestation classified in the imagery.

Image Processing Methods

The 2002 and 2003 imagery were preprocessed by HyVista, Inc., utilizing the HyCorr algorithm for atmospheric correction and conversion of radiance to reflectance data. The vendor also geocorrected the images, however a residual georegistration error was estimated as < 15 m using ground control points (Glenn et al., 2005). Minimum Noise Fraction (MNF; Green *et al.*, 1988)

transforms were applied to the full spectral range of the reflectance data using a large subset of the entire mosaic to estimate image noise statistics. Leafy spurge endmembers for each year were image derived from the same training area using known geographic locations and comparing to known spectral profiles of leafy spurge (Glenn et al., 2005). For each year's dataset, the MNF transformed reflectance data were classified using the Mixture Tuned Matched Filter (MTMF; Boardman, 1998) algorithm. MTMF has demonstrated a high degree of success in similar studies (Parker-Williams and Hunt, 2002; Dudek et al., 2004). The MTMF algorithm produces two values for each pixel in an image: 1) a value of infeasibility; and 2) a Matched Filter value (MF). Pixels predicted to contain leafy spurge were interactively selected from a scatter plot of MF values versus infeasibility values using the criteria of a maximum infeasibility threshold of 20 and a range of MF values between 0.1 and 1.0. Pixels with high MF values and low infeasibility values were considered to likely contain leafy spurge. Pixels with low MF values and low infeasibility values were also considered. In these cases, the infeasibility threshold was adjusted to accommodate the lower MF values. Further discussion on this methodology is presented in Glenn et al. (2005) and Mundt *et al*. (2005).

Validation Methods

Field validation crews were sent to sites predicted to be either leafy spurge present or leafy spurge absent (selected using a stratified random method) to validate the model. This validation occurred in 2003 and in 2004, but unlike the Oxford study, this was not an iterative process. For the purpose of correcting for georegistration error, both positive and negative GPS validation samples were buffered by 15 m (just over 4 pixels). An error matrix of validation samples (polygons) was constructed following methods presented by Congalton and Green (1999). Kappa statistic was also used to test whether the remotely sensed classifications were better than randomly assigning classifications.

Classification Results

Results of the accuracy assessments for leafy spurge presence demonstrated overall accuracies of 86% and 87% for 2002 and 2003, respectively (Figure 2). For all validation sites, producer's accuracies were 56% in 2002 and 63% in 2003 while user accuracies were 81% in 2002 and 88% in 2003, and Kappa values were 0.58 in 2002 and 0.63 in 2003. When considering only validation sites with at least 40% cover leafy spurge, however, Producer's accuracies rose to over 70% in both 2002 and 2003 (Glenn *et al.*, 2005).

Accuracy Assessment

While it is important to represent the sensitivity limits of the classifier, it is also necessary to provide land managers with a useful product that meets their needs for reliability and confidence. When this project was initiated, local weed managers identified user accuracy (percentage of pixels classified on the map which actually represent that category on the ground) assessment criteria of 70%.

Accuracy assessment in high resolution imagery is a developing science, and recent publications have emphasized the importance of decisions pertaining to expressing the accuracy of thematic classifications (Story and Congalton, 1986; Stehman and Czaplewski, 1998; Congalton and Green, 1999; Foody, 2002; Lopez et al., 2004). In both studies presented here, the approach to accuracy assessment addressed two criteria: 1) quantify the reliability of leafy spurge discrimination; and 2) determine the advantages/disadvantages of improved spatial and spectral resolution for land cover modeling.

RESULTS AND DISCUSSION

CASE STUDY COMPARISON

The resulting accuracies of the two case studies presented above were compared using the metrics of detection accuracy, ease of processing, and cost effectiveness. Different software and classification techniques were employed in this study in order to optimize each case study to yield the best results and take advantage of the software and techniques specifically designed for the imagery. A study comparing multispectral and hyperspectral image classification using one standard classification algorithm such as spectral angle mapper is feasible, however this technique was not considered optimal for either case study.

DETECTION ACCURACY

Only one multispectral platform (SPOT) satisfied the minimum user accuracy requirement specified above (70%). The HyMap hyperspectral sensor also satisfied the minimum user accuracy requirement. Overall accuracy was very similar when comparing SPOT and HyMap. Landsat and Quickbird imagery failed to yield satisfactory user accuracies. The low user accuracy of Landsat is likely due to the patchy nature of leafy spurge relative to the size of each pixel (approximately 900 m^2). The high spatial resolution of Quickbird (2.4 meters) likely reduces spectral confusion, and thus the poor accuracy is hypothesized to be due to co-registration errors between the GPS-acquired field training sites and image georectification. As noted above, the georectification RMS was 5 meters for Quickbird imagery, equating to roughly 2 pixels. While a buffering technique could have been applied to absorb this error, we would have subsequently included a large proportion of non-target features due to the small patch sizes of the target features, thus further complicating the accurate classification of the target. With patchy targets compounded by training site positional error, this level of positional error can help explain the unacceptable user accuracy. In addition, it should be pointed out that the acquisition date of Quickbird imagery was not as well timed, phenologically, as either SPOT or Landsat imagery. Therefore this imagery had a slight disadvantage. However, the disadvantage is considered minimal because all infestations were fairly small and patchy and not readily apparent even when in full bloom stage. Lastly, while the spatial resolution of SPOT 5 and Quickbird imagery varies greatly (10 m and 2.4 m respectively), the spectral resolution is very similar, especially in the green, red, and near infrared bands.

The accuracies from the hyperspectral case study were similar to accuracies derived by Dudek *et al.* (2004), Kokaly *et al.* (2004), and Parker-Williams and Hunt (2002). Using hyperspectral data we were detected 40% cover plots of leafy spurge in both 2002 and 2003. While some areas of 10% leafy spurge cover were detected in either 2002 or 2003, these low percent cover predictions were not repeatable (see a full description in Glenn et al., 2005).

It should be noted that two differences existed in how accuracy was assessed in these case studies. First, the sample size used in the hyperspectral study consisted of 270 and 215 validation samples for 2002 and 2003, respectively (Table 1 reflects the 2003 accuracy, see Glenn et al (2005) for all reported accuracies). In the Oxford study area, the validation sample size was 85 (Table 1). The second difference in accuracy assessment was that the hyperspectral study was validated using polygon ground-truth sites (to absorb georegistration error) whereas the Oxford multispectral study used point ground-truth sites. Another factor that may affect accuracy assessment is the number of samples used in the accuracy assessment.. For example, the larger number of absent polygons with the hyperspectral data may increase the overall accuracy while the small number of leafy spurge presence sites in the Oxford study may positively bias the user accuracy. Because co-registration error was not a concern with SPOT imagery, we doubt that its classification would have been improved by using polygon ground-truth sites. Therefore, the only tangible difference is in the number and distribution of validation sites used.

Table 1. Comparison between leafy spurge classification accuracies derived using SPOT (2002) and HyMap (2003) imagery.

		Ground-truth sites							
		Leafy spurge		Non-leafy spurge		Total		User Accuracy	
		SPOT	HyMap	SPOT	HyMap	SPOT	HyMap	SPOT	HyMap
Model Prediction	Leafy spurge	13	43	4	6	17	49	76%	88%
	Non-leafy spurge	0	25	68	140	68	165	100%	85%
	Total	13	69	72	146	85	214		
	Producer's Accuracy	100%	63%	94%	96%	Overall Accuracy		95%	86%

EASE OF PROCESSING

Processing SPOT imagery was minimal. In general, SPOT imagery was processed very easily, especially when using imagery already corrected for systematic and atmospheric errors. Apart from the basic processing already described above, the SPOT imagery was projected from Universal Transverse Mercator to Idaho Transverse Mercator (using cubic convolution resampling) and georectified to an RMS of 2.62 using a 1st order polynomial (affine) transformation. Classification was then performed using maximum likelihood within Idrisi.

While the processing of the hyperspectral imagery had a steep learning curve, similar processing steps were performed between the multispectral and hyperspectral datasets. Hyperspectral datasets are large, commonly over 1GB, and as such require significant computational resources. Hyperspectral processing is a relatively new application, and much of the methodology that is well defined for multispectral processing is not as clear for hyperspectral applications. As such, much time was spent evaluating methods and procedures while processing hyperspectral data, however once the methods were learned, the image processing was smooth and easily iterated.

COST EFFECTIVENESS

To quantify cost-effectiveness, we developed an effectiveness rating which was the quotient of percent user accuracy (when user accuracy satisfied the minimum requirement threshold (i.e., $\geq$70%)) and cost/km^2. It should be noted that a single square kilometer of imagery cannot be purchased as most all data providers require a minimum acquisition area. When minimum requirements were not met, the effectiveness rating was set to 100. The results of the cost-effectiveness evaluation are given in Table 2.

Table 2. Cost-effectiveness (A / B = C) comparison between satellite platforms for detection of leafy spurge in southeastern Idaho.

Platform		(A) Cost / km^2	(B) User Accuracy obtained	(C) Cost-effectiveness
SPOT	$	0.94	74%	0.01
HyMap	$	150.00	88%	1.70
Quickbird	$	30.00	25%	n/a
Landsat	$	0.01	52%	n/a

CONCLUSIONS

While overall accuracy, producer's accuracy and user accuracy are each important to understand how well a classification performed (Congalton 1991), User accuracy was the focus of this paper

as it is a good measure of a predictive model's reliability and subsequent success with a land manager. This study demonstrated that both SPOT multispectral and HyMap hyperspectral imagery can be used to reliably predict the location of a patchy invasive weed such as leafy spurge. One advantage of HyMap hyperspectral imagery is that its pixel size is only 3.5 x 3.5 m. Importantly, we note that HyMap pixels are approximately 85% smaller (12.25m^2 versus 100.00m^2) than SPOT pixels offering a distinct advantage in early detection over numerous other sensors. However, SPOT's cost-effectiveness clearly has an advantage over hyperspectral imagery. In summary, for land management applications, cost- and field-effectiveness, along with time must be considered for each individual project.

ACKNOWLEDGEMENTS

This study was made possible by a grant from the National Aeronautics and Space Administration Goddard Space Flight Center and from the NASA BAA program (BAA-01-0ES-01; NAG13-02029). ISU would also like to acknowledge the Idaho Delegation for their assistance in obtaining this grant. Additional funding was contributed by the NOAA Environmental Technology Laboratory (ETL).The authors would like to thank Mr. Jeffrey Pettingill, Bonneville County Idaho Weed Supervisor, for his support and assistance.

LITERATURE CITED

Boardman, J.W. 1998. Leveraging the high dimensionality of AVIRIS data for improved sub-pixel target unmixing and rejection of false positives: Mixture Tuned Matched Filtering. In Proceedings of the 7th Annual JPL Airborne Geoscience Workshop, JPL Publication 97-1, pp. 55. Pasadena, CA

Casady, G. M., R. S. Hanley, and S. K Seelan. 2005. Detection of Leafy Spurge ( ) using multi-date high resolution satellite imagery. Weed Technology: Vol. 19, No. 2, pp. 462–467.

Cocks, T., Jenssen, R., Stewart A., Wilson, I., Shields, T., 1998. The HYMAP airborne hyperspectral sensor: the system, calibration and performance, Presented at 1st EARSEL Workshop on Imaging Spectroscopy, Zurich, October 1998

Congalton, R. G. 1991. A Review of Assessing the Accuracy of Classifications of Remotely Sensed Data. Remote Sensing of Environment, 37:35-46

Congalton, R. G., and Green, K. (1999). Assessing the Accuracy of Remotely Sensed Data: Principles and Practices. Boca Raton7 Lewis Publishers 137 pp.

Du Toit, J. T. and D. H. M. Cumming. 1999. Functional significance of ungulate diversity in African savannas and the ecological implications of the spread of pastoralism, Biodiversity and Conservation, Volume 8, Issue 12, Pages 1643 – 1661

Dudek, K. B., Root, R. R., Kokaly, R. F., Anderson, G. L., Brown, K. E., Mladinich, C. S. 2004. Temporal monitoring of leafy spurge: An example using 1999 and 2001 airborne visible/infrared imaging spectrometer (AVIRIS) data over Theodore Roosevelt National Park. Proceedings of the Society for Range Management 57th Annual Meeting. Salt Lake City, UT7 Society for Range Management.

Eastman, J. R. 2003. Idrisi Kilimanjaro: Guide to GIS and Image Processing. URL= http://www.clarklabs.org/

Efron, B. 1979. 1979. Bootstrap Methods: Another look at the Jackknife. Annals of Statistics. 7(1) 1-26.

Foody, G. M. 2002. Status of land cover classification accuracy assessment. Remote Sensing of Environment, 80, 185– 201.

Glenn, N.F., J. T. Mundt, K. T. Weber, T. S. Prather, L. W. Lass, and J. Pettingill. 2005. Repeat hyperspectral data processing for the detection of small infestations of leafy spurge. *Remote Sensing of Environment*, 95: 399–412.

Green, A.A., Berman, M., Switzer, P., & Craig, M.D. (1988). A transformation for ordering multispectral data in terms of image quality with implications for noise removal. Transactions on Geoscience and Remote Sensing, 26(1), 65-74

Holecheck, J. L., R. D. Pieper, and C. H. Herbel. 2001. Range Management- Principles and Practices. 4th ed. Prentice-Hall. 587 pp.

Kemble J. and D. Carrol 2005. Researchers use new approaches to pumpkins in the South. URL: http://www.vegetablegrowersnews.com/pages/2003/issue_03_04/03_04_se_pumpkins.html visited 6-April-2005.

Kokaly, R. F., Anderson, G. L., Root, R. R., Brown, K. E., Mladinich, C. S., Hager, S. 2004. Mapping leafy spurge by identifying signatures of vegetation field spectra in compact airborne spectrographic imager (CASI) data. Proceedings of the Society for Range Management 57th Annual Meeting (pp. 249–260). Salt Lake City, UT7 Society for Range Management.

Lass. L., Prather, T., Glenn, N., Weber, K., Mundt, J., Pettingill, J., 2005. Early Detection of Spotted Knapweed and Babysbreath with a Hyperspectral Sensor, *Weed Science*, 53: 242–251.

Lopez, R. D., Edmonds, C. M., Neal, A. C., Slonecker, T., Jones, B. K. Heggem, D. T., et al. 2004. Accuracy assessments of airborne hyperspectral data for mapping opportunistic plant species in freshwater coastal wetlands. In R. S. Lunetta, & J. G. Lyon (Eds.), Remote Sensing and GIS Accuracy Assessment (pp. 253–267). Boca Raton7 CRC Press LLC.

McKay, R.J. and N. A. Campbell. 1982, Variable selection techniques in discriminant analysis II: Allocation, British Journal of Mathematical and Statistical Psychology, 35, 30-41.

Mundt, J., N. F. Glenn, K. T. Weber, T. S. Prather, L. W. Lass, and J. Pettingill. 2005. Discrimination of hoary cress and determination of its detection limits via hyperspectral image processing and accuracy assessment techniques. *Remote Sensing of Environment*, 96: 509–517.

National Land and Water Resources Audit. 2001. URL: http://www.rangelands-australia.com.au/textsite/our_rangelands.html visited 9-November-2004

National Research Council. 1994. Rangeland Health- New Methods to Classify, Inventory, and Monitor Rangelands. National Academy Press. 180 pp.

Northwest Natural Resource Group. 2003. Preparing to Meet the Challenge: An Assessment of Invasive Species Management in Idaho. Boca Raton7 Idaho State Department of Agriculture brochure.

O'Brien, R. A., C. M. Johnson, A. M. Wilson, and V. C. Elsbernd. 2003. Indicators of Rangeland Health and Functionality in the Intermountain West. USDA Forest Service Gen. Tech. RMRS-GTR-104.

Parker-Williams A. & Hunt E. R. 2002. Estimation of leafy spurge cover from hyperspectral imagery using mixture tuned matched filtering. Remote Sensing of Environment 82: 446-456.

Pellant M., P. Shaver, D. A. Pyke, J. E. Herrick. 2003. Interpreting indicators of rangeland health, ver. 4. Technical Reference, USDI, BLM, National Science and Technology Center, Denver, CO, U.S.A

Pyke D. A., J. E. Herrick, P. Shaver, M. Pellant. 2002. Rangeland health attributes and indicators for qualitative assessment. Journal of Range Management 55: 584-597.

Settle J.J. and N.A. Drake, 1993, Linear mixing and the estimation of ground proportions, International Journal of Remote Sensing, 14(6), pp. 1159-1177.

Serr, K., T. K. Windholz, and K. T. Weber. 2006. Comparing GPS Receivers: A Field Study. URISA Journal (in review).

Sohn, Y. and R.M. McCoy. 1997. Mapping desert shrub rangeland using spectra unmixing and modeling spectral mixtures with TM data, Photogrammetric Engineering and Remote Sensing, 63(6) pp.707-716.

Stehman, S. V., & Czaplewski, R. L. 1998. Design and analysis for thematic map accuracy assessment: Fundamental principles. Remote Sensing of Environment, 64, 331– 344.

Story, M., and Congalton, R. G. 1986. Accuracy assessment: A user's perspective. Photogrammetric Engineering & Remote Sensing, 52,397– 399.

Thurow, T. L. and J. W. Hester. 1997. How an increase or reduction in juniper cover alters range-land hydrology. In Taylor, C. A. (ed.) 1997 Juniper Symposium. Texas Agricultural Experiment Station, Texas A&M University System, Tech. Rep. 97-1, January 9-10, 1997, San Angelo Texas.

Titus, K., J. A. Mosher, and B. K. Williams. 1984. Chance-corrected classification for use in discriminant analysis: ecological applications. Am. Midl. Nat. 111:1-7.